AD_____
(Leave blank)

Award Number: W81XWH-06-1-0432

TITLE: A New In Vitro Model of Breast Cancer Metastasis to Bone

PRINCIPAL INVESTIGATOR: Andrea M. Mastro, Ph.D
Erwin A Vogler, Ph.D., Carol V. Gay, Ph.D.

CONTRACTING ORGANIZATION: Pennsylvania State University
University Park, PA 16802-7000

REPORT DATE: April 2009

TYPE OF REPORT: Annual Report

PREPARED FOR: U.S. Army Medical Research and Materiel Command
Fort Detrick, Maryland 21702-5012

DISTRIBUTION STATEMENT: (Check one)

X Approved for public release; distribution unlimited

Distribution limited to U.S. Government agencies only; report contains proprietary information

REPORT DOCUMENTATION PAGE

Form Approved
OMB No. 0704-0188

1. REPORT DATE *(DD-MM-YYYY)*	2. REPORT TYPE	3. DATES COVERED *(From - To)*
14-04-2009	Annual	15 MAR 2008 - 14 MAR 2009

4. TITLE AND SUBTITLE
A New In Vitro Model of Breast Cancer Metastasis to Bone

5a. CONTRACT NUMBER

5b. GRANT NUMBER
W81XWH-06-1-0432

5c. PROGRAM ELEMENT NUMBER

6. AUTHOR(S)
Andrea M. Mastro

Erwin A. Vogler

Carol V. Gay

5d. PROJECT NUMBER

5e. TASK NUMBER

5f. WORK UNIT NUMBER

7. PERFORMING ORGANIZATION NAME(S) AND ADDRESS(ES)

*

Pennsylvania State University
University Park, PA 16802-7000

8. PERFORMING ORGANIZATION REPORT NUMBER

9. SPONSORING / MONITORING AGENCY NAME(S) AND ADDRESS(ES)

U.S.Army Medical and Materiel Command
Ft. Detrick, MD 21702-5012.

10. SPONSOR/MONITOR'S ACRONYM(S)

11. SPONSOR/MONITOR'S REPORT NUMBER(S)

12. DISTRIBUTION / AVAILABILITY STATEMENT

Distribution unlimited.

13. SUPPLEMENTARY NOTES

14. ABSTRACT Osteoblasts (OB) grew into bone-like tissue in a 3D model system. Pre-OB matured to OB and eventually to osteocyte-like cells. These cells met the criteria of osteocytes based on shape and protein expression. In addition, the density was similar to that reported for calvaria bone. The 3-D system was used to examine the interaction of metastatic breast cancer cells, MDA-MB-231, with OB. The cancer cells brought about profound effects on the osteoid tissue. The OB changed from cuboidal to spindle shape.The cancer cells aligned into an "Indian filing" pattern, and penetrated the osteoid. Using RT-PCR, we found that cancer cells downregulated OB differentiation proteins but increased inflammatory cytokines. We have tried to modify these effects by changing the oxidative status of the microenvironment with selenium and by adding drugs commonly used to treat metastatic breast cancer, zoledronc acid (ZOL). ZOL's main known target is the osteoclast but we found that it clearly affects osteoblasts and cancer cells. The OB morphology changes were inhibited. Selenium supplementation caused changes in the osteoblast cell morphology and permitted cancer cell growth but in a different pattern than seen in the deficient cultures.

15. SUBJECT TERMS
3D model, osteoblasts, metastatic breast cancer, bone.

16. SECURITY CLASSIFICATION OF:			17. LIMITATION OF ABSTRACT	18. NUMBER OF PAGES	19a. NAME OF RESPONSIBLE PERSON *e)USAMRMC*
a. REPORT	b. ABSTRACT	c. THIS PAGE	UU	181	19b. TELEPHONE NUMBER *(include area code)*
U	U	U			

Table of Contents

Progress Report: A New In Vitro Model of Breast Cancer Metastasis to Bone

Andrea M. Mastro, Carol V. Gay and Erwin A. Vogler

INTRODUCTION:

Breast cancer frequently metastasizes to the bone where it disrupts the balance between osteoblasts and osteoclasts and leads to osteolytic degradation (Bussard et al. 2008). The objective of this study was to test the hypothesis that osteolytic bone metastases results partly from the affect of the cancer cells on the osteoblasts, i.e. the cancer cells prevent osteoblasts from accreting mineralized tissue ultimately leading to accelerated skeletal degradation. In order to test this idea, we proposed to develop an existing three-dimensional culture system into an *in vitro* test system for studying the interactions between osteoblasts and metastatic breast cancer cells. The objectives were to characterize the morphology and physiology of osteoblasts (MC3T3-E1) cultured as a 3D osteoid in a bioreactor and to determine how they reacted to the presence of human metastatic breast cancer cells (MDA-MB-231). In addition we proposed to determine how this interaction was affected by changing the oxidative state of the microenvironment with selenium spupplementation. We also used this system to determine how the currently used drugs, zoledronic acid and doxetaxel, affected osteoblasts and cancer cells in the 3D model.

BODY:

***Task 1*. To determine the effects of metastatic breast cancer cells on the physiology of osteoblasts cultured in a long term culture system that fosters growth in three-dimensions. (months 1-6)**

a. Establish cultures of MC3T3-E1 cells in bioreactors and add metastatic breast cancer cells at various times after the establishment of culture (4,7,15,30 days). Periodically sample the secreted materials in the growth chamber that will indicate osteoblast function. ELISA or RIA will be carried out for OCN, IL-6, MIP-2, MCP-1. Alkaline phosphatase will be assayed by a biochemical assay. Culture medium from cells grown in standard tissue culture will be compared. For control cells in selected assays, a human immortalized non-tumorgenic cell line, such as h-TERT–HME1 will be used.

b. Establish cultures of MC3T3-E1 cells in bioreactors and add metastatic breast cancer cells at various times after the establishment of culture bioreactors as in task 1-a. Terminate the cultures periodically to assay the cells for cell associated alkaline phosphatase, Type I collagen, mineralization (alizarin red, von Kossa) and for apoptosis (TUNEL).

***Task 2*. To determine the effects of metastatic breast cancer cells on osteoblast morphology in a long term bioreactor culture system that fosters growth in 3-dimensions. (months 7-13)**

a. Co –cultures of osteoblasts and breast cancer cells will be prepared as in task 1. The stage of differentiation of the osteoblasts and the time of the addition of the cancer cells will be decided based on the results of task 1. Co-cultures from the bioreactor and conventional cultures will be fixed to preserve morphological detail.

b. Part of each culture will be fixed with paraformaldehyde following a protocol to preserve GFP. These cultures will be imaged with confocal fluorescence microscopy to detect the metastatic breast cancer cell migration.

c. Part of each culture will be prepared for detection of apoptosis (TUNEL). The GFP tag of the cancer cells will allow us to distinguish apoptotic cancer cells from apoptotic osteoblasts.

d. Part of each culture will be prepared for scanning electron microscopic observation. We anticipate that we will be able to distinguish cancer cells from osteoblasts in these preparations based on size and shape.

e. Part of each culture will be prepared for the transmission electron microscopy. We will view the cells with an eye to fine structural detail.

Task 3. To test known stimulators and/or protectors of osteoblast function in the presence and absence of breast cancer cells in order to develop a means of blocking the destructive effects of breast cancer cells have on bone forming osteoblasts. (months 14-34)

Summary of the results at the end of the third year of investigation

Parts of tasks 1 and 2 were pursued in parallel to maximize efficiency in achieving aims of proposed work and to provide internal consistency in the work by using living cells/biological materials in a conserved timeframe. Much of aims 1 and 2 were reported last year and are now published.

Tasks 1 and 2: Characterization of the osteoblasts in the bioreactor

Main finding: Osteoblast lines and as well as primary osteoblasts grew into bone osteoid-like tissue in the bioreactor. They express characteristic differentiation genes and osteoblast-secreted molecules and cytokines. Most of these findings were presented in last year's report and are now published [see appendix (Dhurjati, Liu et al. 2006; Liu, Lim et al. 2007; Dhurjati, Krishnan et al. 2008; Kinder, Chislock et al. 2008)]. In addition we allowed some cultures to grow for about 10 months. We made two major observations: the osteoblasts developed into cells that were characteristically

osteocytes; bone deposition occurred. This information is included in the appended manuscript (Krishnan et al) and is summarized here.

Differentiation of osteoblasts into osteocytes

We had found that growing osteoblast for about 2 months was optimal for studying the interaction of the osteoblastic tissue with breast cancer cells. However, we allowed a few of the cultures to grow for approximately 10 months. We followed the morphology of the MC3T3-E1 cells over this time. We found that MC3T3E-1, developed into 3D tissue about 22 μm thick within 15 days (Figure 1, Panels A, B), comprised of 6-8 layers (Panel C, D) of actively-mineralizing (positive for alkaline phosphatase activity and for mineralization by von Kossa stain), differentiated osteoblasts. Transmission electron microscopy (TEM) showed that this tissue was densely packed with close cell contacts (Panels C, D). Continuous culture reproducibly resulted in transformation of spindle-shaped pre-osteoblasts into cobble-stone shaped osteoblasts that secreted and mineralized an extensive, collagenous extracellular matrix that completely enveloped the cells.

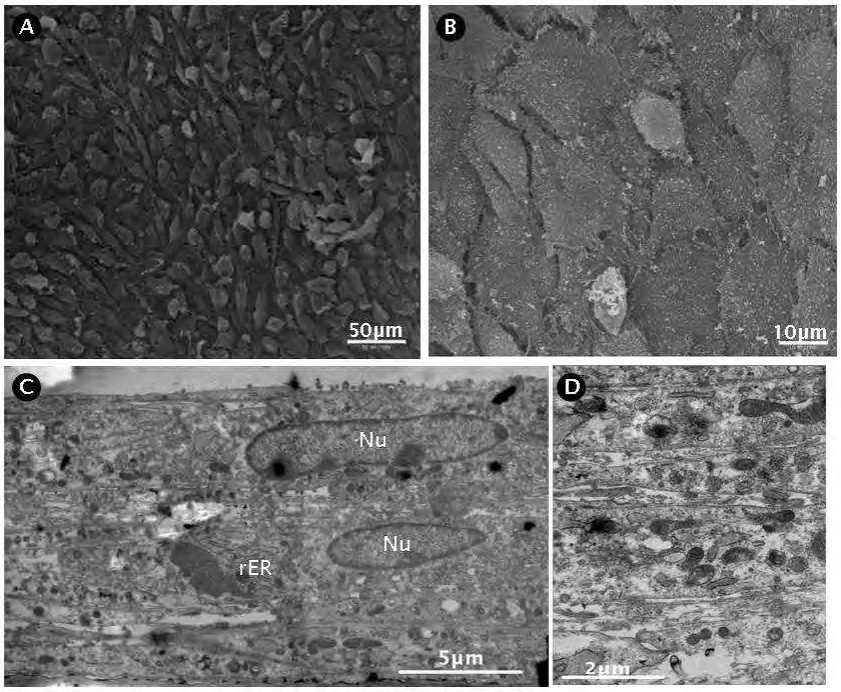

Figure 1: *MC3T3E-1 pre-osteoblasts grown for 15 days within the bioreactor. Panels A, B: SEM images of a dense 3D tissue about 22 μm thick. Panels C, D: Cross-sectional TEM images showing 6-8 layers of actively-mineralizing and densely packed cells with close cell contacts (Nu = nucleus, rER = rough*

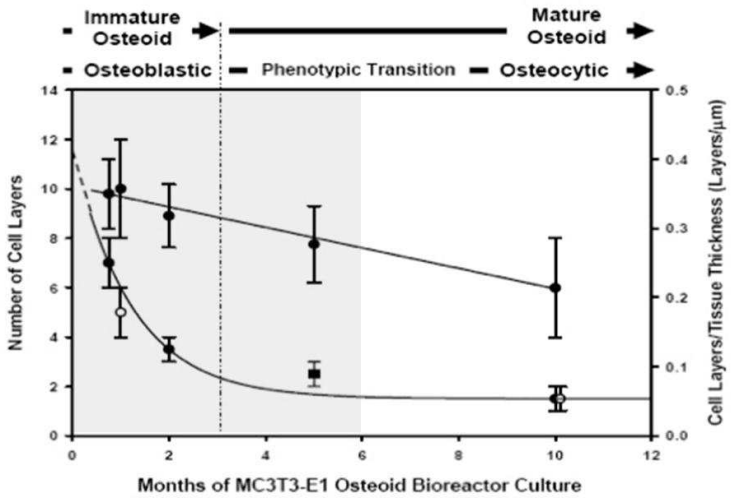

Initially the cells were closely packed (high cell/matrix ratio) but transformed into a more mature phenotype (low cell/matrix) after about 5 months (Figure 2). Confocal microscopy (Figures 3A-D) further revealed that this transformation was associated with a progression in cell morphology from cuboidal to stellate with many intercellular contacts (indicated by arrows). □

Figure 2: *Phenotypic maturation of MC3T3E-1 within the bioreactor over 10 months continuous culture. An exponential-like decrease in the number of cell layers with time (left-hand axis) translated into a linear-like decrease in cell-layer/tissue-thickness ratio (right-hand axis). This finding was consistent with the process of bone maturation that resulted in transformation of proliferating pre-osteoblasts into non-dividing osteoblasts that become engulfed in mineralized matrix and mature into osteocytes.*

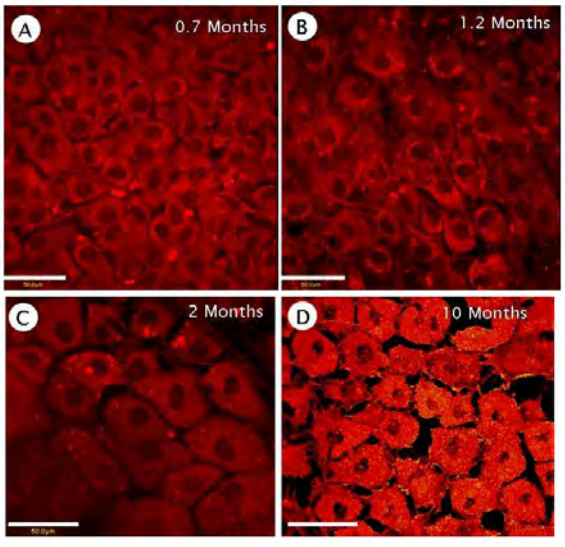

Figure 3: *Progression in cell morphology monitored by confocal microscopy of Alexa Fluor 568 phalloidin stained MC3T3E-1 within the bioreactor over 10 months of culture (compare with Fig. 2). Panel A: "cobble-stone" shaped osteoblast-like cells matured from fibroblastic pre-osteoblasts within 3 weeks. Panel B: elongated cells appeared with development of many cellular processes within 1.2 months. Panel C: density of cells enmeshed in a dense collagenous matrix (appears black,) decreased over 2 months. Panel D: 1-2 layers of stellate cells with many intercellular contacts after 2-10 months of continuous culture. Scale bar represents 50µm.*

We carried out scanning electron microscopy (SEM) a bioreactor after 10 months of continuous culture (Figure 4A,B) and saw that the tissue was about 50 μm thick. Furthermore, it was comprised of stellate cells interconnected with many processes with different lengths ranging from about one cell diameter ("short") to many cell lengths ("long"). Examination of many TEM images (e.g. Figure 4D) revealed that intercellular connections terminated in over-lapping protrusions (see arrows). From these images and molecular biology (Table 1), we concluded that the entire tissue was comprised of osteocytic cells.

Table 1: Temporal gene expression of differentiation markers in MC3T3-E1 cultured in the bioreactor

Markers	Months in Culture			
	0.7	1	2	10
Osteocalcin	0.54[a]	0.14	0.55	0.015
Osteonectin	0.53	0.53	0.34	0.19
Osteopontin	0.21	0.054	0.51	0.11
Type I Collagen	1.49	1.36	1.21	0.76
MMP13	0.11	0.23	1.46	na
E-11	1.15	0.93	1.01	0.78
DMP-1	0.09	0.04	0.63	0.06
Sclerostin	nd	nd	*	*
Yield of RNA	1100 ng/uL	160 ng/uL	180 ng/uL	12 ng/uL

We counted the cells to determine how the numbers compared with human bone. We found 36 osteocytes in a 4 μm^2 confocal-images field (Figure 4C), suggesting that there were about $9X10^4$ osteocytes/cm^2. This value further translated into 2 million osteocytes/bioreactor; assuming that the 27 μm tissue shown was uniform across the entire 25 cm^2 growth space (see Figure 5, panel D). We further estimated that there were about $3.4X10^4$ osteocytes/mm^3. This number compared favorably with $1.3X10^4$ osteocytes/mm^3 measurements on human bone.

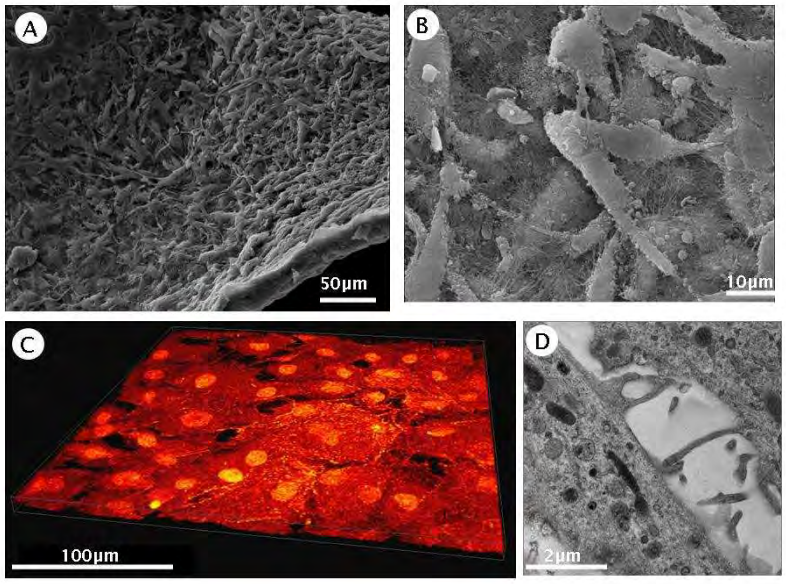

Figure 4: *Osteocyte-like cells mature within the bioreactor over 10 months continuous culture. Panels A, B: SEM image of ~23 µm thick tissue showing closely packed stellate cells interconnected with many cellular processes. Panel C: confocal image of Alexa Fluor 568 phalloidin stained osteocytes showing 1- 2 cell layers with many intercellular processes. Panel D: high-magnification TEM image of overlapping cell protrusions (arrows) typical of osteocytes.*

As osteoblasts differentiate from pre-osteoblasts to mature osteoblasts to osteocytes, characteristic genes are expressed. We determined gene expression by PCR. The phenotypic progression suggested by cell morphology also was reflected in the characteristic expression of genes such as Type I collagen, osteonectin, osteocalcin and osteopontin (Table 1). Up-regulation of matrix-metallo proteinase (MMP)-13 (indicative of extracellular matrix remodeling) and the proteins E11, DMP-1, and sclerostin, indicative of osteocytic transformation, (Franz-Odendaal, Hall et al. 2006) occurred in more mature cultures. In spite of the fact that there were numerous viable cells within the bioreactor after 10 months, RNA recovery was lower than that of younger bioreactors (Table 1), consistent with fewer cells.

After about 2 months of continuous culture, bioreactors occasionally exhibited contiguous, cm^2-scale macroscopic mineral deposits on the growth-chamber side of the dialysis membrane. Dialysis membranes from bioreactors without visually-apparent mineral were found by FTIR spectroscopy to produce weak signals consistent with hydroxyapatite, suggesting that osteoblasts may have passed too quickly through the mineral-deposition phase to produce visually-apparent aggregates. Too few bioreactors have been studied to date to discover the exact conditions that led to bioreactor ossification, but there was no doubt that unknown experimental factors (e.g. inoculum concentration, precise timing of media replacement, *etc*.) occasionally led to deposition of macroscopic bone-like mineral. This material did not appear in bioreactors kept with differentiation medium alone in the absence of cells. X-ray diffraction of a mineral “chip” (Figure 5A) also was consistent with bovine bone (see inset of Figure 5A). SEM of the chip revealed that the deposit was comprised of many nodules (Figure 5B), consistent with a nucleation-and-growth deposition phenomenon. Comparison of FTIR spectra of

chips recovered from 5 and 10 month bioreactors suggested an evolution of chemical composition with deposition time (Figure 5C).

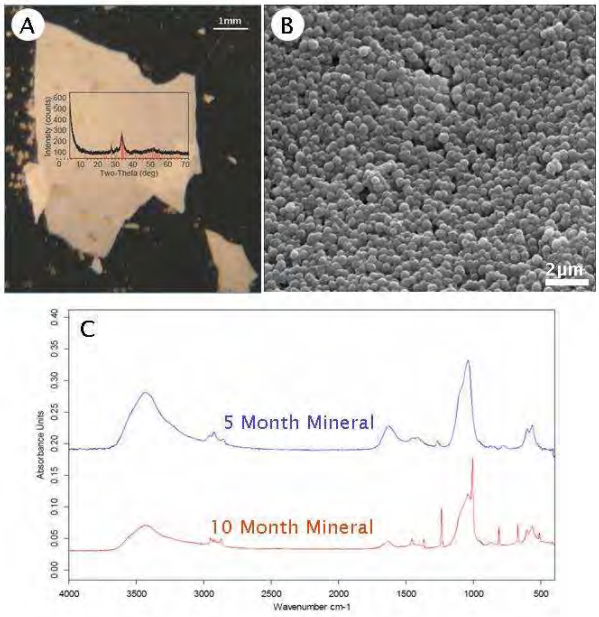

Figure 5: *Macroscopic mineral deposits on the growth-chamber side of the bioreactor dialysis membrane. Mineral chip taken from a 10 month bioreactor dialysis membrane were prepared for X-ray diffraction or FTIR spectral analyses as described in the method. Panle A: The X-ray diffraction pattern was similar to bovine bone (inset). Panel B: Reveals that the chip was comprised of close-packed spherical nodules. Panel C compares FTIR spectra of chips recovered from 5 and 10 month bioreactors* showing changes in chemical composition with deposition time.

In summary, the use of the bioreactor makes it possible to grow osteocytes in culture. Currently is it only possible to use a cell line or to isolate the cells usually from calavaria from neonatal mice or rats. Further manipulation of the bioreactor may allow the time frame to be shortened. We have not seen osteocytes at 5 months but we have seen them at 8 months.

Task 3. To test known stimulators and/or protectors of osteoblast function in the presence and absence of breast cancer cells in order to develop a means of blocking the destructive effects of breast cancer cells have on bone forming osteoblasts. (months 14-34)

Establish cultures of osteoblasts at various stages of differentiation in the presence and absence of metastatic breast cancer cells as determined in task 1.

Main findings

The bisphosphonate, zeledronic acid (ZOL), when added to a bioreactor in the presence of cancer cells, had an obvious impact on the cancer cells in the co-culture system. The cancer cells formed smaller colonies and did not form projections or penetrate the matrix as seen with cultures without ZOL. The gene expression of the cancer cells and osteoblasts is currently underway. Further analyses are in progress.

Selenium supplementation appeared to affect the osteoblasts more than the cancer cells. The osteoblast appeared to have long cell extensions. The cancer cells colonized the osteoblast tissue of the Se deficient and supplemented cultures but with different patterns.

1. Selenium will be increased or reduced (by used of selenium depleted serum) and the cultures will be followed as described in task 1.

Selenium supplementation

Based on our findings in task1 and a series of cell culture studies we grew MC3T3-E1 cells in the bioreactor under low Se conditions or supplemented with 2 μm methylseleninic acid (MeSa). Selenium was reduced to < 20 nM by using 5% serum. We based this choice of a selenium supplement and concentration on reports in the literature and on experiments carried out in our laboratory with MC3T3-E1 in standard culture dishes ((Chen, Y-C, see appended Ms). This concentraton of MeSa was not toxic to either the MC3T3-E1 or to the MDA-MB-231 cells. Under both conditions the osteoblasts grew and differentiated; i.e. alkaline phosphatase production and von Kossa staining, in standard cell culture.

We added MDA-MB-231^{GFP} cells to bioreactors of MC3T3-E1 that were approximately 2.5 months old. The osteoblasts were first labeled with Cell Tracker Orange in order to visualize them with the confocal microscope (Figure 6). We noticed that the Se supplemented cells did not take up the dye as well as those grown in under conditions of low Se. We monitored the cultures by confocal microscopy for a week. We saw that cancer cells attached and grew under both conditions. Unlike our previous observations (Dhurjati et al. 2008) with Se adequate medium, the cancer cells failed to align themselves into single file and the osteoblasts did not change from cuboidal to spindle shape. Rather the Se supplemented osteoblasts formed long processes (Figure 6E). They also did not appear as well-defined microscopically (cf Figure 6 A with D, G). The cancer cells in the Se deficient medium formed colonies (Figure 6 C), as previously seen. In the presence of MSA, they grew more randomly and covered the osteoblast tissue (Figure 6 F). This pattern of growth was reminiscent of that seen with cancer cells and osteoblasts that were relatively undifferentiated after 15 days of culture in the bioreactor. It is possible that the MSA supplementation affected osteoblast differentiation in the bioreactor in spite of the fact that in standard culture plates, the osteoblasts with MSA produce alkaline phosphatase. The RNA and cell culture supernatants from the bioreactors have been collected. RT-PCR will be carried out to measure gene expression patterns of the osteoblasts and cancer cells under both

growth conditions. The supernatants will be assayed by ELISA for inflammatory cytokines.

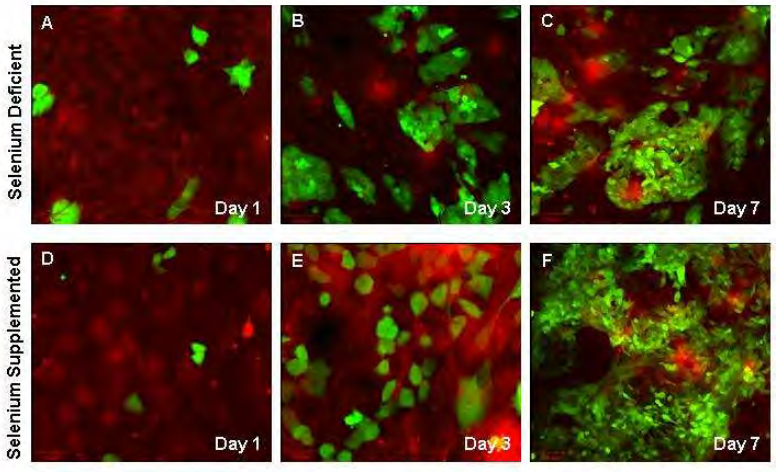

Figure 6. Confocal micrograph of Selenium defecient (A, B, C) and selenium supplemented (D, E, F) MC3T3-E1 (red) co-cultured with MDA-MB-231-GFP for a period of 7 days. Representative images indicate breast cancer cell adhesion (A, D), proliferation (B, E) and colonization (C, F). Panel G is a representative image of osteoblast cells cultured without any cancer cells in deficient medium..

2. Bisphosphonates

We also are in the process of testing compounds currently being used to treat patients with bone metastatic breast cancer.

Bisphosphonates are synthetic analogues of inorganic pyrophosphates, normal regulators of bone mineralization (Rogers, Gordon et al. 2000). Bisphosphonates are widely used to treat metastatic breast cancer as well as prostate cancer and other cancers that metastasize to the skeleton. They also are prescribed in much lower doses for individuals with osteoporosis or osteopenia (Green 2003). Zoledronic acid (Zoledronate) is one of the most aggressive in targeting bone metastasis. It is a nitrogen containing analogue of inorganic pyrophosphate. Bisphosphonates bind strongly to bone mineral particularly where there is bone turnover. In the process of bone resorption, osteoclasts internalize the molecule which then inhibits certain critical enzymes. The nitrogen containing bisphosphonates such as ZOL act on the mevalonate pathway and inhibit geranylgeranylation and farnesylation. These molecules are required for post-translational prenylation (transfer of long chain isoprenoid lipids) of proteins. Among the proteins affected are the GTP-binding proteins such as Ras, Rho, Rac and Rab which leads to apoptosis in osteoclasts. Although these drugs are effective against osteoclasts, they may affect cancers cells and OBs since prenylation is

not limited to osteoclasts. The extent of these other-cell effects and mechanisms are not known.

The theory is that once bone degradation is inhibited, growth factors released in the process of bone resporption will no longer be available to stimulate cancer cell growth. The "vicious cycle" of bone metastasis will be stopped (Mundy 2002). There is evidence to suggest that in bone, bisphosphonates might also inhibit tumor growth directly, although this does not seem to be the case for metastases to soft tissues. What effect does this class of molecule have on osteoblasts?

Studies have been carried out *in vitro* with cell lines in standard tissue culture or *in vivo* in a mouse model. The *in vitro* studies may not impart a complete representation of how OBs or cancer cells react in the bone microenvironment. *In vivo* it is very difficult to separate the effects that numerous cell types have upon others. There are numerous studies of the effects of bisphosphonates on OBs (Reinholz, Getz et al. 2000; Chaplet, Detry et al. 2004; Pan, Farrugia et al. 2004). The results vary, possibly due to the type and age of OBs used. Several studies lead to the conclusion that ZOL enhances OB anabolism and causes increased bone formation. Some report that human primary OBs increased in differentiation in culture in the presence of ZOL. There was increased expression of osteocalcin, bone morphogenic protein 2 and mineralization. They found no increase in the message for RANKL or OPG but there was an increase in OPG secretion and a decrease in transmembrane RANK-L expression possibly due to the effects of prenylation and expression of a metalloprotease (TACE). In contrast report no effect of CLOD, PAM or ZOL on differentiation of human mesenchynal derived OB but did see a drop in OB calcium deposition.

From these few examples, it is clear that ZOL and other bisphosphonates affect OBs. Do they affect tumor cells? It has been found that bisphosphonates have cytostatic and pro-apoptotic effects on myeloma, prostate and breast cancer cells. Other steps in the metastatic process, *i.e*. tumor cell adhesion and invasion, were inhibited by bisphosphonates. Some of these effects are believed due to metalloproteinase (MMP) activity. The blockage of cytokine secretions by OBs, stromal cells and monocytes may also be relevant to tumor cell growth.

In summary, there are numerous studies *in vivo* and *in vitro* with N-bisphosphonates, especially ZOL, to indicate that these drugs inhibit osteoclastic activity. The effects on OBs and other cells including tumor cells are not as clear. *In vitro* studies have yielded conflicting results with regard to OB differentiation is increased but some find a decrease. Tumor cells may be directly affected but there may indirect effects related to bone-tumor microenvironment.

We plan to study the effects of these molecules in the bioreactor. We first conducted a series of cell culture studies to determine the concentrations to use. In vivo, the ZOL binds to the bone matrix so there is an initial blood level and then a concentrated amount in the bone. These studies were carried out by a honors student in bioengeering

student as part of her McNair fellowship research program. The work is ongoing. Appended is the paper that she wrote at the end of the summer 2008, program.

We tested ZOL on osteoblast proliferation (Figure 1 below from Miller) both in a pulse experiment (24 hr exposes) or continuous exposure. We tested 0.05, 0.5 and 5.0 μM over 96 hours. Cells were released with pronase and counted using a hemacytometer. Trypan blue staining was used to detect dead cells. We found that 5 μM was cytotoxic in both protocols. 0.5 μM was less toxic in the pulse protocol.

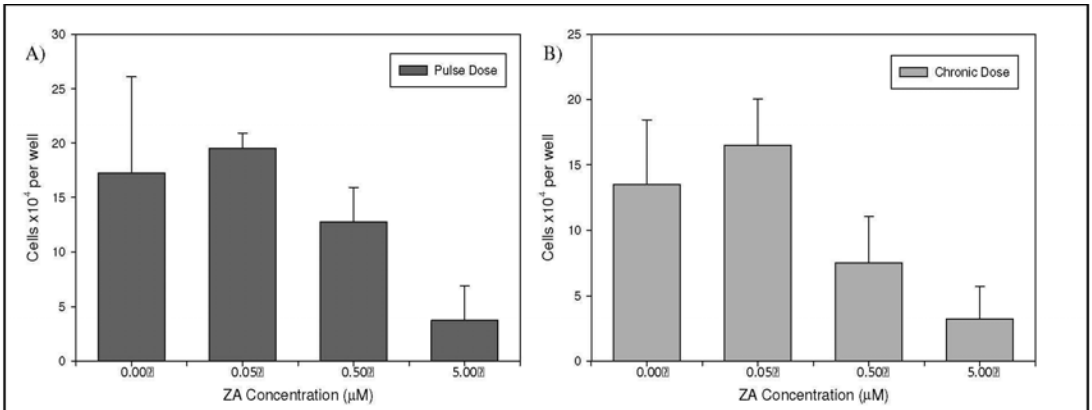

FIGURE 1. Effect of zoledronic acid (ZA) on osteoblast proliferation. Osteoblasts were plated at $1x10^4$ cells/cm^2 in a 24-well plate and ZA was added in concentrations of 0.00, 0.05, 0.50 and 5.00 μM. After 24 hours, medium was removed and replaced according to a dosing regimen. Wells designated for acute exposure (A) were replenished with osteoblast growth medium, while those for chronic exposure (B) received another drug dose. Proliferation was assessed with a trypan blue stain.

Based on the assumption that the concentrations of ZOL in 2 month cultures of osteoblasts in the bioreactor might be different than those found in cells grown under standard tissue culture conditions, we added either 0.05 μM or 0.5 μM to the cell chambers. As the ZOL diffused into the upper reservoir, over time the final concentrations reached 7 nM and 70 nM. We followed the cutures by confocal microscopy for several days and noted several paratmeters (Table 1).
The results are summarized in Table 1. The figures are included in the appended material as a power point presentation.

- In the presence of ZOL, fewer colonies of breast cancer cells formed.
- The colonies that formed with ZOL were more rounded and showed fewer elongated processes.
- The cultures treated with ZOL showed less cancer cell alignment.
- We saw what appeared to be lysed or broken cancer cells in the cultures treated with ZOL.
- The osteoblasts in the culture with ZOL did not show the modified spindle shape that they normally acquire in the presence of cancer cells.
- The cancer cells in the presence of ZOL did not appear to penentrate through the osteoblast multilayer as they did without the ZOL..

Table 1. The effects of zoledronic acid on the interaction of breast cancer cells with osteoblasts in a 3D culture system.

Experimental Parameter	Culture/Treatment			
	OB	OB + BC	OB + BC + 0.05µM ZOL	OB + BC + 0.5µM ZOL
BC Colony Formation	n/a	+++	+	++
BC Processes	n/a	+++	+	+
Rounded BC Morphology	n/a	+	+++	++
BC Alignment	n/a	+++	+	++
Ruptured BC Cells	n/a	-	++	++
Spindle-shaped OB Morphology	---	+++	+	+
Tissue Penetration	n/a	+++	+	++

The RNA from these co-cultures has been isolated. We are currently preparing to carry out RT-PCR to determine the effects of ZOL on the osteoblast differentiation proteins. Because both the human cancer cells and the murine osteoblasts contributed to the RNA, we must design primers to distinguish murine from human RNA. We will use a housekeeping gene to normalize the RNA to account for differences in cell numbers. This work is in progress.

In summary, ZOL affected the interaction of breast cancer cells and osteoblasts in the absence of osteoclasts. The next step is to examine the effect of doxetaxel on two month cultures of OB grown in the bioreactor. We would expect doxetaxel to block l proliferation of dividing cells. However, the two month cutures will be non-dividing and well differentiated. Thus we expect there to be little effect on the osteoblasts. In contrast, the cancer cells in the cultures continue to divide. We anticipate that the cancer cells will be affected. There are reports that cancer cells in co-culture with normal cells are protected from cytoxic agents. We will first test a range of concentrations of doxetaxel for cytotoxicity of cancer cells grown alone or co-cultured with differentiated cultures of osteoblasts in standard culture. Based on the results, we will choose a concentration to test in the bioreactor culture. We anticipate that we will be able to selectively affect the cancer cells. The final step will be to combine treatments with ZOl and dxetaxel.

Future Goals

As we have presented this work at meetings and conferences it has become clear that a culture that included osteoclasts as well as osteoblasts would be very valuable. These together would comprise a " bone remodeling unit." To that end, a graduate student has been learning to differentiate both human and mouse osteoclasts in culture. We are currently writing proposals to obtain funding for this work.

He has successfully cultured human osteoclasts (Lonza) in the bioreactor and shown them to be functional osteoclasts (Figure 7). They developed into multinucleated cells that stained with acridine orange, indicative of an acid cytolplasm (Figure 7 A). They stained with TRAP and also formed actin rings, indicative of mature osteoclasts (Figure 7, B,C). When cultured on a bone slice, these cells degraded the bone as evidenced by formation of "resorption pits."

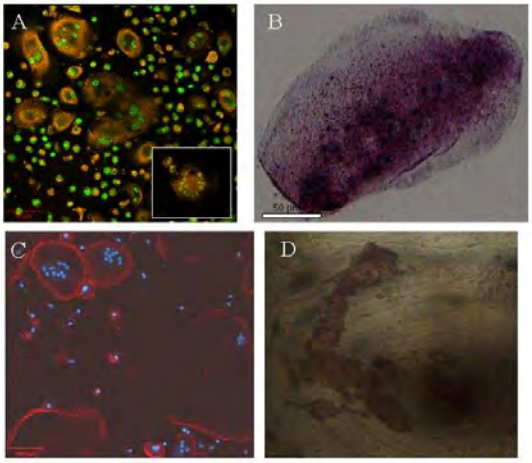

Figure 7. Micrographs of Human pre-osteoclasts cultured for 7 days in Bioreactor (A, B) and 96 well tissue culture dishes (C, D)- (A) Acid compartments (orange) of mature multi-nucleated (green) osteoclasts visualized using acridine orange staining. Inset shows staining for actin ring on cells that were also stained for acridine orange. (B) TRAcP positive mature osteoclasts that were stained for acridine orange and actin ring. (C) Phalloidin stained multi-nucleated (blue) osteoclast depicting actin-ring (red) formation. (D) Phase image of osteoclast-made resorption pit on bovine cortical bone slice.

KEY RESEARCH ACCOMPLISHMENTS

- Primary osteoblasts and the MC3T3-E1 osteoblast line can be grown for extended periods in the bioreactor.
- The osteoblasts appeared to differentiate and undergo an osteogenesis program from pre-osteoblasts to mature osteoblasts to osteocytes. Gene expression and morphology indicated this progression. Cells resemble in vivo calvaria osteocytes.
- MDA-MB-231 metastatic breast cancer cells when co-cultured with the osteoblasts, caused a change in morphology of the osteoblasts. The cancer cells aligned themselves in a manner reminiscent of "Indian Filing."
- With both the primary osteoblasts and the MC3T3-E1 cell line, the cancer cells inhibited osteoblast differentiation genes. On the other hand they stimulated expression of inflammatory cytokines.

- The currently used drug, zoledronic acid, when added to co-cultures, prevented the cancer cells from forming large colonies and from pentrating the osteoid.
- Selenium supplementation of the cultures affected osteoblasts and cancer cells.
- Osteoclasts can be cultured in the bioreactor.

REPORTABLE OUTCOMES

Manuscripts (inclusive for project)

Liu, X., J.Y. Lim, H.J. Donahue, R. Dhurjati, A.M. Mastro, E.A. Vogler. Influence of substratum surface chemistry/energy and topography of the human fetal osteoblastic cell line. 2007. Biomaterials. hFOB1.19: phenotypic and genotypic responses observed in *in vitro*. 28:4535-4550.

Kinder M, E. Chislock, K.M. Bussard, L. Shuman, and A. M. Mastro. Metastatic breast cancer induces an osteoblast inflammatory response. 2008. Experimental Cell Research. 314 173-189.

Dhurjati, R., V. Krishnan, L.A. Shuman, A. M. Mastro, and E.A. Vogler. Metastatic Breast Cancer Cell Colonization Degrades Three-Dimensional Osteoblast Tissue *In Vivo. 2008* Clinical and Experimental Metastasis 25: 741-752. (appendix)

Bussard, K.M.,C. V. Gay, A. M. Mastro. The bone microenvironment in metastasis: what is special about bone? 2008. Cancer Metastasis Reviews. 27:41-55. (appendix)

Mastro, A.M**.**, E. A. Vogler. 2009. A 3D Osteogenic-Tissue Model for the Study of Metastatic Tumor-Cell Interactions with Bone (minireview). Cancer Research, in press. (appended)

Shuman, L.A., V. Krishnan, R. Dhurjati, E.A. Vogler and A.M. Mastro. Metastatic Breast Cancer Cells Colonize and Penetrate Osteoblast Multilayers in a 3-D Culture System. Submitted to Experimental Cell Research.

Krishnan, V, R. Dhurjati, E.A. Vogler and Andrea. M. Mastro. Osteogenesis *In Vitro*: From Pre-Osteoblasts to Osteocytes. (manuscript to be submitted). (appended)

Abstracts/Presentations since last report

Shuman, Laurie A. and Mastro, Andrea M. Mechanisms By Which Metastatic Breast Cancer Cells Initiate an Osteoblast Inflammatory Response, 27th Annual Summer Symposium, Penn State University, University Park, PA June 18 – 21, 2008 *Poster Presentation*

Shuman, L.A., Krishnan, V., Dhjurati, R., Sosnoski, D.M., Vogler, E.A., and A.M. Mastro. A physiologically relevant 3D in vitro tissue culture system for monitoring the interaction of metastatic breast cancer cells with osteoblasts The Annual Meeting of the American Association for Cancer Research , San Diego, CA, April 2008. Proceedings of the 98th Annual Meeting vol 49.

Krishnan, V., Ravi, D., Shuman, L.A., Vogler, E.A., Mastro, A. *In vitro Model of Breast cancer Colonization of Bone.*Talk and Poster presentation at the Joint Mestasis Research Society – American Association for Cancer Research Conference on Metastasis, Vancouver, BC, Canada, August 2008

Krishnan, V, D. Ravi, L.A. Shuman, S.A. Vogler and A.M.Mastro. *In vitro Model of Breast cancer Colonization of Bone*. The McArdle Symposium on Cancer. The Initiation – Promotion Paradigm November 8, 2008. The University of Wisconsin, Madison, Wisconsin.

Shuman, Laurie A. and Mastro, Andrea M. Mechanisms By Which Metastatic Breast Cancer Cells Initiate an Osteoblast Inflammatory Response, 27th Annual Summer Symposium, Penn State University, University Park, PA June 18 – 21, 2008 *Poster Presentation*

Miller, Genevieve. 2008 Penn State McNair Summer Research Conference "Bisphosphonate and taxane effects on osteoblast proliferation and differentiation." July 20, 2008.

Miller, Genevieve. "Bisphosphonate and taxane effects on breast-cancer cell colonization of osteoblast tissue." McNair & Summer Research Opportunities Program (SROP) Alumni Gathering. Penn State, February 26, 2009.

Miller, Genevieve. Becoming an Effective Presenter of Engineering and Science: Guidelines and Video Examples. "The role of the bioreactor in breast cancer research." Leonhard Center for Enhancement of Engineering Education, Penn State,

Mastro, A. M. Bone metastasis. Invited speaker, The International Metastasis Research Society Meeting / AACR Conference "Metastasis to Bone." Vancouver, British Columbia, August 2008.

Applications for Funding based on this work

Miller, Genevieve. 2009 The effect of combination bisphonates and taxane therapy on breast cancer cell colonization of osteoblast tissue. Undergraduate Summer Discovery Grant from Penn State University. Awarded.

Miller, Genevieve. Pennsylvania Space Grant Consortium Sylvia Stein Memorial Scholarship for undergraduates, pending.

Based on our results thus far, the following proposals were submitted. However, none were funded. We are in the process of writing more!

Agency: NASA
Project title: Gravitational Effects on the Osteoblastic Inflammatory Response
Principal Investigator: Erwin Vogler
Co-Investigator: A. Mastro

Agency: NIH
Project title: Growing Osteocytes *in vitro*
Principal Investigator: Erwin Vogler
Co-Investigators: A. Mastro

Agency: NIH
Project title: An *in vitro* model of Cancer in Bone
Principle Investigator: E. Vogler
Co-Investigators: A. Mastro

CONCLUSIONS

A specialized bioreactor has allowed us to grow osteoblasts into a 3D osteoid tissue. Short term growth, up to several months led to multilayers of osteoblasts and an extracellular matrix. Longer term growth, up to 10 months, led to the differentiation of osteocytes. Challenge of the 3-D culture with breast cancer cells created a system that simulated metastatic breast cancer colonization of bone. Within hours the osteoblasts respond with an inflammatory stress response. They also show reduced expression of osteoblast differentiation genes. The cancer cells adhere to the osteoid- like tissue and penetrate the cell layer. The also cause loss of extracellular matrix. Both osteoblasts and cancer cells change to more spindle-shaped cells. The cancer cells line up in a pattern described as “Indian filing.” Attempts to “cure” the cancer containing cultures with the bisphosphonate, zoledronic acid, showed that the addition of this drug after the cancer cells were present for three days, led to smaller cancer colonies and less penetration of the extracellular matrix. Selenium supplementation appeared to affect osteoblast morphology. It did not inhibit cancer cell growth in the bioreactor but the cells did not form colonies.

REFERENCES

1. Bussard, KM. C.V. Gay, A.M. Mastro. The bone microenvironment in metastasis: what is special about bone? Cancer Metastasis Reviews. 2008; 27:41-55.

2. Dhurjati R, Liu X, Gay CV, Mastro AM, Vogler EA. Extended-Term Culture of Bone Cells in a Compartmentalized Bioreactor. Tissue Engineering 2006;12:3045-3054.

3. Kinder, M., E. Chislock, K.M. Bussard, L. Shuman, and Andrea M. Mastro. Metastatic breast cancer induces an osteoblast inflammatory response. Exp, Cell Res. 2008; 314:173-189.

4. Liu, X., J.Y. Lim, H.J. Donahue, R. Dhurjati, A.M. Mastro, E.A. Vogler. Influence of substratum surface chemistry / energy and topography of the human fetal osteoblastic cell line. Biomaterials. hFOB1.19: phenotypic and genotypic responses observed in *in vitro*. 2007;28:4535-4550.

5. Mercer R, Miyasaka C, Mastro A. Metastatic breast cancer cells suppress osteoblast adhesion and differentiation. Clin Exp Metastasis 2004;21:427-35.

6. Mercer R, and Mastro AM. Cytlines secreted by bone-metastatic breast cancer cells alger the expression pattern of f-actin and reduce focal adhesion plaques in osteoblasts through PI3K. Exp. Cell Res. 2005; 310: 270-281.

OTHER REFERENCES CITED

Chaplet, M., C. Detry, et al. (2004). "Zoledronic acid up-regulates bone sialoprotein expression in osteoblastic cells through Rho GTPase inhibition." Biochem J 384(Pt 3): 591-8.

Franz-Odendaal, T. A., B. K. Hall, et al. (2006). "Buried Alive: How Osteoblasts Become Osteocytes." Developmental dynamics 235(1): 176-190.

Green, J. R. (2003). "Antitumor effects of bisphosphonates." Cancer 97(3 Suppl): 840-7.

Mundy, G. (2002). "Metastasis to bone: causes, consequences and therapeutic opportunities." Nat Rev Cancer 2: 584-593.

Pan, B., A. N. Farrugia, et al. (2004). "The nitrogen-containing bisphosphonate, zoledronic acid, influences RANKL expression in human osteoblast-like cells by activating TNF-alpha converting enzyme (TACE)." J Bone Miner Res 19(1): 147-54.

Reinholz, G. G., B. Getz, et al. (2000). "Bisphosphonates directly regulate cell proliferation, differentiation, and gene expression in human osteoblasts." Cancer Res 60(21): 6001-7.

Rogers, M. J., S. Gordon, et al. (2000). "Cellular and molecular mechanisms of action of bisphosphonates." Cancer 88(12 Suppl): 2961-78.

Osteogenesis *In Vitro*: From Pre-Osteoblasts to Osteocytes

A Contribution from the Osteobiology Research Group
The Pennsylvania State University

Venkatesh Krishnan[Φ‡a], Ravi Dhurjati[†a], Erwin A. Vogler[†‡§],
and Andrea M. Mastro[Φ‡*]

Departments of Materials Science and Engineering[†],
Biochemistry and Molecular Biology[Φ],

Materials Research Institute[§] and the Huck Institutes of Life Sciences[‡],
Pennsylvania State University, University Park, PA 16802.

[*] **Author to whom correspondence should be addressed:**

Andrea M. Mastro

431, South Frear

University park, PA-16802

Phone: 814-863-0152, Fax: 814-863-7024

A36@PSU.EDU

[a] Authors contributed equally

Keywords: osteocyte, osteoblast, bone formation, bioreactor,

three-dimensional cell culture model, bone tissue engineering

Abstract

Murine calvariae pre-osteoblasts (MC3T3-E1), grown in a novel bioreactor, proliferate into a mineralizing three-dimensional (3D) osteoblastic tissue that undergoes progressive phenotypic maturation into osteocyte-like cells. This process recapitulates stages of bone development observed *in vivo* in that: (i) both tissue structure and composition undergo continuous maturation with tissue thickness and cell-to-extra-cellular-matrix (ECM) volume ratio decreasing with decreasing cell number; (ii) cell morphology concomitantly evolves from spindle-shaped pre-osteoblasts through cobble-stone shaped osteoblasts to stellate-shaped osteocyte-like cells interconnected by many intercellular processes spanning a range of lengths from short to long and (iii) gene-expression profiles parallel cell morphological changes, up-to-and-including increased expression of osteocyte associated-genes such as E11, DMP1 and sclerostin. X-ray scattering and infrared spectroscopy of contiguous, cm^2-scale macroscopic mineral deposits are consistent with bone hydroxyapatite, showing that bioreactor conditions can lead to ossification reminiscent of bone formation. Thus, extended-term osteoblast culture ($\leq$ 10 months) in a bioreactor based on the concept of simultaneous-growth-and-dialysis, captures the full continuum of bone development otherwise inaccessible with conventional cell culture, resulting in an *in vitro* model of osteogenesis and a source of terminally-differentiated osteocytes that does not require demineralization of fully-formed bone.

Introduction

Diseases of bone such as osteoarthritis, osteomalacia, and osteoporosis negatively affect the quality of life for millions and cause commensurate socioeconomic burden [1,2]. Likewise, cancers in bone are pernicious diseases with characteristically high levels of morbidity and mortality [3-5]. Resolution of these healthcare issues, as well as development of therapeutic approaches to bone restoration [1] depends, in part, on a firm understanding of the cellular-and-molecular basis of osteogenesis.

Osteoblasts, cells of mesenchymal origin, are responsible for bone accretion [6] through a tightly regulated, spatiotemporal sequence [7] that includes proliferation of pre-osteoblasts, differentiation into functional osteoblasts capable of depositing collagenous matrix, and progressive mineralization of that matrix. In the final stage of bone development, mature osteoblasts either undergo apoptosis or terminally differentiate into osteocytes that inhabit lacunar spaces within hard bone [8]. Throughout this sequence, cells maintain extensive intercellular networks through gap junctions (osteoblasts) or intercellular processes (osteocytes) [9]. Thus bone tissue is a functional syncytium that transduces mechanochemical stimuli through dynamic cell-cell contacts [10]. This syncytium is disrupted by bone diseases [11], including metastases of cancers in bone [3], emphasizing the importance of three-dimensional (3D) tissue organization in osteopathologies.

Conventional cell culture has proven to be a valuable tool for studying the physiology of bone-forming cells. In particular, enzymatic isolation of osteoblasts has yielded reproducible and widely-applied methods for studying osteoblast biology *in vitro* [12]. However, osteoblasts grown by conventional-culture methods are limited to a 2D monolayer and do not emulate the 3D network that characterizes bone tissue. Also, conventional culture is not generally suitable

for maintaining cells over the long period required for completion of all stages of bone development. Importantly, the pericellular microenvironment, perturbed by the periodic replacement of the medium, prevents development of chemical gradients (cytokines and other factors) thought to mediate phenotypic development [13]. As a consequence, differentiation of osteoblasts into osteocytes has not been reproduced under *in vitro* conditions conducive to probing with modern genomic and proteomic tools.

We have developed a novel bioreactor [14,15] based on the principle of simultaneous-growth-and-dialysis [16] that permits extended-term, uninterrupted growth of a 3D mineralizing osteoblastic tissue [14]. This system permits phenotypic maturation of pre-osteoblasts into terminally-differentiated osteocytes. Bioreactors have occasionally exhibited mineralization yielding contiguous, cm^2-scale mineral deposits, that prove to be consistent with bone hydroxyapatite. Simultaneous-growth-and-dialysis culture has thus provided unprecedented access to osteocyte biology.

Materials and Methods

Bioreactor: Bioreactors based on the principle of simultaneous-growth and-dialysis [16] were implemented as described previously [3,14,15] (see also S.Figure 1). Briefly, the cell-growth compartment (5 mL) was separated from a 30 mL medium-reservoir by a dialysis membrane. Cells were inoculated into the growth chamber in complete medium including serum. The reservoir was filled with basal medium without serum. Serum constituents or macromolecules synthesized by cells with molecular weights in excess of the dialysis membrane cutoff (6-8 kDa) were retained and concentrated within the growth compartment.

Cells and Cell Culture: Murine calvarial pre-osteoblasts (MC3T3-E1), a gift from Dr. Norman Karin, Pacific Northwest National Laboratories, were inoculated into the growth chamber (10^4 cells/cm^2) and cultured with growth medium [alpha minimum-essential medium (α-MEM) (Mediatech, Herdon, VA), 10% neonatal FBS (Cansera, Roxdale, Ontario), 100 U/ml penicillin 100 μg/ml streptomycin (Sigma Aldrich, St. Louis, MO)]. The reservoir contained the same medium but without serum. Once the cells reached confluence, usually 4-5 days, the medium in the growth chamber was replaced with differentiation medium containing 50 μg/mL ascorbic acid and 10 mM β-glycerophosphate (Sigma Aldrich). Every 30 days the basal medium within the medium reservoir was refreshed. This medium change prevented the build up of metabolic wastes. Bioreactors were maintained at 37°C in a humidified, 5% CO_2 incubator.

Reverse Transcriptase Polymerase Chain Reaction: After indicated times, MC3T3-E1 were harvested and RNA isolated (RNeasy, Qiagen, Valencia, CA). All RNA samples had a A260/280 ratio >1.8. CDNA was generated from 0.5 μg RNA using the SuperScript® VILO™ kit (Invitrogen, Carlsbad, CA). PCR was carried out with a thermo cycler (DeltaCycler 1™ System, Ericomp San Diego, CA) as described previously [3]. The sequences of the primer pairs are available in supplementary table 1. Expression levels for each gene were normalized by determining the ratio of the band volume to that of β-actin.

Confocal Microscopy: The cells were fixed with 2.5% gluteraldehyde in cacodylate buffer and stained with Alexa Fluor 568 phalloidin according to the manufacturer's instructions (Molecular Probes, Invitrogen). *In situ* laser-scanning was performed using an Olympus FV-300 laser scanning microscope (Olympus America Inc., Center Valley, PA) [3].

Fourier Transform Infrared Spectroscopy (FTIR) and X-ray Analyses: A bone chip from the bioreactor or from bovine bone, was placed in a stainless steel vial along with a large ball bearing, and then put in a Wig-L-Bug vibrating mill. The bone was ground for 30 seconds. A small amount of oven dried KBr powder (International Crystal Laboratories, Garfield, NJ) was added, the ball bearing removed, and the materials mixed for 30 seconds. A translucent 7mm pellet was pressed (Quick-Press) and analyzed in transmission mode using a FTIR spectrometer (Bruker IFS 66/s, Bruker Optics, Billerica, MA). Other bone chips were dried with hexamethyldisilazane (HDMS)and ground in a ball mill into a powder. The X-ray diffraction pattern of the powder was collected using a Phillips MPD theta-2-theta powder diffractometer (PANalytical Inc., Westborough, MA), and compared to that of authentic bone.

Scanning (SEM) and Transmission Electron Microscopy (TEM): Tissue from the bioreactor was fixed overnight with 2.5% glutaraldehyde in 0.1M sodium cacodylate buffer at 4^{o}C and processed for TEM as described previously [4]. For SEM the tissues were further incubated with 1% osmium tetroxide in cacodylate [4].

Results

Osteoblastic Tissue Growth and Maturation Under Continuous Long-term Culture: MC3T3E-1, developed into 3D tissue about 22 μm thick within 15 days (Figure 1, Panels A, B), comprised of 6-8 layers (Panel C, D) of actively-mineralizing (positive for alkaline phosphatase activity and for mineralization by von Kossa stain), differentiated osteoblasts [3,14]. TEM showed that this tissue was densely packed with close cell contacts (Panels C, D). Continuous culture reproducibly resulted in transformation of spindle-shaped pre-osteoblasts into cobble-

stone shaped osteoblasts that secreted and mineralized an extensive, collagenous extracellular matrix that completely enveloped the cells [3,14].

Quantitative evaluation of ~30-50 histological and ultra-structural sections taken from bioreactor cultures at different times (Figure 2) revealed continuous transformation of tissue. Initially the cells were closely packed (high cell/matrix ratio) but transformed into a more mature phenotype (low cell/matrix) after about 5 months. Confocal microscopy (Figures 3A-D) further revealed that this transformation was associated with a progression in cell morphology from cuboidal to stellate with many intercellular contacts (indicated by arrows).

SEM images of a bioreactor after 10 months of continuous culture (Figure 4A,B) showed that tissue was about 50 μm thick and was comprised of stellate cells interconnected with many processes with different lengths ranging from about one cell diameter ("short") to many cell lengths ("long"). Examination of many TEM images (e.g. Figure 4D) revealed that intercellular connections terminated in over-lapping protrusions (see arrows). From these images and molecular biology (Table 1), we concluded that the entire tissue was comprised of osteocytic cells. We counted 36 osteocytes in a 4 μm^2 confocal-images field (Figure 4C), suggesting that there were about $9X10^4$ osteocytes/cm^2. This value further translated into 2 million osteocytes/bioreactor; assuming that the 27 μm tissue shown was uniform across the entire 25 cm^2 growth space (see Figure 5, panel D). We further estimated that there were about $3.4X10^4$ osteocytes/mm^3, which compared favorably with $1.3X10^4$ osteocytes/mm^3 measurements on human bone [17,18].

Gene expression. The phenotypic progression suggested by cell morphology was reflected in the characteristic expression of genes such as Type I collagen, osteonectin, osteocalcin and

osteopontin (Table 1) [7]. Up-regulation of matrix-metallo proteinase (MMP)-13 (indicative of extracellular matrix remodeling) and the proteins E11, DMP-1, and sclerostin, indicative of osteocytic transformation, [19] occurred in more mature cultures. In spite of the fact that there were numerous viable cells within the bioreactor after 10 months, RNA recovery was lower than that of younger bioreactors (Table 1), consistent with fewer cells and perhaps related to the relatively low metabolic activity attributed to osteocytes (see Discussion).

Formation of Macroscopic Bone: After about 2 months of continuous culture, bioreactors occasionally exhibited contiguous, cm^2-scale macroscopic mineral deposits on the growth-chamber side of the dialysis membrane (see S.Figure 1). Dialysis membranes from bioreactors without visually-apparent mineral were found by FTIR spectroscopy to produce weak signals consistent with hydroxyapatite (data not shown), suggesting that osteoblasts may have passed too quickly through the mineral-deposition phase to produce visually-apparent aggregates. Too few bioreactors have been studied to date to discover the exact conditions that led to bioreactor ossification, but there was no doubt that unknown experimental factors (e.g. inoculum concentration, precise timing of media replacement, *etc*.) occasionally led to deposition of macroscopic bone-like mineral. This material did not appear in bioreactors kept with differentiation medium alone in the absence of cells. X-ray diffraction of a mineral “chip” (Figure 5A) also was consistent with bovine bone (see inset of Figure 5A). SEM of the chip revealed that the deposit was comprised of many nodules (Figure 5B), consistent with a nucleation-and-growth deposition phenomenon. Comparison of FTIR spectra of chips recovered from 5 and 10 month bioreactors suggested an evolution of chemical composition with deposition time (Figure 5C).

Discussion

Osteoblastic Tissue Growth and Phenotypic Maturation Under Continuous Long-term Culture: Cell and tissue morphological evidence (Figures 1-4) combined with gene expression data (Table 1) has led us to conclude that growth and maturation of MC3T3-E1 derived osteoblastic tissue over 10 months of continuous culture in the bioreactor recapitulated the normal sequence of bone deposition characterized by stages of proliferation, matrix maturation, mineralization, and terminal differentiation into osteocytes [7]. In particular, the tissue progressed through these stages (Figure 2) showing no apparent signs of necrosis. In fact, microscopy revealed that tissue recovered from 10 month bioreactors was quite similar to 5 month tissue (not shown), suggesting that viability through the phenotypic-transition stage (Figure 2) was nearly constant. We therefore speculate that osteoblastic tissue can be sustained indefinitely within the bioreactor with only occasional refreshment of basal media in the reservoir, but we have not yet experimentally examined cultures longer than 10 months. Gene expression was likewise consistent with phenotypic maturation into osteocytes indicated by the expression E-11, DMP-1 and sclerostin.

Osteocytes developed to densities similar to that seen in calvarial bone [18]. If this osteocytic tissue has an architecture similar to authentic bone, (Figure 4A) then at least calvarial osteocytes are quite closely packed in bone in a way that is different from osteocytes in shafts of long bone where they are separated by several cell diameters interconnected by long processes [20]. Textbook images convey the idea that osteocytes are rather sparse in bone. Neither our data nor measurements of osteocyte density in authentic bone [17,18] support such a perspective for calvaria-derived bone. Since carrying out this work, we became aware of a paper by Murshid *et al* [21] comparing primary chicken osteoblasts to MC3T3-E1 grown in a 3D matrigel matrix.

The cells that grew in both cultures were similar but not identical. This group did not assay for osteocyte proteins, i.e. sclerostin, DMP-1 or E-11, so we cannot compare our work directly with theirs.

Formation of Macroscopic Bone: Deposition of contiguous, cm^2-scale macroscopic mineral is, to our knowledge, unprecedented in the culture of bone cells *in vitro*. Failure to routinely reproduce bioreactor ossification suggests uncontrolled variable(s) in the culture, that once discovered, may help understand critical variables involved in bone restoration after trauma or disease. We were struck by the observation that this cell-mediated mineral deposition formed on the cell side of the dialysis membrane (see S. Figure 1). Osteoblasts exocytose vesicles containing enzymes responsible for mineral formation [22] which were observed in TEM sections of osteoblastic tissues (e.g. Figure 1C). Presumably, these secreted enzymes caused nucleation of mineral nodules on the dialysis membrane that aggregated into a contiguous layer with time. This mineral deposit had the X-ray and FITR characteristics of bone and did not appear to be due to the microcrystalline apatite deposition described by Cisar et al. [23]. Clearly, more research is required to fully trace steps involved in formation of macroscopic mineral deposits by osteoblasts in the environment of the bioreactor.

Implications for Osteobiology: We suggest that the ability to monitor and control the maturation of osteoblastic tissue *in vitro* is useful to the study of osteogenesis and osteopathologies. Foremost is the ability to create readily-accessible osteocytes that are otherwise accessible only by extraction from bone using rigorous extraction protocols [12]. Growth of osteocytes from isolated pre-osteoblasts offers the distinct advantage that

demineralization is not required. Furthermore in the bioreactor, cells can be directly observed by microscopy. Moreover, the conditions of culture can be controlled and modified to better understand the process of osteogenesis. We have already used the bone model to study the affect of metastatic breast cancer known to invade skeleton on osteoblastic tissue [19]. We directly observed cancer cell adhesion, penetration, colony formation, and osteoblast reorganization heretofore only inferred in 2D culture models. This result encourages use of 3D tissue models in the study of other pathologies, such as osteoarthritis, osteomalacia, and osteoporosis.

The bioreactor employed in this work is probably only one of many that can produce bone tissue with varying phenotype ranging from pre-osetoblast to terminally-differentiated osteocytes. However, a critical attribute of this method is creation of a pericellular microenvironment that mimics growing bone. The simultaneous-growth-and-dialysis method is crucial in this regard because it allows concentration gradients to form that guide cell maturation.

Acknowledgments: Supported by U.S. Army Medical and Material Command Breast Cancer Program WX81XWH-06-1-0432, Susan G. Komen for the Cure BCTR 0601044, with additional support from the National Foundation for Cancer Research. Authors appreciate the expert technical assistance of Ms. Donna Sosnoski and the Cytometry and the Electron Microscopy Facilities at Penn State. We thank Dr. Carol Gay for her thoughtful discussions and critique.

Reference:

1. Rodan, G.A., Martin, T.J. 2000. Therapeutic Approaches to Bone Diseases. Science 289: 1508-1514.

2. Service, R.F. 2000. Tissue Engineers Build New Bone. Science 289: 1498-1500.

3. Dhurjati, R., Krishnan, V., Shuman, L.A., Mastro, A.M., Vogler, E.A. 2008. Metastatic breast cancer cells colonize and degrade three-dimensional osteoblastic tissue in vitro. Clin Exp Metastasis 25: 753-763.

4. Rubens, R.D. 1998. Bone metastases—The clinical problem. European Journal of Cancer 34: 210-213.

5. Rubens, R.D., Mundy, G.R. 2000. Cancer and the Skeleton. Informa Health Care. 286. p

6. Ducy, P., Schinke, T., Karsenty, G. 2000. The Osteoblast: A Sophisticated Fibroblast under Central Surveillance. Science 289: 1501-1504.

7. Lian, J.B., Stein, G.S. 1992. Concepts of osteoblast growth and differentiation: basis for modulation of bone cell development and tissue formation. Crit Rev Oral Biol Med 3: 269-305.

8. Knothe Tate, M.L., Adamson, J.R., Tami, A.E., Bauer, T.W. 2004. The osteocyte. The International Journal of Biochemistry & Cell Biology 36: 1-8.

9. Doty, S.B. 1981. Morphological evidence of gap junctions between bone cells. Calcif Tissue Int 33: 509-512.

10. Palumbo, C., Palazzini, S., Marotti, G. 1990. Morphological study of intercellular junctions during osteocyte differentiation. Bone 11: 401-406.

11. Knothe Tate, M.L., Tami, A., Bauer, T.W., Knothe, U. 2002. Micropathoanatomy of ostoeporosis-indications for a cellular basis for bone disease. Advances in Osteoporotic Fracture Management 2: 9-14.

12. Nijweide, P.J., Burger, E.H. 1990. Mechanisms of Bone Formation In Vitro. In, Bone : The Osteoblast and Osteocyte. Caldwell: The Teleford Press.

13. Chaudhuri, J., Al-Rubeai, M. 2005. Bioreactors for Tissue Engineering: Principles, Design And Operation. Springer. 375. p

14. Dhurjati, R., Liu, X., Gay, C.V., Mastro, A.M., Vogler, E.A. 2006. Extended-term culture of bone cells in a compartmentalized bioreactor. Tissue Engineering 12: 3045-3054.

15. Vogler, E.A. 1989. A compartmentalized device for the culture of animal cells. J. Biomaterials, Artificial Cells, and Artificial Organs 17: 597-610.

16. Rose, G.G. 1966. Cytopathophysiology of Tissue Cultures Growing Under Cellophane Membranes. In, Int. Rev. Exp. Pathology, pp. 111-178.

17. Mullender, M.G., van der Meer, D.D., Huiskes, R., Lips, P. 1996. Osteocyte density changes in aging and osteoporosis. Bone 18: 109-113.

18. Sugawara, Y., Kamioka, H., Honjo, T., Tezuka, K., Takano-Yamamoto, T. 2005. Three-dimensional reconstruction of chick calvarial osteocytes and their cell processes using confocal microscopy. Bone 36: 877-883.

19. Franz-Odendaal, T.A., Hall, B.K., Witten, P.E. 2006. Buried Alive: How Osteoblasts Become Osteocytes. Developmental dynamics 235: 176-190.

20. Eriksen, E.F., Eghbali-Fatourechi, G.Z., Khosla, S. 2007. Remodeling and vascular spaces in bone. J Bone Miner Res 22: 1-6.

21. Murshid, S.A., Kamioka, H., Ishihara, Y., Ando, R., Sugawara, Y., Takano-Yamamoto, T. 2007. Actin and microtubule cytoskeletons of the processes of 3D-cultured MC3T3-E1 cells and osteocytes. J Bone Miner Metab 25: 151-158.

22. Anderson, H.C., Garimella, R., Tague, S.E. 2005. The role of matrix vesicles in growth plate development and biomineralization. Front Biosci 10: 822-837.

23. Cisar, J.O., Xu, D.Q., Thompson, J., Swaim, W., Hu, L., Kopecko, D.J. 2000. An alternative interpretation of nanobacteria-induced biomineralization. Proceedings of the National Academy of Sciences 97: 11511-11515.

Table 1: Temporal gene expression of differentiation markers in MC3T3-E1 cultured in the bioreactor

Markers	Months in Culture			
	0.7	1	2	10
Osteocalcin	0.54[a]	0.14	0.55	0.015
Osteonectin	0.53	0.53	0.34	0.19
Osteopontin	0.21	0.054	0.51	0.11
Type I Collagen	1.49	1.36	1.21	0.76
MMP13	0.11	0.23	1.46	na
E-11	1.15	0.93	1.01	0.78
DMP-1	0.09	0.04	0.63	0.06
Sclerostin	nd	nd	*	*
Yield of RNA	1100 ng/uL	160 ng/uL	180 ng/uL	12 ng/uL

MC3T3-E1 cells were cultured in the bioreactor for various intervals (22, 30, 60 days, 10 months). Cells were harvested and RNA isolated (RNeasy, Qiagen, Valencia, CA) as described in the methods section. PCR was carried out on a thermocycler (DeltaCycler 1™ System. Ericomp San Diego, CA). PCR reactions were run on a 2% agarose gel, stained with ethidium bromide and imaged under UV illumination. Gel documentation was performed on the Kodak Gel Logic 100 Imaging System (Eastman Kodak, Rochester, NY) and band volume quantitation was done by ImageQuant software (Molecular Dynamics, Sunnyvale, CA). [a]- Shown are expression levels of each gene normalized by determining the ratio of the band volume for each message relative to the band volume for β-actin for the same cDNA. nd- Not Detected, n=2, na- Not Assayed, *- Detected at faint levels that could not be quantified.

List of Figure Legends

Figure 1: MC3T3E-1 pre-osteoblasts grown for 15 days within the bioreactor. Panels A, B: SEM images of a dense 3D tissue about 22 μm thick. Panels C, D: Cross-sectional TEM images showing 6-8 layers of actively-mineralizing and densely packed cells with close cell contacts (Nu = nucleus, rER = rough endoplasmic reticulum).

Figure 2: Phenotypic maturation of MC3T3E-1 within the bioreactor over 10 months continuous culture. An exponential-like decrease in the number of cell layers with time (left-hand axis) translated into a linear-like decrease in cell-layer/tissue-thickness ratio (right-hand axis). This finding was consistent with the process of bone maturation that resulted in transformation of proliferating pre-osteoblasts into non-dividing osteoblasts that become engulfed in mineralized matrix and mature into osteocytes [20]. Data within grey box was previously reported in [3].

Figure 3: Progression in cell morphology monitored by confocal microscopy of Alexa Fluor 568 phalloidin stained MC3T3E-1 within the bioreactor over 10 months of culture (compare with Fig. 2). Panel A: “cobble-stone” shaped osteoblast-like cells matured from fibroblastic pre-osteoblasts within 3 weeks. Panel B: elongated cells appeared with development of many cellular processes within 1.2 months. Panel C: density of cells enmeshed in a dense collagenous matrix (appears black, and see Figures 4 and 8 in [14]) decreased over 2 months. Panel D: 1-2 layers of stellate cells with many intercellular contacts after 2-10 months of continuous culture. Scale bar represents 50μm.

Figure 4: Osteocyte-like cells mature within the bioreactor over 10 months continuous culture. Panels A, B: SEM image of ~23 μm thick tissue showing closely packed stellate cells interconnected with many cellular processes. Panel C: confocal image of Alexa Fluor 568 phalloidin stained osteocytes showing 1- 2 cell layers with many intercellular processes. Panel D: high-magnification TEM image of overlapping cell protrusions (arrows) typical of osteocytes.

Figure 5: Macroscopic mineral deposits on the growth-chamber side of the bioreactor dialysis membrane. Mineral chip taken from a 10 month bioreactor dialysis membrane were prepared for X-ray diffraction or FTIR spectral analyses as described in the method. Panle A: The X-ray diffraction pattern was similar to bovine bone (inset). Panel B: Reveals that the chip was comprised of close-packed spherical nodules. Panel C compares FTIR spectra of chips recovered from 5 and 10 month bioreactors showing changes in chemical composition with deposition time.

Supplementary Figure 1: Compartmentalized bioreactor design. Panel (a) is a cross-section diagram showing separation of the cell-growth space (A) from the basal-medium reservoir (B) by a dialysis membrane (C). Cells are grown on gas-permeable but liquid-impermeable film (E). The device is ventilated through film (D), which is the same material as (E). The whole device is brought together in a liquid-tight fashion using screws Panel (b) and Panel (c), which is an exploded-view identifying separate components. Liquid-access is through leur-taper ports (J, K), which mate to standard pipettes. Reproduced from [14] with permission.

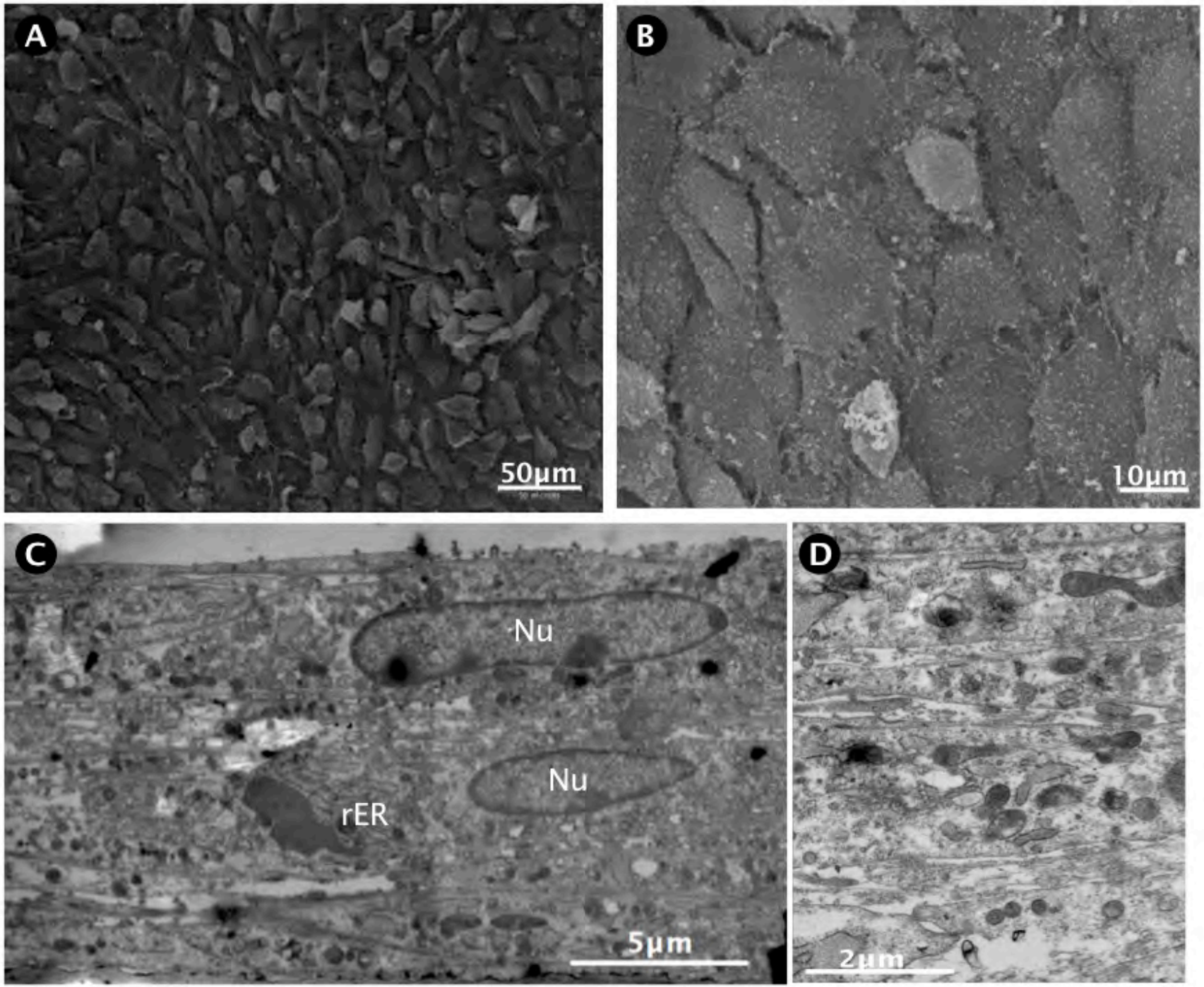
A
50µm
B
10µm
C
Nu
Nu
rER
5µm
D
2µm

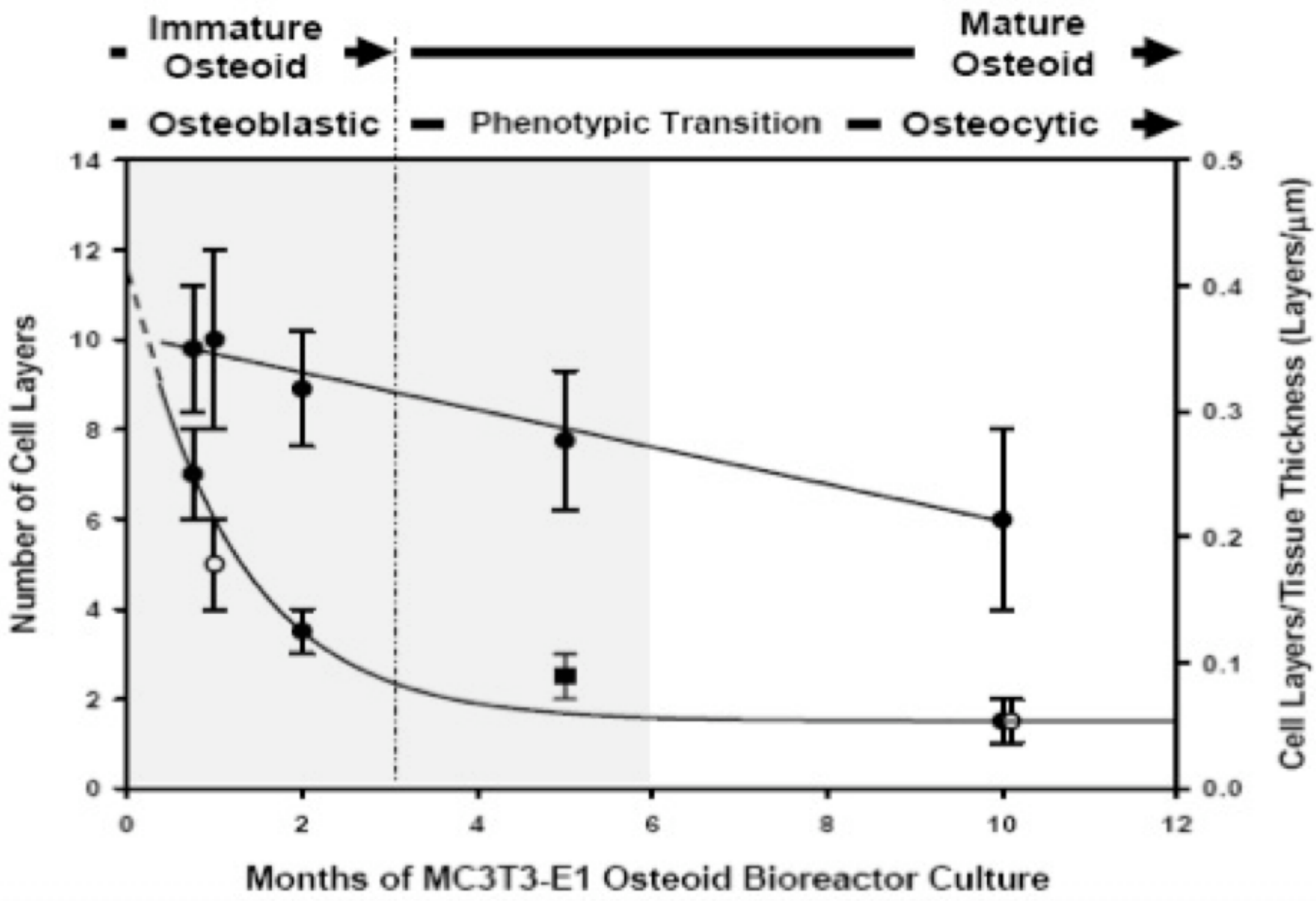
Immature Osteoid
Mature Osteoid
Osteoblastic
Phenotypic Transition
Osteocytic
Number of Cell Layers
Cell Layers/Tissue Thickness (Layers/μm)
Months of MC3T3-E1 Osteoid Bioreactor Culture
0
2
4
6
8
10
12
14
0.0
0.1
0.2
0.3
0.4
0.5

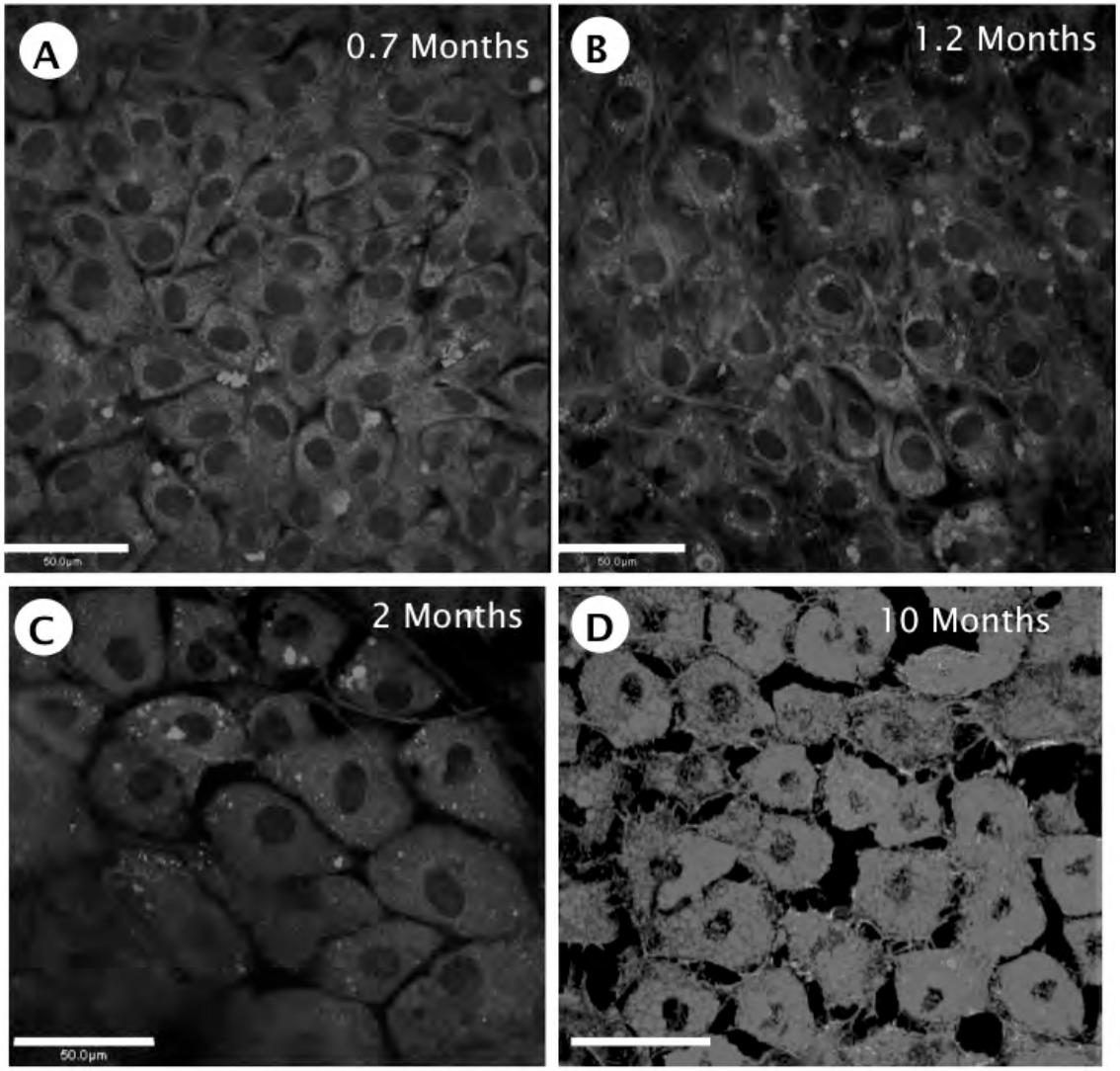
A
0.7 Months
50.0µm
B
1.2 Months
50.0µm
C
2 Months
50.0µm
D
10 Months

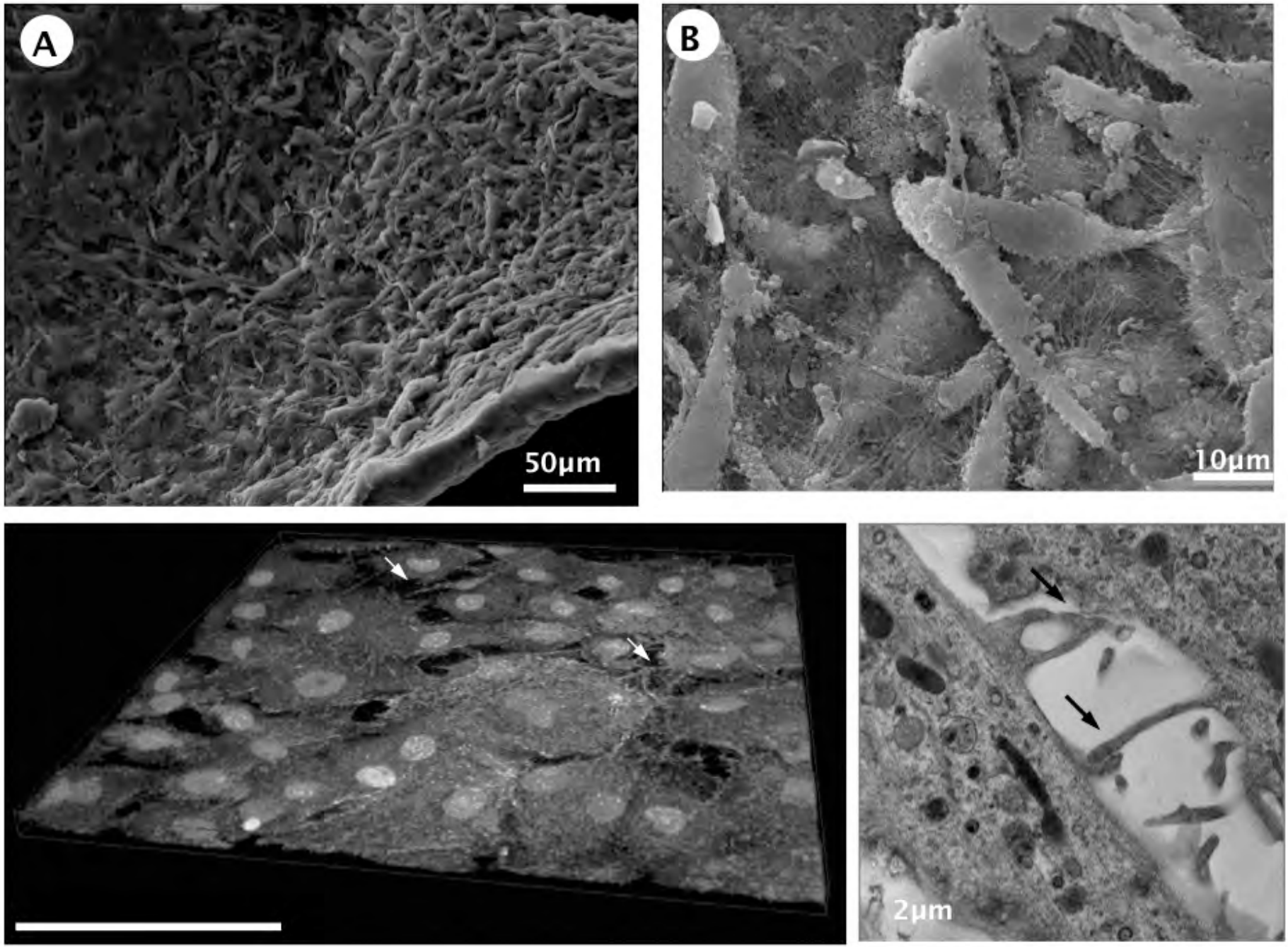
A
50µm
B
10µm
2µm

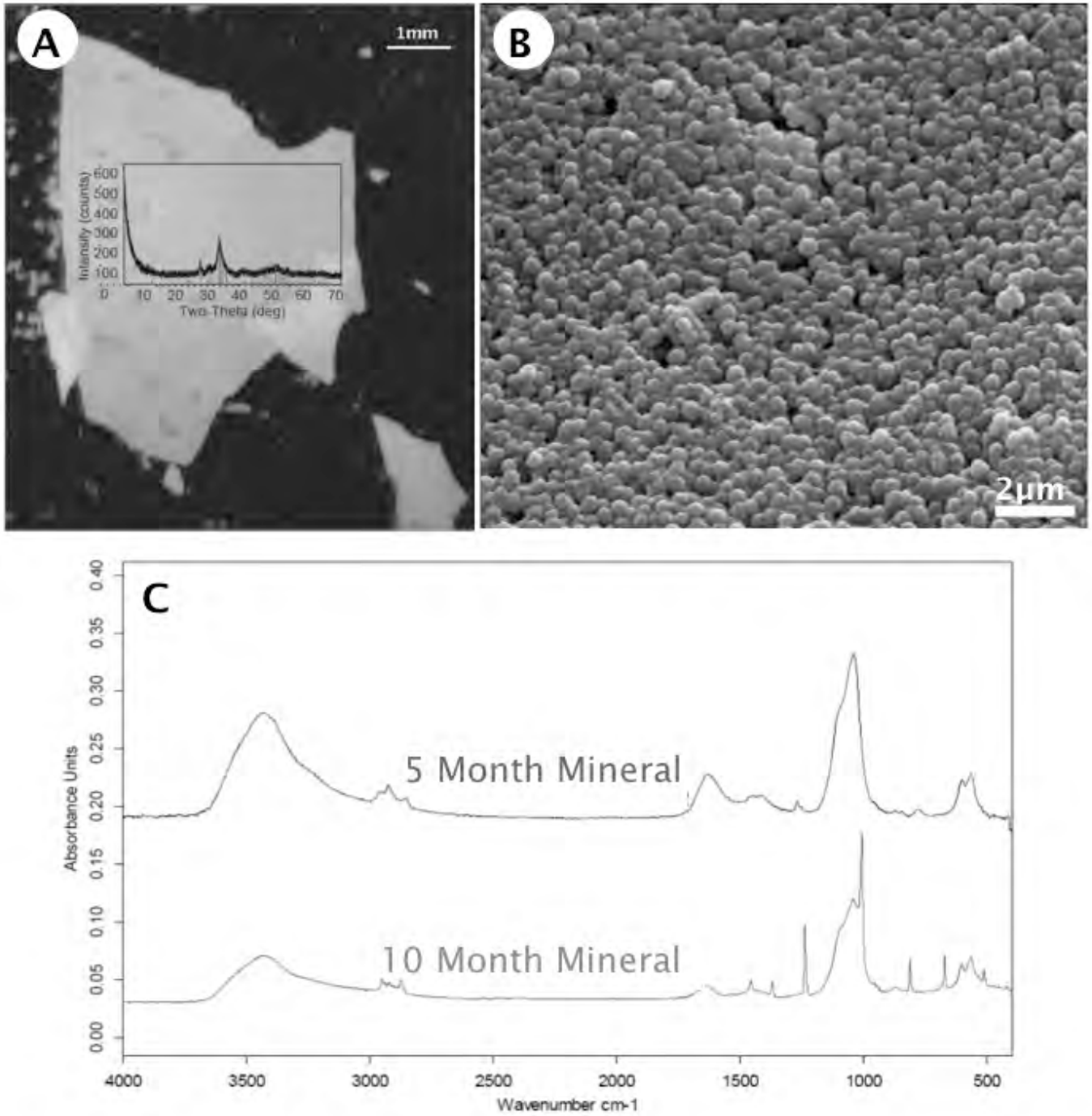
A
1mm
Intensity (counts)
600
500
400
300
200
100
0
10 20 30 40 50 60 70
Two-Theta (deg)
B
2µm
C
Absorbance Units
0.00 0.05 0.10 0.15 0.20 0.25 0.30 0.35 0.40
5 Month Mineral
10 Month Mineral
4000 3500 3000 2500 2000 1500 1000 500
Wavenumber cm-1

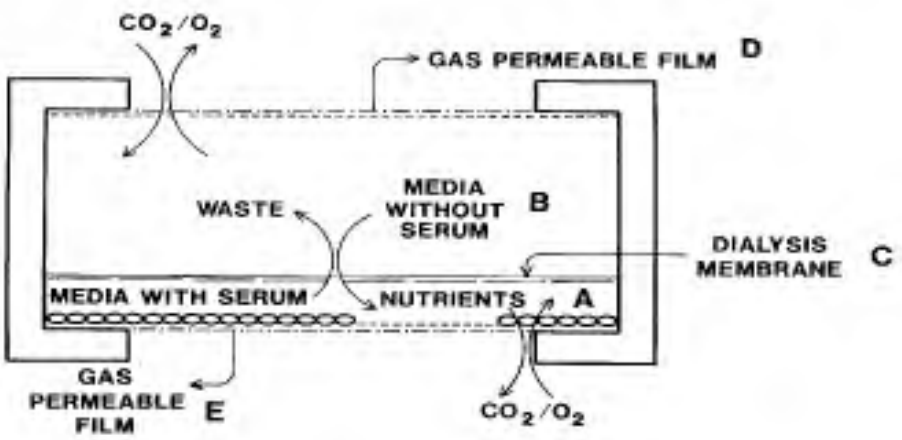
a
CO_2/O_2
GAS PERMEABLE FILM
D
MEDIA WITHOUT SERUM
B
WASTE
DIALYSIS MEMBRANE
C
MEDIA WITH SERUM
NUTRIENTS
A
GAS PERMEABLE FILM
E
CO_2/O_2

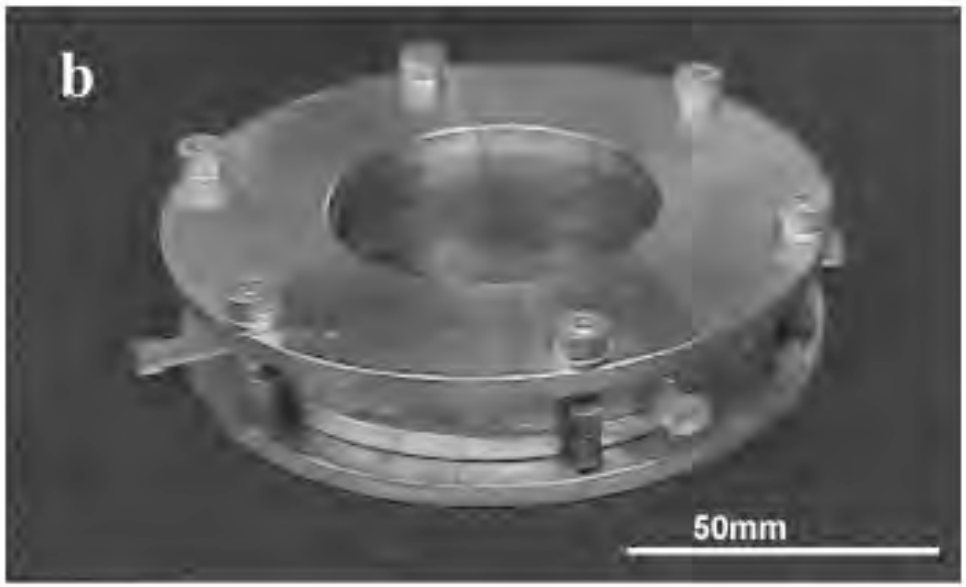
b
50mm

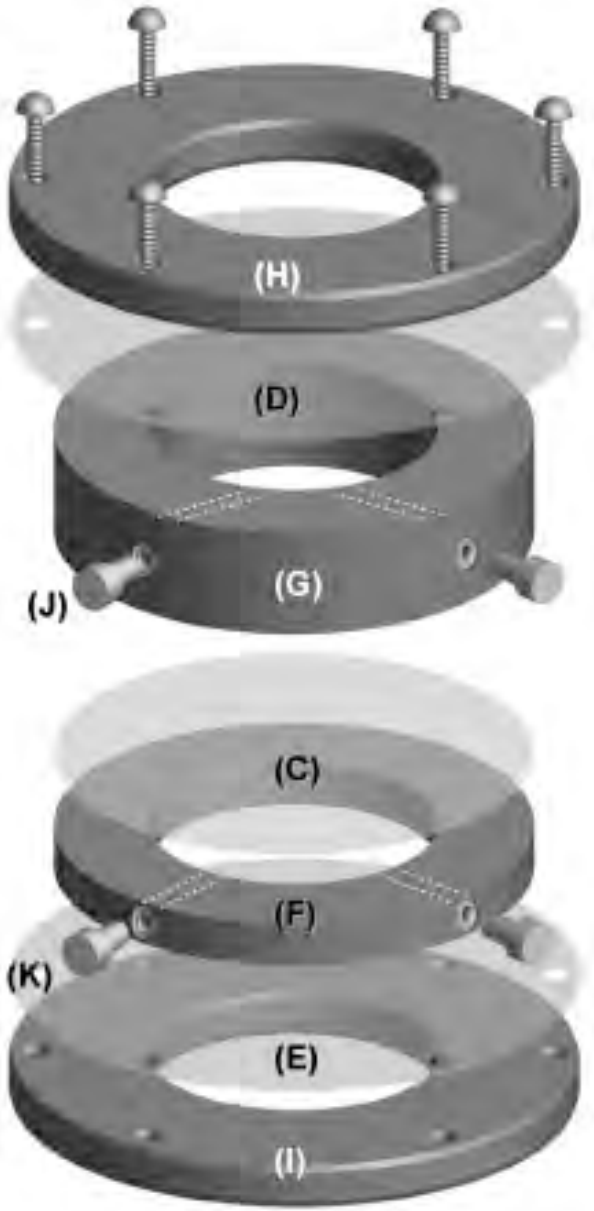
c
(H)
(D)
(G)
(J)
(C)
(F)
(K)
(E)
(I)

A 3D Osteogenic-Tissue Model for the Study of Metastatic Tumor-Cell Interactions with Bone

A Contribution from the Osteobiology Research Group
The Pennsylvania State University

Andrea M. Mastro[Φ‡*] and Erwin A. Vogler[†‡§]

Departments of Materials Science and Engineering[†],
Biochemistry and Molecular Biology,

Materials Research Institute[§] and the Huck Institutes of Life Sciences[‡],
Pennsylvania State University, University Park, PA 16802.

* Author to whom correspondence should be addressed

Andrea M. Mastro

a36@psu.edu

431 S. Frear Laboratory
University Park PA 16803
USA

Phone: 814-863-0152
Fax: 814-863-7024

Running title: 3D Model of Breast Cancer Colonization of Bone

Keywords: 3D model, bone, breast cancer, metastasis, osteoblasts

Abstract

A specialized bioreactor based on the principle of simultaneous-growth-and-dialysis permits growth of three-dimensional (3D), multiple-cell-layer osteogenic tissue from isolated osteoblasts over long, continuous-culture intervals (tested up to 10 months with no sign of necrosis). The resulting tissue recapitulates the stages of bone development observed *in vivo*, including phenotypic maturation of cobble-stone-shaped osteoblasts into stellate-shaped osteocytes interconnected by many intercellular processes. Gene-expression profiles parallel cell-morphological changes with time, ultimately leading to increased expression of osteocyte-associated molecules such as E11, DMP1 and sclerostin. Contiguous, cm^2-scale macroscopic mineral deposits that form within the bioreactor are consistent with bone hydroxyapatite. The simple-to-use bioreactor system provides an *in vitro* model that permits the study and manipulation of cancer-cell interactions with bone tissue in real time. Metastatic human-breast-cancer cells, MDA-MB-231^{GFP} introduced into the model grow and colonize osteoblastic tissue in a manner reflecting various characteristics of pathological tissue observed in the clinic. Specifically, MDA-MB-231 cells are observed to penetrate the thick extracellular matrix in which osteoblasts are embedded and to form chains reminiscent of “Indian files” described for infiltrating lobular or metaplastic breast carcinomas. Osteoblasts appear to be marshaled into a parallel alignment with cancer cells followed by erosion of extracellular matrix structural integrity. Tissue degradation appears to be accompanied by increased expression of osteoblast inflammatory cytokines.

The skeleton is a favored site for the metastatic spread of breast, prostate, lung, and multiple myeloma cancers (1). Metastasis to the bone often progresses with significant morbidity related to substantial bone loss (osteolytic cancers) or gain (blastic cancers), bone pain, hypercalcemia, pathological fractures, and spinal cord compression (2). Bone metastasis is particularly pernicious because early-stage detection is obscured by the refractory nature of bone; once bone colonization occurs, the cure rate drops precipitously (1-3). Inaccessibility also hampers a full understanding of the cellular-and-molecular mechanisms underlying cancer colonization of bone, thereby slowing drug development. Whole-animal models are thus too complex for detailed mechanistic studies and, although excised tissue faithfully captures end stages of bone metastasis associated with fully-developed tumors, the critical initial stages of disease remain substantially obscured in this surrogate (4, 5). Standard monolayer cell culture sharply reduces complexity and permits direct access to bone cells but, in so doing, loses biological relevance of a fully-developed tissue architecture. For these reasons, as well as for reducing the use of animals for research, three-dimensional (3D) tissue models have become a focus of recent investigation (6, 7) and a challenging target for tissue engineering (8).

Effective *in vitro* bone models must strike a difficult balance between experimental efficiency and retention of biological complexity. For example, the metaphysis region of long bone, where cancer cells are known to traffic early in the metastasis process (9), is chiefly comprised of cancellous bone in the form of thin trabeculae intertwined with blood vessels, connective tissue, and hematopoietic cells of the bone marrow. Trabeculae, in turn, are comprised of a calcified collagenous matrix populated and lined by osteoblasts that are responsible for bone accretion, interacting with osteoclasts that are responsible for bone resorption. A minimal model of bone accretion consisting of only osteoblasts must simulate the microenvironment wherein spatially-and-temporally sequenced secretion of growth factors and cytokines associated with bone development can occur (10) over long periods measured in months. Generally speaking,

neither conventional cell culture nor advanced-bioreactor systems that rely on scheduled-or-continuous culture refeeding can reproduce this microenvironment because removal of spent growth medium also eliminates, or significantly perturbs, pericellular-concentration gradients.

We have adapted a specific type of bioreactor (11) based on the principle of simultaneous-growth-and-dialysis first pioneered by G. G. Rose (12) for the purpose of developing an *in vitro* model of bone with systematically-increasing biological complexity (6, 13). The core idea behind this compartmentalized bioreactor is to continuously feed cells with low-molecular-weight nutrients by dialysis through a cellulose membrane that also retains cell-secreted macromolecules within a cell-growth compartment bounded by this membrane. In this way, metabolic-waste products such as lactic acid continuously dialyze out of the cell-growth compartment and into a basal-medium compartment for eventual removal and replacement with fresh growth medium. Growth-and-feeding functions are thus separated (compartmentalized) and the pericellular space is not perturbed by wholesale growth-medium removal. The result is an extraordinarily-stable culture environment wherein concentration gradients can develop.

Using this method of culture, we have grown multiple-cell-layer osteogenic tissue from two lines of osteoblasts; human fetal hFOB1.19 (ATCC CRL-11372) and mouse calvaria MC3T3-E1 (ATCC CRL-2593) (13). Focusing on MC3T3E-1 derived tissue, we have observed *in vitro* the progression of osteoblast development as it occurs in natural bone; *i.e*. from proliferation and differentiation to engulfment of osteoblasts in a thick cell-secreted mineralized matrix, followed by subsequent phenotypic maturation into a network of osteocytes with distinctive stellate shape (Figure 1, panels A, B). In some cultures, contiguous, cm^2-scale macroscopic mineral deposits were formed that proved consistent with bone hydroxyapatite by X-ray scattering and infrared spectroscopy. In addition, the gene expression profiles of characteristic osteoblast proteins such as Type 1 collagen, alkaline phosphatase, osteonectin, osteopontin and osteocalcin,

mirrored that observed *in vivo*. After several months the cultures also expressed molecules indicative of osteocytes, *i.e.* E11, DMP1, and sclerostin. RNA recovery from these mature cultures was low compared to less-mature bioreactors, consistent with decreased cell density (due to apoptosis) and the reduced metabolic activity attributed to osteocytes. To our knowledge, these are the first *in vitro* observations of massive osteoblast-mediated ossification and phenotypic transformation into osteocytes reported in the literature. The compartmentalized bioreactor thus presents itself as an *in vitro* model for studies of bone biology and pathology.

The bioreactor is amenable to real-time live-cell analysis by fluorescence confocal microscopy. We have labeled osteoblasts with Cell Tracker Orange ™, for example, and followed cell morphology over time. At the end of the culture period, the tissue can be fixed and the cells stained for alkaline phosphatase or with phalloidin and/or labeled with other fluorescent molecule probes (Figure 1). Tissue can be further processed using conventional histological methods including conventional light-and-electron microscopies (13). We have combined fluorescence with TEM by using fluorescent, electron-dense Quantum Dots ™ (In Vitrogen-Molecular Probes). Following protocol similar to that discussed below, we introduced MDA-MB-231 metastatic cancer cells which had internalized Q Tracker 655 dots (10nm nominal diameter with cadmium cores) into osteoblast cultures and followed cancer-cell/osteoblast interactions by confocal microscopy before processing the tissue for TEM. The electron-dense dots were observed to collect within perinuclear vacuoles only in the cancer cells and did not transfer to the osteoblasts. In this way we were able to distinguish cancer cells from osteoblasts and study cell-cell interactions at the TEM level. Finally, all-or-part of the culture can be released from the membrane for RNA isolation suitable for gene expression by PCR or lysed for protein expression by western blotting.

Introduction of MDA-MB-231^{GFP} human metastatic breast cancer cells (genetically engineered to produce green-fluorescent protein, GFP, and known to invade the murine skeleton (14)) onto MC3T3-E1 osteoblastic tissue grown in the compartmentalized bioreactor to various stages of phenotypic maturity allowed us to follow early stages of cancer-cell colonization in real time by confocal microscopy (Figure 1, panels C-E). In this way, we observed cancer cell/osteoblast-tissue adhesion, cancer-cell proliferation, tissue penetration, formation of non-vascularized micro-tumors, and ultimate degradation of osteoblast-derived extracellular matrix (ECM). Cancer cells proliferated and formed into columns of cells that penetrated the collagenous tissue matrix, organizing into rows similar to the "Indian files" described for infiltrating lobular or metaplastic breast carcinomas (Figure 1, panels E,F) (15). Migration of cancer cells along tracks of remodeled ECM produced by preceding invading cell(s) apparently results in characteristic cell-alignment patterns (16). Invasion by chains of tumor cells linked together by cell-cell contacts is considered to be an effective penetration mechanism (17), conferring high metastatic capacity and commensurately poor prognosis (15, 16). Observation of filing in the osteoblastic-tissue model suggests a considerable degree of physiological relevance. Indian filing is common in soft tissue but also found in bone metastasis (Figure 1, panels G,H,I).

We also observed an increased expression of inflammatory cytokines such as IL-6 in the presence of the breast cancer cells, as well as a decrease in secretion of soluble (newly formed) collagen and osteocalcin (a marker of osteoblast maturity) (6). A strong osteoblastic stress response and decrease in collagen production correlated with loss of ECM integrity seen after seven days of co-culture with MDA-MB-231^{GFP}. These results parallel previous studies in conventional culture showing that exposure of osteoblasts to MDA-MB-231^{GFP} conditioned medium produced an osteoblastic inflammatory stress response with sharply increased expression of the inflammatory cytokines, IL-6, IL-8 and MCP-1 (18). These cytokines are known to attract and activate osteoclasts, and are likely to contribute to the tumor-host

microenvironment *in vivo*. In particular, IL-6 a pleiotropic cytokine, has been implicated in the pathogenesis of osteolysis associated with Paget's disease, Gorham-Stout syndrome, and multiple myeloma. IL-6 levels in breast-cancer patients have been found to correlate to the clinical stage of the disease as well to the rate of recurrence. High IL-6 serum levels in breast-cancer patients have been found to be an unfavorable prognosis indicator (see ref. (6) and citations therein). IL-8, and the murine-related molecules KC and MIP-2, have also been found to correlate with increase bone metastasis *in vivo* and with stimulation of osteoclast differentiation followed by bone resorption. Interestingly, MCP-1, a principal chemokine involved in normal bone remodeling, is produced primarily by osteoblasts and not the metastatic MDA-MB-231^{GFP} cells upon interaction. Thus, the osteoblastic response to the cancer cells, even in the absence of osteoclasts, changes the tumor microenvironment to favor osteolysis in this particular cancer-cell model (6).

Interestingly, we found that that the above-described pattern of cancer colonization was dependent on osteoblastic tissue maturity (Figure 1, Panel B table portion). MDA-MB-231^{GFP} cells failed to penetrate immature osteoblast tissue (less than 30 days in culture); instead forming colonies substantially on, not in, tissue. Significant penetration, remodeling, and characteristic cancer-cell-alignment patterns were observed only in relatively-mature osteoblastic tissue. Cancer cell induced changes in osteoblast shape and in the production of inflammatory cytokines were seen after as few as three days of co-culture. We speculate that cancer-cell penetration was slowed by close contacts among osteoblasts comprising immature tissue and becomes more efficient as the cell/ECM ratio decreases, creating a more permeable tissue.

Comparison of results obtained with tissue grown in the bioreactor to cells grown using conventional tissue culture clearly showed that 3D tissue was superior in modeling details of

cancer-cell colonization. In the first place, osteoblasts do not grow into more than 1-2 cell layers in conventional cell culture. Furthermore, these cultures usually did not remain healthy for more than about a one month of before showing signs of necrosis or sharply-increased apoptosis (13). These substantially 2D cultures never achieved the phenotypic maturity observed in the bioreactor and, in particular, there was no evidence of an osteoblast-to-osteocyte transition. In the second place, although the MDA-MB-231^{GFP} proliferated in contact with 2D osteoblast monolayers and formed colonies, these cancer cells did not penetrate the osteoblast monolayers and did not form cell files. It is thus apparent that the 3D osteoblastic tissue model is a better tool for discovery of therapeutic interventions to cancer colonization of bone.

In summary, we have found that the easy-to-use bioreactor design based on the principle of simultaneous-growth-and-dialysis permitted *in vitro* culture of 3D, multiple-cell-layer osteoblastic tissue from isolated cells and their maintenance for much longer periods than in conventional culture (demonstrated up to 10 months with no indication of tissue necrosis). This osteoblastic tissue exhibited important hallmarks of osteoblast-to-osteocyte phenotypic transition and deposition of macroscopic bone. We conclude that the resulting tissue is a relevant *in vitro* model of osteoblasts within regions of growing bone such as the metaphysial areas of long bone that are otherwise difficult to access *in vivo*. Challenge with breast cancer cells known to invade skeleton permitted, for the first time, direct and real-time observation of cancer-cell colonization of the osteoblast tissue. Important pathological events such as cancer-cell filing and colony (microtumor) formation observed clinically were reproduced *in vitro*. These studies have revealed that breast-cancer cell colonization strongly depends on osteoblastic-tissue maturity, and point to a potentially important point of therapeutic intervention for cancer metastases in bone. Comparison of breast-cancer cell interactions with osteoblasts in conventional culture to interactions with osteoblastic tissue in the bioreactor strongly suggested that monolayer cell culture is not the optimal model for studying the cancer-cell colonization of bone.

In the future, we plan to use primary osteoblasts (especially human) as source cells for growth of osteogenic tissue. In addition we plan to increase the biological complexity of the system by adding other cell types including osteoclasts. We have already successfully cultured primary osteoblasts isolated from mouse calvaria in the bioreactor. After three months, these cells formed a multilayer complex that expressed characteristic osteoblast-differentiation proteins, in a manner similar to that obtained with the pure MC3T-E1 osteoblast cell line. Once we have a human-derived 3D osteogenic-tissue model in hand, we plan to study interactions with other bone-metastatic cancers (*e.g.* blastic prostate cancer cells or osteolytic multiple myeloma cells) to determine if human cancer colonization of human osteoblastic tissue parallels pathogenesis *in vivo*. We intend to explore development of an *in vitro* bone-remodeling unit by co-culture of primary osteoclasts with osteogenic tissue. Challenging such a mimic with cancer cells should permit close examination of how cancer cells influence osteoblast/osteoclast interactions and upset normal bone remodeling. Toward ultimate biological complexity in an *in vitro* bone model, we aim to recreate the hematopoietic/cancer cell niche by culturing osteoblastic tissue in the presence of mesenchymal stromal cell from bone-marrow cells. There is strong evidence in the literature that osteoblasts provide the endosteal niche for hematopoietic stem cells (19) and that this niche both receives and harbors metastatic cancer cells early in the colonization process. Finally, while this bioreactor system is not an appropriate tool for rapid drug screening, it can serve as an efficient system to test therapeutics at a level above 2D cell culture but below costly and slow animal testing. While the described compartmentalized device is not commercially available, engineering plans have been published (11) and the bioreactor is straightforward to make in a standard engineering shop.

Acknowledgements

Grant support: U.S. Army Medical and Materiel Command Breast Cancer Research Program (WX81XWH-06-1-0432) and The Susan G. Koman Breast Cancer Foundation (BCTR 0601044). We thank Ravi Dhurjati, Laurie Shuman, Venkatesh Krishnan and Donna Sosnoski for their work with various aspects of this project. We also thank Dr. Elizabeth Frauenhoffer of the Penn State Hershey Medical Center for images of metastatic breast cancer in bone.

Figure legend

Figure 1: Osteogenic tissue maturation in the bioreactor recapitulates development of native bone by systematic and reproducible phenotypic maturation of pre-osteoblasts through mineralizing osteoblasts to terminally-differentiated osteocytes (Panel A). MC3T3-E1 produce and mineralize a thick, engulfing extracellular matrix (ECM) that slowly decreases in thickness and number of cell layers through progressive apoptosis to a final stable state exhibiting no sign of tissue necrosis over 10 months of continuous culture (Panel B graph). Interaction of MDA-MB-231^{GFP} human cancer cells (green, GFP) with osteogenic tissue (red = osteoblasts, black = ECM) depends on tissue maturity (Panel B table) and exhibits stages of cancer-cell adhesion (C), penetration (D), and alignment of cancer-cell into files (E) that are reminiscent of events observed in pathological tissue. Filing is especially evident in corresponding 3D confocal reconstructions (F). For comparison, Indian Filing is shown in a section from bone with metastatic breast cancer (G,H,I). Scale bar Panel A, C, D = 50 μm, Panel F = 100 μm, Panel G = 200 μm; H,I = 50 μm.

Citations

1. Rubens RD, Mundy GR. Cancer and the Skeleton. London: Martin Dunitz; 2000.

2. Nielsen OS, Munro AJ, Tannock IF. Bone Metastases: Pathophysiology and Management policy. J Clin Oncol 1991; 9: 509-24.

3. Rubens RD. Bone Metastases--The Clinical Problem. Eur J Cancer 1998; 34: 210-3.

4. Nemeth JA, Harb JF, Barroso U, Jr., He Z, Grignon DJ, Cher ML. Severe combined immunodeficient model of human prostate cancer metastasis to human bone. Cancer Res 1999; 59: 1987-93.

5. Welch DR. Technical considerations for studying cancer metastasis in vivo. 1997. p. 272 - 301.

6. Dhurjati R, Krishnan V, Shuman LA, Mastro AM, Vogler EA. Metastatic breast cancer cells colonize and degrade three-dimensional osteoblastic tissue in vitro. Clin Exp Metastasis 2008; 25 741-52.

7. Schmeichel KL, Bissell MJ. Modeling tissue-specific signaling and organ function in three dimensions. 2003; 116: 2377-88.

8. Rose FRAJ, Oreffo ROC. Breakthroughs and Views: Bone Tissue Engineering: Hope vs Hype. Biochem and Biophys Res Comm 2002; 292: 1-7.

9. Phadke PA, Mercer RR, Harms JF, et al. Kinetics of metastatic breast cancer cell trafficking in bone. Clinical cancer research 2006; 12: 1431-40.

10. Lian JB, Stein GS. Concepts of osteoblast growth and differentiation: basis for modulation of bone cell development and tissue formation. Crit Rev Oral Biol Med 1992; 3: 269-305.

11. Vogler EA. A Compartmentalized Device for the Culture of Animal Cells. J Biomaterials, Artificial Cells, and Artificial Organs 1989; 17: 597-610.

12. Rose GG. Cytopathophysiology of Tissue Cultures Growing Under Cellophane Membranes. In: Richter GW, Epstein MA, editors. Int Rev Exp Pathology. New York: Academic Press; 1966. p. 111-78.

13. Dhurjati R, Liu X, Gay CV, Mastro AM, Vogler EA. Extended-Term Culture of Bone Cells in a Compartmentalized Bioreactor. Tissue Engineering 2006; 12: 3045-54.

14. Rusciano D, Burger M. In vivo cancer metastasis assays. In: Welch D, editor. CANCER METASTASIS: EXPERIMENTAL APPROACHES: Elsevier; 2000. p. 207-42.

15. Page DL, Anderson TJ, Sakamoto G. Diagnostic Histopathology of the Breast. 1987. p. 219-22.

16. Friedl P, Wolf K. Tumor-cell invasion and migration: diversity and escape mechanisms. Nat Rev Cancer 2003; 3: 362-74.

17. Friedl P, Wolf K. Tube Travel: The Role of Proteases in Individual and Collective Cancer Cell Invasion. Cancer Res 2008; 68: 7247-9.

18. Kinder M, Chislock E, Bussard KM, Shuman L, Mastro AM. Metastatic breast cancer induces an osteoblast inflammatory response. Exp Cell Res 2008; 314: 173-83.

19. Taichman RS. Blood and bone: two tissues whose fates are intertwined to create the hematopoietic stem-cell niche. Blood 2005; 105: 2631-9.

Tissue Maturation

A

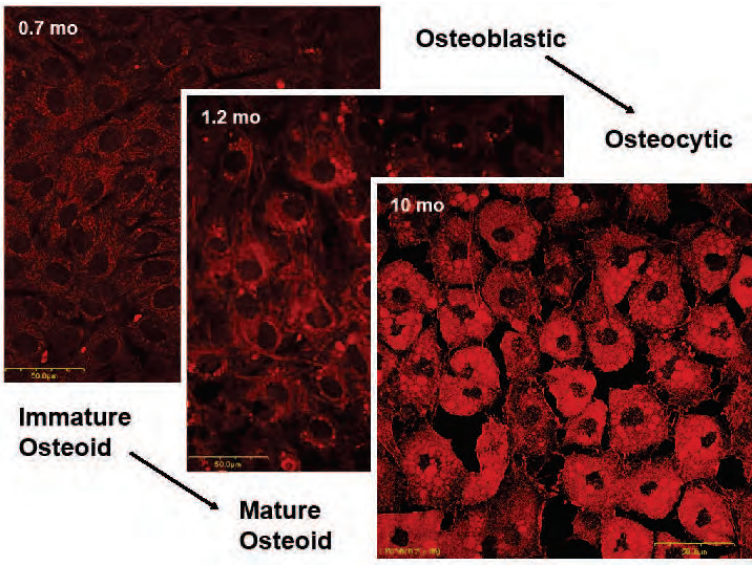

B

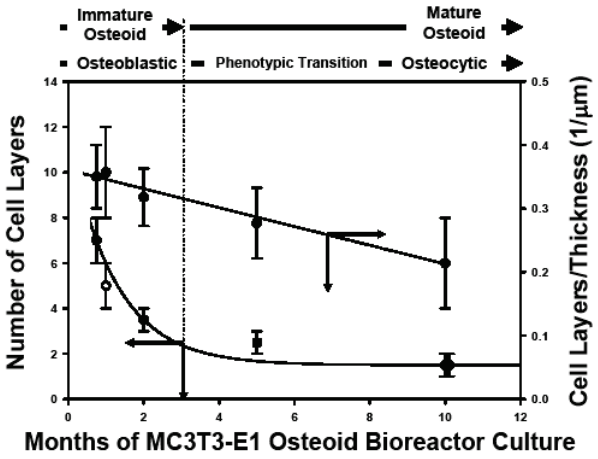

Experimental Parameter @ BC:OB=1:10	Months of Bioreactor Culture			
	0.75	1	2	5
BC Colonization	(+++)	(++)	(+)	(+)
Tissue Penetration	(-)	(+/-)	(+)	(+)
BC Filing	(-)	(+)	(++)	(++)
Tumor Formation	(-)	(+)	(++)	(++)

Cancer Colonization

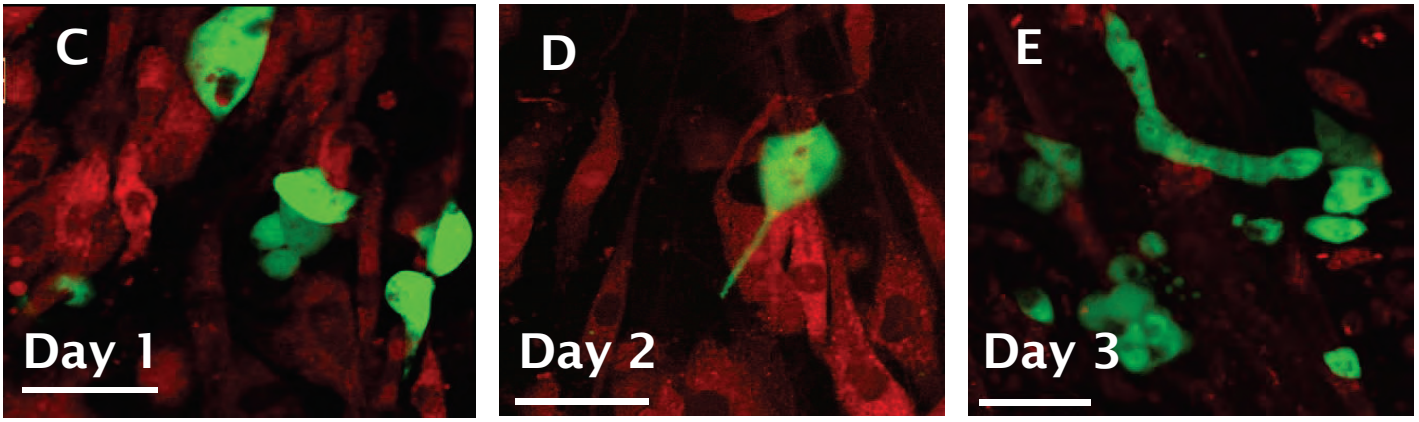

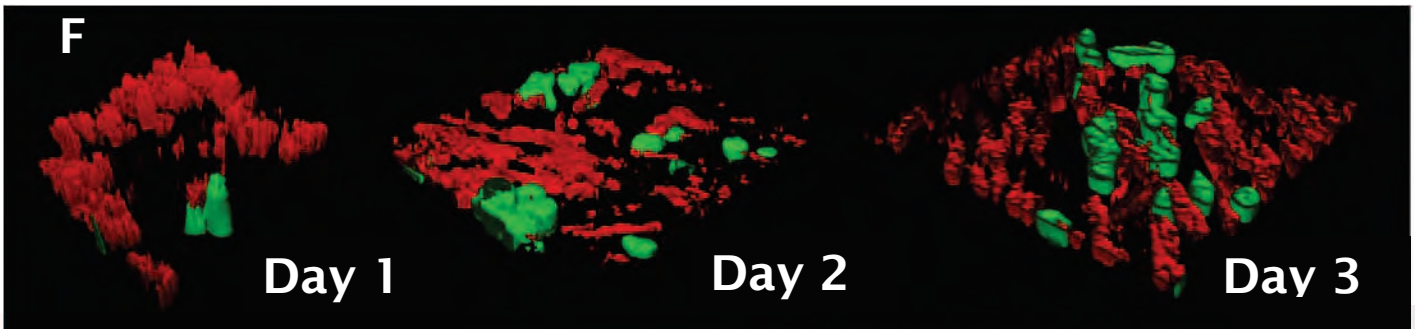

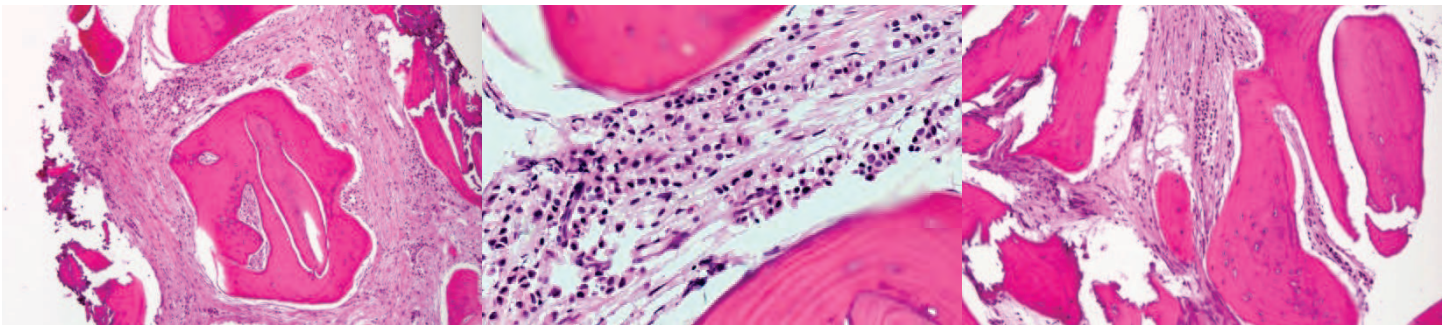

Cancer Metastasis Rev (2008) 27:41–55
DOI 10.1007/s10555-007-9109-4

The bone microenvironment in metastasis; what is special about bone?

Karen M. Bussard · Carol V. Gay · Andrea M. Mastro

Published online: 11 December 2007

Abstract The skeleton is a common destination for many cancer metastases including breast and prostate cancer. There are many characteristics of bone that make it an ideal environment for cancer cell migration and colonization. Metaphyseal bone, found at the ends of long bone, in ribs, and in vertebrae, is comprised of trabecular bone interspersed with marrow and rich vasculature. The specialized microvasculature is adapted for the easy passage of cells in and out of the bone marrow. Moreover, the metasphyseal regions of bone are constantly undergoing remodeling, a process that releases growth factors from the matrix. Bone turnover also involves the production of numerous cytokines and chemokines that provide a means of communication between osteoblasts and osteoclasts, but co-incidentally can also attract and support metastatic cells. Once in the marrow, cancer cells can interact directly and indirectly with osteoblasts and osteclasts, as well as hematopoietic and stromal cells. Cancer cells secrete factors that affect the network of cells in the bone microenvironment as well as interact with other cytokines. Additionally, transient cells of the immune system may join the local mileau to ultimately support cancer cell growth. However, most metastasized cells that enter the bone marrow are transient; a few may remain in a dormant state for many years. Advances in understanding the bone cell-tumor cell interactions are key to controlling, if not preventing metastasis to bone.

Keywords Bone metastasis · Osteoblasts · Osteoclasts · Cytokines · Chemokines

K. M. Bussard · C. V. Gay · A. M. Mastro (✉)
Department of Biochemistry and Molecular Biology,
The Pennsylvania State University,
University Park, PA 16802, USA
e-mail: a36@psu.edu

C. V. Gay
e-mail: cvg1@psu.edu

K. M. Bussard
Department of Veterinary and Biomedical Sciences:
The Pathobiology Graduate Program,
The Pennsylvania State University,
University Park, PA 16802, USA
e-mail: kmb337@psu.edu

1 Tumor cell metastasis

The skeleton is a favored site of metastasis for a number of common tumors. Bone metastases are by far more prevalent than primary tumors of the bone. Based on post-mortem examination, approximately 70% of patients who die from breast or prostate cancer have bone metastases [1]. The incidences from thyroid, kidney, and lung cancer also are high (about 40%). In contrast, it has been noted that bone metastases from cancers of the gastrointestinal tract are uncommon. In many cases, cancer cell metastases are diagnosed in patients before diagnosis of the primary disease. A better understanding of the specificity and the pathogenesis of metastasis will allow for better therapeutic treatments and quality of life for patients.

The metastasis of a primary tumor to distant organs requires a series of coordinated steps. Proliferation of the primary tumor is supported by tumor autocrine factors or local growth factors, such as vascular endothelial growth factor (VEGF), tumor growth factor-beta (TGF-β), and interleukin-6 (IL-6). For a tumor to reach a clinically detectable size, localized neovascularization or angiogenesis must occur. The development of new blood vessels provide an endless supply of nutrients as well as a route for tumor cell migration to secondary sites. Subsequently, local

invasion takes place, which is accomplished by the destruction of the extracellular matrix, including the basement membrane and connective tissue. The process of invasion through a basement membrane is a hallmark characteristic of a metastatic cell. Additionally, tumor cells experience increased motility and reduced adherence allowing them to migrate into lymph or blood vessels. Intravasation into blood vessels at the primary site may occur as a result of excess force or response to a soluble chemotactic factor gradient. After circulating through the vasculature, tumor cells may adhere to vessel endothelium of the target organ and extravasate into the tissue. This movement is facilitated by cancer cell secretion of matrix metalloproteinases (MMPs) and cathepsin-K that destroy surrounding tissue. Finally, tumor cells thrive at the secondary site, a defining characteristic of metastatic tumor cells, only if there is an appropriate environment of paracrine or autocrine factors that aid in growth and vascularization [2–4]. The distribution pattern of cancer cells to the bone is believed to be due to the venous flow from breast and prostate towards the vena cava and into the vertebral venous plexus [5]. Once in the circulation, entry of the cancer cells into the venous circulation of the bone marrow may be facilitated by the slow blood flow and particular anatomy of the venous sinusoids. Nonetheless these steps alone do not explain survival and growth of the cancer cells in the bone.

2 Bone structure

In order to understand the bone-tumor microenvironment, one must consider bone structure and function. Bone is a specialized type of connective tissue, which provides structural support, protective functions, and plays a major role in the regulation of calcium levels in the body [6]. Type I collagen accounts for 95% of the organic bone matrix [7]. The remaining 5% includes proteoglycans and a variety of other non-collagenous proteins [6]. This largely collagenous matrix is hardened through the mineralization process, in which hydroxyapatite ($3Ca[PO_4]_2[OH]_2$) crystals are deposited in the organic matrix [8]. Mineralization increases bone resistance to compression [9], and also contains numerous growth factors, including TGF-β, which are released upon bone resorption [10].

The bones of the body are classified as long bones (e.g. the tibia, femur, and humerus) and flat bones (e.g. the skull, ileum, and mandible). Both types contain cortical and trabecular bone, albeit in different concentrations. Cortical bone, the compact, dense outer protective layer of bone, is made up of tightly packed collagen fibrils [6]. This form of bone is vital for supporting the weight load of the body. On the other hand, trabecular bone, also known as cancellous bone, has a loosely organized, porous matrix and is located in the interior of bone, near the ends. Trabecular bone is metabolically active. All bone matrix undergoes remodeling, but trabecular bone has a greater turnover rate than cortical bone [6].

Long bones are divided into the diaphysis, metaphysis, and epiphysis in a growing individual [11] (Fig. 1). The long bone ends, or epiphyses, are located above the growth plate, where bone elongation occurs. The diaphysis, which is the long, narrow shaft of the bone, is primarily composed of cortical bone. The metaphysis, located near the ends of bones just below the growth plate, is predominantly composed of trabecular bone and is surrounded by hematopoietic marrow, fatty marrow, and blood vessels [11].

3 Cells in the bone microenvironment

Bone is a dynamic structure that undergoes constant remodeling in order to respond to mechanical strain and maintain calcium homeostasis. Bone resorption and deposition occur in a tightly regulated fashion that is orchestrated by three cell types: osteoblasts, osteocytes, and osteoclasts. Osteoblasts are derived from mesenchymal stem cells located in the bone marrow stroma. They synthesize osteoid (i.e. new bone matrix), comprised primarily of collagen and non-collagenous proteins, and also aid in mineralization of the bone matrix. Upon stimulation by bone morphogenetic proteins and local growth factors, the mesenchymal stem cells proliferate and form pre-osteoblasts, which subsequently differentiate into mature osteoblasts [12]. After synthesizing new bone

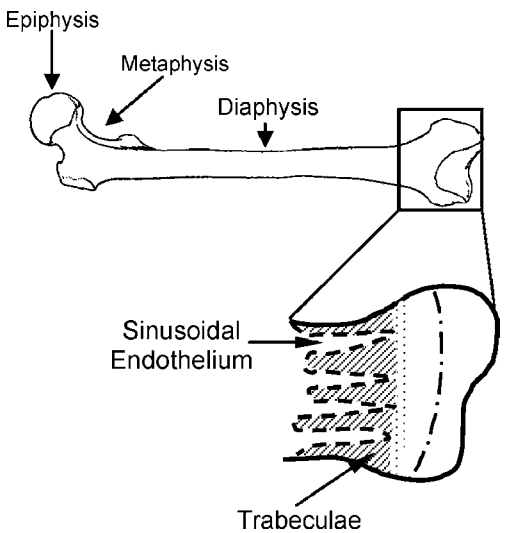

Fig. 1 Diagram of a long bone indicating the major regions and the major structures within the metaphysis, i.e. trabecular bone and the sinusoidal endothelium

matrix, the osteoblast either undergoes apoptosis or becomes embedded in the bone as an osteocyte [13]. These cells have long processes that allow them to remain in contact with other osteocytes and with osteoblasts that line the bone surface. The processes connect the entire matrix through a series of canaliculi [14, 15].

Osteoclasts, responsible for bone resorption, are derived from monocytes in the bone marrow [16]. Monocytes are activated to form osteoclasts through osteoblasts. Osteoblasts express the receptor-activator for NF-κB ligand (RANK-L) on their external surfaces; RANK-L binds to the receptor RANK found on the surface of monocytes. In the presence of macrophage colony stimulating factor (M-CSF), RANK-L promotes cellular fusion of several monocytes to form a multinucleated osteoclast [16]. Activated osteoclasts bind to the bone matrix through $\alpha_v\beta_3$, $\alpha_v\beta_5$, $\alpha_2\beta_1$ integrins located on the membrane surface and also secrete acid and lysosomal enzymes which degrade bone [13, 16].

Other cell types located within the bone microenvironment may also contribute to the bone metastatic niche. These cells can generally be grouped into two categories: stromal and transient. Mesenchymal stem cells in the bone marrow give rise to stromal cells which can differentiate into adipocytes, fibroblasts, chrondrocytes, or osteoblasts. Stromal cells have been found to support the differentiation, proliferation, and survival of both hematopoetic and cancer cells. In particular, it has been found that stromal cells express vascular cell adhesion molecule (VCAM-1). Michigami and colleagues discovered that the presence of VCAM-1 on stromal cells increased the production of bone-resorbing cytokines by myeloma cells. Neutralizing antibody to VCAM-1 or to $\alpha_4\beta_1$ integrin reduced osteolysis [17]. The adipocyte has been found to secrete tumor necrosis factor-alpha (TNF-α), IL-6, and leptin, which stimulate bone resorption and inhibit osteoblast proliferation [18, 19]. Factors secreted by adipocytes have also been implicated in breast cancer proliferation, invasiveness, survival, and angiogenesis [19]. Another type of mesenchymal cell, the fibroblast, has been shown to affect breast cancer cell invasion and contribute to metastatic bone disease. Fibroblast-secreted syndecan-1 was found to increase breast cancer cell proliferation *in vivo* [20]. In addition, fibroblasts secrete inactive MMP-2, which can be activated by breast cancer cells to subsequently increase their invasiveness and migration [21]. Fibroblasts have also been found to stimulate osteoclasts, and thus bone resorption, in a RANK-L dependent manner [22].

Vascular endothelial cells contribute to the formation of a favorable cancer cell microenvironment. New blood vessels, which arise from endothelial cells, are essential for the survival of cancer cells. Investigators have shown that the bone marrow, which has a high microvessel density, is associated with increased bone-tumor metastasis and survival of tumor cells [23]. It has also been found that many tumor-cell secreted factors stimulate endothelial cell proliferation, differentiation, and angiogenesis [23], thus producing a feedback loop that facilitates tumor cell survival in a secondary location.

Transient cells also contribute to the metastatic bone microenvironment. These cells include erythrocytes, T cells, and platelets, all derived from hematopoietic stem cells. In one study it was shown that platelets were directed by MDA-MB-231, a metastatic breast cancer cell line, to secrete LPA (Lysophosphatidic acid ([1-acyl-sn-glycero-3-phosphate]), a phospholipid with diverse biological activities [24]. Overexpression of this molecule and its receptor has been shown to increase tumor growth and metastasis [25]. Platelets may also adhere to cancer cells in the blood stream, allowing them to evade natural killer immune cell surveillance [26]. In addition, platelets may aid in cancer cell attachment to vascular endothelial cell walls [26]. T lymphocytes have been found to express RANKL, also known as TRANCE, and aid in osteoclast formation and activation [16, 27]. Peripheral T cells also secrete TNF-α, which is involved in osteoclastogenesis, inhibits osteoblast cell differentiation, and is a pro-apoptotic factor for osteoblasts [27, 28]. Besides enhancing osteoclastic bone resorption, T cells may be affected by bone metastatic cancer cells as well. As bone resorption is enhanced, TGF-β is released from the bone. This factor can inhibit both T cell proliferation and activity, and natural killer cell function [29]. Thus the immune response is suppressed and tumor cells may escape surveillance. In addition, tumor cell-secreted parathyroid hormone related peptide (PTHrP) and IL-8 may activate T cells, thus enhancing bone resorption and suppressing T cell function [29]. Plasma cells, or antibody-producing B cells, upregulate the receptor CXCR4 upon completion of differentiation [27]. Breast cancer cells, as well as stromal cells, express the ligand to this receptor CXCL12 [Stromal-derived factor-1 (SDF-1)] [27]. This ligand-receptor interaction may facilitate cancer cell migration into and within the bone microenvironment.

Tumor-associated macrophages (TAMs) are an important component of the inflammatory response in tissues [30]. These cells are derived from monocytes and are recruited by monocyte chemotactic peptide (MCP) chemokines [30]. Although activated TAMs kill many cancerous cells through secretion of IL-2, interferon, and IL-12, they also secrete a variety of potent angiogenic and lymphangiogenic growth factors, cytokines, and proteases [31, 32], all of which are involved in the promotion of tumor cell growth and survival. TAMs, as well as tumor cells, produce IL-10 which suppresses the anti-tumor response of cytotoxic T cells [33]. TAMs also induce the expression of VCAM-1 on mesothelial cells, which can aid in tumor cell invasion [34].

4 Bone remodeling

Mineralized bone has an abundance of growth factors, calcium ions, cell adhesion molecules, cytokines, and chemokines that, when released into the microenvironment during bone remodeling, make the skeleton an attractive site for metastatic cancer cells. This observation was first described in 1889 by Stephen Paget, who recognized the nonrandom movement of cancer cells within the body that was unexplained by blood flow. Paget stated "When a plant goes to seed, its seeds are carried in all directions; but they can only grow if they fall on congenial soil" [35]. This 'seed and soil' hypothesis helps to explain the preferential metastasis of certain types of cancers to the bone microenvironment, which provides a fertile soil where cancer cells can grow. Osteoclasts further contribute to this environment by acting as plows to break up the 'soil' and release its 'nutrients' for cancer cell growth and maintenance. Studies have shown that there is a close relationship between bone resorption and tumor cell growth [36].

The relative activities of osteoblasts and osteoclasts are normally tightly coupled in order to maintain a balance between bone formation and degradation. Bone remodeling is regulated both by systemic hormones and locally produced cytokines [37]. Cells in the bone marrow, especially stromal and immune cells, produce cytokines and growth factors that influence the activities of osteoblasts and osteoclasts [38]. However, this balance between bone synthesis and resorption is disturbed in several pathological conditions, including osteoporosis, rheumatoid arthritis, and skeletal metastases, resulting in osteoclast activity in excess of bone deposition by osteoblasts with net bone loss [38].

Osteoclasts likely prime the bone microenvironment for tumor cell growth through bone resorption. Although there is no definitive evidence linking increased bone resorption to increased tumor cell mass, a variety of studies have been carried out with bisphosphonates to investigate this relationship. Bisphosphonates are inorganic pyrophosphates with powerful inhibitory effects on bone resorption. One of their main targets is the osteoclast. Powles et al. showed that the administration of a bisphosphonate, clodronate, was associated with both decreased bone metastasis and death rate in patients with breast cancer [39]. Risedronate was found to reduce tumor burden in addition to osteolytic bone lesions in a nude mouse model [40]. Furthermore, nude mice treated with neutralizing antibodies to PTHrP (key factor involved in the 'vicious cycle' of bone metastasis), also experienced a decrease in tumor burden compared to controls [41, 42]. Even though inhibitors to bone resorption seem to reduce tumor burden in bone, the same does not hold true for soft tissues [39]. In the study carried out by Powles et al., the idea that inhibitors of osteolysis slowed tumor growth in soft tissue was refuted [39]. In addition, there are pre-clinical data suggesting that bisphosphonates have no effect on tumor burden in soft tissues if the drugs are administered after the metastases are already formed [3]. Taken together, these studies illustrate the importance of osteoclasts and the uniqueness of the bone microenvironment for tumor cell growth.

In patients with bone metastatic cancer, usually one of two types of lesions predominate: osteolytic or osteoblastic, although mixed lesions may occur especially early on [36]. During osteolytic metastases, typical for breast cancer metastases, osteoclastogenesis and osteoclast activation results from direct and indirect actions by metastatic cancer cells. Increased bone resorption results. Mastro and colleagues additionally found that bone metastatic breast cancer cells suppress osteoblast function, which includes decreased matrix deposition, decreased proliferation, altered adhesion, and loss of osteoblast differentiation [43–45]. These phenomanae together favor a microenvironment of increased bone turnover with decreased bone deposition similar to that seen in osteoporosis.

On the other hand, cancers such as prostate cancer tend to be predominantly osteoblastic in nature. Excess bone deposition occurs but not necessarily in an ordered fashion. While little is known about the exact mechanisms, endothelin-1 has been implicated in osteoblastic breast cancer metastases [46, 47]. Endothelin-1 has been found to stimulate the formation of new bone through osteoblast proliferation [48], and serum endothelin-1 levels were found to be increased in patients with osteoblastic prostate cancer metastases [49]. In addition to endothelin-1, platelet derived growth factor-BB (PDGF-BB) may also be a mediator for osteoblastic metastases. In a study done by Yi et al., increased expression of PDGF-BB by human metastatic breast cancer cells was correlated with increased bone formation [50]. The exact mechanism has yet to be determined. Regardless of the lesion type, these observations underscore the importance of crosstalk between cancer cells and the bone microenvironment which facilitates bone metastases.

Clinically, patients with breast cancer and other osteolytic metastases but also with osteoblastic prostate bone metastases are treated with bisphosphonate drugs that block osteoclast activity. However, therapies utilizing bisphosphonates, such as ibandronate (Boniva™), are not curative [51]. Lesion progression is slowed, but the pre-existing lesions do not heal [52–55]. Severe bone pain, fractures, hypercalcemia, and spinal cord compression may still occur [3, 10, 56, 57]. The inability of bone to regenerate following bisphosphonate treatment supports the *in vitro* finding that breast cancer cells alter osteoblast function in addition to stimulating osteoclast activity.

Not all bones of the skeleton are equally favored for metastases. The spinal vertebrate, ribs, and the ends of long

bones are preferred destinations of metastases. In general, well vascularized areas and areas of the skeleton containing red marrow are the sites of metastatic colonization. In osteoblastic metastases, bone deposition is usually made on trabecular bone surfaces without prior removal of old bone, but it may also be at sites of prior resorption. In myeloma, a malignancy of B cells, the plasma cells accumulate in the bone marrow and lead to osteolysis. Activation of osteoclasts and bone resorption far exceed bone deposition in this disease. Whether the lesions are overall lytic or blastic, the outcome is bone pain, pathological fracture, nerve compression syndromes and hypercalcemia [58].

5 The metaphyseal region of the bone has unique properties that distinguish it from the diaphysis

Scintigrams of humans with advanced disease clearly indicate that highly vascularized metaphyseal bone is a preferred site for secondary metastasis [1]. A trafficking study with a nude mouse model of metastatic breast cancer revealed that within 2 h of an inoculation of a bolus of metastatic breast cancer cells into the left ventricle of the heart, cancer cells were detected throughout the femur. However, by 24 h they had been cleared from the shaft (diaphysis) but remained at the metaphysis where they grew into large tumor masses [59]. The unique properties of the bone metaphysis make it an attractive site for metastatic cancer cells.

6 Metaphyseal bone: structure and vascularity

Metaphyseal bone is a highly vascularized structure found near the ends of long bone, in ribs and in vertebrate. It is composed of a network of thin bone spicules, sometimes referred to as “spongy bone.” In long bones, these spicules appear as mineralized fingers interspersed with red marrow and are in close proximity to the blood supply. The marrow contains hematopoietic, mesenchymal, and stromal cells. The vascular supply is sinusoidal in nature rather than a bed of capillaries. Lining the trabecular bone surfaces are osteoblasts and bone lining cells which share many properties [60]. Bone lining cells are believed to differentiate into osteoblasts when necessary for bone remodeling. The osteoblasts, as well as the marrow cells, provide an environment rich in growth factors, cytokines and chemotactic factors. These factors, and the vascular structure of the trabecular bone, are crucial for metastatic cancer cell colonization and growth.

The interactions of metastatic breast cancer cells with the vasculature has recently been well documented by Glinsky [61] and is only briefly summarized here. Metastatic foci are often seen where the sinusoid microvasculature is abundant [62]. This phenomenon is likely related to the unique anatomic, hemodynamic, and epithelial properties of the metaphyseal vascular bed. For one, the vasculature does not end in capillaries of small diameter as in most tissues. Instead it consists of voluminous sinusoids with lumens many times the diameter of cancer cells [63]. The sinusoids are within a few microns of the trabecular bone [64]. This unique structure leads to a sluggish flow of blood compared to that seen in the capillary networks of most other tissues [63]. For example, Mazo et al. found the blood flow in venous sinusoids of mouse calvaria to be 30 fold lower than the arterial rate. In another animal model, blood flow rates in canine long bone were assessed with microspheres [65]. It was found that metaphyseal and marrow cavity flow rates in sinusoids were 7–14 ml/min/g tissue, much slower than more rapidly metastasizing tissue such as the post-prandial intestine [66]. Thus cells entering the sinusoids are more “in a lake than in a stream.” In addition, sinusoids are specialized to allow easy movement of hematopoietic cells in and out of the marrow. The walls of the sinusoids are trilaminar and their structure helps explain why tumor cells can easily enter and leave [63]. Stromal endothelial cells line the sinusoidal lumen. These cells do not have tight junctions but may overlap or interdigitate. They rest on a basement membrane, the middle layer, which is irregular and discontinuous. The third layer, facing the bone marrow, is composed of adventitial cells, a type of phagocytic cell, which also do not form a tight layer. Thus the nature of the sinusoidal walls allows for easy two-way movement of hematopoietic and lymphoid cells. This structure is used advantageously by cancer cells [67].

Nevertheless, cellular entry into the sinusoids and migration into the marrow are not sufficient to insure colonization by the cancer cells. In a mouse study, it was observed that many more cancer cells entered the marrow cavity of the femur than remained to colonize it [59]. Presumably, many metastatic cancer cells in the blood can circulate through the bone, but few remain. Cancer cells, similar to leukocytes, migrate through the vasculature using a process of attachment-detachment through cell-adhesion molecules. The endothelial cells of the bone sinusoids constitutively and simultaneously express an array of tethering and adhesive proteins including P-selectin, E-selectin, intercellular adhesion molecule (ICAM-1) and VCAM-1. The vasculature of other tissues only express these molecules when stimulated by inflammatory cytokines [63]. Moreover, vasculature in one part of the bone may be different than other parts. Indeed Makuch et al. [68] found expression of P-selectin, E-selectin, ICAM and VCAM by vascular endothelial cells isolated from trabecular bone and from diaphyseal bone. However the endothelial cells from the trabecular bone but not diaphy-

seal bone showed a significantly increased expression in E-selectin when exposed to conditioned medium from immature osteoblasts. These data can be interpreted to suggest that osteoblasts of immature, metabolically active bone enhance E-selectin expression by nearby endothelial cells. This increase in cell attachment molecules would in turn enhance cancer cell extravasation into the bone marrow. Furthermore as discussed further on, inflammatory cytokines produced by osteoblasts in the presence of breast cancer cells may cause an even greater increase in cancer cell migration. In complementary approaches, others found that prostate cancer cells showed increased adherence to bone marrow microvasculature endothelium than from endothelium of other anatomical sites [69, 70]. Similar findings were reported for breast cancer [71, 72].

7 Adhesion molecules of the vascular endothelium

There has been an ongoing discussion of the roles of adhesion vs. entrapment in the movement of cancer cells into organs. The "leaky" vasculature suggests that entrapment is not the limiting event in bone metastasis. To the contrary, adhesion of metastatic cancer cells to the endothelium appears to play a specific and critical role. Evidence for the role of adhesion molecules has been found, both with prostate and breast cancer cells, which may explain their predilection to the bone [61]. For tumor cells to reach the bone marrow there must be a selective adhesion of the circulatory tumor cells to the endothelium of the bone marrow sinusoids. Therefore the adhesion molecules of the endothelium are of utmost importance.

The movement of cancer cells across the endothelium in the bone marrow has been likened to the movement of leukocytes across the endothelium. While the general patterns are likely the same, the actual molecules involved may differ [73–75]. The reported roles of various adhesion molecules may relate to the particular system, i.e. primary or secondary tumors and the specific organ. For example, selectin-mediated binding of colon cancer cells has been demonstrated to be important for their adhesion to the hepatic microvasculature [76]. This association may not hold for other metastatic tumors [61]. Makuch et al. [68] reported that active osteoblasts influenced E-selectin (but not P or S-selectin) expression on metaphyseal endothelium. The expression of E-selectin depended both on the stage of differentiation of the osteoblasts and the source of the microvasculature endothelium within the bone marrow. Galactin-3 is another molecule that participates in tumor cell, bone microvasculature associations. Galactin-3 and its ligand Thomsen–Friedenreich (TF) antigen are found both on many cancer cells and on microvasculature endothelium. Their interaction appears to be important for the primary arrest of the tumor cells [71, 77]. Another well studied molecule is CD44, the principle cell surface receptor for hyaluronic acid (HA). It is frequently over-expressed on malignant cells. In model systems, its expression correlates with the rate and strength of cancer cell interaction with bone marrow endothelium. CD44 expression on the surface of bone marrow endothelial cells likely acts to bind HA. Cancer cells and bone marrow endothelial cells both appear to express CD44 and HA, and the interaction of the two leads to tethering of the cancer cells to the bone marrow. In addition, there are associated data to suggest that activation of CD44 by HA or by osteopontin is important in downstream signaling through CD44 in bone.

8 Adhesion molecules within the bone marrow cavity

Coordinated bone remodeling involves extensive cell–cell and cell–matrix interactions among osteoblasts, osteoclasts, and bone marrow resident stromal and hematopoietic cells. The sinusoidal endothelium of the bone marrow is a two-way gate, allowing movement in both directions of newly formed and recirculating lymphocytes, hematopoietic stem cells as well as neoplastic cells. The trafficking patterns are organized by adhesion molecules on the circulating cells as well as on the bone marrow reticulocytes. VCAM-1, a member of the immunoglobulin family of cell adhesion molecules, was shown by a radiolabeling technique to be constitutively expressed by bone marrow reticular cells as well as the entire endothelium of the bone marrow sinusoids [78]. Its counter receptor, VLA-4 ($\alpha_4\beta_1$), and ICAM-1, which belongs to a similar family and binds $\alpha_2\beta_1$ integrins, are found on many cancer cells. Thus adhesion molecules which serve normal bone metabolism can be used to the advantage of metastatic tumor cells.

Another integrin member, $\alpha_v\beta_3$ is associated both with breast cancer [79] and osteoblast function [80, 81]. Interestingly, it is over-expressed in metastatic breast cancer cells once they enter the bone [82]. It is the predominant integrin on osteoclasts and appears to be important for syncytia formation and attaching to the bone matrix [83]. Peptomimetic inhibitors of $\alpha_v\beta_3$ were found to significantly reduce metastatic cancer formation when injected prior to tumor cells in a mouse model. However, there was less of an effect when administered after tumor inoculation [84]. The expression of adhesion molecules by osteoclasts has been fairly well determined [85]. Three integrins, $\alpha_v\beta_3$, $\alpha_2\beta_1$, and $\alpha_v\beta_1$, and CD44 are present on osteoclasts.

The survival of cancer cells in the bone depends on their interactions with other cells. Interactions may be physical, with cell adhesion molecules, or through secreted molecules, such cytokines, chemokines, and other growth factors. Adhesion to various cells in the metastatic site

controls anti-apoptotic and proliferative signals (see [84]). Thus the bone marrow displays numerous adhesion molecules that offer opportunities for interactions between cancer cells and normal cells. Some of these interactions do not occur until the cancer cells are in the bone marrow environment after they express new adhesion molecules.

9 Bone remodeling and inflammation

Rodan [86] in an overview of skeletal development and function, points out the similarities between bone remodeling and inflammation. Many of the same cytokines produced by the immune cells as part of an inflammatory response are also produced by osteoblasts. Some of these, IL-1, IL-11, IL-6, PGE and PTHrP, are also osteoclastogenic. Furthermore, both osteoblasts and osteoclasts express toll-like-receptors [87] and respond to trauma, bacterial infection, and metastases with the production of these same molecules [88–90]. In particular, a set of inflammatory stress molecules (IL-6, IL-8, MCP-1, COX-2) appears in normal bone remodeling as well as under these pathogenic conditions [88]. These factors are made by osteoblasts but can also be produced by macrophages. They attract and activate osteoclasts. Osteoclasts degrade bone matrix, leading to the release of many growth factors. This combination of factors creates a very hospitable environment for cancer cells.

10 Cytokines and chemokines

Once established in the bone microenvironment, a 'vicious cycle' is created among metastatic tumor cells, osteoblasts, and osteoclasts that facilitates increased bone turnover and metastatic cell survival. Guise et al. developed a model of breast cancer metastasis to the bone, based on breast cancer cell overproduction of PTHrP [3, 91] that activates osteoblasts to produce RANK-L. Osteoblast-secreted RANK-L binds the RANK receptor on osteoclasts, inducing osteoclast differentiation and bone matrix degradation. In turn, TGF-β, released from the bone matrix, stimulates the cancer cells to produce more PTHrP [43], thus establishing a positive feedback loop. There is additional evidence that breast cancer-derived IL-8 acts prior to PTHrP to stimulate osteoclastogenesis via both RANK-L dependent and independent mechanisms [92–94]. As a result of constituitive osteoclast activation and an inability of osteoblasts to lay down bone matrix, sustained bone degradation occurs [45, 54]. This feedback establishes a vicious cycle, resulting in continued activation of osteoclasts and breast cancer cells. Ultimately, osteolytic lesions are formed at sites of metastases [10, 57].

It should be noted that the presence of PTHrP is not sufficient for cancer cell metastases to the bone. In a study in which 526 patients with operable breast cancer were examined, it was found that those with PTHrP-positive primary tumors had improved survival and were less likely to develop bone metastases [95]. In those patients with bone metastases, PTHrP presence was found not to be significantly associated with tumor size, vascular invasion, or tumor grade [95]. Thus, it is likely that bone metastases are influenced by other factors in the bone microenvironment besides PTHrP.

In addition to the PTHrP, Bendre et al. found an important role for IL-8. IL-8, the human homolog to murine MIP-2, belongs to the family of CXC chemokines and is naturally constitutively produced by osteoblasts [93, 96, 97]. IL-8 is overexpressed in a bone-homing derivative of MDA-MB-231 human metastatic breast cancer cells suggesting an important role in bone metastasis [94]. IL-8 can stimulate osteoclastogenesis by increasing RANK-L or stimulate the formation of osteoclasts in the absence of RANK-L [92]. It is believed that IL-8 is involved in the early stages of breast cancer metastasis by initiating the bone resorption process [93]. IL-8 also has been shown to increase angiogenesis and suppress osteoblast activity [98, 99]. In addition, IL-8 increases cell motility, invasion, and metastatic potential in breast cancer [93]. If overexpressed in breast cancer cells, IL-8 will lead to increased bone metastasis and osteolytic activity [94]. IL-8 stimulates osteoclast activity independently of RANK-L [92]. Bendre et al. suggested that the vicious cycle with PTHrP is first initiated by breast cancer cells secreting IL-8, thereby stimulating bone resorption by osteoclasts. The release of TGF-β from the bone matrix then stimulates cancer cells to produce more PTHrP, thus continuing the vicious cycle [93].

COX-2 and PGE_2 also have been found to contribute to osteoclast activitation and facilitate the creation of a microenvironment favorable for cancer cell metastasis. COX-2 levels and activity correlate with cancer cell metastasis both *in vitro* and *in vivo* [100–102]. COX-2 expression also has been implicated in the growth, invasion, apoptosis, and angiogenesis of breast cancer [103–105]. COX-2 expression in patients with cancer has shown to be a negative prognostic factor [106]. Singh et al. recently conducted a study investigating the involvement of COX-2 in breast cancer metastases to the bone [107]. Interestingly, overexpression of COX-2 correlated with increased production of IL-8 [108], which has also been linked to increased metastatic occurrence [94]. Singh et al. found that COX-2 induced both the formation of PGE_2 and IL-8 specifically in bone metastatic breast cancer cells. Since PGE_2 and IL-8 are mediators of osteoclast activation [109] (through direct or indirect mechanisms of stimulation of RANKL [92]), a system in which there is overexpression of

COX-2 would favor osteolytic cancer metastases. In addition, Hiraga et al. discovered that bone-derived TGF-β stimulated COX-2 expression, thus enhancing bone metastases in breast cancer [110]. TGF-β, released from the bone during bone resorption, stimulates COX-2 expression and subsequently PGE_2 expression in breast cancer cells. PGE_2 upregulates RANKL expression on osteoblasts, leading to osteoclast activation and increased bone turnover [110]. Finally, Hall et al. investigated the involvement of Wnts, a family of glycoproteins [111], in the promotion of osteoblastic bone metastases in prostate cancer [112]. They found that promotion of Wnt activity (by blocking the Wnt antagonist DKK-1), led to enhanced osteoblastic bone metastases in typically osteolytic PC-3 prostate cancer cells [112]. These results suggest that the involvement of DKK-1 dictates whether bone metastases are osteoblastic or osteolytic, and once again emphasize the importance of the bone microenvironment.

Cancer cell secreted IL-1, IL-6, and IL-11 have also been found to increase osteoclast activation. IL-6 is a pleiotropic cytokine that is naturally expressed by osteoblasts in low quantities. IL-6 receptors are found on osteoclasts and when stimulated, cause osteoclast differentiation and bone resorption [113]. There is a correlation of poor prognosis with increased IL-6 expression and metastatic breast cancer. IL-6 additionally has been implicated with increased breast cancer cell migration [114–116]. IL-1 is also a potent stimulator of osteoclast activation. To explore the notion that increased bone turnover attracts metastatic cancer cells, Sasaki et al. increased bone resorption by injecting recombinant IL-1β locally over the calvaria of nude mice [117]. Four weeks after cancer cell inoculation, osteolytic metastatic cancer cells were found in the calvariae of IL-1 treated mice. None were seen in the control. IL-11 is an additional key player in osteoclast activation. It has been reported that IL-11 mediates the actions of IL-1 on osteoclast development [118]; however, IL-11 has independent effects on osteoclast activity [119]. IL-11, IL-1, and IL-6 have all been found to be involved in an interacting cascade of cytokines which play a large part in osteoclast development and activity. Increased osteoclast activity subsequently creates a bone microenvironment that favors cancer cell metastasis, growth, and development. IL-1 contributes to the production of IL-11 and IL-6 [118]. IL-6 and IL-11 production are also regulated by IL-1, growth factors such as PDGF, IGF-1, and TGF-β, vitamin D, PTHrP, and PTH [119, 120].

11 Bone matrix is fertile soil for metastatic cancer cells

During bone deposition, osteoblasts secrete a variety of growth factors, such as IGF, TGF-β, FGF, and BMPs, that become incorporated into the bone matrix [121]. As bone resorption occurs, these factors are released into the bone microenvironment, making it an attractive place for cancer cells to metastasize and grow [122]. TGF-β released from the bone, in particular, has been found to stimulate the expression of CTGF, IL-11, and PTHrP by cancer cells [42, 123]. These factors are involved in tumor metastasis to bone and subsequently promote additional bone resorption, leading to the release of more growth factors and further preferential tumor metastasis to bone. Growth factors released during bone remodeling and present in the bone microenvironment may be chemoattractive molecules for the cancer cells. Orr et al. and Mundy et al. using a Boyden Chamber assay both demonstrated that the release of growth factors during bone resorption stimulated the chemotaxis of cancer cells [124, 125]. Additionally, cytokines have been implicated in cancer cell chemotaxis to bone. The SDF-1/CXCR4 axis is a ubiquitous chemotaxis mechanism in normal biology and is used for directed migration of a variety of immune and hematopoetic cells [126–129]. Jung et al. found that SDF-1 is secreted by osteoblasts, and that certain factors, namely IL-1β, PDGF-BB, VEGF, tumor necrosis factor-alpha (TNF-α), and PTH, act on osteoblasts to increase SDF-1 production [130]. Consequently, many of these cytokines play a role in increasing osteoclast activity during bone resorption [119, 120]. Furthermore, the results of this study suggested that osteoblast secretion of SDF-1 may be a chemotactic mechanism for stem cell homing. It goes without saying that the SDF-1/CXCR4 axis may be involved in cancer cell chemoattraction as well. In fact, Muller et al., among others [131, 132], explored the idea that metastatic breast cancer cells were responsive to gradients of chemokines [133]. CXCR4 was found to be highly expressed on metastatic breast cancer cells, and its ligand, SDF-1 was found to be highly expressed in organs to which cancer cells preferentially metastasizes (such as bone) [133]. Treatment with a neutralizing antibody to CXCR4 suppressed bone metastatic breast cancer [133]. Sun et al. conducted a similar study using prostate cancer as a model and found comparable results [134]. Once in bone, cancer cells become tethered by integrins and cell adhesion molecules as previously described [135, 136].

Current models suggest that chemokines and cytokines produced by breast cancer cells are key to breast cancer cell metastasis [92–94, 137]. Elevated levels of IL-8 production by human breast cancer cells have been correlated with increased bone metastasis *in vivo* and with stimulation of osteoclast differentiation and bone resorption [92, 94]. Tumor-derived IL-1, IL-6, and IL-11, insulin-growth factor-II, TNF-α, and a variety of other factors can also contribute to osteoclast activation and bone destruction [98, 138].

While breast cancer cells undoubtedly play an important role in breast cancer metastasis to the bone, data have shown that osteoblasts can be directed by the breast cancer cells to produce several inflammatory cytokines that have been implicated in osteoclast activation as well as breast cancer cell migration and survival [93, 139–143]. (Table 1 gives a brief summary of some relevant cytokines and their sources in the bone.) Kinder et al. demonstrated that osteoblasts undergo an inflammatory stress response in the presence of human metastatic breast cancer cells and produce elevated levels of IL-6, human IL-8 (murine KC, MIP-2), and MCP-1 [144]. These cytokines are known to attract, differentiate, and activate osteoclasts; thus co-opting osteoblasts into creating a bone microenvironment that exacerbates bone loss [144]. Similar findings were seen with murine osteoblasts and primary calvarial osteoblasts [144]. These results support the idea that cancer metastases create a unique niche in the bone microenvironment by co-opting normal cells of the bone to favor tumor growth and development.

Furthermore, Mastro and colleagues have preliminary *in vivo* evidence that osteoblasts themselves in the bone naturally produce cytokines that may be chemoattractants for metastatic breast cancer cells. In particular, they showed that metaphyses of bone cleared of bone marrow produced chemokines and cytokines that were different from those in the diaphysis (shaft). Prominent among these were KC (present only in the metaphyses), MIP-2 (murine homolog to human IL-8), and MCP-1 (Fig. 2) (Bussard and Mastro, 2007, unpublished data).

These cytokines were strongly observed in cultures of the bone metaphysis alone and not found in cultures of bone marrow from the metaphysis (Bussard and Mastro, 2007, unpublished data). This observation suggests that the cytokines were specifically produced by the cells of the bone (i.e. osteoblasts) and not the stromal cells. Murine IL-6, KC, and MIP-2 located in femur metaphyses were also found to be increased in the presence of human metastatic breast cancer cells compared with femur metaphyses from control mice (Bussard and Mastro, 2007, unpublished data). Finally, a novel experiment was conducted to monitor and quantify the initial stages (arrival, localization, and initial colonization) of breast cancer cell trafficking in the bone [59]. The DNA from femurs of mice inoculated with MDA-MB-435^{GFP} cells via intracardiac injection were isolated at various times, purified, and subjected to quantitative PCR for a human gene, HERV-1, and the number of breast cancer cells calculated. Femurs were separated into metaphyses and diaphyses. Results indicated that breast cancer cells preferentially migrated within days directly to the distal then proximal metaphyses. Few were found in the diaphyses [59]. These results additionally support the idea that metastatic breast cancer cells may follow a gradient of chemoattractant cytokines as well as suggests the importance of the local bone microenvironment.

In addition to IL-6 and IL-8, KC and MCP-1 are osteoblast-derived cytokines that greatly increase in response to metastatic breast cancer cells (Bussard and Mastro, 2007, unpublished data). MCP-1, a member of the CC chemokine family, is naturally produced by osteoblasts [96]. It regulates bone resorption by stimulating the migration of common monocyte-osteoclast progenitor cells from the blood or the bone marrow to the bone. MCP-1 concentrations are increased in metastatic cell lines, and it is associated with angiogenesis and increased cancer cell survival [145–147]. KC is another member of the CXC chemokine family with homology to IL-8 [148]. KC stimulates angiogenesis and is involved in neutrophil chemotaxis and activation [148, 149]. KC is also expressed by osteoblasts [149].

In addition to directing osteoblasts to secrete cytokines which alter the bone microenvironment, cancer cells affect the bone building cells in other ways as well. Mercer et al. demonstrated that culturing mouse osteoblasts with the conditioned medium from a human metastatic breast cancer cell line inhibited expression of osteoblast differentiation and blocked osteoblast ability to mineralize bone matrix [45]. This *in vitro* observation was confirmed in a mouse study [59]. Since osteoblasts do not differentiate properly in the presence of breast cancer cells, it is possible that the

Table 1 Source of several important chemokines and cytokines in the bone microenvironment in the presence of metastatic breast cancer cells

	Osteoblasts	Bone matrix	Breast cancer cells	Other cells in the bone microenvironment
IL-6	[153, 154]	–	[138, 155]	Bone Marrow Stromal Cells [156], Monocytes, Macrophages [157], and Osteoclasts [158]
IL-8	[155, 159]	–	[94, 155, 160]	Osteoclasts [155, 161], Bone Marrow Stromal Cells [159], Macrophages [162], Endothelial Cells [162]
PTHrP	–	–	[91, 94, 155]	–
TGFβ	[121, 155]	[155, 163]	[155]	Bone Marrow Stromal Cells [164], Endothelial Cells [165]

Many cells in the metastatic bone environment produce cytokines and chemokines. The cell sources of several important ones are indicated. The dash indicates that we were unable to find evidence from the literature or in our laboratory that the molecule was produced in the indicated cell type.

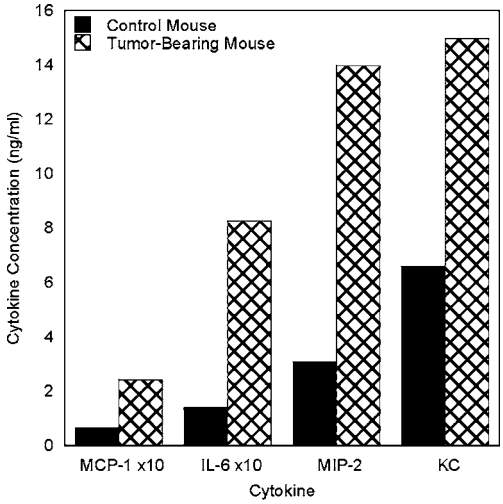

Fig. 2 Cytokine expression of murine femur metaphyses ex-vivo following intracardiac inoculation. MDA-MB-231^{GFP} cells (3×10^5 cells) were inoculated into the left cardiac ventricle of 4–6 week old athymic, female mice. Control mice were untreated. Mice were euthanized at 4 weeks and femurs harvested. The bone marrow was removed and the femur metaphyses were fractionated. Isolated metasphyseal bone pieces were crushed and cultured. Media were collected and tested after 24 h. Murine MCP-1 cytokine production was quantified using ELISAs. Murine IL-6, MIP-2, and KC were quantified using a Bio-Rad Bio-Plex™ murine cytokine quantification assay. Shown is a representative experiment. MCP-1 and IL-6 concentrations were multiplied by 10 in order to be shown on the same graph as MIP-2 and KC

cancer cells may alter the overall protein secretion profile of osteoblasts. This alteration may involve preventing osteoblasts from producing the differentiation proteins necessary for developing into mature, bone-depositing cells, as well as inducing osteoblast production of cytokines that could contribute to progression of bone metastasis, increase activation of osteoclasts, and contribute to the formation of osteolytic lesions.

12 Conclusions

Clearly, the organ microenvironment is extremely influential in cancer cell metastasis to a specific location. Crosstalk between the cancer cell "seed" and the target organ microenvironment "soil" will determine if the cancer cell metastasizes to a specific site and if that microenvironment supports growth and proliferation of the metastatic cancer cell. Only then will the metastatic cancer cell population flourish. Bone provides an especially attractive site for a variety of reasons. Metabolically active areas of bone are well-vascularized with a system that allows various cells to easily enter and exit. The normal remodeling process provides chemotactic and growth factors that attract cancer cells and support them once in place. The bone matrix contains a rich storehouse of growth factors such as TGF-β that are released during bone turnover. Resident cancer cells thrive in the rich cocktail of released cytokines. Finally, both osteoblast and octeoclast activities can be modulated by cancer cells to their advantage. The release of characteristic sets of cytokines by the bone matrix of an osteolytic lesion or osteoblastic lesion (e.g. MCP-1, IL-6, IL-8) will facilitate the chemoattraction and survival of metastatic cancer cells. Understanding the mechanisms behind these events will aid in the development of therapeutics to combat specific metastases and manipulate their target organ microenvironments. While the origin of metastatic variants remains unclear, is it certain that the target organ microenvironment contributes greatly to their metastasis.

13 Unanswered questions

Many unanswered questions remain. One of the most critical is to determine a 'metastatic signature' for the primary tumor which would indicate the possibility of metastasis. However, not all tumor cells that arrive in the bone, even from the same primary tumor, will remain or grow there. Dormant metastases in the bone remain a mystery. It is known that individual cells or micrometastases can be found in patients with no evidence of metastasis [150]. These individuals may never exhibit bone metastasis. On the other hand, bone micrometastases can remain dormant for years in spite of the rich microenvironment. What event triggers that cell to begin to grow?

14 Future studies

It is difficult to study bone metastases and the tumor microenvironment for many reasons. (1) The marrow space is relatively inaccessible. (2) It is also a complex space containing not only bone cells, osteoblasts and osteoclasts, but also hematopoietic cells and transient immune cells. Cell lines, particularly osteoblasts, have been developed that recapitulate in culture the stages of osteoblast differentiation. However, these lines have limitations when compared to intact bone.

We have recently developed a specialized bioreactor that allows extended-term culture of osteoblasts. The cells have been grown uninterrupted for up to 10 months. They proliferate and form a multilayer (>6 cell layers) of mature osteoblasts that begin to mineralize and form macroscopic bone chips [151]. By 10 months the morphology of the cells resembles osteocytes. We have inoculated human metastatic breast cancer cells, MDA-MB-231^{GFP}, into these chambers and have seen by microscopy that the cells adhere, grow, and move through the cell layers, mimicking *in vivo* migration and invasion [152]. We have evidence

that the osteoblasts likewise undergo a stress response and produce increased amounts of IL-6, for example. While the bioreactor has been used to study osteoblast-cancer cell interactions, it will allow introduction of other cell types, e.g. macrophages, lymphocytes. Thus, the bioreactor promises to be a useful 3-D culture system to study and to manipulate the bone-tumor microenvironment.

Acknowledgments KMB was supported by a predoctoral traineeship from the U.S. Army Medical and Materiel Research Command Breast Cancer Program (W81XWH-06-1-0363). The authors' work was supported by was supported by the U.S. Army Medical and Material Research Command Breast Cancer Program; (DAMD 17-02-1-0358 and W81XWH-06-1-0432 to AMM,); National Foundation for Cancer Research, Center for Metastasis Research; The Susan G. Komen Breast Cancer Foundation, BCTR104406; The American Institute of Cancer Research, #06A027-REV2; The authors thank Richard Ball of the Immunomodulation Core, Penn State GCRC (work supported by NIHM01RR10732) for technical advice regarding ELISAs.

References

1. Rubens, R. D., & Mundy, G. R. (2000). *Cancer and the skeleton*. London: Martin Dunitz.
2. Price, J. E. (2004). *The breast comprehensive management of benign and malignant disorders* pp. 537–557. St. Louis: Saunders.
3. Mundy, G. R. (2002). Metastasis to bone: Causes, consequences and therapeutic opportunities. *Nature Reviews. Cancer*, *2*, 584–593.
4. Chambers, A. F., Groom, A. C., & MacDonald, I. C. (2002). Dissemination and growth of cancer cells in metastatic sites. *Nature Reviews. Cancer*, *2*, 563–572.
5. Batson, O. V. (1942). *Annals of Internal Medicine*, *16*, 38–45.
6. Marks, S. C., & Odgren, P. R. (2002). Structure and development of the skeleton. In J. P. Bilezikian, L. G. Raisz, & G. A. Rodan (Eds.) *Principles of bone biology* (vol. 1 (pp. 3–15). New York: Academic.
7. Hancox, N. M. (1972). *Biology of bone*. Cambridge: University Press.
8. Baron, R. (2003). General principles of bone biology. In M. J. Favus (Ed.) *Primer on the metabolic bone diseases and disorders of mineral metabolism* (pp. 1–8). Washington, D.C.: American Society for Bone and Mineral Research.
9. Alberts, B., Johnson, A., Lewis, J., Raff, M., Roberts, K., & Walter, P. (2002). *Molecular biology of the cell* p. 1308. New York: Garland Science.
10. Guise, T. A., & Mundy, G. R. (1998). Cancer and bone. *Endocrine Reviews*, *19*, 18–54.
11. Price, J. S., Oyajobi, B. O., & Russell, R. G. (1994). The cell biology of bone growth. *European Journal of Clinical Nutrition*, *48*(Suppl 1), S131–S149.
12. Minguell, J. J., Erices, A., & Conget, P. (2001). Mesenchymal stem cells. *Experimental Biology and Medicine*, *226*, 507–520.
13. Kanis, J. A., & McCloskey, E. V. (1997). Bone turnover and biochemical markers in malignancy. *Cancer*, *80*, 1538–1545.
14. Gartner, L. P., & Hiatt, J. L. (1997). *Color textbook of histology*. Philadelphia: Saunders.
15. Baron, R. (2003). General principles of bone biology. In J. B. Lian, & S. R. Goldring (Eds.) *Primer on the metabolic bone diseases and disorders of mineral metabolism*. Washington, D.C: American Society for Bone and Mineral Research.
16. Takahashi, N., Udagawa, N., Takami, M., & Suda, T. (2002). Cells of bone: Osteoclast generation. In J. P. Bilezikian, L. G. Raisz, & G. A. Rodan (Eds.) *Principles of bone biology* (vol. 1 (pp. 109–126). San Diego: Academic.
17. Michigami, T., Shimizu, N., Williams, P. J., Miewolna, M., Dallas, S. L., Mundy, G. R., et al. (2000). Cell–cell contact between marrow stromal cells and myeloma cells via VCAM-1 and α4B1 integrin enhances production of osteoclast-stimulating activity. *Blood*, *96*, 1953–1960.
18. Iyengar, P., Combs, T. P., Shah, S. J., Gouon-Evans, V., Pollard, J. W., Albanese, C., et al. (2003). Adipocyte-secreted factors synergistically promote mammary tumorigenesis through induction of anti-apoptotic transcriptional programs and proto-oncogene stabilization. *Oncogene*, *22*, 6408–6423.
19. Maurin, A. C., Chavassieux, P. M., Frappart, L., Delmas, P., Serre, C.-M., & Meunier, P. J. (2000). Influence of mature adipocytes on osteoblast proliferation in human primary cocultures. *Bone*, *26*, 485–489.
20. Maeda, T., Alexander, C. M., & Friedl, A. (2004). Induction of syndecan-1 expression in stromal fibroblasts promotes proliferation of human breast cancer cells. *Cancer Research*, *64*, 612–621.
21. Saad, S., Gottlieb, D. J., Bradstock, K. F., Overall, C. M., & Bendall, L. J. (2002). Cancer cell-associated fibronectin induces release of matrix metalloproteinase-2 from normal fibroblasts. *Cancer Research*, *62*, 283–289.
22. Lau, Y. S., Sabokbar, A., Giele, H., Cerundolo, V., Hofstetter, W., & Athanasou, N. A. (2006). Malignant melanoma and bone resorption. *British Journal of Cancer*, *94*, 1496–1503.
23. Chavez-Macgregor, M., Aviles-Salas, A., Green, D., Fuentes-Alburo, A., Gomez-Ruiz, C., & Aguayo, A. (2005). Angiogenesis in the bone marrow of patients with breast cancer. *Clinical Cancer Research*, *11*, 5396–5400.
24. Eberhardt, C., Gray, P. W., & Tjoelker, L. W. (1997). Human lysophosphatidic acid acyltransferase: cDNA cloning, expression, and localization to chromosome 9q34.3. *Journal of Biological Chemistry*, *272*, 20299–20305.
25. Boucharaba, A., Serre, C. M., Gres, S., Saulnier-Blache, J. S., Bordet, J. C., Guglielmi, J., et al. (2004). Platelet-derived lysophosphatidic acid supports the progression of osteolytic bone metastases in breast cancer. *Journal of Clinical Investigation*, *114*, 1714–1725.
26. Lapumbo, J. S., Talmage, K. E., Massari, J. B., La Jeunesse, C. M., Flick, M. J., Kombrinck, K. W., et al. (2005). Platelets and fibrin(ogen) increase metastatic potential by impeding natural killer cell-mediated elimination of tumor cells. *Blood*, *105*, 178–185.
27. Walsh, M. C., Kim, N., Kadono, Y., Rho, J., Lee, S. Y., Lorenzo, J., et al. (2006). Osteoimmunology: Interplay between the immune system and bone metabolism. In W. E. Paul, C. G. Fathman, & L. H. Glimcher (Eds.) *Annual review of immunology* (vol. 24 (pp. 33–63). Palo Alto: Annual Reviews.
28. Sroato, I., Grano, N., Brunetti, G., Colucci, S., Mussa, A., & Bertetto, O. (2005). Mechanisms of spontaneous osteoclastogenesis in cancer with bone involvement. *FASEB Journal*, *19*, 228–230.
29. Fournier, P. G., Chirgwin, J. M., & Guise, T. A. (2006). New insights into the role of T cells in the vicious cycle of bone metastases. *Current Opinion in Rheumatology*, *18*, 396–404.
30. Coussens, L. M., & Werb, Z. (2002). Inflammation and cancer. *Nature*, *420*, 860–867.
31. Brigati, C., Noonan, D. N., Albini, A., & Benelli, R. (2002). Tumors and inflammatory infiltrates: Friends or foes? *Clinical & Experimental Metastasis*, *19*, 247–258.
32. Schoppmann, S. F., Birner, P., Stockl, J., Kalt, R., Ullrich, R., Caucig, C., et al. (2002). Tumor-associated macrophages express lymphatic endothelial growth factors and are related to peritu-

moral lymphangiogenesis. *American Journal of Pathology*, *161*, 947–956.
33. Torisu, H., Ono, M., Kiryu, H., Furue, M., Ohmoto, Y., Nakayama, J., et al. (2000). Macrophage infiltration correlates with tumor stage and angiogenesis in human malignant melanoma: Possible involvement of TNF-α and IL-1α. *International Journal of Cancer*, *85*, 182–188.
34. Jonjic, N., Peri, G., Bernasconi, S., Sciacca, F. L., Colotta, F., Pelicci, P., et al. (1992). Expression of adhesion molecules and chemotactic cytokines in cultured human mesothelial cells. *Journal of Experimental Medicine*, *176*, 1165–1174.
35. Paget, S. (1889). The distribution of secondary growths in cancer of the breast. *Cancer and Metastasis Reviews*, *8*, 98–101.
36. Roodman, G. D. (2004). Mechanisms of bone metastasis. *New England Journal of Medicine*, *350*, 1655–1664.
37. Roodman, G. D. (2001). Biology of osteoclast activation in cancer. *Journal of Clinical Oncology*, *19*, 3562–3571.
38. Yoneda, T. (1996). Mechanisms of preferential metastasis of breast cancer to bone. *Journal of Clinical Oncology*, *9*, 103–109.
39. Powles, T., Paterson, S., Kanis, J. A., McCloskey, E. V., Ashley, S., Tidy, A., et al. (2002). Randomized, placebo-controlled trial of clodronate in patients with primary operable breast cancer. *Journal of Clinical Oncology*, *20*, 3219–3224.
40. Sasaki, A., Boyce, B. F., Story, B., Wright, K. R., Chapman, M., Boyce, R., et al. (1995). Bisphosphonate risedronate reduces metastatic human breast cancer cells and bone metastases development. *Journal of Clinical Investigation*, *103*, 197–206.
41. Guise, T. A., Yin, J. J., Taylor, S. D., Kumagai, Y., Dallas, M. R., Boyce, B. F., et al. (1996). Evidence for a causal role of parathyroid-hormone-related protein in the pathogenesis of human breast cancer-mediated osteolysis. *Journal of Clinical Investigation*, *98*, 1544–1549.
42. Yin, J.-J., Selander, K., Chirgwin, J. M., Dallas, M. R., Grubbs, B. G., Wieser, R., et al. (1999). TGF-β signaling blockade inhibits PTHrP secretion by breast cancer cells and bone metastases development. *Journal of Clinical Investigation*, *103*, 197–206.
43. Mastro, A. M., Gay, C. V., Welch, D. R., Donahue, H. J., Jewell, J., Mercer, R., et al. (2004). Breast cancer cells induce osteoblast apoptosis: a possible contributor to bone degradation. *Journal of Cell Biology*, *91*, 265–276.
44. Mastro, A. M., Gay, C. V., & Welch, D. R. (2003). The skeleton as a unique environment for breast cancer cells. *Clinical & Experimental Metastasis*, *20*, 275–284.
45. Mercer, R., Miyasaka, C., & Mastro, A. M. (2004). Metastatic breast cancer cells suppress osteoblast adhesion and differentiation. *Clinical & Experimental Metastasis*, *21*, 427–435.
46. Guise, T. A., Yin, J. J., & Mohammad, K. S. (2003). Role of endothelin-1 in osteoblastic bone metastases. *Cancer*, *97*, 779–784.
47. Yin, J. J., Mohammad, K. S., Käkönen, S. M., Harris, S., Wu-Wong, J. R., Wessale, J. L., et al. (2003). A causal role for endothelin-1 in the pathogenesis of osteoblastic bone metastases. *Proceedings of the National Academy of Sciences*, *100*, 10954–10959.
48. Kasperk, C. H., Borcsok, I., Schairer, H. U., Schneider, U., Nawroth, P. P., Niethard, F. U., et al. (1997). Endothelin-1 is a potent regulator of human bone cell metabolism *in vitro*. *Calcified Tissue International*, *60*, 368–374.
49. Nelson, J. B., Hedican, S. P., George, D. J., Reddi, A. H., Piantadosi, S., Eisenberger, M. A., et al. (1995). Identification of endothelin-1 in the pathophysiology of metastatic adenocarcinoma of the prostate. *Nature Medicine*, *1*, 944–949.
50. Yi, B., Williams, P. J., Niewolna, M., Wang, Y., & Yoneda, T. (2002). Tumor-derived platelet-derived growth factor-BB plays a critical role in osteosclerotic bone metastasis in an animal model of human breast cancer. *Cancer Research*, *62*, 917–923.
51. Hiraga, T., Williams, P. J., & Mundy, G. R. (2001). The bisphosphonate ibandronate promotes apoptosis in MDA-MB-231 human breast cancer cells in bone metastases. *Cancer Research*, *61*, 4418–4424.
52. Delmas, P. D., Demiaux, B., Malaval, L., Chapuy, M. C., Edouard, C., & Meunier, P. J. (1986). Serum bone gamma carboxyglutamic acid-containing protein in primary hyperthyroidism and in malignant hypercalcemia. *Journal of Clinical Investigation*, *77*, 985–991.
53. Kukreja, S. C., Rosol, T. J., Shevrin, D. H., & York, P. A. (1998). Quantitative bone histomorphometry in nude mice bearing a human squamous cell lung cancer. *Journal of Bone and Mineral Research*, *3*, 341–346.
54. Stewart, A. F., Vignery, A., Silverglate, A., Ravin, N. D., Livolsi, V., Broadus, A. E., et al. (1982). Quantitative bone histomorphology in humoral hypercalcemia of malignancy: Uncoupling of bone cell activity. *Journal of Clinical Endocrinology and Metabolism*, *55*, 219–227.
55. Taube, T., Elomaa, I., Blomqvist, C., Benton, N. C., & Kanis, J. A. (1994). Histomorphometric evidence for osteoclast-mediated bone resorption in metastatic breast cancer. *Bone*, *15*, 161–166.
56. Galasko, C. S. (1982). Mechanisms of lytic and blastic metastatic disease of bone. *Clinica Ortopedica*, *169*, 20–27.
57. Martin, T. J., & Moseley, J. M. (2000). Mechanisms in the skeletal complications of breast cancer. *Endocrine Related Cancer*, *7*, 271–284.
58. Mundy, G. R., & Guise, T. A. (2000). Pathophysiology of bone metastasis. In R. D. Rubens, & G. R. Mundy (Eds.) *Cancer and the skeleton* (pp. 43–64). London: Martin Dunitz Ltd.
59. Phadke, P. A., Mercer, R. R., Harms, J. F., Jia, Y., Kappes, J. C., Frost, A. R., et al. (2006). Kinetics of metastatic breast cancer cell trafficking in bone. *Clinical Cancer Research*, *12*, 1431–1440.
60. Everts, V., Delaisse, J. M., Korper, W., Jansen, D. C., Tigchelaar-Gutter, W., Saftig, P., et al. (2002). The bone lining cell: Its role in cleaning Howship's lacunae and initiating bone formation. *Journal of Bone and Mineral Research*, *17*, 77–90.
61. Glinsky, V. V. (2006). Intravascular cell-to-cell adhesive interactions and bone metastasis. *Cancer and Metastasis Reviews*, *25*, 531–540.
62. Sasaki, A., Boyce, B. F., Story, B., Wright, K. R., Chapman, M., Boyce, R., et al. (1995). Bisphosphonate risedronate reduces metastatic human breast cancer burden in bone in nude mice. *Cancer Research*, *55*, 3551–3557.
63. Mazo, I. B., & von Andrian, U. H. (1999). Adhesion and homing of blood-borne cells in bone marrow microvessels. *Journal of Leukocyte Biology*, *66*, 25–32.
64. Buckwalter, J. A. (1995). Pharmacological treatment of soft-tissue injuries. *Journal of Bone and Joint Surgery. American Volume*, *77*, 1902–1914.
65. Schnitzer, J. E., McKinstry, P., Light, T. R., & Ogden, J. A. (1982). Quantitation of regional chondro-osseous circulation in canine tibia and femur. *American Journal of Physiology*, *242*, H365–H375.
66. Stephenson, R. B. (1989). The splanchnic circulation. In H. D. Patton, A. F. Fuchs, B. Hille, A. M. Scher, & R. Steiner (Eds.) *Textbook of physiology* (pp. 911–923). Philadelphia: Saunders.
67. Mastro, A. M., Gay, C. V., & Welch, D. R. (2003). The skeleton as a unique environment for breast cancer cells. *Clinical & Experimental Metastasis*, *20*, 275–284.
68. Makuch, L. A., Sosnoski, D. M., & Gay, C. V. (2006). Osteoblast-conditioned media influence the expression of E-selectin on bone-derived vascular endothelial cells. *Journal of Cellular Biochemistry*, *98*, 1221–1229.
69. Lehr, J. E., & Pienta, K. J. (1998). Preferential adhesion of prostate cancer cells to a human bone marrow endothelial cell line. *Journal of the National Cancer Institute*, *90*, 118–123.

70. Scott, L. J., Clarke, N. W., George, N. J., Shanks, J. H., Testa, N. G., & Lang, S. H. (2001). Interactions of human prostatic epithelial cells with bone marrow endothelium: Binding and invasion. *British Journal of Cancer*, *84*, 1417–1423.
71. Glinsky, V. V., Glinsky, G. V., Rittenhouse-Olson, K., Huflejt, M. E., Glinskii, O. V., Deutscher, S. L., et al. (2001). The role of Thomsen–Friedenreich antigen in adhesion of human breast and prostate cancer cells to the endothelium. *Cancer Research*, *61*, 4851–4857.
72. Glinsky, V. V., Huflejt, M. E., Glinsky, G. V., Deutscher, S. L., & Quinn, T. P. (2000). Effects of Thomsen–Friedenreich antigen-specific peptide P-30 on beta-galactoside-mediated homotypic aggregation and adhesion to the endothelium of MDA-MB-435 human breast carcinoma cells. *Cancer Research*, *60*, 2584–2588.
73. McEver, R. P. (1997). Selectin-carbohydrate interactions during inflammation and metastasis. *Glycoconjugate Journal*, *14*, 585–591.
74. Cooper, C. R., Bhatia, J. K., Muenchen, H. J., McLean, L., Hayasaka, S., Taylor, J., et al. (2002). The regulation of prostate cancer cell adhesion to human bone marrow endothelial cell monolayers by androgen dihydrotestosterone and cytokines. *Clinical & Experimental Metastasis*, *19*, 25–33.
75. Glinskii, O. V., Turk, J. R., Pienta, K. J., Huxley, V. H., & Glinsky, V. V. (2004). Evidence of porcine and human endothelium activation by cancer-associated carbohydrates expressed on glycoproteins and tumour cells. *Journal of Physiology*, *554*, 89–99.
76. Krause, T., & Turner, G. A. (1999). Are selectins involved in metastasis? *Clinical & Experimental Metastasis*, *17*, 183–192.
77. Khaldoyanidi, S. K., Glinsky, V. V., Sikora, L., Glinskii, A. B., Mossine, V. V., Quinn, T. P., et al. (2003). MDA-MB-435 human breast carcinoma cell homo- and heterotypic adhesion under flow conditions is mediated in part by Thomsen–Friedenreich antigen-galectin-3 interactions. *Journal of Biological Chemistry*, *278*, 4127–4134.
78. Jacobsen, K., Kravitz, J., Kincade, P. W., & Osmond, D. G. (1996). Adhesion receptors on bone marrow stromal cells: *in vivo* expression of vascular cell adhesion molecule-1 by reticular cells and sinusoidal endothelium in normal and gamma-irradiated mice. *Blood*, *87*, 73–82.
79. Pecheur, I., Peyruchaud, O., Serre, C. M., Guglielmi, J., Voland, C., Bourre, F., et al. (2002). Integrin alpha(v)beta3 expression confers on tumor cells a greater propensity to metastasize to bone. *FASEB Journal*, *16*, 1266–1268.
80. Faccio, R., Grano, M., Colucci, S., Zallone, A. Z., Quaranta, V., & Pelletier, A. J. (1998). Activation of alphav beta3 integrin on human osteoclast-like cells stimulates adhesion and migration in response to osteopontin. *Biochemical and Biophysical Research Communications*, *249*, 522–525.
81. Carron, C. P., Meyer, D. M., Engleman, V. W., Rico, J. G., Ruminski, P. G., Ornberg, R. L., et al. (2000). Peptidomimetic antagonists of alphavbeta3 inhibit bone resorption by inhibiting osteoclast bone resorptive activity, not osteoclast adhesion to bone. *Journal of Endocrinology*, *165*, 587–598.
82. Liapis, H., Flath, A., & Kitazawa, S. (1996). Integrin alpha V beta 3 expression by bone-residing breast cancer metastases. *Diagnostic Molecular Pathology*, *5*, 127–135.
83. Chellaiah, M., Kizer, N., Silva, M., Alvarez, U., Kwiatkowski, D., & Hruska, K. A. (2000). Gelsolin deficiency blocks podosome assembly and produces increased bone mass and strength. *Journal of Cell Biology*, *148*, 665–678.
84. Harms, J. F., Welch, D. R., Samant, R. S., Shevde, L. A., Miele, M. E., Babu, G. R., et al. (2003). A small molecule antagonist of the alpha v beta 3 integrin suppresses MDA-MB-435 skeletal metastasis. *Clinical & Experimental Metastasis*, *21*, 119–128.
85. Horton, M. A., Nesbitt, S. A., Bennett, J. H., & Stenbeck, G. (2002). Integrins and other cell surface attachment molecules of bone cells. In J. P. Bilezikian, L. G. Raisz, & G. A. Rodan (Eds.) *Principles of bone biology* (vol. 1 (pp. 265–286). San Diego: Academic.
86. Rodan, G. A. (2003). The development and function of the skeleton and bone metastases. *Cancer*, *97*, 726–732.
87. Kikuchi, T., Matsuguchi, T., Tsuboi, N., Mitani, A., Tanaka, S., Matsuoka, M., et al. (2001). Gene expression of osteoclast differentiation factor is induced by lipopolysaccharide in mouse osteoblasts via Toll-like receptors. *Journal of Immunology*, *166*, 3574–3579.
88. Fritz, E., Jacobs, J., Glant, T., & Roebuck, K. (2005). Chemokine IL-8 induction by particulate wear debris in osteoblasts is mediated by NF-kappaB. *Journal of Orthopaedic Research*, *23*, 1249–1257.
89. Lisignoli, G., Toneguzzi, S., Grassi, F., Piacentini, A., Tschon, M., Cristino, S., et al. (2002). Different chemokines are expressed in human arthritic bone biopsies: IFN-gamma and IL-6 differently modulate IL-8, MCP-1 and rantes production by arthritic osteoblasts. *Cytokine*, *20*, 231–238.
90. Fritz, E., Glant, T., Vermes, C., Jacobs, J., & Roebuck, K. (2005). Chemokine gene activation in human bone marrow-derived osteoblasts following exposure to particulate wear debris. *Journal of Biomedical Materials Research A*, *77*, 192–201.
91. Guise, T. A., Yin, J. J., Taylor, S. D., Kumagai, Y., Dallas, M., Boyce, B. F., et al. (1996). Evidence for a causal role of parathyroid hormone-related protein in the pathogenesis of human breast-cancer-mediated osteolysis. *Journal of Clinical Investigation*, *98*, 1544–1549.
92. Bendre, M., Montague, D. C., Peery, T., Akel, N. S., Gaddy, D., & Suva, L. J. (2003). Interleukin-8 stimulation of osteoclastogenesis and bone resorption is a mechanism for the increased osteolysis of metastatic bone disease. *Bone*, *33*, 28–37.
93. Bendre, M., Gaddy, D., Nicholas, R. W., & Suva, L. J. (2003). Breast cancer metastasis to bone. *Clinical Orthopaedics and Related Research*, *415S*, S39–S45.
94. Bendre, M., Gaddy-Kurten, D., Foote-Mon, T., Akel, N. S., Skinner, R. A., Nicholas, R. W., et al. (2002). Expression of interleukin 8 and not parathyroid hormone-related protein by human breast cancer cells correlates with bone metastasis *in vivo*. *Cancer Research*, *62*, 5571–5579.
95. Henderson, M. A., Danks, J. A., Slavin, J. L., Bryrnes, G. B., Choong, P. F. M., Spillane, J. B., et al. (2006). Parathyroid hormone-related protein localization in breast cancers predict improved prognosis. *Cancer Research*, *66*, 2250–2256.
96. Horowitz, M. C., & Lorenzo, J. A. (2002). *Principles of bone biology*. San Diego: Academic.
97. Graves, D. T., Jiang, Y., & Valente, A. J. (1999). The expression of monocyte chemoattractant protein-1 and other chemokines by osteoblasts. *Frontiers in Bioscience*, *4*, 571–580.
98. Guise, T. A., & Chirgwin, J. M. (2003). Transforming growth factor-beta in osteolytic breast cancer bone metastases. *Clinical Orthopaedics and Related Research*, *4155*, 532–538.
99. Dovio, A., Sartori, M. L., Masera, R. G., Peretti, L., Perotti, L., & Angeli, A. (2004). Effects of physiological concentrations of steriod hormones and interleukin-11 on basal and stimulated production of interleukin-8 by human osteoblast-like cells with different functional profiles. *Clinical and Experimental Rheumatology*, *22*, 79–84.
100. Kundu, N., Yang, Q., Dorsey, R., & Fulton, A. M. (2001). Increased cyclooxygenase-2 (COX-2) expression and activity in a murine model of metastatic breast cancer. *International Journal of Cancer*, *94*, 681–686.
101. Liu, C. H., Chang, S.-H., Narko, K., Trifan, O. C., Wu, M.-T., Smith, E., et al. (2001). Overexpression of cyclooxygenase-2 is sufficient to induce tumorigenesis in transgenic mice. *Journal of Biological Chemistry*, *276*, 18563–18569.
102. Ristimaki, A., Sivula, A., Lundin, J., Lundin, M., Salminen, T., Haglund, C., et al. (2002). Prognostic significance of elevated

cycloozygenase-2 expression in breast cancer. *Cancer Research*, *62*, 632–635.
103. Rozic, J. G., Chakraborty, C., & Lala, P. K. (2001). Cyclo-oxygenase inhibitors retard murine mammary tumor progression by reducing tumor cell migration, invasiveness and angiogenesis. *International Journal of Cancer*, *93*, 497–506.
104. Witters, L. M., Crispino, J., Fraterrigo, T., Green, J., Lipton, A. (2003). Effects of the combination of docetaxel, zoledronic acid, and a COX-2 inhibitor on the growth of human breast cancer cell line. *American Journal of Clinical Oncology*, *26*.
105. Davies, G., Salter, J., Hills, M., Martin, L. A., Sacks, N., & Dowsett, M. (2003). Correlation between cyclooxygenase-2 expression and angiogenesis in human breast cancer. *Clinical Cancer Research*, *9*, 2651–2656.
106. Denkert, C., Winzer, K. J., Muller, B. M., Weichert, W., Pest, S., Kobel, M., et al. (2003). Elevated expression of cyclooxygenase-2 is a negative prognostic factor for disease free survival and overall survival in patients with breast carcinoma. *Cancer*, *97*, 2978–2987.
107. Singh, B., Berry, J. A., Vincent, L. E., & Lucci, A.(2006). Involvement of IL-8 in COX-2-mediated bone metastases from breast cancer. *Journal of Surgical Research*.
108. Benoy, I. H., Salgado, R., Van Dam, P., Geboers, K., Van Marck, E., Scharpe, S., et al. (2004). Increased serum interleukin-8 in patients with early and metastatic breast cancer correlates with early dissemination and survival. *Clinical Cancer Research*, *10*, 7157–7162.
109. Li, X., Pilbeam, C. C., Pan, L., Breyer, R. M., & Raisz, L. G. (2002). Effects of prostaglandin E_2 on gene expression in primary osteoblastic cells from prostaglandin receptor knockout mice. *Bone*, *30*, 567–573.
110. Hiraga, T., Myoui, A., Choi, M. E., Yoshikawa, H., & Yoneda, T. (2006). Stimulation of cyclooxygenase-2 expression by bone-derived transforming growth factor-β enhances bone metastases in breast cancer. *Cancer Research*, *66*, 2067–2073.
111. Westendorf, J. J., Kahler, R. A., & Schroeder, T. M. (2004). Wnt signaling in osteoblasts and bone diseases. *Gene*, *341*, 19–39.
112. Hall, C. L., Bafico, A., Dai, J., Aaronson, S. A., & Keller, E. T. (2005). Prostate cancer cells promote osteoblastic bone metastases through Wnts. *Cancer Research*, *65*, 7554–7560.
113. Manolagas, S. C. (1995). Role of cytokines in bone resorption. *Bone*, *17*, 63S–67S.
114. Morinaga, Y., Fujita, N., Ohishi, K., & Tsurot, T. (1997). Stimulation of interleukin-11 production from osteoclast-like cells by transforming growth factor-beta and tumor cell factors. *International Journal of Cancer*, *71*, 422–428.
115. Zhang, G. J., & Adachi, I. (1999). Serum interleukin-6 levels correlate to tumor progression and prognosis in metastatic breast carcinoma. *Anticancer Research*, *19*, 1427–1432.
116. Yoneda, T., Sasaki, A., & Mundy, G. R. (1994). Osteolytic bone metastasis in breast cancer. *Breast Cancer Research and Treatment*, *32*, 273–284.
117. Sasaki, A., Williams, P., Mundy, G. R., & Yoneda, T. (1994). Osteolysis and tumor growth are enhanced in sites of increased bone turnover *in vivo*. *Journal of Bone and Mineral Research*, *9*, S294.
118. Manolagas, S. C. (1995). Role of cytokines in bone resorption. *Bone*, *17*, 63S–67S.
119. Girasole, G., Passeri, G., Jilka, R. L., & Monolagas, S. C. (1994). Interleukin-11: A new cytokine critical for osteoclast development. *Journal of Clinical Investigation*, *93*, 1516–1524.
120. Manolagas, S. C., Jilka, R. L., Girasole, G., Passeri, G., & Bellido, T. (1994). Estrogens, cytokines, and the pathophysiology of osteoporosis. In P. O. Kohler (Ed.) *Current opinion in endocrinology and diabetes* (pp. 275–281). Philadelphia: Current Science.
121. Hauschka, P. V., Mavrakos, A. E., Iafrati, M. D., Doleman, S. E., & Klagsburn, M. (1986). Growth factors in bone matrix. Isolation of multiple types by affinity chromatography on heparin-Sepharose. *Journal of Biological Chemistry*, *261*, 12665–12674.
122. Pfeilschifter, J., & Mundy, G. R. (1987). Modulation of transforming growth factor beta activity in bone cultures by osteotropic hormones. *Proceedings of the National Academy of Sciences*, *84*, 2024–2028.
123. Kang, Y., Siegel, P. M., Shu, W., Drobnjak, M., Kakonen, S. M., Cordon-Cardo, C., et al. (2003). A multigenic program mediating breast cancer metastasis to bone. *Cancer Research*, *3*, 537–549.
124. Mundy, G. R., DeMartino, S., & Rowe, D. W. (1981). Collagen and collagen fragments are chemotactic for tumor cells. *Journal of Clinical Investigation*, *68*, 1102–1105.
125. Orr, F. W., Varani, J., Gondek, M. D., Ward, P. A., & Mundy, G. R. (1979). Chemotactic response of tumor cells to productions of resorbing bone. *Science*, *203*, 176–179.
126. Zou, Y.-R., Kottmann, A. H., Kuroda, M., Tainwchi, I., & Littman, D. R. (1998). Function of the chemokine receptor CXCR4 in hematopoiesis and in cerebellar development. *Nature*, *393*, 595–599.
127. Nagasawa, T., Hirota, S., Tachibana, K., Takakura, N., Nishikawa, S., Kitamura, Y., et al. (1996). Defects of B-cell lymphopoiesis and bone marrow myelopoiesis in mice lacking the CXC chemokine PBSF/SDF-1. *Nature*, *382*, 635–638.
128. Bluel, C. C., Fuhlbrigge, R. C., Casanovas, J. M., Aiuiti, A., & Springer, T. A. (1996). Highly efficacious lymphocyte chemo-attractant, stromal cell-derived factor 1 (SDF-1). *Journal of Experimental Medicine*, *184*, 1101–1109.
129. D'Apuzzo, M., Rolink, A., Loetscher, M., Hoxie, J. A., Clark-Lewis, I., Melchers, F., et al. (1997). The chemokine SDF-1, stromal cell-derived factor-1, attracts early stage B cell precursors via the chemokine receptor CXCR4. *European Journal of Immunology*, *27*, 1788–1793.
130. Jung, Y., Wang, J., Schneider, A., Sun, Y.-X., Koh-Paige, A. J., Osman, N. I., et al. (2006). Regulation of SDF-1 (CXCL12) production by osteoblasts; a possible mechanism for stem cell homing. *Bone*, *38*, 497–508.
131. Wang, J., Wang, J., Sun, Y.-X., Song, W., Nor, J. E., Wang, C. Y., et al. (2005). Diverse signaling pathways through the SDF-1/CXCR4 chemokine axis in prostate cancer cell lines leads to altered patterns of cytokine secretion and angiogenesis. *Cellular Signalling*, *17*, 1578–1592.
132. Luker, K. E., & Luker, G. D. (2005). Functions of CXCL12 and CXCR4 in breast cancer. *Cancer Letters*.
133. Muller, A., Homey, B., Soto, H., Ge, N., Catron, D., Buchanan, M. E., et al. (2001). Involvement of chemokine receptors in breast cancer metastasis. *Nature*, *410*, 50–56.
134. Sun, Y.-X., Schneider, A., Jung, Y., Wang, J., Dai, J., Wang, J., et al. (2005). Skeletal localization and neutralization of the SDF-1 (CXCL12)/CXCR4 axis blocks prostate cancer metastasis and growth in osseous sites *in vivo*. *Journal of Bone and Mineral Research*, *20*, 318–329.
135. Siclari, V. A., Guise, T. A., & Chirgwin, J. M. (2006). Molecular interactions between breast cancer cells and the bone microenvironment drive skeletal metastases. *Cancer and Metastasis Reviews*, *25*, 621–633.
136. Yoneda, T. (2000). Cellular and molecular basis of preferential metastasis of breast cancer to bone. *Journal of Orthopaedic Science*, *5*, 75–81.
137. Guise, T. A. (2000). Molecular mechanisms of osteolytic bone metastases. *Cancer*, *88*, 2892–2898.
138. Pederson, L., Winding, B., Foged, N. T., Spelsberg, T. C., & Oursler, M. J. (1999). Identification of breast cancer cell line-derived paracrine factors that stimulate osteoclast activity. *Cancer Research*, *59*, 5849–5855.
139. Badache, A., & Hynes, N. E. (2001). Interleukin 6 inhibits proliferation and, in cooperation with an epidermal growth factor

receptor autocrine loop, increases migration of T47D breast cancer cells. *Cancer Research*, *61*, 383–391.
140. Kotake, S., Sato, K., Kim, K. J., Takahashi, N., Udagawa, N., Nakamura, I., et al. (1996). Interleukin-6 and soluble interleukin-6 receptors in the synovial fluids from rheumatoid arthritis patients are responsible for osteoclast-like cell formation. *Journal of Bone and Mineral Research*, *11*, 88–95.
141. Scapini, P., Morini, M., Tecchio, C., Minghelli, S., Di Carlo, E., Tanghetti, E., et al. (2004). CXCL1/macrophage inflammatory protein-2-induced angiogenesis *in vivo* is mediated by neutrophil-derived vascular endothelial growth factor-A. *Journal of Immunology*, *172*, 5034–5040.
142. Goede, V., Brogelli, L., Ziche, M., & Augustin, H. G. (1999). Induction of inflammatory angiogenesis by monocyte chemoattractant protein-1. *International Journal of Cancer*, *82*, 765–770.
143. Fitzgerald, K. A., O'Neill, L. A. J., Gearing, A. J. H., & Callard, R. E. (2001). *The cytokine facts book*. New York: Academic.
144. Kinder, M. , Chislock, E. M., Bussard, K. M., Shuman, L. A., & Mastro, A. M. (2007). Metastatic breast cancer induces an osteoblast inflammatory response. *Experimental Cell Research*, Oct. 4 (in press).
145. Neumark, E., Cohn, M. A., Lukanidin, E., Witz, I. P., & Ben-Baruch, A. (2002). Possible co-regulation of genes associated with enhanced progression of mammary adenocarcinomas. *Immunology Letters*, *82*, 111–121.
146. Neumark, E., Sagi-Assif, O., Shalmon, B., Ben-Baruch, A., & Witz, I. P. (2003). Progression of mouse mammary tumors: MCP-1-TNF-alpha cross regulatory pathway and clonal expression of promalignancy and antimalignancy factors. *International Journal of Cancer*, *106*, 879–886.
147. Ueno, T., Toi, M., Saji, J., Muta, M., Bando, H., Kuroi, K., et al. (2000). Significance of macrophage chemoattractant protein-1 in macrophage recruitment, angiogenesis, and survival in human breast cancer. *Clinical Cancer Research*, *6*, 3282–3289.
148. Mukaida, N., Ketlunsky, S. A., & Matsushima, K. (2003). *The cytokine handbook*. Amsterdam: Academic.
149. Bischoff, D. S., Zhu, J. H., Makhijani, N. S., & Yamaguchi, D. T. (2005). KC chemokine expression by TGF-B in C3H10T1/2 cells induced towards osteoblasts. *Biochemical and Biophysical Research Communications*, *326*, 364–370.
150. Wolfle, U., Muller, V., & Pantel, K. (2006). Disseminated tumor cells in breast cancer: detection, characterization and clinical relevance. *Future Oncology*, *2*, 553–561.
151. Dhurjati, R., Liu, X., Gay, C. V., Mastro, A. M., & Vogler, E. A. (2006). Extended-term culture of bone cells in a compartmentalized bioreactor. *Tissue Engineering*, *12*, 3045–3054.
152. Dhurjati, R., Shuman, L. A., Krishnan, V., Mastro, A. M., Gay, C. V., & Vogler, E. A. (2006). Compartmentalized bioreactor: *In vitro* model for osteobiology and osteopathology. *28th Annual Meeting of the American Society for Bone and Mineral Research*, *21*, 349.
153. Deyama, Y., Takeyama, S., Suzuki, K., Yoshimura, Y., Nishikata, M., & Matsumoto, A. (2001). Inactivation of NF-KB involved in osteoblast development through interleukin-6. *Biochemical and Biophysical Research Communications*, *282*, 1080–1084.
154. Ishimi, Y., Miyaura, C., Jin, C. H., Akatsu, T., Abe, E., Nakamura, Y., et al. (1990). IL-6 is produced by osteoblasts and induces bone resorption. *Journal of Immunology*, *145*, 3297–3303.
155. Bendre, M., Gaddy, D., Nicholas, R. W., & Suva, L. J. (2003). Breast cancer metastasis to bone: It is not all about PTHrP. *Clinical Orthopaedics and Related Research*, *415S*, S39–S45.
156. Girasole, G., Jilka, R. L., Passeri, G., Boswell, S., Boder, G., Williams, D. C., et al. (1992). 17 beta-estradiol inhibits interleukin-6 production by bone marrow-derived stromal cells and osteoblasts *in vitro*: A potential mechanism for the antiosteoporotic effect of estrogens. *Journal of Clinical Investigation*, *89*, 883–891.
157. Linkhart, T. A., Linkhart, S. G., MacCharles, D. C., Long, D. L., & Strong, D. D. (1991). Interleukin-6 messenger RNA expression and interleukin-6 protein secretion in cells isolated from normal human bone. *Journal of Bone and Mineral Research*, *6*, 1285–1294.
158. O'Keefe, R. J., Teot, L. A., Singh, D., Puzas, J. E., Rosier, R. N., & Hicks, D. G. (1997). Osteoclasts constitutively express regulators of bone resorption: An immunohistochemical and in situ hybridization study. *Laboratory Investigation*, *76*, 457–465.
159. Chaudhary, L. R., & Avioli, L. V. (1994). Dexamethasone regulates IL-1 beta and TNF-alpha-induced interleukin-8 production in human bone marrow stromal and osteoblast-like cells. *Calcified Tissue International*, *55*, 16–20.
160. Bendre, M. S., Margulies, A. G., Walser, B., Akel, N. S., Bhattacharrya, S., Skinner, R. A., et al. (2005). Tumor-derived interleukin-8 stimulates osteolysis independent of the receptor activator of nuclear factor-kappaB ligand pathway. *Cancer Research*, *65*, 11001–11009.
161. Rothe, L., Collin-Osdoby, P., Chen, Y., Sunyer, T., Chaudhary, L., Tsay, A., et al. (1998). Human osteoclasts and osteoclast-like cells synthesize and release high basal and inflammatory stimulated levels of the potent chemokine interleukin-8. *Endocrinology*, *139*, 4353–4363.
162. Sozzani, S., Locati, M., Allavena, P., Van Damme, J., & Mantovani, A. (1996). Chemokines: A superfamily of chemotactic cytokines. *International Journal of Clinical & Laboratory Research*, *26*, 69–82.
163. Lipton, A. (2000). Bisphosphonates and breast carcinoma: Present and future. *Cancer*, *88*, 3033–3037.
164. Oslen, N. J., Gu, X., & Kovacs, W. J. (2001). Bone marrow stromal cells mediate androgenic suppression of B lymphocyte development. *Journal of Clinical Investigation*, *108*, 1697–1704.
165. Schultz-Cherry, S., Ribeiro, S., Gentry, L., & Murphy-Ullrich, J. E. (1994). Thrombospondin binds and activates the small and large forms of latent transforming growth factor-beta in a chemically defined system. *Journal of Biological Chemistry*, *269*, 26775–26782.

Clin Exp Metastasis
DOI 10.1007/s10585-008-9185-z

RESEARCH PAPER

Metastatic breast cancer cells colonize and degrade three-dimensional osteoblastic tissue in vitro

Ravi Dhurjati · Venkatesh Krishnan · Laurie A. Shuman · Andrea M. Mastro · Erwin A. Vogler

Received: 20 March 2008 / Accepted: 20 May 2008

Abstract Metastatic breast cancer cells (BCs) colonize a mineralized three-dimensional (3D) osteoblastic tissue (OT) grown from isolated pre-osteoblasts for up to 5 months in a specialized bioreactor. Sequential stages of BC interaction with OT include BC adhesion, penetration, colony formation, and OT reorganization into "Indian files" paralleling BC colonies, heretofore observed only in authentic pathological cancer tissue. BCs permeabilize OT by degrading the extracellular collagenous matrix (ECM) in which the osteoblasts are embedded. OT maturity (characterized by culture age and cell phenotype) profoundly affects the patterns of BC colonization. BCs rapidly form colonies on immature OT (higher cell/ECM ratio, osteoblastic phenotype) but fail to completely penetrate OT. By contrast, BCs efficiently penetrate mature OT (lower cell/ECM ratio, osteocytic phenotype) and reorganize OT. BC colonization provokes a strong osteoblast inflammatory response marked by increased expression of the pro-inflammatory cytokine IL-6. Furthermore, BCs inhibit osteoblastic bone formation by down-regulating synthesis of collagen and osteocalcin. Results strongly suggest that breast cancer disrupts the process of osteoblastic bone formation, in addition to upregulating osteoclastic bone resorption as widely reported. These observations may help explain why administration of bisphosphonates to humans with osteolytic metastases slows lesion progression by inhibiting osteoclasts but does not bring about osteoblast-mediated healing.

Keywords Bone metastases · Breast cancer · Colonization · Inflammation · Invasion · Osteoblast · Three-dimensional cell culture model

Ravi Dhurjati and Venkatesh Krishnan contributed equally to this work.

This work is a contribution from the Osteobiology Research Group, The Pennsylvania State University.

R. Dhurjati · E. A. Vogler
Department of Materials Science and Engineering, The Pennsylvania State University, University Park, PA 16802, USA

V. Krishnan · L. A. Shuman · A. M. Mastro
Department of Biochemistry and Molecular Biology, The Pennsylvania State University, University Park, PA 16802, USA

E. A. Vogler
Materials Research Institute and the Huck Institutes of Life Sciences, The Pennsylvania State University, University Park, PA 16802, USA

E. A. Vogler (✉)
Department of Bioengineering, The Pennsylvania State University, University Park, PA 16802, USA
e-mail: eav3@psu.edu

Introduction

Skeleton is a favored site for the metastatic spread of breast, prostrate, lung, and multiple myeloma cancers [1]. Metastatic cancer in bone is particularly pernicious because, once bone colonization occurs, the cure rate is almost zero [1–3]. Cancers in bone progress with significant morbidity related to bone loss (lytic cancer) or gain (blastic cancer), hypercalcemia, pathological fractures, and spinal compression [3]. Specific aspects of cancer cell growth in bone such as dormancy [4, 5] contribute to a protracted disease progression with intervals of remission that can sometimes last up to decades [6]. Metastatic colonization of bone is the culmination of a sequence of steps beginning with migration of cancer cells to bone, survival and adaptation to the bone environment, proliferation to form micrometastases, and finally development of vascularized

tumors [7]. Successful progression through these different stages requires reciprocal interactions between cancer cells and the bone microenvironment [8]. Of the cancer cells that reach bone, only a small percentage of cells develop into clinically detectable tumors; the remaining either die, persist as solitary dormant cells, or develop into pre-angiogenic micrometastases that fail to develop into overt tumors [7, 9].

The specific cellular and molecular mechanisms responsible for the variable fate of cancer cells in bone are incompletely understood [7]. Investigations of metastasis suppressor genes [10] and cell trafficking studies using intravital videomicroscopy [11, 12] have revealed that early stage, pre-angiogenic interactions between the cancer cells and the bone environment are crucial regulators of cancer cell growth and disease progression. Evidence from these two independent lines of investigation suggest that early stages of metastatic colonization constitute a rate-limiting step in disease progression that can be an effective target for therapeutic intervention [13]. Consequently, a full appreciation of the mechanistic basis of metastatic colonization can greatly enhance discovery of drugs aimed at the arrest of cancer cell growth that will limit disease progression to a minimal residual, asymptomatic stage [14].

One difficulty encountered in drug development is that early stage detection of cancer cell colonization is difficult, both in the clinic and laboratory, because of the refractory nature of whole bone and lack of relevant in vitro models, respectively. Excised tissue [15] faithfully captures end stages of cancer in bone associated with fully-developed tumors, but the critical initial stages of disease remain largely inaccessible in this surrogate. Effective in vitro bone models must strike a balance between experimental efficiency and retention of biological complexity. In particular, the model must recapitulate the in vivo bone microenvironment to the greatest extent possible. Three-dimensional (3D) tissue models have become a focus of recent investigation for this reason [16]. Herein, we report use of a multiple-cell layer (3D) mineralizing osteoblastic tissue (OT) grown from isolated osteoblasts in a specialized bioreactor as an effective surrogate for studies of cancer colonization of bone. By challenging OT with metastatic breast cancer cells (BCs) known to invade the skeleton, important hallmarks of the metastatic process including cancer cell/tissue adhesion, tissue penetration, and ultimate degradation of the osteoblast-derived extracellular matrix were directly observed in vitro.

Materials and methods

Bioreactor design and implementation

Bioreactors based on the principle of simultaneous-growth-and-dialysis [17, 18] were implemented using a two-compartment bioreactor design described previously [19, 20]. One of the compartments was a cell growth chamber (5 ml total volume) that was separated from a 30-ml medium reservoir compartment by a dialysis-membrane (6–8 KDa cutoff). Cells were inoculated into the growth chamber in complete medium including serum. The reservoir was filled with basal medium consisting of nutrients such as glucose and amino acids but no proteins. The entire vessel was ventilated through transparent, gas-permeable but liquid-impermeable films that offered optimum cell adhesion and delivered requisite oxygen tension to the cells. The bioreactor was specifically designed to enable non-invasive, live-cell analysis with an inverted (phase-contrast, fluorescence, or confocal) microscope. Completely assembled units used in this work had a cell growth space of 25 cm^2 total area emulating a standard T25 flask. Bioreactors were sterilized by gamma radiation at the Breazeale Nuclear Reactor on the campus of The Pennsylvania State University.

During culture, cells were bathed in pH-equilibrated and oxygenated medium that continuously dialyzed from the medium reservoir. At the same time, metabolic waste products such as lactic acid dialyzed out of the growth compartment, maintaining low pericellular concentrations. The medium reservoir was periodically replenished to provide additional nutrients and remove accumulated waste products without disturbing the cell growth chamber. Serum constituents or macromolecules synthesized by cells with molecular weights in excess of the dialysis membrane cutoff (8–10 kDa) were retained and concentrated within the growth compartment. This simple-to-use bioreactor design was integrated into conventional tissue culture protocols. The system conferred an extraordinarily stable pericellular environment that improved cell recovery from "culture shock" [21], and resulted in development of OT with a normal phenotype over extended, uninterrupted culture intervals tested for as long as 10 months with no sign of necrosis [19, 20]. In the course of defining the experimental bioreactor system, we have cultured MC3T3-E1 for various times from 1 week to 10 months. Cocultures with BCs were carried out at three ratios of cancer cells to osteoblasts (1:10, 1:100, and 1:1,000). Tissue with up to 5 months maturity was utilized in this work. Data from other times of culture is shown as indicated for individual experiments.

Cells and cell culture

Murine calvarial pre-osteoblasts (MC3T3-E1) were a gift from Dr. Norman Karin at the Pacific Northwest National Laboratories (ATCC CRL-2593 presumptive equivalent). MC3T3-E1 were inoculated into the growth chamber of the bioreactors at a sub-confluent density (10^4 cells/cm^2) and

cultured in alpha minimum-essential medium (α-MEM) (Mediatech, Herdon, VA) supplemented with 10% neonatal FBS (Cansera, Roxdale, Ontario) and 100 U/ml penicillin and 100 μg/ml streptomycin (Sigma Aldrich, St. Louis, MO). The medium reservoir of the bioreactor was filled with α-MEM supplemented with 100 U/ml penicillin and 100 μg/ml streptomycin but no serum. Once the cells reached confluence, usually 4–5 days, the medium in the growth chamber was replaced with differentiation medium containing the additional ingredients of 50 μg/ml ascorbic acid and 10 mM β-glycerophosphate (Sigma Aldrich, St. Louis, MO). This change to differentiation medium was the only time during the course of the experiment that medium in the cell chamber was replaced. Subsequent medium changes involved only the basal medium within the medium reservoir that was refreshed every 30 days. Bioreactors were maintained in a water-jacketed 5% CO_2 incubator (Model 3110, Thermo Fisher Scientific, Waltham, MA) held at 37°C. In this way, MC3T3-E1 cultures have been maintained continuously in the bioreactor without subculture for extended intervals up to 10 months, generating a multiple-cell layer tissue with controllable age (maturity), herein referred to as OT.

Human metastatic BCs (MDA-MB-231, ATCC-HTB 26 presumptive equivalent) genetically engineered to produce green fluorescent protein (GFP), were a gift from Dr. Danny Welch, University of Alabama at Birmingham, and herein referred to as BCs. Derived from a pleural effusion [22], MDA-MB-231^{GFP} cells are known to invade the murine skeleton [23].

MDA-MB-231^{GFP} cells were cultured in standard tissue culture dishes in Dulbecco's Modified Eagle's Medium (DMEM) (Mediatech, Herdon, VA) containing 5% neonatal bovine serum and 100 U/ml penicillin and 100 μg/ml streptomycin for 3–4 days before coculture with bioreactor-derived OT.

Reverse transcription polymerase chain reaction

Relative quantitative PCR was performed on RNA isolated from MC3T3-E1 cells cultured in the bioreactor for various intervals (7, 22, 30 or 60 days) to determine expression levels of osteopontin, osteonectin, type I collagen, osteocalcin, MMP-13, E11, and β-actin. Total RNA was isolated from the cells using the RNeasy kit (Qiagen, Valencia, CA) with on-column DNase treatment. Five hundred nanograms of total RNA was reverse transcribed from an oligo dT primer using the RETROscript kit (Ambion, Austin, TX). Two microliters of the cDNA were used in PCR reactions that had been previously optimized by varying the cycle number to determine the linear range of amplification. PCR reactions for each of the proteins of interest were performed using the primer pairs, annealing temperatures and cycle numbers listed in Table 1. PCR products were separated by electrophoresis on a 2% agarose gel in Tris-borate EDTA buffer and stained with ethidium bromide. Gel documentation was performed on the Kodak Gel Logic 100 Imaging System (Eastman Kodak, Rochester, NY) and band volume quantitation was done by ImageQuant software (Molecular Dynamics, Sunnyvale, CA). Expression levels were normalized by determining the ratio of the band volume for each message relative to the band volume for β-actin for the same cDNA.

Bioreactor cocultures

BCs were inoculated into bioreactor cell growth chambers containing OT at maturities between 15 and 145 days of

Table 1 Primer sequences and experimental conditions for RT-PCR

Gene	Primers (F = Forward; R = Reverse)	Annealing temperature (°C)	Cycles	Amplicon size (bp)
Osteocalcin	F: 5′-CAA GTC CCA CAC AGC AGC TT-3′	55	23	370
	R: 5′-AAA GCC GAG CTG CCA GAG TT-3′			
Osteonectin	F: 5′-CTG CCT GCC TGT GCC GAG AGT TCC-3′	55	17	653
	R: 5′-CCA GCC TCC AGG CGC TTC TCA TTC-3′			
Type I collagen	F: 5′-TCT CCA CTC TTC TAG TTC CT-3′	55	16	269
	R: 5′-TTG GGT CAT TTC CAC ATG-3′			
MMP-13	F: 5′-GAT GAC CTG TCT GAG GAA G-3′	58	21	357
	R: 5′-ATC AGA CCA GAC CTT GAA G-3′			
E11	F: 5′-TCCAACGAGACCAAGATGTG-3′	60	24	539
	R: 5′-AGCTCTTTAGGGCGAGAACCT-3′			
Osteopontin	F: 5′-ACA CTT TCA CTC CAA TCG TCC-3′	58	16	240
	R: 5′-TGC CCT TTC CGT TGT TGT CC-3′			
β-Actin	F: 5′-CGT GGG CCG CCC TAG GCA-3′	62	20	242
	R: 5′-TTG GCC TTA GGG TTC AGG-3′			

culture at an estimated 1:10, 1:100, or 1:1,000 breast cancer-to-osteoblast cell ratio; corresponding to 10^5, 10^4, or 10^3 BCs/bioreactor, respectively. BC challenged bioreactors were monitored microscopically for 7 days. On day 7, bioreactors were dismantled and substratum film with adherent tissue was carefully cut into pieces for various assays, avoiding loss of OT that was conspicuously degraded by BC challenge. Medium from the cell growth space of the bioreactor was collected and used for various analyses. Tissue was fixed in 2.5% glutaraldehyde (in cacodylate buffer) and stained for actin filaments with Alexa Fluor 568 phalloidin stain (Invitrogen, Carlsbad, CA). Osteoblasts were optionally stained with Cell Tracker Orange™ (Invitrogen, Carlsbad, CA) for live in situ confocal imaging to monitor cell growth dynamics, prior to staining with actin stain.

Conditioned media experiments

BCs were grown to 90% confluency in standard tissue culture plates and growth medium was removed. Adherent BCs were rinsed with PBS and the original growth medium replaced with fresh α-MEM (20 ml in a T-150 flask, $\sim 1.3 \times 10^5$ cells/cm^2). Cultures were incubated for an additional 24 h, the medium collected and centrifuged ($300\times$ *g* for 10 min) to remove cellular debris resulting in "BC-conditioned medium". At desired OT maturity, medium in the growth chamber of the bioreactor was completely replaced with a mixture of 50% breast cancer conditioned medium and 50% differentiation medium as previously described [24]. Osteoblast tissue in the bioreactor was exposed to BC-conditioned medium for 2 weeks.

Confocal microscopy

In situ laser-scanning confocal microscopy of cocultures in the bioreactor was performed using Olympus FV-300 laser-scanning microscope (Olympus America Inc., Center Valley, PA). Sections were observed with a 40X Olympus UPlanF1 objective with an 0.85 numerical aperture. Cell Tracker Orange ™ was excited using a 543 nm line from a helium-neon laser and collected through a 565 nm long-pass filter. GFP was excited using a 488-nm argon laser and collected through 510 nm long-pass and 530 nm short-pass filters. A 570 nm dichroic long-pass filter was used to split the emission. Serial optical sections were taken at 1 μm intervals throughout the tissue. Confocal images were processed using image processing software (Fluoview 300, Version 4.3b, Olympus, Center Valley, PA). 3D optical reconstructions of 2D serial sections were obtained using AutoQuant, AutoDeblur and AutoVisualize software (Version 9.3, Media Cybernetics, Bethesda, MD). Number of cell layers within the tissue was determined visually by counting and by following the sub-volumes of cells in the 3D-reconstructed Z-stack images.

Biochemical and immunochemical assays

Soluble collagen (indicative of collagen synthesis) was quantified using Sircol Assay (Biocolor, Carrickfergus, UK). Prior to running the assay following manufacturer's protocol, the collagen was extracted/precipitated from cell culture supernatants by addition of 4 M NaCl. Supernatants were centrifuged and the resulting collagen pellet was re-suspended in 0.5 M acetic acid. Levels of osteocalcin and IL-6 secreted into the medium were quantified using multiplex ELISA kit (LINCOplex™ Mouse Bone Panel 2B, Millipore, Billerica, MA). Alkaline phosphatase activity was quantitated using the QuantiChrom™ Alkaline Phosphatase Assay Kit (DALP-250), BioAssay Systems, Hayward, CA according to manufacturers protocol. Briefly, cells were lysed in a solution of 100 mM glycine, 0.1% Triton-X 100, 1 mM $MgCl_2$, pH 10, and the lysate was added to 96-well plates coated with tartrazine standard working solution containing the pNPP substrate. The 96-well plate was gently tapped to mix all components, and immediately read at 405 nm. The plate was read again after 4 minutes at 405 nm and the optical densities from the two readings were used to calculate the alkaline phosphatase enzyme activity. Each sample was tested three times.

Results

Osteoblast tissue model

Murine MC3T3E-1 pre-osteoblasts maintained in the bioreactor developed into a 3D osteoblast tissue (OT, Panel A of Fig. 1) comprised of 6–8 layers of differentiated cells (Panels B, top layer; Panel C, bottom layer) that stained positive for alkaline phosphatase activity and for mineralization by von Kossa (not shown). Continuous culture in the bioreactor resulted in transformation of spindle shaped pre-osteoblasts (Fig. 2, Panel A) to cuboidal osteoblasts (Panel B) that secreted and mineralized an extensive, collagenous extracellular matrix (Panel C) that completely enveloped the cells (Panel D). Examination of numerous histological and ultra-structural (not shown), and confocal sections of tissue from bioreactor cultures at different times revealed reproducible and continuous transformation of tissue in which cells were initially closely packed (high cell/ECM ratio; Fig. 2 Panel A) to a more mature phenotype characterized by lower cell density (low cell/ECM ratio; Fig. 2 Panels C, D) with intercellular contacts maintained by a network of cellular processes [20]. Growth and maturation of OT in the bioreactor thus recapitulated

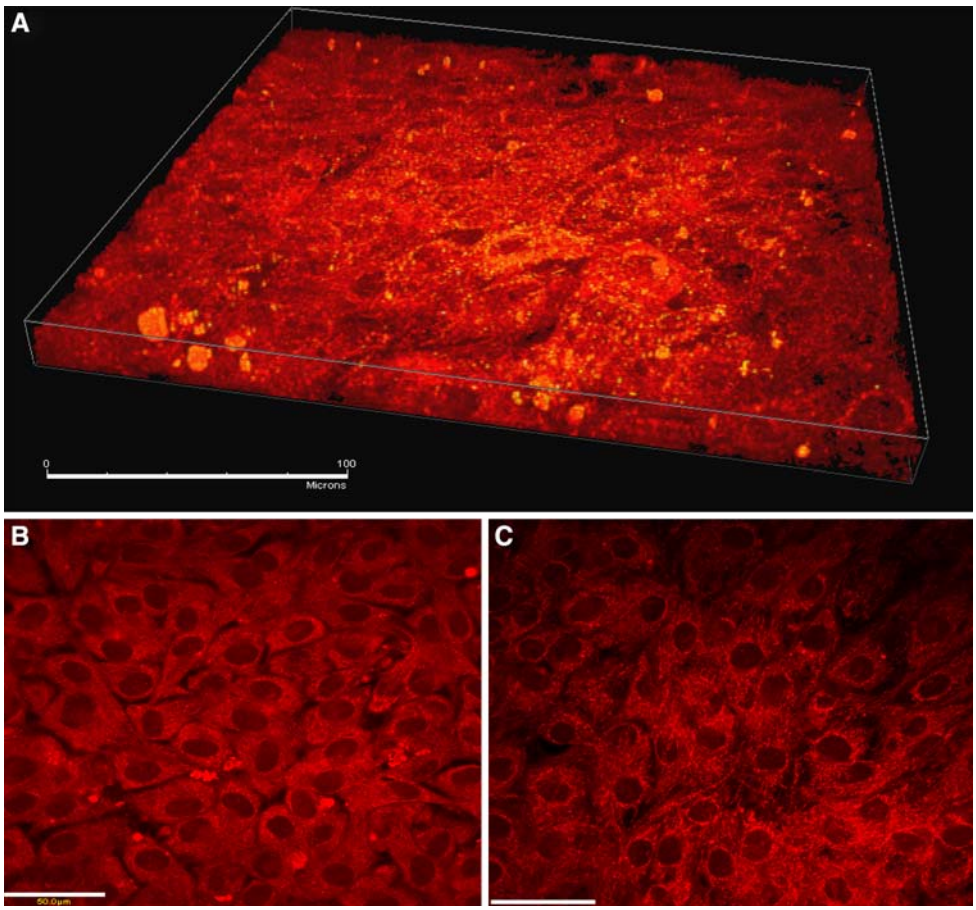

Fig. 1 Phalloidin-stained MC3T3-E1 osteoblast-derived tissue (OT) after 22 days of continuous culture in the bioreactor. MC3T3-E1 pre-osteoblasts grow into a 3D OT comprised of 6–8 cell layers enmeshed in a collagenous matrix (see also Figs. 2, 5). Panel A is a 3D reconstruction of serial confocal optical sections (magnification = 40×, scale bar = 100 μm). A morphological gradient in the tissue was evident wherein top layer of cells (Panel B) were conspicuously more cuboidal than bottom layer of cells (Panel C) which exhibited filamentous inter-cell connections reminiscent of osteocyte morphology

the normal sequence of bone development characterized by stages of proliferation, matrix maturation, and mineralization. This phenotypic progression was also reflected in the characteristic expression of genes such as Type I collagen, osteonectin, osteocalcin and osteopontin (Fig. 2, Panel E) [25]. Up-regulation of matrix-metallo protease (MMP)-13 (indicative of extracellular matrix remodeling) and the protein E11 (indicative of osteocytic transformation) occurred in mature cultures (Fig. 2, Panel E).

Breast cancer cell challenge to osteoblast tissue

Interaction of cancer cells with OT were followed by fluorescence microscopy after injecting MDA-MB-231^{GFP} human BCs directly onto 5-month OT stained with Cell Tracker Orange^{TM} to clearly differentiate osteoblasts from cancer cells. BCs adhered to OT (Fig. 3 Panel A) in the first 24 h. By the second day, the BC cells penetrated tissue (Panel B), apparently through the agency of cellular processes extended by BCs (see Fig. 3). Within 3 days of coculture, BCs proliferated and organized into lines of cells (Panels C). Close inspection of 2D optical sections (Fig. 4, Panel A, Day 3) and 3D reconstructions (Fig. 4, Panel D) revealed concomitant re-organization of OT. Before cancer cell challenge, osteoblasts exhibited a cuboidal morphology. Over 3 days of BC coculture, osteoblasts took on a definitively elongated appearance and aligned with cancer cells which also became spindle shaped. In particular, osteoblasts paralleled the BC cells, as though marshaled into an order that seemed to permeabilize OT structure. The BC alignment in the bioreactor was reminiscent of the classical "Indian filing" pattern that is one of the defining characteristics of breast cancer invasion [26–28].

Breast cancer cell conditioned medium effects on osteoblast tissue

Prior work determined that exposure of MC3T3-E1 cells to conditioned medium (CM) from MDA-MB-231 cells caused a change in osteoblast morphology and adherence to the substrate under standard tissue culture conditions [29]. In order to determine if this effect occurred with 3D OT, 16 day OT in the bioreactor was maintained in CM for 2 weeks (see Materials and methods). Exposure of OT to BC-conditioned medium induced significant cytoskeletal reorganization in response to factors secreted by BCs, as revealed by actin stress-fiber reorganization (Fig. 3, compare control Panel D to test Panel E). Control OT were

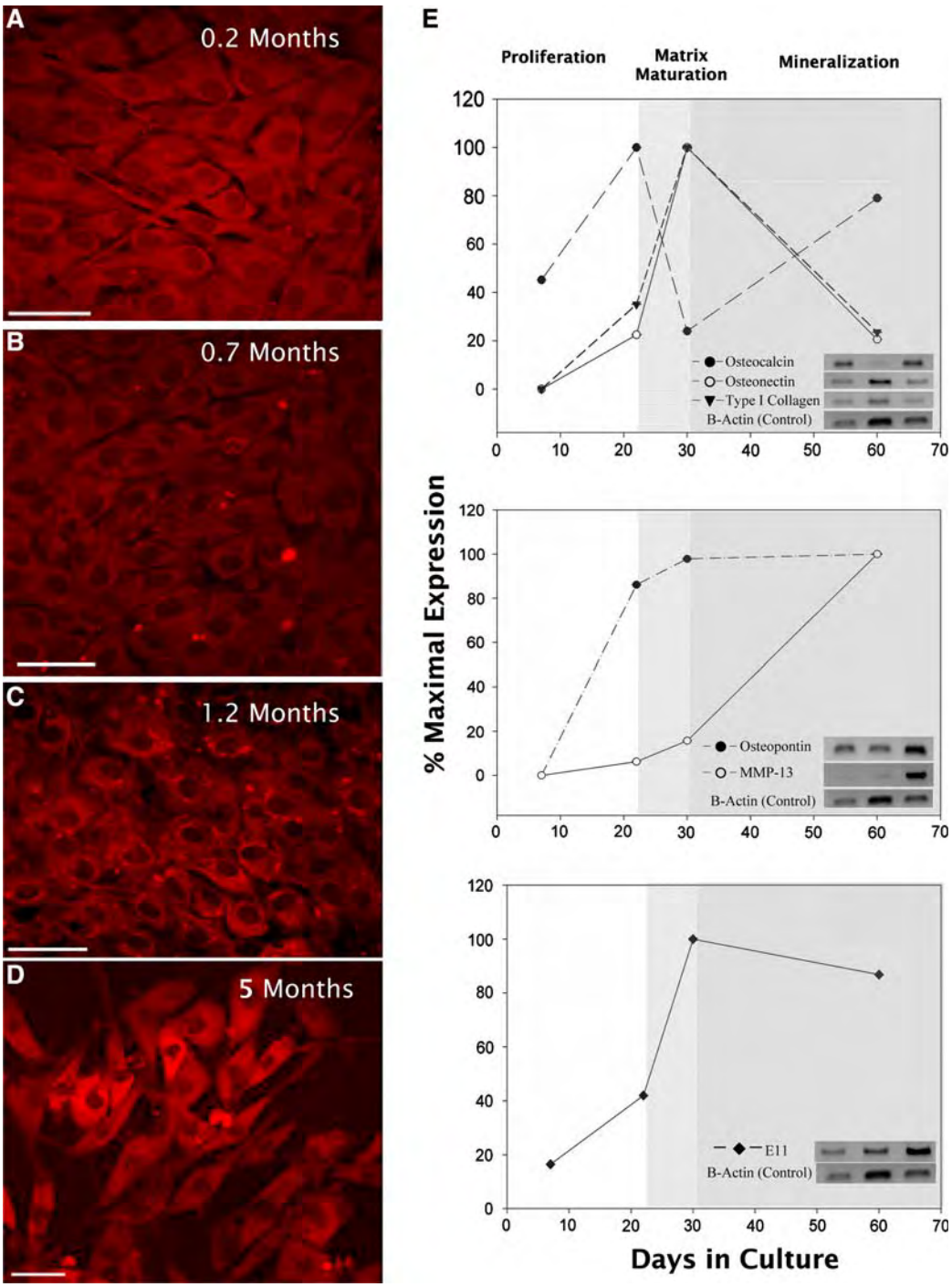

Fig. 2 Maturation of MC3T3-E1 derived OT within the bioreactor (see also Figs. 1, 5). Panels (A–D) are confocal images of actin-stained cells over several months of continuous culture (scale bar = 50 μm, annotations give culture age). Spindle shaped pre-osteoblasts (Panel A) progressively transformed into cuboidal osteoblasts (Panel B) that became enmeshed in a collagenous matrix (Panel C appearing black) that eventually buried cells exhibiting an osteocytic-like morphology (Panel D). Relative quantitative PCR was performed on RNA isolated from MC3T3-E1 cells cultured in the bioreactor for various intervals (7, 22, 30 or 60 days) to determine expression levels of osteopontin, osteonectin, type I collagen, osteocalcin, MMP-13, E11 and β-actin (Panel E). Insets show ethidium bromide stained bands for the genes indicated for 22, 30 and 60 days. The gene expression for the 7 day cultures was very faint, and is not shown. Samples from replicate bioreactors at days 22 and 30 were also tested with similar results. Expression levels were normalized by determining the ratio of the band volume for each message relative to the band volume for β-actin for the same cDNA. The data are expressed as percent of maximum expression following the work of Lian et al. [25]. Changes in gene expression were consistent with progression of the osteoblast phenotype through the stages of proliferation, matrix maturation and mineralization as indicated by the shaded vertical bars in Panel E. Two bioreactors were tested but data from only one of each age are shown

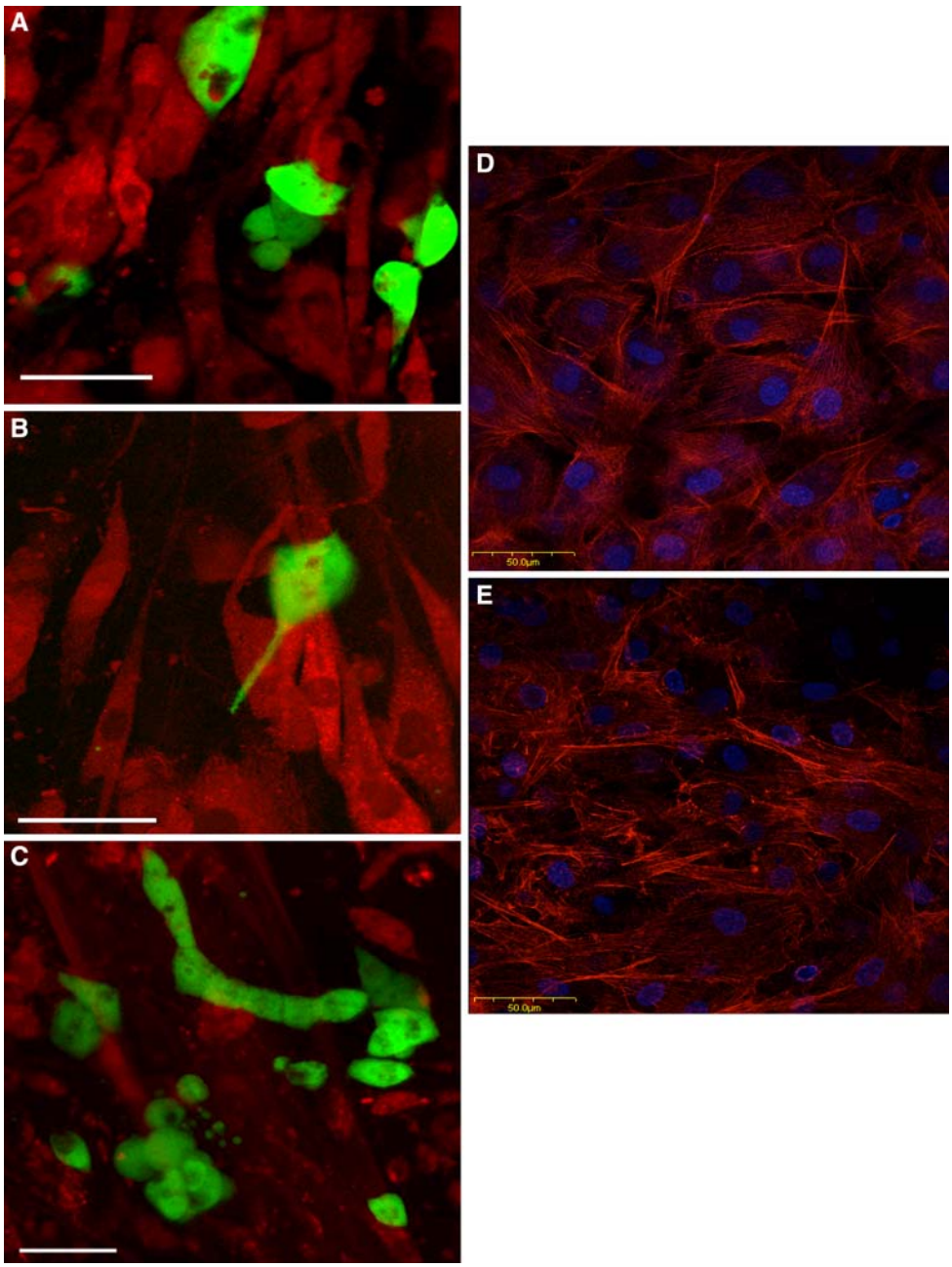

Fig. 3 MDA-MB-231^{GFP} breast cancer cell invasion of MC3T3-E1 derived OT grown for 5 months within the bioreactor. OT (stained with Cell Tracker Orange^{TM}) was cocultured with MDA-MB-231 breast cancer cells (BCs) genetically engineered to produce GFP. Confocal images (scale bar = 50 µm, magnification = 40×) were collected over 3 days (Panels A–C). These representative images are interpreted as stages of BC adhesion (Panel A, day one), penetration (Panel B, day two), and replication/ organization into characteristic filing patterns (Panel C, day three), respectively (see also Fig. 4). Phalloidin-stained OT grown for 16 days in the bioreactor (Panel D) was compared to similar tissue exposed to MDA-MB-231 conditioned medium for 2 weeks (Panel E, scale bar = 50 µm, magnification = 40×). Note that exposure to conditioned media disrupted actin fiber organization in OT. Draq5 (Biostatus, Shepshed, UK) stained nuclei (blue) reveal concomitant nuclear shrinkage. Breast cancer conditioned medium was prepared as reported previously [24]

characterized by smooth, long actin stress fibers (Panel D), whereas, F-actin stress fibers were clumped and punctate in OT exposed to conditioned medium (Panel E). These cytoskeletal changes correlated with the observation that OT from coculture experiments was consistently more fragile than OT not exposed to cancer cells. In fact, very careful processing was required to prevent wholesale cell sloughing during the wash steps involved in preparation of specimens for histology and electron microscopy. It was plainly evident from these latter observations that OT structure and adhesion to the bioreactor substratum film was significantly eroded by BC exposure. Details of BC interaction with OT were followed using the confocal microscopy study outlined in the legend to Fig. 4 and as detailed in the section Discussion.

Effect of osteoblast tissue maturity on breast cancer cell interactions

The interaction of BC cells with OT depended on the stage of OT maturity. As the OT matured, there was decrease in the number of cell layers with increasing culture time (Fig. 5, left-hand axis of graphic portion) that translated into a linear-like decrease in cell layer/tissue-thickness ratio (Fig. 5, right-hand axis). Qualitative aspects of BC interactions were correlated with OT characteristics (Fig. 5,

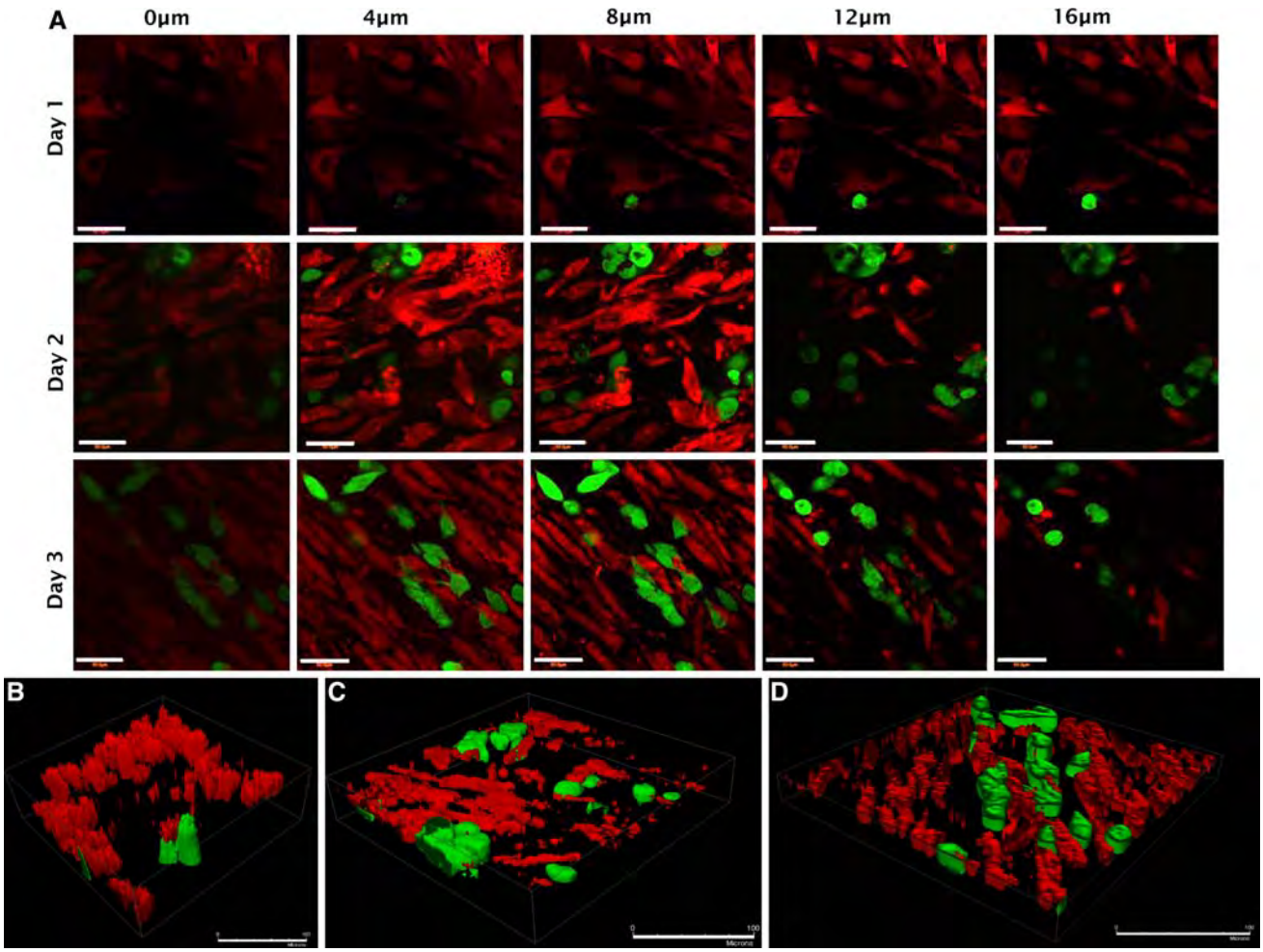

Fig. 4 MDA-MB-231 breast cancer cell (BC) invasion of MC3T3-E1 derived OT grown for 5 months the bioreactor (see also Figs. 1, 3). BCs were added to a 5 month OT culture as described as in the legend to Fig. 3. Optical sections (40×, scale bar = 50 μm) at various depths within OT at successive days in culture were collected by laser scanning confocal microscopy. It appeared that BCs fully penetrated OT only in a few locations within day 1 of coculture. Penetration increased over days 2 and 3. Linear-like organization of breast cancer cells and osteoblasts within the tissue was evident beginning at day 2 but more obvious at day 3. Optical reconstructions of serial sections over 3 days (Panels B–D respectively, 40×) revealed significant re-organization and permeablization of OT

table portion), suggesting that declining rates of BC colonization and increasing efficiency of tissue penetration, filing, and colony formation were related to OT maturity.

The effect of BCs on OT was further assessed by measuring the changes in levels of secreted factors representing primary osteoblast functions of extracellular matrix production (secreted collagen) and mineralization (osteocalcin). Introduction of BCs led to reduced production of new collagen (Fig. 6, Panel A) and to less secretion of osteocalcin (Fig. 6, Panel B) at all tested OT maturities. Alkaline phosphatase activity deceased as the cultures aged (Fig. 6, Panel C). This effect has been reported previously [30]. Nevertheless, at each time tested, the alkaline phosphatase in the presence of the cancer cells was less than in the OT alone. Furthermore, BCs stimulated increased production of IL-6, indicative of an inflammatory stress response (Fig. 6, Panel D) [24].

Discussion

Osteoblastic tissue model

A relatively simple bioreactor was used to grow a 3D OT from murine MC3T3E-1 pre-osteoblasts for culture periods up to 5 months. This extended culture interval allowed maturation of OT through successive stages of phenotypic development, up-to-and-including osteocyte-like cells. A morphologically stratified tissue developed within the first month of culture (Fig. 1; compare top layer Panel B to bottom layer Panel C). Over successive months of culture, cuboidal osteoblastic cells underwent continued morphological changes (Fig. 2) accompanied by characteristic expression of genes such as Type I collagen, osteonectin, osteocalcin and osteopontin; as well as up-regulation of

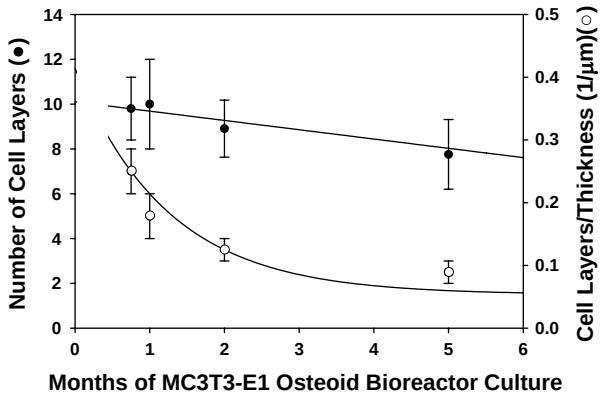

Experimental Parameter @ BC:OB=1:10	Months of Bioreactor Culture			
	0.75	1	2	5
BC Colonization	(+++)	(++)	(+)	(+)
Tissue Penetration	(-)	(+/-)	(+)	(+)
BC Filing	(-)	(+)	(++)	(++)
Tumor Formation	(-)	(+)	(++)	(++)

Fig. 5 Qualitative aspects of MDA-MB-231 metastatic breast cancer cell (BC) interaction correlate with MC3T3-E1 derived OT maturity. An exponential-like decrease in the number of cell layers with time (left-hand axis, graph) translated into a linear-like decrease in cell layer/tissue-thickness ratio (right-hand axis, graph). This observation was consistent with the process of bone-tissue maturation that resulted in transformation of proliferating pre-osteoblasts into non-dividing osteoblasts that become engulfed in mineralized matrix and mature into osteocytes through a process of phenotypic transformation marked by increased osteoblast apoptosis [31]. The data presented in the summary table suggested that declining rates of BC colonization and increasing efficiency of tissue penetration, cell organization into chains, and colony formation were related to OT maturity

MMP-13 (suggestive of active matrix turnover) and protein E11 (indicative of osteocytic transformation). The number of cell layers comprising OT and tissue-thickness decreased with culture time (Fig. 5) in a manner consistent with the increased osteoblast apoptosis observed in the formation of natural bone [31]. These observations were collectively interpreted to mean that continuous culture of MC3T3-E1 cells in the bioreactor recapitulated growth and phenotypic development of native bone-tissue in vivo, excluding osteoclast-mediated remodeling. Osteoclasts were purposely excluded from the bioreactor-based model so that osteoblast biology could be clearly observed.

Breast cancer cell challenge to osteoblast tissue

Confocal microscopy indicated that MDA-MB-231 human BCs adhered to and penetrated OT (Figs. 3, 4). BCs penetrated OT by extending long cellular protrusions that were enriched in filamentous actin and formed chains of cells similar to "Indian files" described for infiltrating lobular or metaplastic breast carcinomas [26, 27]. Migration of cancer cells along tracks of remodeled ECM produced by preceding invading cell(s) results in characteristic cell alignment patterns [28]. Invasion by chains of tumor cells linked together by cell–cell contacts is considered to be an effective penetration mechanism conferring high metastatic capacity and commensurately poor prognosis [26, 28]. Observation of BC invasion "Indian files" in the OT model suggests a considerable degree of physiological relevance.

BC attachment and penetration varied significantly with OT maturity (Fig. 5). BCs failed to penetrate immature OT (less than 30 days in culture); instead forming colonies substantially on, not in, OT. Significant penetration, remodeling, and characteristic cancer cell alignment patterns were observed only in relatively mature OT. We speculate that BC penetration is inhibited by close contacts among osteoblasts comprising immature OT and becomes more efficient as the cell/ECM ratio decreases, creating a more permeable tissue. The first penetrating BC remodels the extracellular matrix in a way that creates a path for other BCs [32], leading to the chains of cells as discussed above. This progressive process marshals OT into a pattern that paralleled the lines of breast cancer cells.

Unlike conventional cell culture wherein continuous or scheduled medium exchanges lead to loss of cell secreted growth factors and cytokines, the compartmentalized bioreactor retains all factors secreted into the cell growth compartment that have molecular weight greater than 6–8 KDa dialysis-membrane cutoff (see Materials and methods). We believe this attribute is critical to simulating the bone microenvironment because osteoblasts are known to secrete a number of growth factors and cytokines in a spatially and temporally ordered sequence that is closely aligned with the specific stages in osteoblast development [25]. Likewise, BC coculture introduces growth factors and cytokines that would presumably concentrate in the microenvironment in physiological conditions. For these reasons, we maintain that the OT model is a relevant model for cancer colonization of bone.

Osteoblast inflammatory response

Inflammation is linked closely with the progression of many cancers [33]. Osteoblasts are able to mount an inflammatory response independent of immune cells [34]. Inflammation appears to play a critical role in bone loss in osteomyelitis due to bacterial infection in the bone [34] and in debris-mediated bone loss associated with titanium implants [35]. Previous studies in conventional culture have shown that exposure to BC-conditioned medium produced a profound osteoblastic inflammatory stress

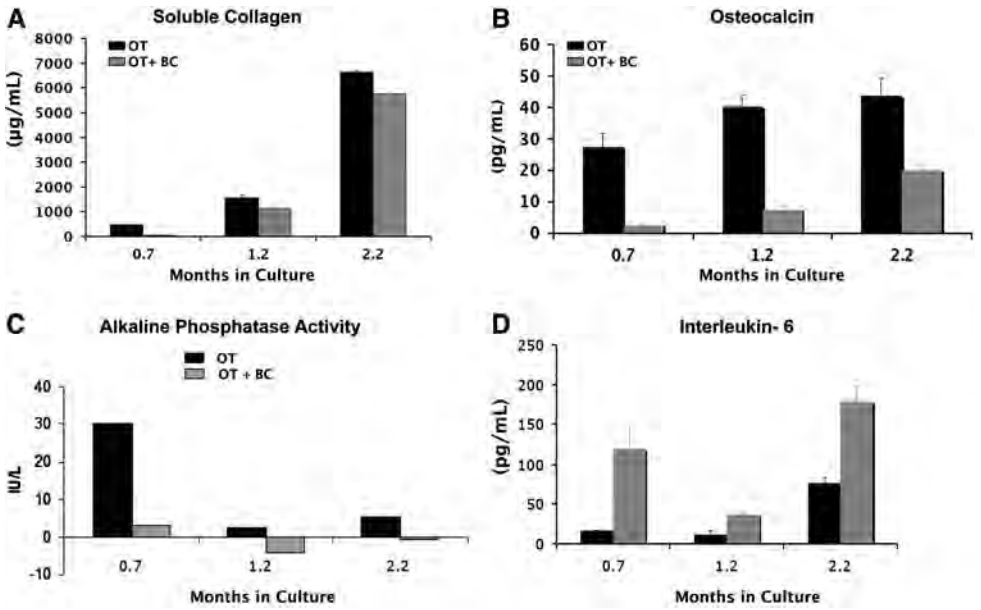

Fig. 6 Osteoblasts cocultured with MDA-MB-231 metastatic breast cancer cells (BC) showed a reduction in the production of osteoblast maturation proteins and an increase in IL-6. MC3T3-E1 derived osteoblast tissue (OT) were grown in the bioreactor for 0.7, 1.2, and 2.2 months before breast cancer cells (BC) were injected onto OT at a 1:10 BC-to-osteoblast cell ratio and cocultured for 7 days. OT with no added BC served as controls. Levels of soluble collagen secreted by osteoblasts into the medium in the presence and absence of breast cancer cells were quantified using Sircol^{TM} Assay (Biocolor) ($n \geq 2$) (Panel A). Levels of osteocalcin (OCN) secreted into the medium in the presence and absence of breast cancer cells were quantified using multiplex ELISA assay (LINCOplex^{TM} Mouse Bone Panel 2B, Millipore). Shown are averages of duplicate sample determination. (Panel B). Alkaline phosphatase activity was quantitated using the QuantiChrom^{TM} Alkaline Phosphatase Assay Kit (DALP-250), Bio-Assay Systems, Hayward, CA as indicated in the methods section. Each sample was tested three times (Panel C). Levels of murine IL-6 released into the culture media were determined with a multiplex ELISA assay (LINCOplex^{TM} Mouse Bone Panel 2B, Millipore). Shown are averages of duplicate sample determinations (Panel D)

response that included increased expression of the inflammatory cytokines, IL-6, IL-8 and MCP-1 [36]. These cytokines are known to attract and activate osteoclasts, and are likely to contribute to the tumor-host microenvironment in vivo. In particular, IL-6 a pleiotropic cytokine [37], has been implicated in pathogenesis of osteolysis associated with Paget's disease [38], Gorham-Stout syndrome [39], and multiple myeloma [40]. IL-6 levels in breast cancer patients have been found to correlate to the clinical stage of the disease [41, 42] as well to the rate of recurrence [43]. High IL-6 serum levels in breast cancer patients were found to be an unfavorable prognosis indicator [44–46]. We thus interpret pronounced IL-6 production by OT in coculture experiments (Fig. 6, Panel D) as a strong osteoblast inflammatory provoked by the presence of BCs. The concomitant decrease in collagen and osteocalcin secreted by OT cocultured with BCs confirms that BC suppress osteoblast function in a manner consistent with inflammation-induced bone loss observed in bone pathologies.

Breast cancer induced bone loss

Cancer-related bone loss appears to occur through multiple pathways. Evidence for osteoclast-mediated resorption is indeed very strong [47]. In addition, destruction of devitalized bone directly by cancer cells has also been reported [48], especially late in metastasis when bone-degradation rate is highest and osteoclast cell numbers are in decline [49]. These lines of evidence support the idea that osteoclasts are not solely responsible for excessive bone-degradation and that cancer cells may directly contribute to bone loss. Degradation of the osteoblast tissue by coculture with BCs observed in the bioreactor model (that purposely excludes osteoclasts) strongly suggests that yet another mechanism of bone loss is related to disruption of the bone-accretion process by destruction of osteoblastic tissue. There is clinical and experimental literature to support this concept. For example, quantitative histomorphometric analyses of bone biopsies from patients with hypercalcemia due to bone metastasis indicated a dramatic decrease in osteoblast activity [50]. Histomorphometric analysis of rodents inoculated with lytic human BCs (MDA-MB-231) indicated that, even though administration of risedronate (a bisphosphonate) reduced the number of osteoclasts, slowed bone lysis, and significantly reduced tumor burden, there was no evidence of new bone deposition or repair [51]. Similarly, administration of bisphosphonates to humans with osteolytic metastasis slowed lesion progression but

did not bring about healing [52]. Our previous work in vivo and in vitro also indicate that metastatic BCs suppress osteoblast adhesion and differentiation and increase osteoblast apoptosis [29, 49, 53]. All taken together, these observations strongly suggest that normal osteoblast function (i.e., deposition and mineralization of matrix) is not only impaired in the presence of BCs but, in fact, OT is degraded by breast cancer invasion, possibly by enlisting a cooperative inflammatory response by osteoblasts themselves. Further understanding of the cellular and molecular basis for breast cancer colonization of bone and discovery of therapeutic interventions will be greatly expedited by the use of 3D tissue models such as the one demonstrated in this study.

Acknowledgments This work was supported by U.S. Army Medical Research and Material Command Breast Cancer Research Program WX81XWH-06-1-0432, and the Susan G. Komen Breast Cancer Foundation BCTR 0601044, National Foundation for Cancer Research, Center for Metastasis Research, The University of Alabama-Birmingham. Authors appreciate the expert technical assistance of Ms. Donna Sosnoki and the assistance of the Cytometry Facility and the Electron Microscopy Facility at the Huck Institutes of Life Sciences, Penn State University.

References

1. Rubens RD, Mundy GR (2000) Cancer and the skeleton. Martin Dunitz, London
2. Rubens RD (1998) Bone metastases—the clinical problem. Eur J Cancer 34:210–213. doi:10.1016/S0959-8049(97)10128-9
3. Nielsen OS, Munro AJ, Tannock IF (1991) Bone metastases: pathophysiology and management policy. J Clin Oncol 9(3): 509–524
4. Aguirre-Ghiso JA (2007) Models, mechanisms and clinical evidence for cancer dormancy. Nat Rev Cancer 7(11):834–846. doi: 10.1038/nrc2256
5. Demicheli R (2001) Tumour dormancy: findings and hypotheses from clinical research on breast cancer. Semin Cancer Biol 11:297–306. doi:10.1006/scbi.2001.0385
6. Kvalheim G, Naume B, Nesland JM (1999) Minimal residual disease in breast cancer. Cancer Metastasis Rev 18:101–108. doi: 10.1023/A:1006216504892
7. Chambers AF, Groom AC, MacDonald IC (2002) Dissemination and growth of cancer cells in metastatic sites. Nat Rev Cancer 2(8):563–572. doi:10.1038/nrc865
8. Mundy GR (2002) Metastasis to bone: causes, consequences and therapeutic opportunities. Nat Rev Cancer 2:584–593. doi: 10.1038/nrc867
9. Holmgren L, O'Reilly MS, Folkman J (1995) Dormancy of micrometastases: balanced proliferation and apoptosis in the presence of angiogenesis suppression. Nat Med 1:149–153. doi: 10.1038/nm0295-149
10. Welch DR, Steeg PS, Rinker-Schaeffer CW (2000) Molecular biology of breast cancer metastasis: genetic regulation of human breast carcinoma metastasis. Breast Cancer Res 2(6):408–416. doi:10.1186/bcr87
11. Chambers AF, MacDonald IC, Schmidt EE et al (1995) Steps in tumor metastasis: new concepts from intravital videomicroscopy. Cancer Metastasis Rev 14:279–301. doi:10.1007/BF00690599
12. Chambers AF, Naumov GN, Vantyghem SA et al (2000) Molecular biology of breast cancer metastasis. Clinical implications of experimental studies on metastatic inefficiency. Breast Cancer Res 2:400–407. doi:10.1186/bcr86
13. Steeg PS (2000) Molecular biology of breast metastasis: 'has it spread?' disarming one of the most terrifying questions. Breast Cancer Res 2(6):396–399. doi:10.1186/bcr85
14. Chambers AF, MacDonald IC, Schmidt EE et al (2000) Clinical targets for anti-metastasis therapy. Adv Cancer Res 79:91–121. doi:10.1016/S0065-230X(00)79003-8
15. Welch DR (1997) Technical considerations for studying cancer metastasis in vivo. Clin Exp Metastasis 15:272–301. doi:10.1023/A:1018477516367
16. Schmeichel KL, Bissell MJ (2003) Modeling tissue-specific signaling and organ function in three-dimensions. J Cell Sci 116(12):2377–2388. doi:10.1242/jcs.00503
17. Rose GG (1966) Cytopathophysiology of tissue cultures growing under cellophane membranes. In: Richter GW, Epstein MA (eds) International review of experimental pathology. Academic Press, New York, pp 111–178
18. Rose GG, Pomerat CM, Shindler TO et al (1958) A cellophane-strip technique for culturing tissue in multipurpose culture chambers. J Cell Biol 4(6):761–764. doi:10.1083/jcb.4.6.761
19. Vogler EA (1989) A compartmentalized device for the culture of animal cells. J Biomater Artif Cells Artif Organs 17:597–610
20. Dhurjati R, Liu X, Gay CV et al (2006) Extended-term culture of bone cells in a compartmentalized bioreactor. Tissue Eng 12(11):3045–3054. doi:10.1089/ten.2006.12.3045
21. Sorkin AM, Dee KC, Knothe Tate ML (2004) "Culture shock" from the bone cell's perspective: emulating physiological conditions for mechanobiological investigations. Am J Physiol Cell Physiol 287(6):C1527–C1536. doi:10.1152/ajpcell.00059.2004
22. Cailleau R, Olive M, Cruciger QV (1978) Long-term human breast carcinoma cell lines of metastatic origin: preliminary characterization. In Vitro 14(11):911–915. doi:10.1007/BF02616120
23. Rusciano D, Burger M (2000) In vivo cancer metastasis assays. In: Welch D (ed) Cancer metastasis: experimental approaches: Elsevier, pp 207–242
24. Kinder M, Chislock E, Bussard KM et al (2008) Metastatic breast cancer induces an osteoblast inflammatory response. Exp Cell Res 314(1):173–183. doi:10.1016/j.yexcr.2007.09.021
25. Lian JB, Stein GS (1992) Concepts of osteoblast growth and differentiation: basis for modulation of bone cell development and tissue formation. Crit Rev Oral Biol Med 3(3):269–305
26. Page DL, Anderson TJ, Sakamoto G (1987) Diagnostic histopathology of the breast, pp 219–222
27. Pitts WC (1991) Carcinomas with metaplasia and sarcomas of the breast. Am J Clin Pathol 95:623–632
28. Friedl P, Wolf K (2003) Tumour-cell invasion and migration: diversity and escape mechanisms. Nat Rev Cancer 3(5):362–374. doi:10.1038/nrc1075
29. Mercer R, Miyasaka C, Mastro AM (2004) Metastatic breast cancer cells suppress osteoblast adhesion and differentiation. Clin Exp Metastasis 21(5):427–435. doi:10.1007/s10585-004-1867-6
30. Chou YF, Dunn JC, Wu BM (2005) In vitro response of MC3T3-E1 pre-osteoblasts within three dimensional apatite-coated PLGA scaffolds. J Biomed Mater Res B Appl Biomater 75(1):81–90. doi:10.1002/jbm.b.30261
31. Franz-Odendaal TA, Hall BK, Witten PE (2006) Buried alive: how osteoblasts become osteocytes. Dev Dyn 235(1):176–190. doi:10.1002/dvdy.20603
32. Stetler-Stevenson WG (1993) Tumor cell interactions with the extracellular matrix during invasion and metastasis. Annu Rev Cell Biol 9(1):541. doi:10.1146/annurev.cb.09.110193.002545

33. Visser Kd, Coussens L (2006) The inflammatory tumor microenvironment and its impact on cancer development. Contrib Microbiol 13:118–137
34. Marriott I (2004) Osteoblast responses to bacterial pathogens: a previously unappreciated role for bone-forming cells in host defense and disease progression. Immunol Res 30:291–308. doi:10.1385/IR:30:3:291
35. Fritz EA, Glant TT, Vermes C et al (2002) Titanium particles induce the immediate early stress responsive chemokines IL-8 and MCP-1 in osteoblasts. J Orthop Res 20:490–498. doi:10.1016/S0736-0266(01)00154-1
36. Kinder M, Chislock E, Bussard KM et al (2008) Metastatic breast cancer induces an osteoblast inflammatory response. Exp Cell Res 314(1):173–183. doi:10.1016/j.yexcr.2007.09.021
37. Papanicolaou DA (1998) The pathophysiologic roles of interleukin-6 in human disease. Ann Intern Med 128(2):127
38. Roodman GD, Kurihara N, Ohsaki Y et al (1992) Interleukin 6. A potential autocrine/paracrine factor in Paget's disease of bone. J Clin Invest 89(1):46–52. doi:10.1172/JCI115584
39. Devlin RD, Bone HG 3rd, Roodman GD (1996) Interleukin-6: a potential mediator of the massive osteolysis in patients with Gorham-Stout disease. J Clin Endocrinol Metab 81(5):1893–1897. doi:10.1210/jc.81.5.1893
40. Klein B, Zhang XG, Lu ZY et al (1995) Interleukin-6 in human multiple myeloma. Blood 85(4):863–872
41. Kozlowski L, Zakrzewska I, Tokajuk P et al (2003) Concentration of interleukin-6 (IL-6), interleukin-8 (IL-8) and interleukin-10 (IL-10) in blood serum of breast cancer patients. Roczniki Akademii Medycznej W Bialymstoku (1995) 48:82–84
42. Benoy I, Salgado R, Colpaert C et al (2002) Serum interleukin 6, plasma VEGF, serum VEGF, and VEGF platelet load in breast cancer patients. Clin Breast Cancer 2(4):311–315
43. Mettler L, Salmassi A, Heyer M et al (2004) Perioperative levels of interleukin-1beta and interleukin-6 in women with breast cancer. Clin Exp Obstet Gynecol 31(1):20–22
44. Salgado R, Junius S, Benoy I et al (2003) Circulating interleukin-6 predicts survival in patients with metastatic breast cancer. Int J Cancer 103(5):642–646
45. Zhang GJ, Adachi I (1999) Serum interleukin-6 levels correlate to tumor progression and prognosis in metastatic breast carcinoma. Anticancer Res 19(2B):1427–1432
46. Bozcuk H, Uslu G, Samur M et al (2004) Tumour necrosis factor-alpha, interleukin-6, and fasting serum insulin correlate with clinical outcome in metastatic breast cancer patients treated with chemotherapy. Cytokine 27(2–3):58–65. doi:10.1016/j.cyto.2004.04.002
47. Kozlow W, Guise TA (2005) Breast cancer metastasis to bone: mechanisms of osteolysis and implications for therapy. J Mammary Gland Biol Neoplasia 10(2):169–180. doi:10.1007/s10911-005-5399-8
48. Sanchez-Sweatman OH, Lee J, Orr FW et al (1997) Direct osteolysis induced by metastatic murine melanoma cells: role of matrix metalloproteinases. Eur J Cancer 33(6):918–925. doi:10.1016/S0959-8049(97)00513-3
49. Phadke PA, Mercer RR, Harms JF et al (2006) Kinetics of metastatic breast cancer cell trafficking in bone. Clin Cancer Res 12(5):1431–1440. doi:10.1158/1078-0432.CCR-05-1806
50. Stewart AF, Vignery A, Silverglate A et al (1982) Quantitative bone histomorphology in humoral hypercalcemia of malignancy: uncoupling of bone cell activity. J Clin Endocrinol Metab 55:219–227
51. Sasaki A, Boyce BF, Story B et al (1995) Bisphosphonate risedronate reduces metastatic human breast cancer burden in bone in nude mice. Cancer Res 55(16):3551–3557
52. Lipton A (2000) Bisphosphonates and breast carcinoma: present and future. Cancer 88:3033–3037. doi:0.1002/1097-0142(20000615)88:12+<3033::AID-CNCR20>3.0.CO;2-C
53. Mastro A, Gay C, Welch D et al (2004) Breast cancer cells induce osteoblast apoptosis: a possible contributor to bone degradation. J Cell Biochem 91(2):265–276. doi:10.1002/jcb.10746

Bisphosphonate and Taxane Effects on Osteoblast Proliferation and Differentiation

Genevieve N. Miller, McNair Scholar, The Pennsylvania State University
Erwin A. Vogler, Ph.D.
Professor of Materials Science and Engineering
Departments of Materials Science and Engineering and Bioengineering
The Pennsylvania State University
Andrea M. Mastro, Ph.D.
Professor of Microbiology and Cell Biology
Department of Biochemistry and Molecular Biology
The Pennsylvania State University

ABSTRACT

Breast cancer is the second most commonly diagnosed cancer in women in the United States. Advanced stages of breast cancer frequently metastasize to bone, where it is difficult to diagnose and treat. Current cancer-in-bone therapeutics focus on bisphosphonates to inhibit osteolysis (bone dissolution by osteoclasts) and taxanes to impede cancer cell growth. Effects of these drugs on osteoblasts (bone forming cells) have not been well studied. The purpose of this study is to observe and quantify the effect of a bisphosphonate (zoledronic acid) and a taxane (docetaxel) on osteoblast proliferation and differentiation. Results of this research serve as preliminary data that will guide studies in an advanced three-dimensional bone tissue model.

INTRODUCTION

Breast Cancer in Bone

Breast cancer is among the most commonly diagnosed cancers in the United States. This year alone, approximately 182,460 women in the United States will develop invasive breast cancer, and 40,480 women are expected to die from the disease. The risk of a woman in the United States developing breast cancer in their lifetime is now 1 in 8[1]. Worldwide, breast cancer has reached epidemic proportions[2].

Metastatic breast cancer is the most advanced stage of breast cancer, and the most frequent site of breast cancer metastases is bone. Of the cases of breast cancer diagnosed each year, approximately 25% of those cancers metastasize, with the first site of metastasis located in bone in 46% of cases and in 70% of cases with first relapse. Once cancerous breast cells colonize bone, the cure rate is almost zero[3].

The normal bone environment is in a dynamic equilibrium – the bone undergoes constant remodeling in which osteoclasts resorb bone, whereas osteoblasts deposit bone. When breast

cancer metastasizes to bone, this balance is shifted to abnormally high osteoclastic resorption. Interactions between osteoclasts and breast-cancer cells establish a vicious cycle in which osteolysis and tumor activity both increase. Activation of osteoclasts results in pain, bone fracture, and hypercalcemia[4-6].

An In Vitro Model of Bone

Modeling the bone environment to study cancer colonization of bone is difficult because few cell culture methods simultaneously provide biological relevance and simplicity required for experimental control. The previous lack of a sophisticated model not only has hindered breast cancer metastasis research, but also has hindered the development of therapeutics for bone metastases. Dhurjati et al. recently developed a compartmentalized culture device, hereafter referred to as the bioreactor, that operates on the principle of continuous growth and dialysis[7]. The bioreactor consists of a cell growth chamber separated from a larger medium reservoir by a dialysis membrane. Waste from the growth compartment and nutrients from the medium reservoir are capable of passing through the dialysis membrane, while macromolecules synthesized by the cells as they develop are maintained in the growth chamber. The bioreactor design creates an extremely stable cellular environment that allows for the growth of three-dimensional tissue for an extended period of time. This cell-culture system allowed development of a three-dimensional multiple-cell layer of osteoblastic tissue over 10 months of continuous culture. Krishnan et al. showed that this three-dimensional tissue was a useful surrogate for studies of cancer in bone[8].

Cancer in Bone Therapy

This research extends the bioreactor model by introducing therapeutic drugs to the system. Two drug families are currently used in the treatment of bone metastases – bisphosphonates to regulate osteoclast activity and taxanes to attack cancer cells. The effects of these drugs on bisphosphonates have not been well studied.

Bisphosphonates are synthetic analogues of inorganic pyrophosphate, in which the oxygen atom connecting the two phosphates is replaced by a carbon atom. This stabilizes the molecule from biological degradation. Nitrogen-containing bisphosphonates have recently proven to be the most aggressive in targeting bone metastases. Bisphosphonates bind strongly to bone mineral, particularly in areas of increased bone activity. As bone resorption occurs, osteoclasts internalize bisphosphonates. Once internalized, the bisphosphonates inhibit an enzyme that contributes to osteoclast function and survival. Recent studies have suggested that bisphosphonates may also have antitumor effects. During bone resorption, growth factors are released that stimulate cancer cell activity; therefore decreased osteoclast activity would have negative effects on cancer cells as well. Bisphosphonates decrease cancer cell proliferation and induce apoptosis[9-13].

Taxanes are widely used chemotherapeutic agents. Taxanes are microtubule interfering agents that bind to β tubulin, causing abnormal assembly of microtubules and preventing disassembly. This arrests the cell cycle in the G_2M phase and induces apoptosis. Taxanes also cause programmed cell death by inducing phosphorylation of Bcl-2, an anti-apoptotic protein[14-15].

Recent work has suggested that the most effective therapy for metastatic breast cancer to bone is combinatorial therapy with a bisphosphonate and a taxane. Bisphosphonates have been shown to enhance the antitumor effects of taxanes *in vitro* on cancer cell invasion, adhesion, and apoptosis[16-17].

The purpose of this research was to assess the effects of a bisphosphonate (zoledronic acid) and taxane (docetaxel) on osteoblast proliferation and differentiation. The goal was to determine an appropriate concentration for use in the bioreactor model. Low concentrations (0.05-0.50 μM) of zoledronic acid enhanced both osteoblast proliferation and differentiation, while high concentrations of docetaxel (10.0 μM) had positive effects on osteoblast differentiation.

MATERIALS AND METHODS

Cells and Cell Culture

Osteoblast Proliferation

Murine calvaria pre-osteoblast (MC3T3-E1) cells were plated at $1x10^4$ cells/cm^2 in a 24-well plate and grown in alpha minimum essential medium (α-MEM) supplemented with 10% heat-inactivated fetal bovine serum (FBS) and 1% penicillin-streptomycin, hereafter referred to as growth medium. Cultures were incubated at 37°C. After 24 hours, zoledronic acid was added to the growth medium in 0.05, 0.5 and 5 μM concentrations. Medium was changed after 24 hours to allow for acute exposure (pulse dose) and chronic exposure (chronic dose).

Osteoblast Differentiation

MC3T3-E1 cells were plated at $1x10^4$ cells/cm^2 in a 24-well plate and grown in α-MEM supplemented with 10% heat-inactivated FBS, 1% penicillin-streptomycin, 10mM β-glycerophosphate and 50 μg/mL ascorbic acid, hereafter referred to as differentiation medium. Cells were allowed to differentiate for 17 days prior to the addition of zoledronic acid in 0.05, 0.5 and 5.0 μM concentrations or docetaxel in 0.1, 1.0 and 10.0 μM concentrations. After 24 hours, the supernatant was collected for cytokine assays and a media change was performed to allow for acute and chronic dosing. Medium was collected and replenished again after three days.

Zoledronic Acid and Docetaxel

A 5 μM stock solution of zoledronic acid was prepared in 0.1N sodium hydroxide. The stock solution was diluted with growth medium and differentiation medium for measures of cell proliferation and differentiation, respectively. A 10 μM stock solution of docetaxel was prepared in 100% ethanol and diluted with differentiation medium.

Assessment of Cell Proliferation

Four day osteoblasts grown in varying concentrations of zoledronic acid were rinsed twice with phosphate buffered saline (PBS) and detached with three rinses of 0.002% pronase in PBS. Upon detachment, the pronase was neutralized with growth medium. The cell suspension was diluted with 0.4% trypan blue dye and both viable and apoptotic cells were counted with a hemocytometer.

Differentiated osteoblasts grown in varying concentrations of zoledronic acid and docetaxel were also counted with a hemocytometer and trypan blue stain. Cells were initially rinsed twice with PBS and detached with three rinses of 0.002% pronase in PBS. The differentiated cells detached as an aggregate accumulated in the collagen matrix. In an attempt to further detach the osteoblasts from the collagen matrix, the pronase solution was neutralized with growth medium and then placed in a centrifuge. The solution was removed and replaced with accutase.

Assessment of Cell Differentiation – Alkaline Phosphatase

Differentiated osteoblasts were stained for alkaline phosphatase (ALP) activity. Cells were rinsed once with PBS and then fixed for 10 minutes with 10% formaldehyde. Cells were then rinsed three times for five minutes each with PBS. The cells were stained with an ALP stain consisting of pre-warmed dH_2O, 0.2M Tris, napthol and Fast Blue RR Salt and incubated at 37°C for 30 minutes. They were then rinsed three times for five minutes each with dH_2O and the dish was set to dry. The cell culture dish was then scanned into a computer. The stain intensity was quantified using ImageQuant software.

MCP-1 and IL-6 Expression

MCP-1 and IL-6 were quantified using a sandwich ELISA. Flat-bottom 96-well plates were coated with antibody at 0.4 μg/ml for MCP-1 and 2 μg/ml for IL-6. Plates were incubated overnight at 4°C. The plates were washed four times with PBS with 0.05% Tween 20 and blocked for 2 hours with PBS and 1% BSA. After three washes, samples and standards were added and incubated overnight at 4°C. The plates were then washed four times and incubated with detection antibody for 2 hours at room temperature. The plates were washed 6 times and incubated with NeutrAvidin horseradish peroxidase conjugate for 30 minutes at room temperature. The plates were washed 8 times and then incubated with ABTS peroxidase substrate at room temperature for 90 minutes. Plates were read at 405 nm in an ELISA reader.

RESULTS

Osteoblast Proliferation

Drug effects on osteoblast proliferation was assessed by means of cell counting and a trypan blue stain. Low concentration zoledronic acid (0.05 μM) enhanced osteoblast growth. As zoledronic acid concentration increased, cell growth declined. Results were the same for both acute and chronic exposures (Fig. 1).

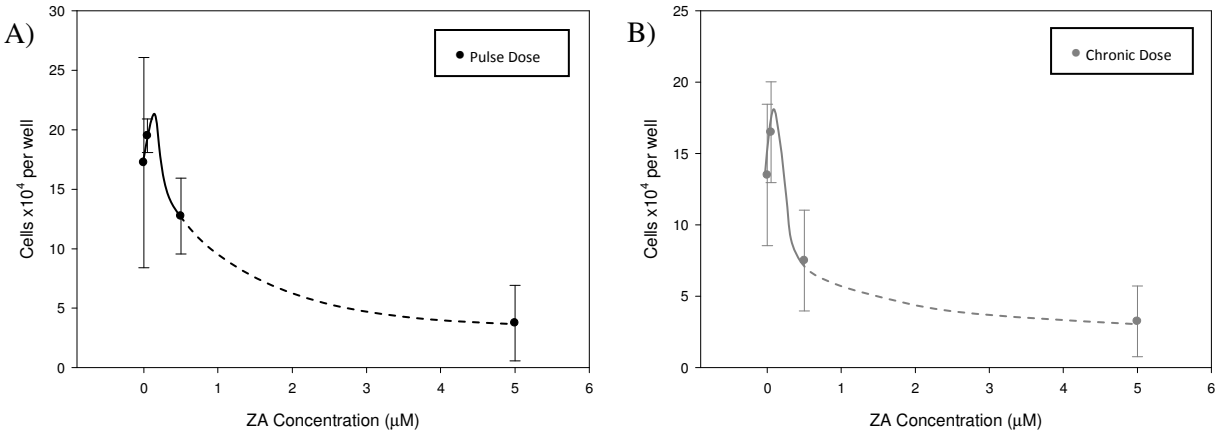

FIGURE 1. Effect of zoledronic acid (ZA) on osteoblast proliferation. Osteoblasts were plated at $1x10^4$ cells/cm^2 and ZA was added in concentrations of 0.00, 0.05, 0.50 and 5.00 μM. After 24 hours, medium was removed and replaced according to a dosing regimen. Wells designated for acute exposure (A) were replenished with osteoblast growth medium, while those for chronic exposure (B) received another drug dose. Proliferation was assessed with a trypan blue stain. Lines are guides to the eye.

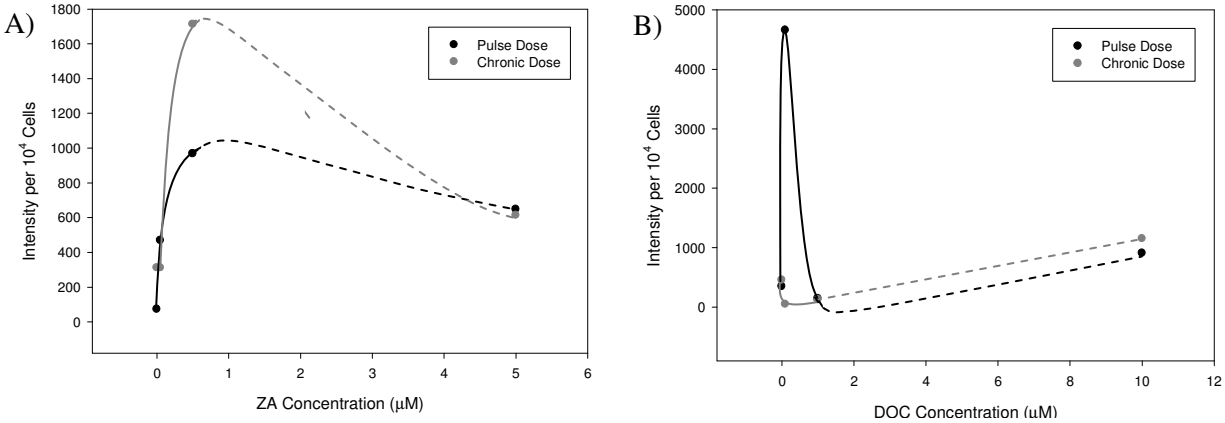

FIGURE 2. Drug effects on alkaline phosphatase production. Osteoblasts were plated at $1x10^4$ cells/cm^2 and grown in differentiation medium for two weeks. Cells were treated with either zoledronic acid (ZA) or docetaxel (DOC). ZA (A) or DOC (B) was added in low, medium, and high concentrations (ZA – 0.00, 0.05, 0.50 and 5.00 μM; DOC – 0.00, 0.10, 1.00 and 10.00 μM). After 24 hours, medium was removed and replaced according to a dosing regimen. Wells designated for acute exposure were replenished with osteoblast differentiation medium, while drug doses were added to wells for chronic exposure. Cells were stained for alkaline phosphatase. The intensity of the stain was quantified using ImageQuant software, and intensity was normalized to viable cell number (cell counts obtained using trypan blue stain). Lines are guides to the eye.

Osteoblast Differentiation

Drug effects on osteoblast differentiation were assessed by measuring alkaline phosphatase production. Alkaline phosphatase (ALP) production increased with low and medium (0.05 and 0.50 μM, respectively) zoledronic acid concentrations, while ALP production declined at the higher concentration. Chronic exposure to zoledronic acid caused a more dramatic rise in ALP than the acute exposure. Docetaxel treated cells showed different responses to pulse and chronic

dosing. Acute exposure to docetaxel resulted in a sharp increase in ALP production for low concentration docetaxel (0.1 μM), followed by a rapid decrease to the medium concentration (1.0 μM) and a slight increase with the higher concentration. Chronic exposure to docetaxel produced an immediate decline in ALP production followed by a slight increase with concentration (Fig. 2).

Osteoblast Inflammatory Response

Drugs effects on MCP-1 and IL-6 expression were analyzed to determine whether either drug elicited an inflammatory response from the osteoblasts. Acute exposure of zoledronic acid decreased expression of MCP-1 as a function of concentration. Chronic exposure, however, increased MCP-1 expression through low and medium concentrations of zoledronic acid (0.05 and 0.50 μM, respectively), followed by a decline in MCP-1 expression (Fig. 3). Most zoledronic acid treated cells produced IL-6 below the level of detection, therefore the data were inconclusive (Table 1).

Both pulse and chronic doses of docetaxel elicited similar osteoblast responses. Low concentration docetaxel (0.1 μM) increased MCP-1 expression, followed by a decline through medium and high concentrations of the drug (Fig. 3). IL-6 concentrations were below the level of detection in both dosing methods. After 24 hours exposure to docetaxel, IL-6 expression was detectable, with IL-6 concentrations decreasing with increasing docetaxel concentration (Table 2).

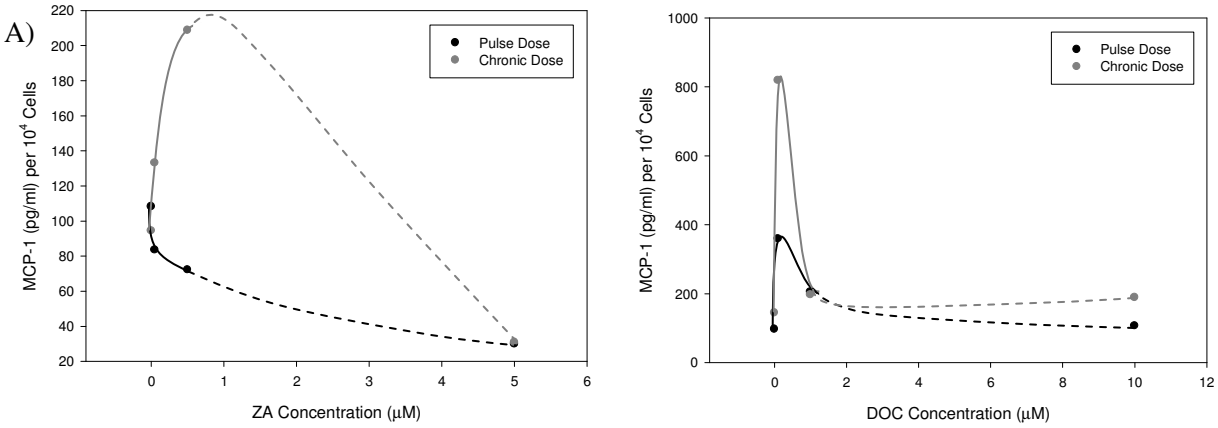

FIGURE 3. Drug effects on MCP-1 expression. Osteoblasts were plated at $1x10^4$ cells/cm^2 and grown in differentiation medium for two weeks. Cells were treated with either zoledronic acid (ZA) or docetaxel (DOC). ZA (A) or DOC (B) was added in low, medium, and high concentrations (ZA – 0.00, 0.05, 0.50 and 5.00 μM; DOC – 0.00, 0.10, 1.00 and 10.00 μM). After 24 hours, medium was removed and replaced according to a dosing regimen. Supernatant was collected after an additional 3 days of culture. Supernatant was assayed for MCP-1 using a sandwich ELISA. MCP-1 concentration was normalized to viable cell number (cell counts obtained using trypan blue stain). Lines are guides to the eye.

TABLE 1. Effects of zoledronic acid (ZA) on IL-6 expression.

	IL-6 Concentration (pg/ml)		
ZA Concentration	**24 Hours**	**Pulse Dose**	**Chronic Dose**
Control - 0	54.0	*	*
Low - 0.05	*	*	22.0
Medium - 0.5	*	*	*
High - 5.0	26.0	18.0	*

Osteoblasts were plated at $1x10^4$ cells/cm^2 and grown in differentiation medium for two weeks. Cells were treated with ZA in control, low, medium and high concentrations (0.00, 0.05, 0.50 and 5.00 μM, respectively). After 24 hours, supernatant was collected and replaced according to a dosing regimen. Supernatant was collected after an additional 3 days of culture. Supernatant was assayed for IL-6 using a sandwich ELISA.

TABLE 2. Effects of docetaxel (DOC) on IL-6 expression.

	IL-6 Concentration (pg/ml)		
DOC Concentration	**24 Hours**	**Pulse Dose**	**Chronic Dose**
Control - 0	139.0	*	*
Low - 0.1	47.0	*	*
Medium - 1.0	84.0	*	*
High - 10.0	91.0	*	*

Osteoblasts were plated at $1x10^4$ cells/cm^2 and grown in differentiation medium for two weeks. Cells were treated with DOC in control, low, medium and high concentrations (0.00, 0.10, 1.00 and 10.00 μM, respectively). After 24 hours, supernatant was collected and replaced according to a dosing regimen. Supernatant was collected after an additional 3 days of culture. Supernatant was assayed for IL-6 using a sandwich ELISA.

DISCUSSION AND FUTURE WORK

The bisphosphonate zoledronic acid and the taxane docetaxel have pronounced effects on osteoblast proliferation and differentiation. Low concentrations of zoledronic acid enhanced both osteoblast proliferation and differentiation. However, low concentrations also elicit the most pronounced inflammatory response. High concentrations of docetaxel incur the lowest inflammatory response and have the most positive effects on osteoblast differentiation. From these observations, zoledronic acid at 0.05 μM and docetaxel at 10 μM are candidates for use in the bioreactor model. Choice of ideal concentrations will depend on the effect on breast-cancer cells from future work. Future experiments include assessing the effects of these drugs on breast-cancer cells and evaluating combinatorial therapy in standard tissue culture.

ACKNOWLEDGEMENTS

I would like to thank my advisors, Dr. Vogler and Dr. Mastro, and the McNair Scholars Program for granting me the opportunity to participate in research and for funding this project. I would also like to thank Donna Sosnoski for providing me with the skills necessary to complete this experiment.

REFERENCES

1. American Cancer Society. *Breast Cancer Facts & Figures 2007-2008.* Atlanta: American Cancer Society, Inc.

2. *Nature Medicine*. Special Web Focus: Breast Cancer. 2001(4).
3. Landis SH, Murray T, Bolden S, Wingo PA. Cancer Statistics. CA Cancer J Clin 1999:49:8-31.
4. Rubens RD. Bone Metastases – The Clinical Problem. Eur J Cancer 1998:34:210-213.
5. Mundy GR. Metastasis to bone: causes, consequences and therapeutic opportunities. Nat Rev Cancer 2002:2:584-593.
6. Coleman RE. Clinical Features of Metastatic Bone Disease and Risk of Skeletal Morbidity. Clin Cancer Res 2006:12(20):6243-6249.
7. Dhurjati R, Liu X, Gay CV, Mastro AM, Vogler EA. Extended-Term Culture of Bone Cells in a Compartmentalized Bioreactor. Tissue Engineering 2006:12:3045-3054.
8. Fleisch H. Development of bisphosphonates. Breast Cancer Res 2002:4(1):30-34.
9. Dhurjati R, Krishnan V, Shuman LA, Mastro AM, Vogler EA. Metastatic breast cancer cells colonize and degrade three-dimensional osteoblastic tissue in vitro. Clin Exp Metastasis 2008:
10. Coleman RE. Bisphosphonates in breast cancer. Annals of Oncology 2005:16:687-695.
11. Green JR. Bisphosphonates: Preclinical Review. The Oncologist 2004:9(4):3-13.
12. Coxon FP, Thompson K, Rogers MJ. Recent advances in understanding the mechanism of action of bisphosphonates. Current Opinion in Pharmacology 2006:6:307-312.
13. Russell RGG, Watts NB, Ebetino FH, Rogers MJ. Mechanisms of action of bisphosphonates: similarities and differences and their potential influence on clinical efficacy. Osteoporos Int 2008:19:733-759.
14. Subbaramaiah K, Hart JC, Norton L, Dannenberg AJ. Microtubule-interfering Agents Stimulate the Transcription of Cyclooxygenase-2. The Journal of Biological Chemistry 2000:20:14838-14845.
15. Olsen SR. Taxanes and COX-2 inhibitors: from molecular pathways to clinical practice. Biomedicine and Pharmacology 2005:59:306-310.
16. Magnetto S, Boissier S, Delmas PD, Clezardin P. Additive antitumor activities of taxoids in combination with the bisphosphonate ibandronate against invasion and adhesion of human breast carcinoma cells to bone. Int J Cancer 1999:83:263-269.
17. Inoue K, Karashima T, Fukata S, Nomura A, Kawada C, Kurabayashi A, Furihata M, Ohtsuki Y, Shuin T. Effect of Combination Therapy with a Novel Bisphosphonate, Minodronate (YM529), and Docetaxel on a Model of Bone Metastasis by Human Transitional Cell Carcinoma. Clin Cancer Res 2005:11(18):6669-6677.

The Effect of Zoledronic Acid on Breast Cancer Colonization of Osteoblast Tissue *In Vitro*

by Genevieve Miller

January 22, 2009

Background on Bisphosphonates

Bisphosphonates…

- **bind avidly to bone mineral**
- **are internalized by osteoclasts during resorption**
- **interfere with functions vital to osteoclast survival**
- **reduce release of factors that stimulate tumor growth**

Recently, bisphosphonates have been established as standard treatment for bone metastases.

New research has suggested that combination treatment of bisphosphonates with chemotherapeutic agents may better treat bone metastases.

Hypothesis and Specific Aims

Hypothesis: Combination therapy of a bisphosphonate (zoledronic acid) and a taxane (docetaxel) will inhibit breast cancer colonization of osteoblast tissue to a greater degree than a bisphosphonate alone.

→ ***Specific Aim 1: To characterize the effect of zoledronic acid on breast cancer colonization of osteoblast tissue.***

Specific Aim 2: To characterize the effect of docetaxel on breast cancer colonization of osteoblast tissue.

Specific Aim 3: To characterize the effect of a combination treatment of zoledronic acid and docetaxel on breast cancer colonization of osteoblast tissue.

The bioreactor is a compartmentalized cell-culture device that allows for long-term growth of three-dimensional tissue.

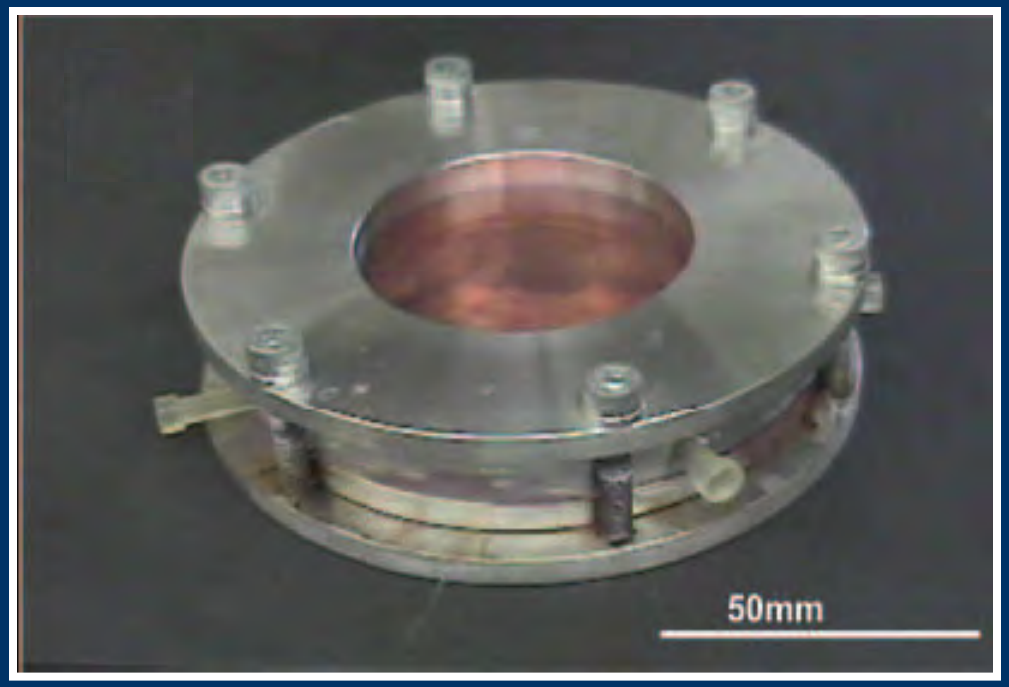

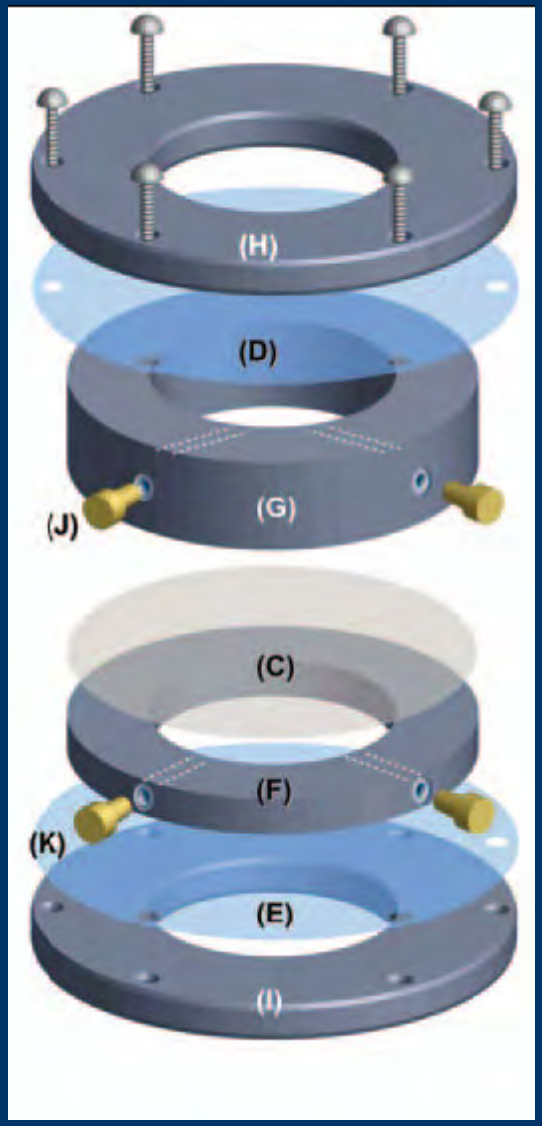

Experimental Protocol

1. Osteoblasts (MC3T3-E1) were allowed to mature for 3 months in the bioreactor.

2. Breast-cancer cells (MDA-MB-231^{GFP}) were added to the cultures and allowed to colonize the osteoblasts for 3 days.

3. Cultures were treated with 0.05 µM and 0.5 µM concentrations of zoledronic acid.

4. Osteoblasts were stained with either CTO or Phalloidin (RED) and cancer cells expressed GFP (Green). Images of the cultures were taken using confocal microscopy.

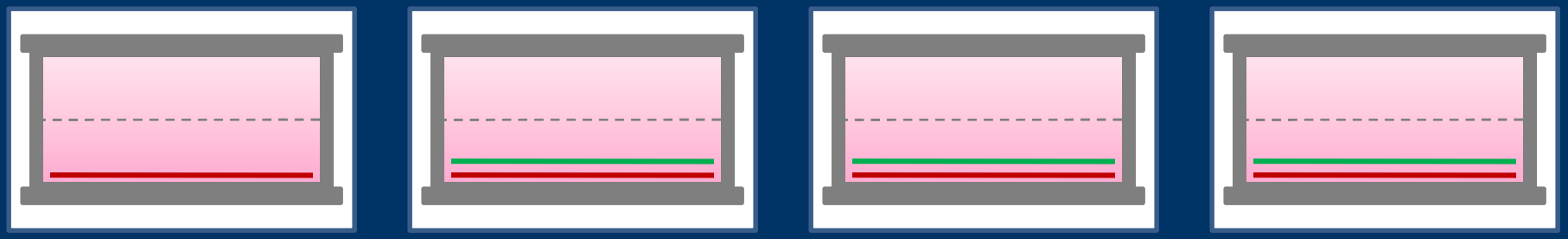

OB (control) | OB + BC | OB + BC + 0.05 µM ZOL | OB + BC + 0.5 µM ZOL

The effect of ZOL was evaluated using confocal microscopy with considerations to the following parameters:

Experimental Parameter	Culture/Treatment			
	OB	OB + BC	OB + BC + 0.05µM ZOL	OB + BC + 0.5µM ZOL
BC Colony Formation	n/a	+++	+	++
BC Processes	n/a	+++	+	+
Rounded BC Morphology	n/a	+	+++	++
BC Alignment	n/a	+++	+	++
Ruptured BC Cells	n/a	-	++	++
Spindle-shaped OB Morphology	---	+++	+	+
Tissue Penetration	n/a	+++	+	++

Treatment with ZOL inhibited the formation of breast-cancer cell colonies.

Experimental Parameter	Culture/Treatment			
	OB	OB + BC	OB + BC + 0.05µM ZOL	OB + BC + 0.5µM ZOL
BC Colony Formation	n/a	+++	+	++
BC Processes	n/a	+++	+	+
Rounded BC Morphology	n/a	+	+++	++
BC Alignment	n/a	+++	+	++
Ruptured BC Cells	n/a	-	++	++
Spindle-shaped OB Morphology	---	+++	+	+
Tissue Penetration	n/a	+++	+	++

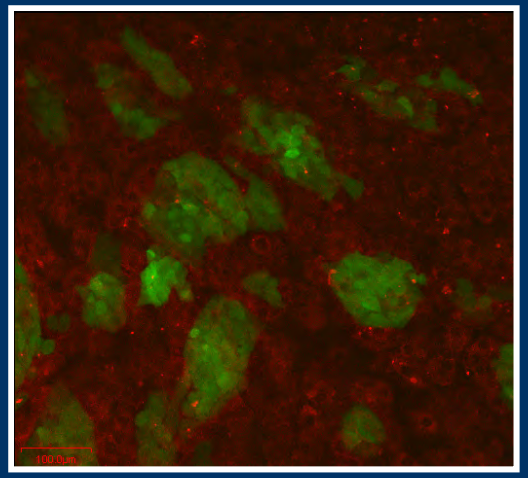

OB + BC

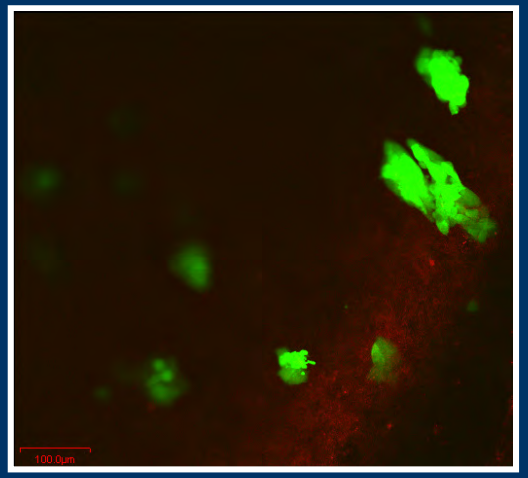

OB + BC + 0.05 µM ZOL

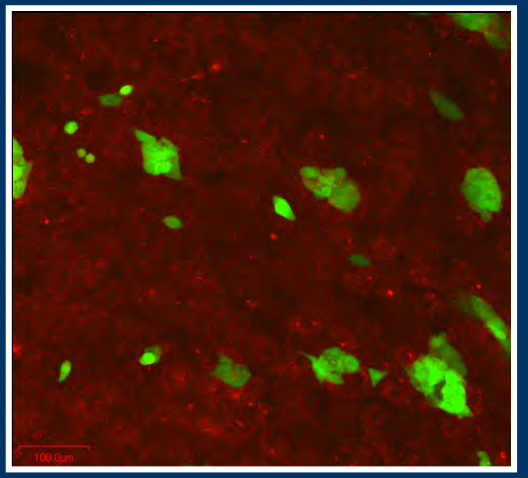

OB + BC + 0.5 µM ZOL

*24 hr. ZOL exposure

Treatment with ZOL inhibited the formation of breast-cancer cell colonies.

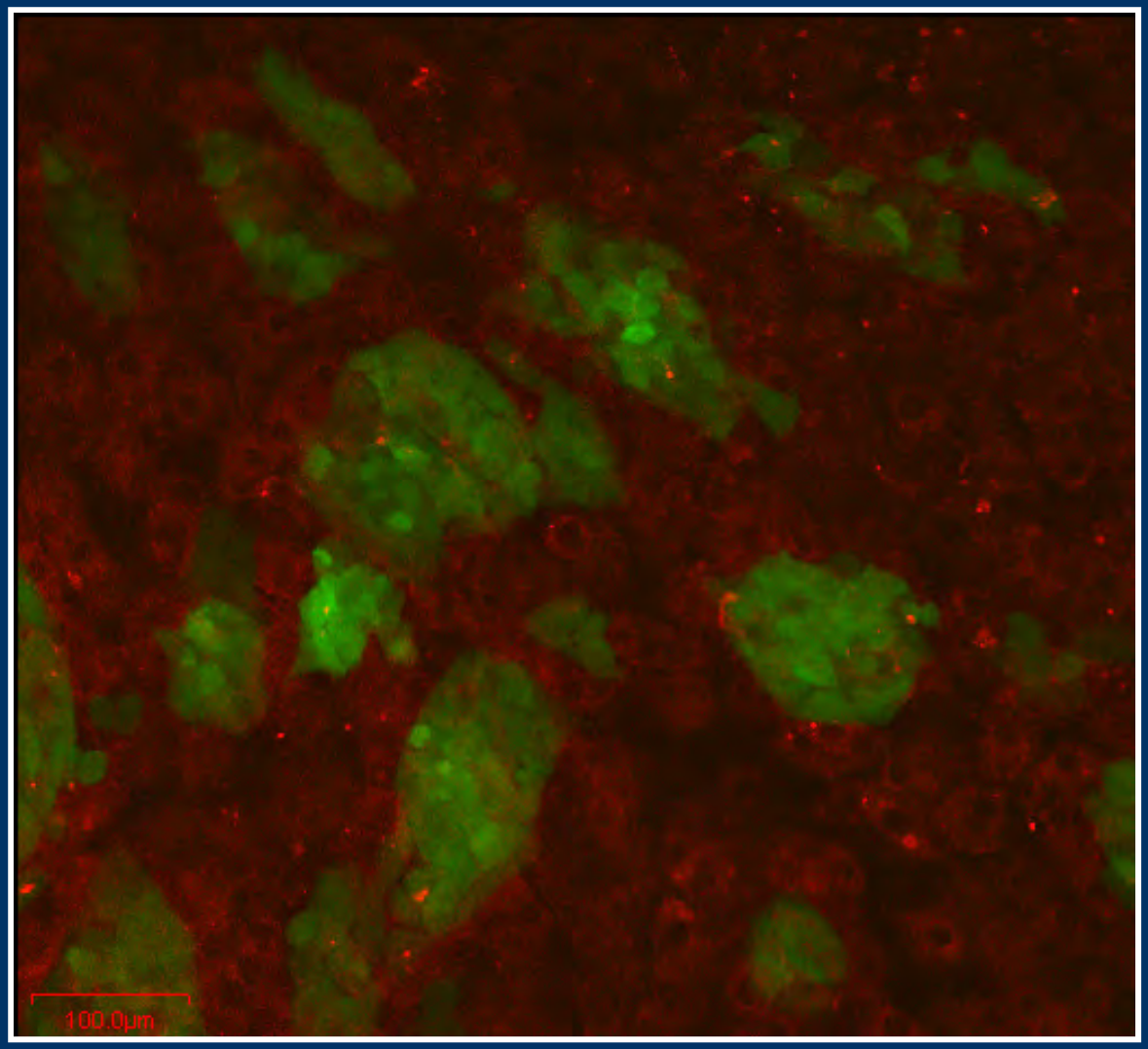

OB + BC

*24 hr. ZOL exposure

Treatment with ZOL inhibited the formation of breast-cancer cell colonies.

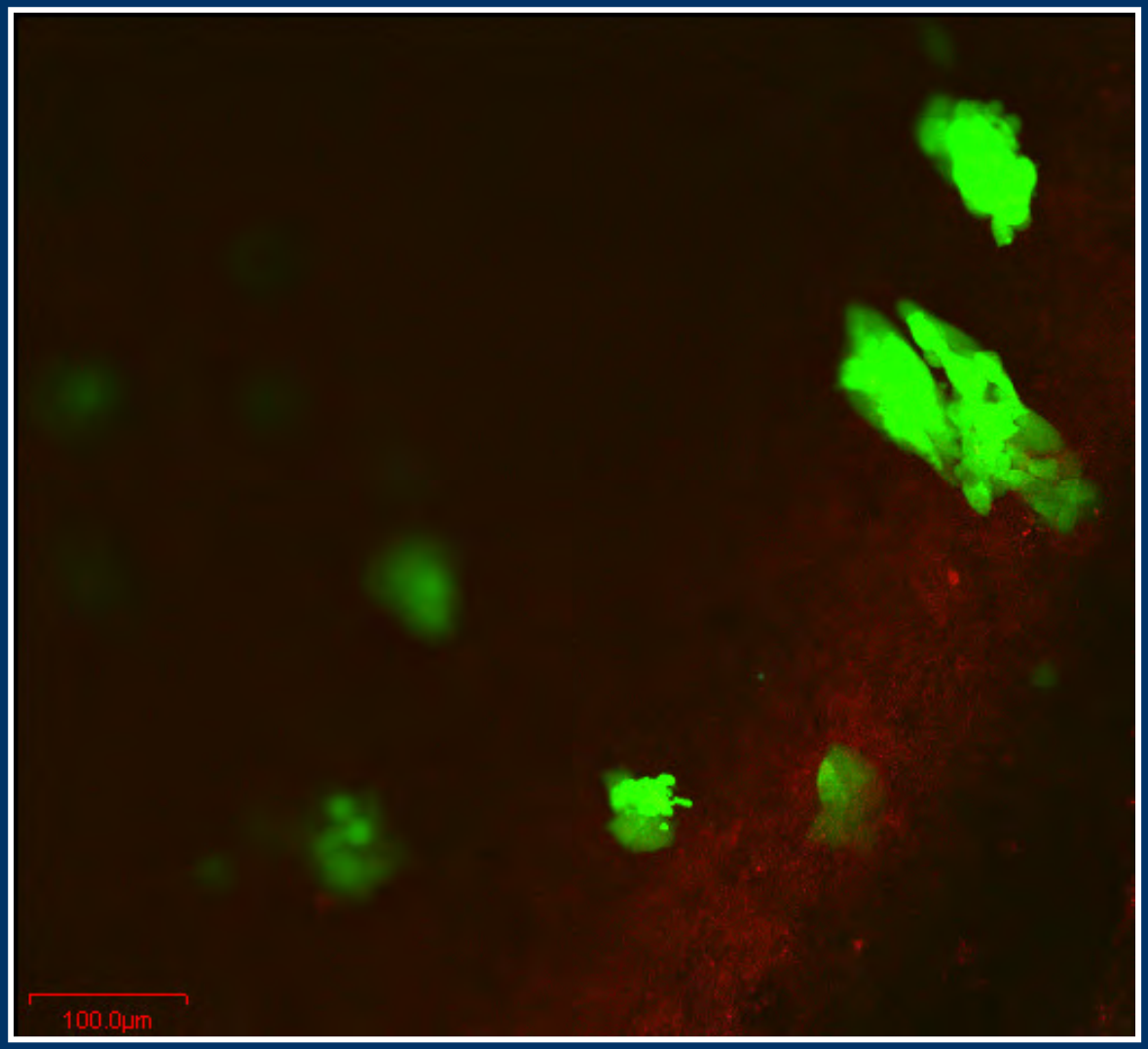

OB + BC +
0.05 µM ZOL

*24 hr. ZOL exposure

Treatment with ZOL inhibited the formation of breast-cancer cell colonies.

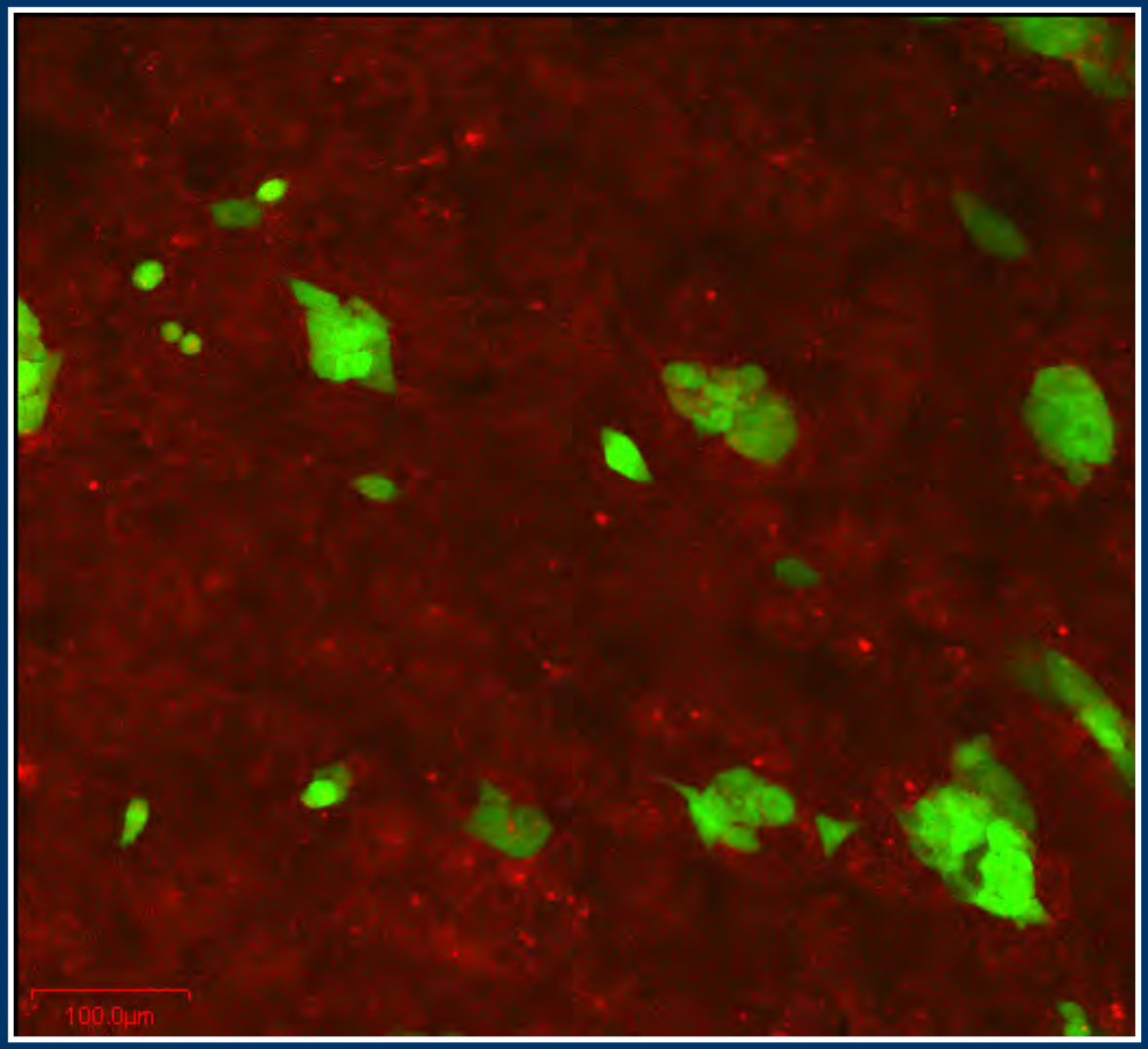

OB + BC +
0.5 µM ZOL

*24 hr. ZOL exposure

Cultures treated with ZOL showed more rounded breast-cancer cell morphology and fewer processes.

Experimental Parameter	Culture/Treatment			
	OB	OB + BC	OB + BC + 0.05µM ZOL	OB + BC + 0.5µM ZOL
BC Colony Formation	n/a	+++	+	++
BC Processes	n/a	+++	+	+
Rounded BC Morphology	n/a	+	+++	++
BC Alignment	n/a	+++	+	++
Ruptured BC Cells	n/a	-	++	++
Spindle-shaped OB Morphology	---	+++	+	+
Tissue Penetration	n/a	+++	+	++

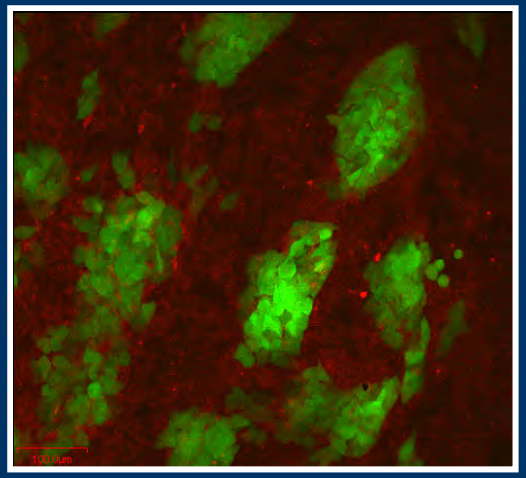

OB + BC

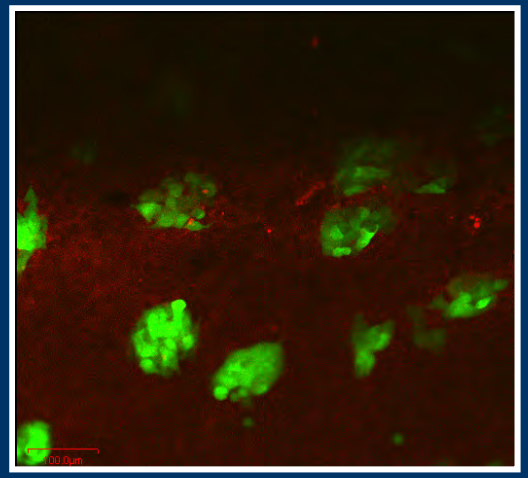

OB + BC + 0.05 µM ZOL

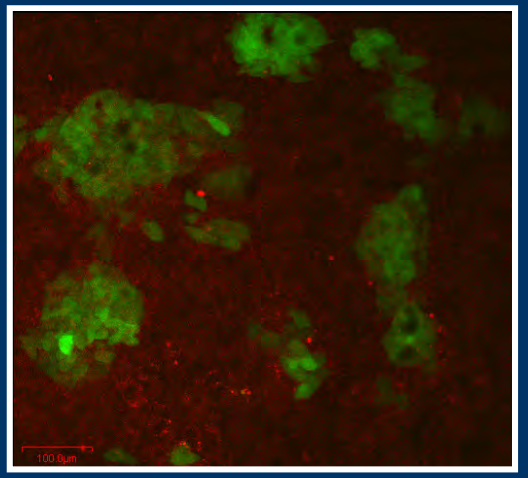

OB + BC + 0.5 µM ZOL

*48 hr. ZOL exposure

Cultures treated with ZOL showed more rounded breast-cancer cell morphology and fewer processes.

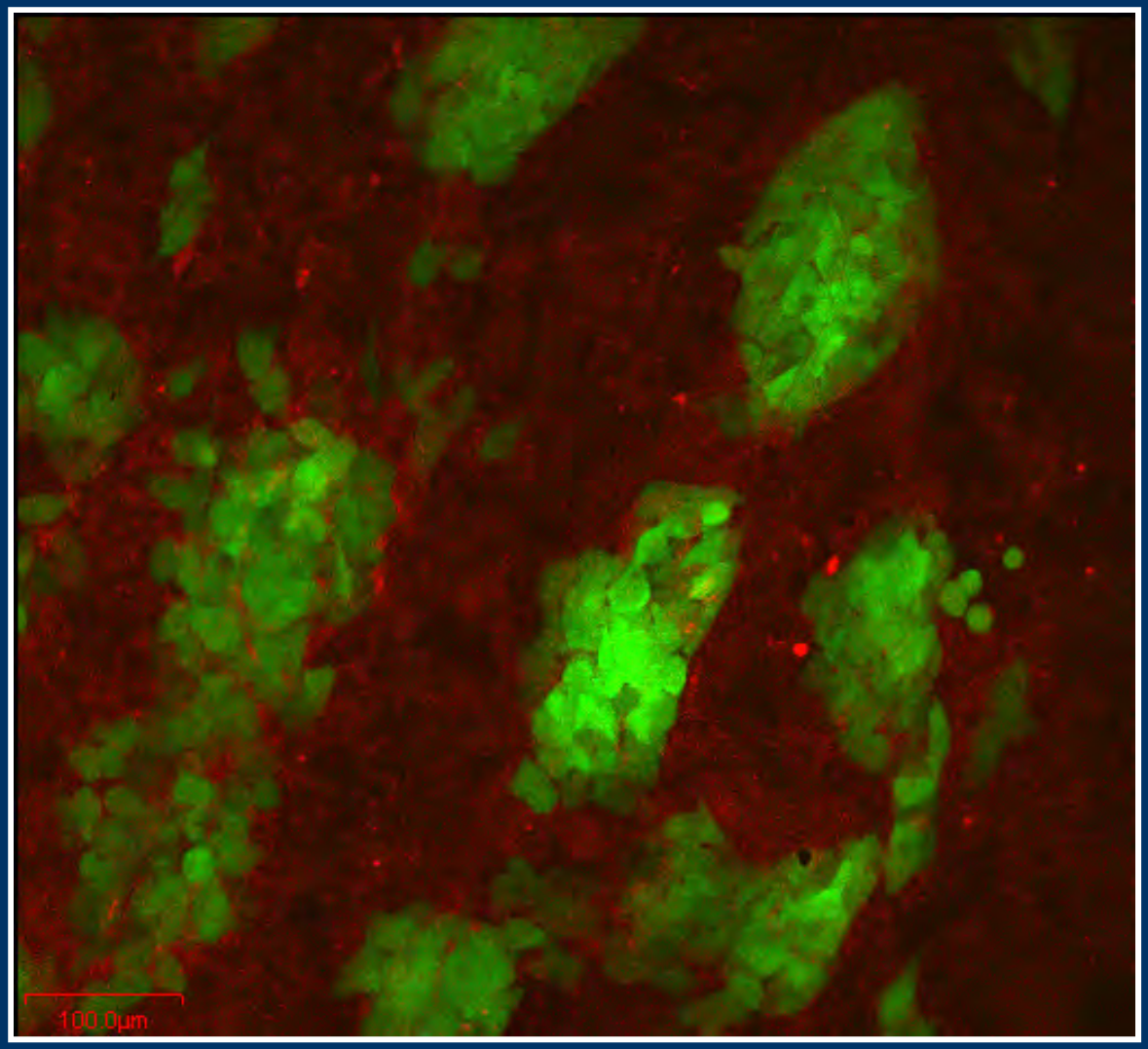

Cultures treated with ZOL showed more rounded breast-cancer cell morphology and fewer processes.

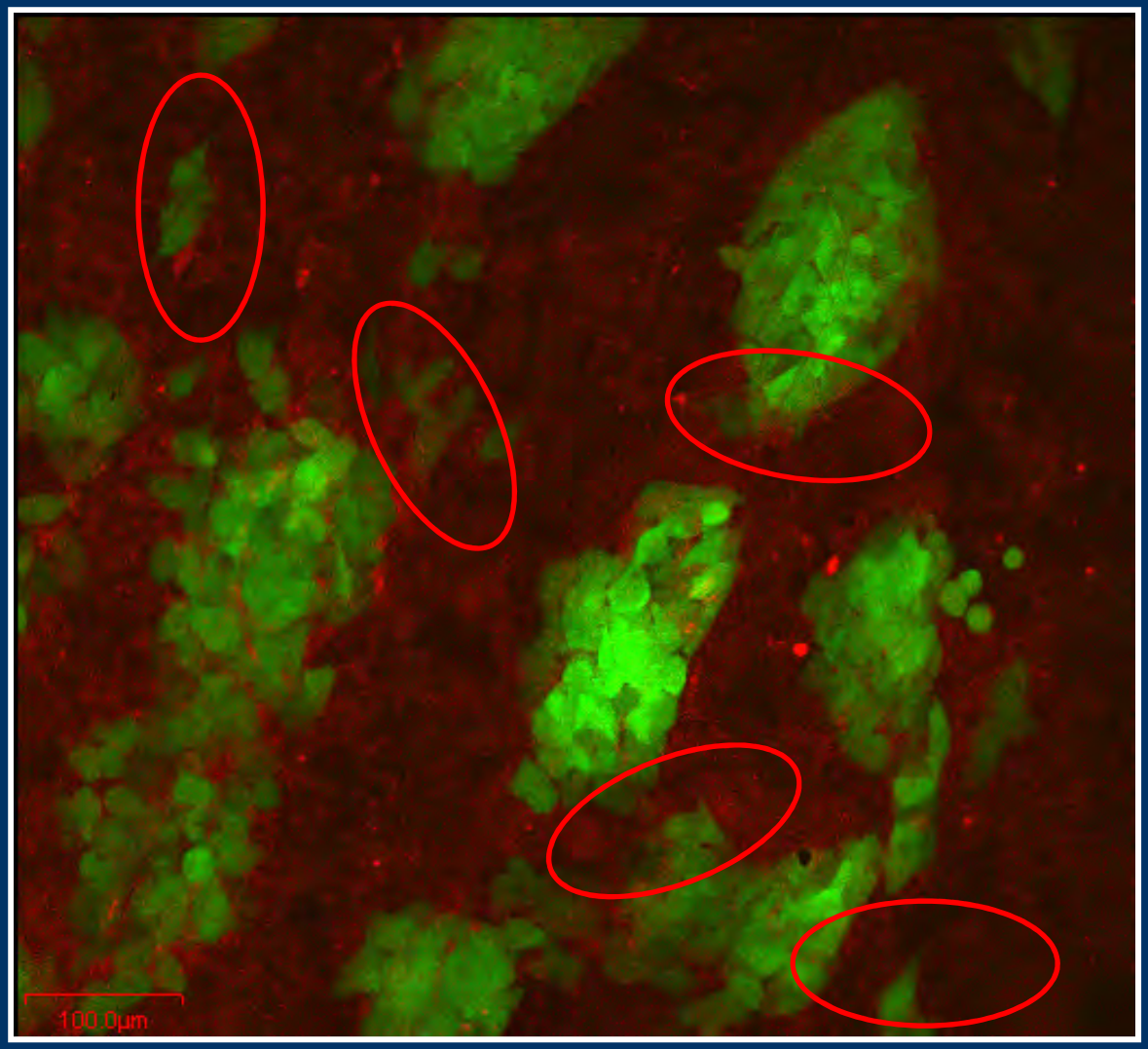

OB + BC

Cultures treated with ZOL showed more rounded breast-cancer cell morphology and fewer processes.

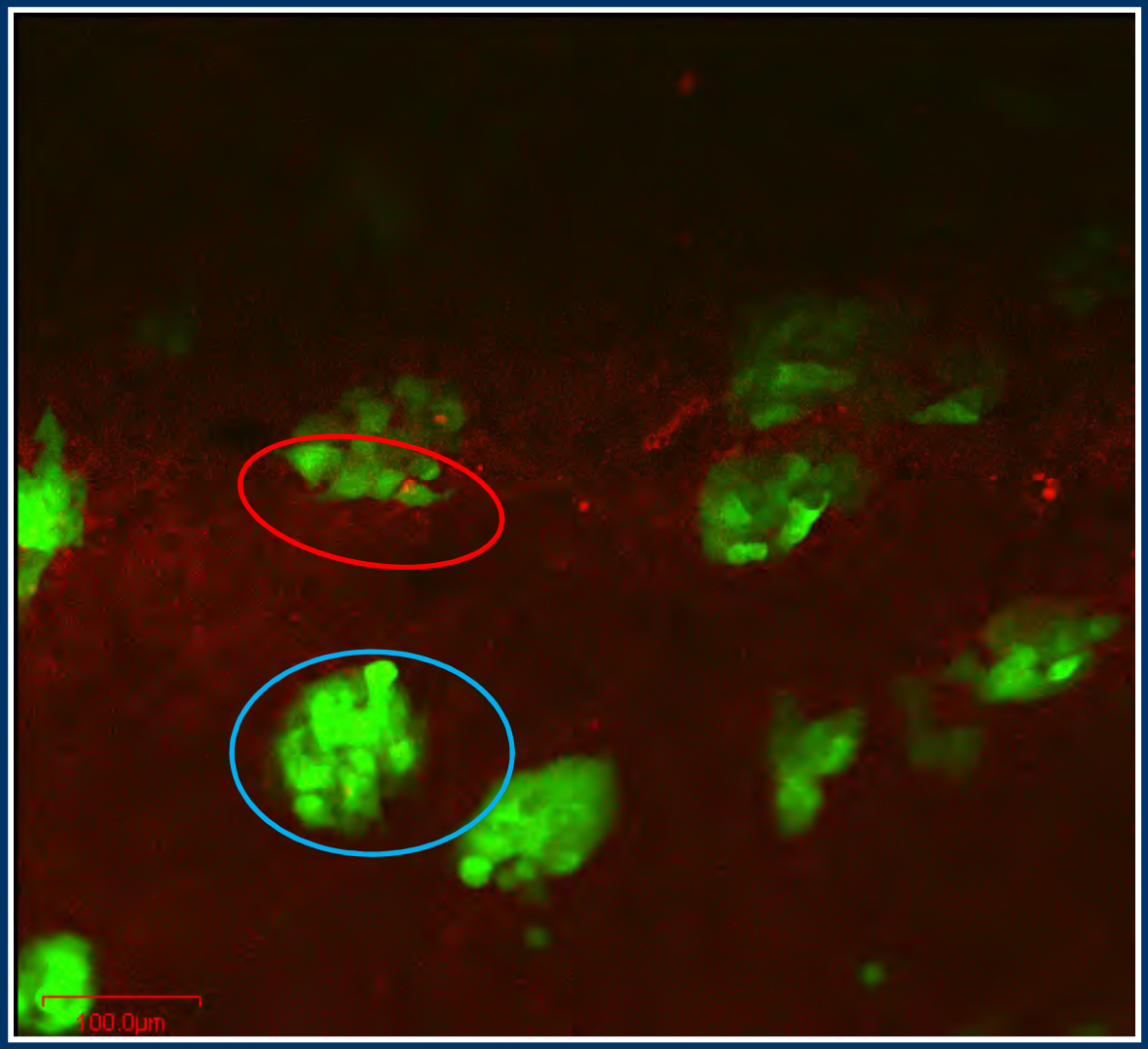

OB + BC +
0.05 µM ZOL

Cultures treated with ZOL showed more rounded breast-cancer cell morphology and fewer processes.

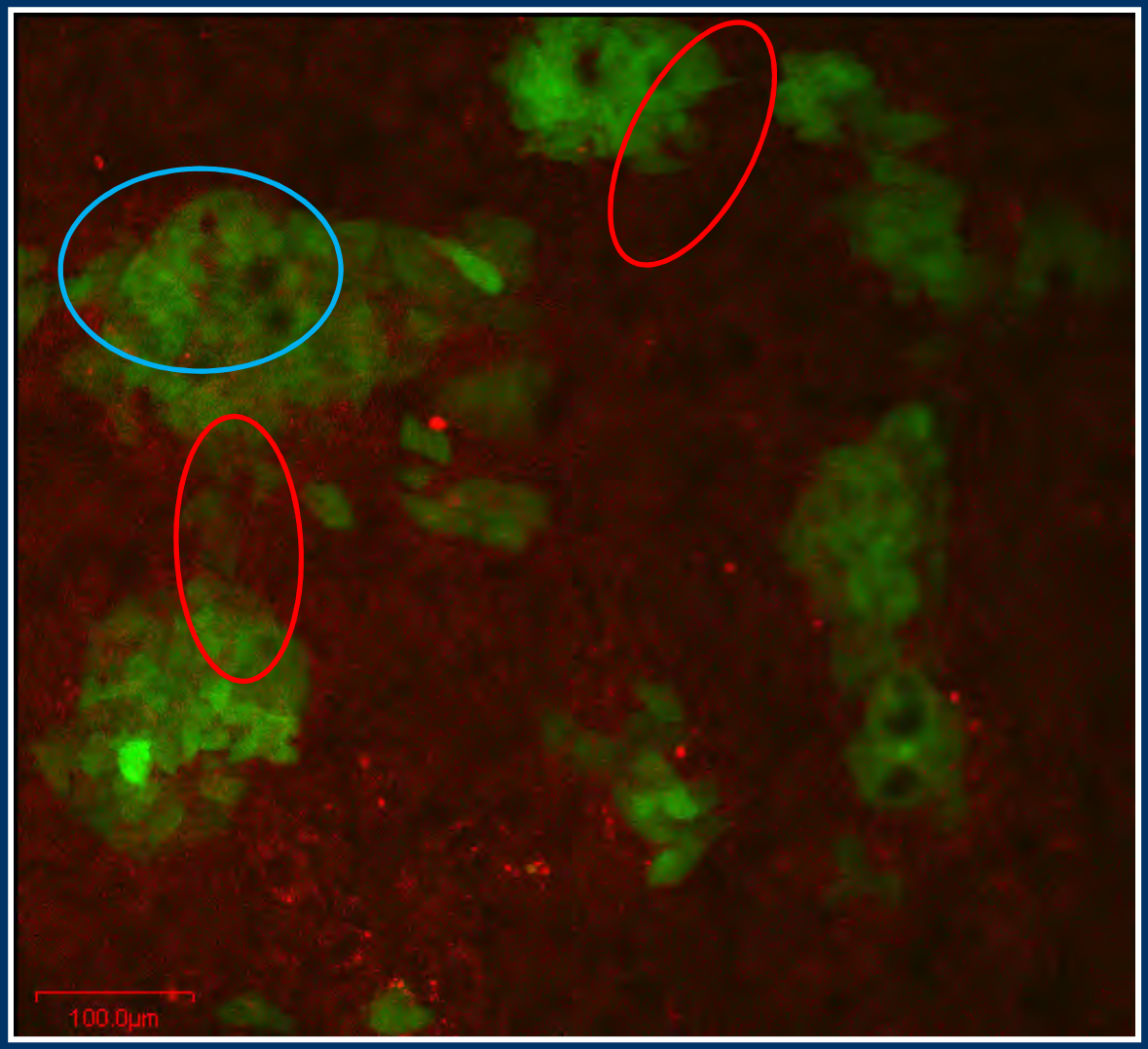

OB + BC +
0.5 µM ZOL

Treatment with ZOL showed disruption in breast-cancer cell alignment.

Experimental Parameter	Culture/Treatment			
	OB	OB + BC	OB + BC + 0.05µM ZOL	OB + BC + 0.5µM ZOL
BC Colony Formation	n/a	+++	+	++
BC Processes	n/a	+++	+	+
Rounded BC Morphology	n/a	+	+++	++
BC Alignment	n/a	+++	+	++
Ruptured BC Cells	n/a	-	++	++
Spindle-shaped OB Morphology	---	+++	+	+
Tissue Penetration	n/a	+++	+	++

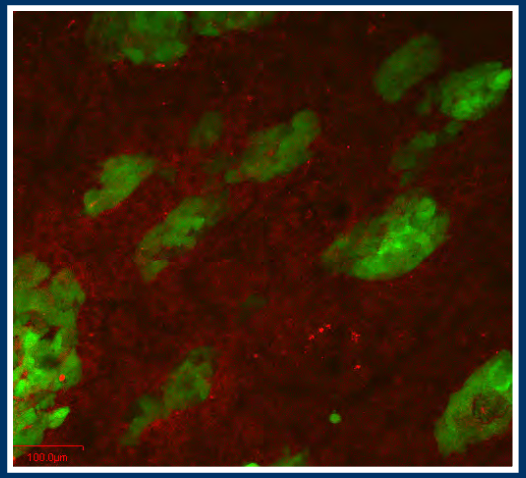

OB + BC

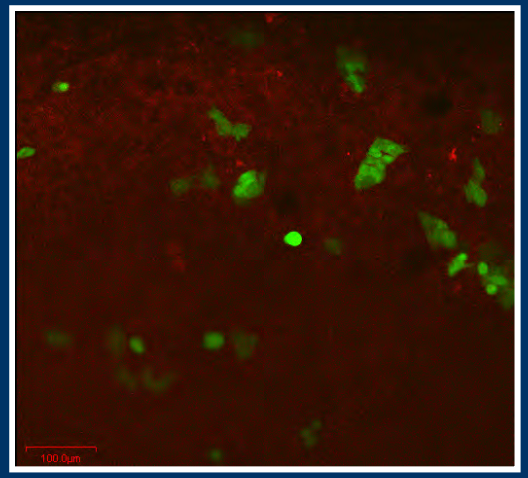

OB + BC + 0.05 µM ZOL

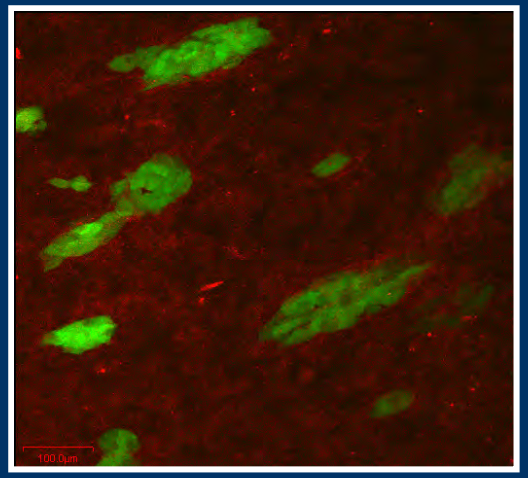

OB + BC + 0.5 µM ZOL

*48 hr. ZOL exposure

Treatment with ZOL showed disruption in breast-cancer cell alignment.

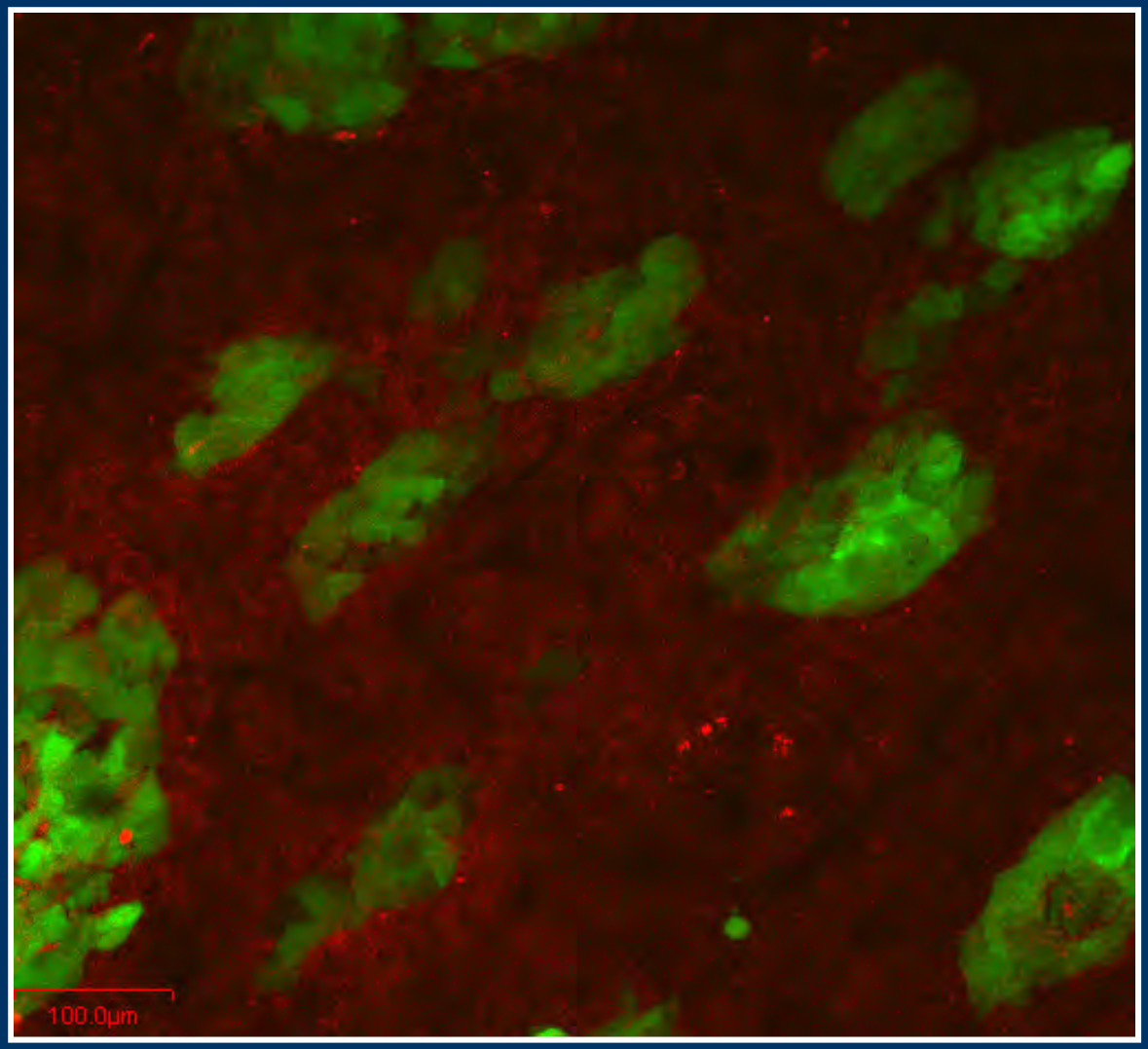

OB + BC

Treatment with ZOL showed disruption in breast-cancer cell alignment.

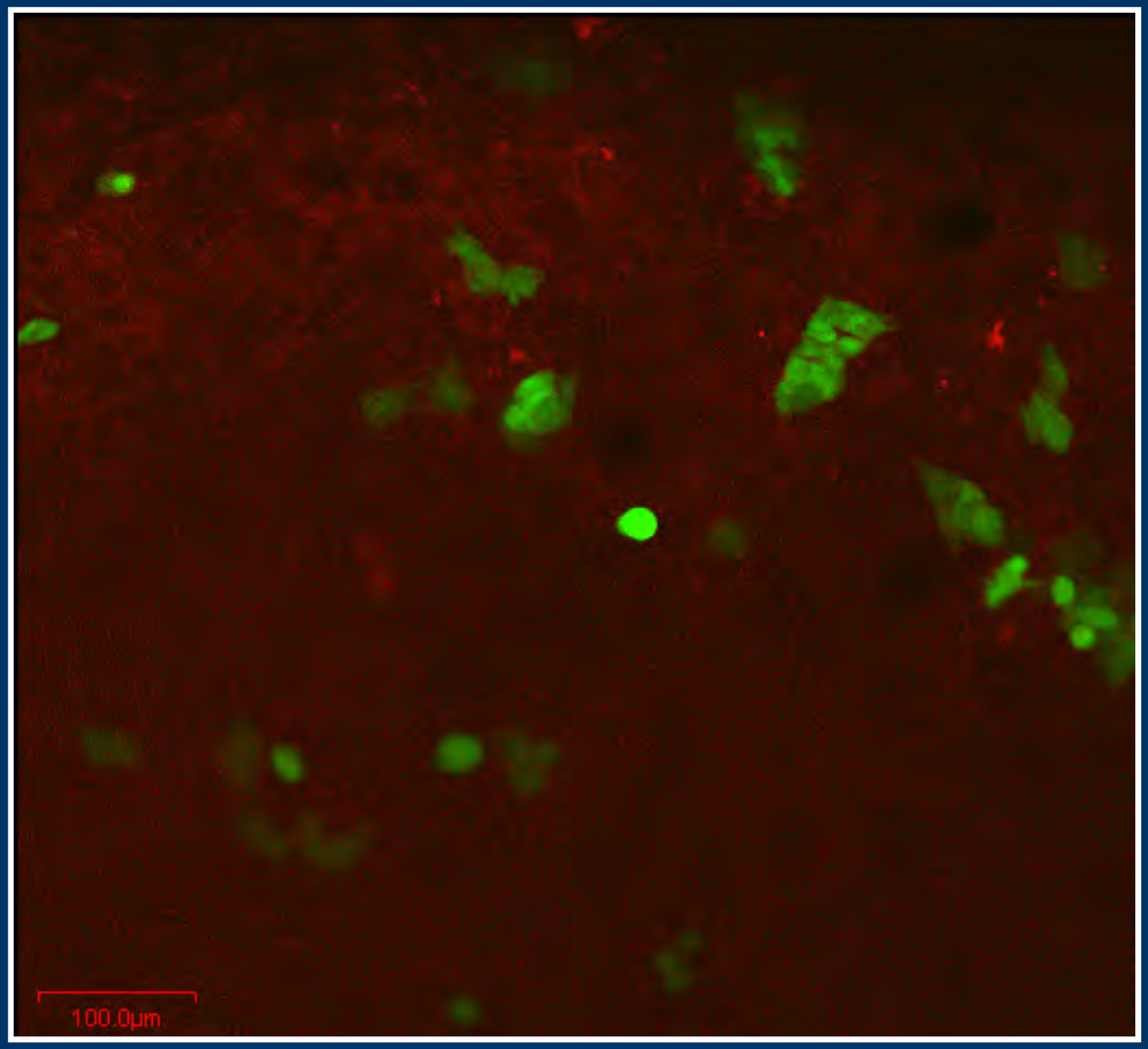

OB + BC +
0.05 µM ZOL

Treatment with ZOL showed disruption in breast-cancer cell alignment.

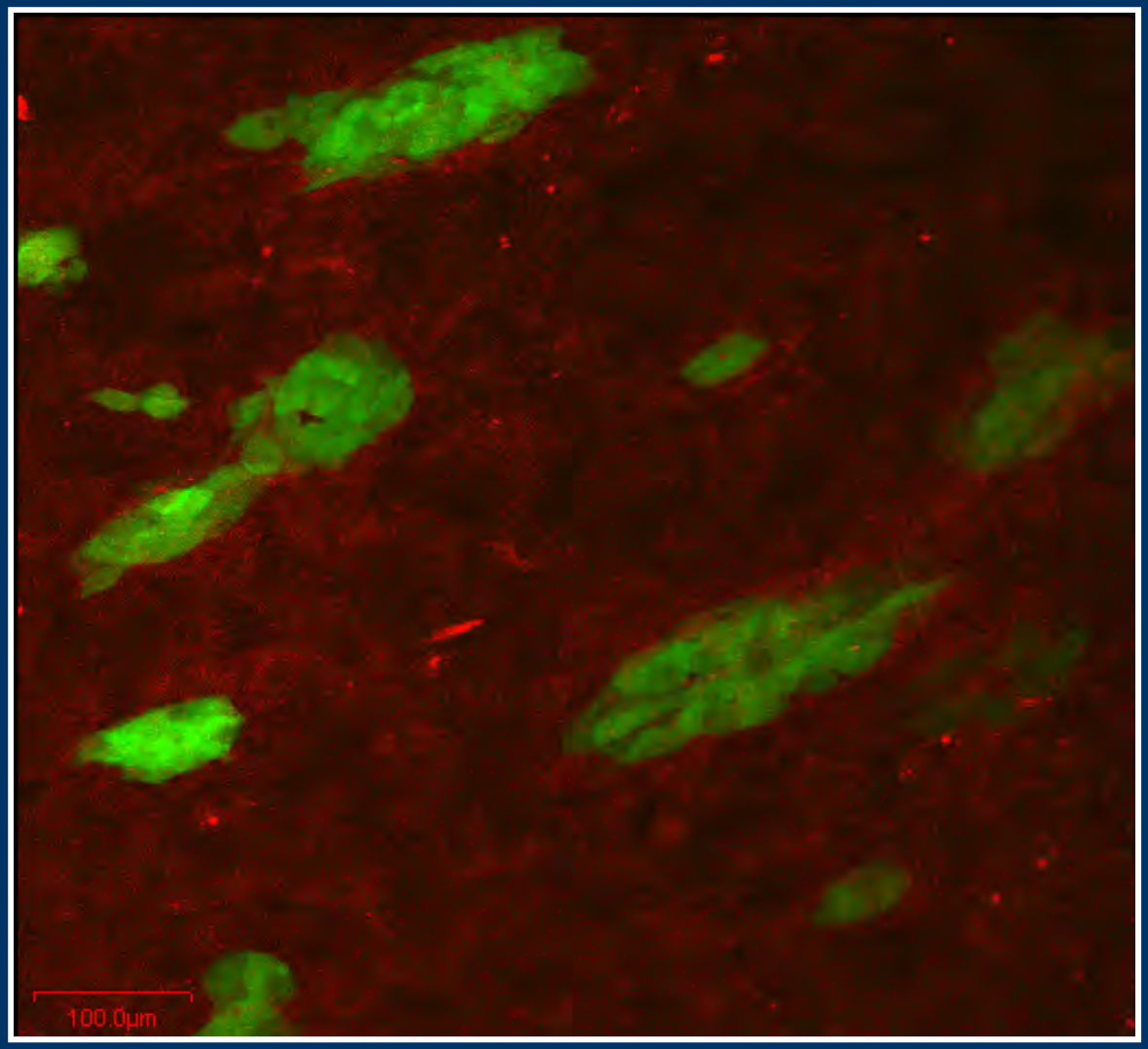

OB + BC +
0.5 µM ZOL

Ruptured breast-cancer cells existed in ZOL treated co-cultures.

Experimental Parameter	Culture/Treatment			
	OB	OB + BC	OB + BC + 0.05µM ZOL	OB + BC + 0.5µM ZOL
BC Colony Formation	n/a	+++	+	++
BC Processes	n/a	+++	+	+
Rounded BC Morphology	n/a	+	+++	++
BC Alignment	n/a	+++	+	++
Ruptured BC Cells	n/a	-	++	++
Spindle-shaped OB Morphology	---	+++	+	+
Tissue Penetration	n/a	+++	+	++

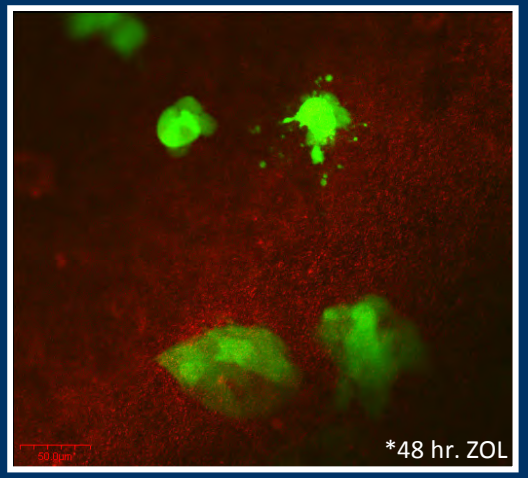

OB + BC + 0.05 µM ZOL

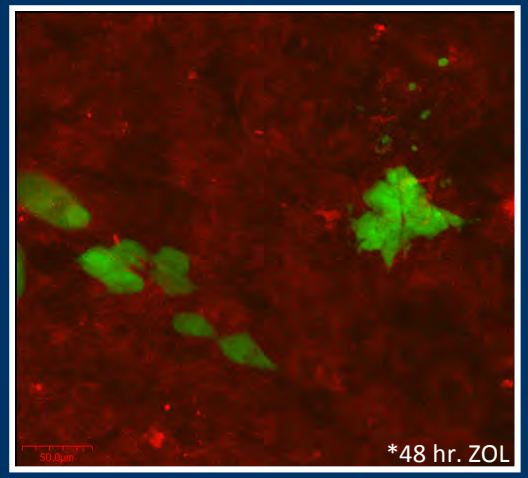

OB + BC + 0.5 µM ZOL

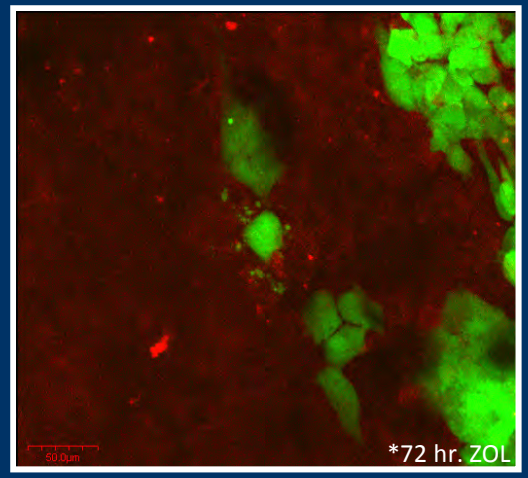

OB + BC + 0.5 µM ZOL

Ruptured breast-cancer cells existed in ZOL treated co-cultures.

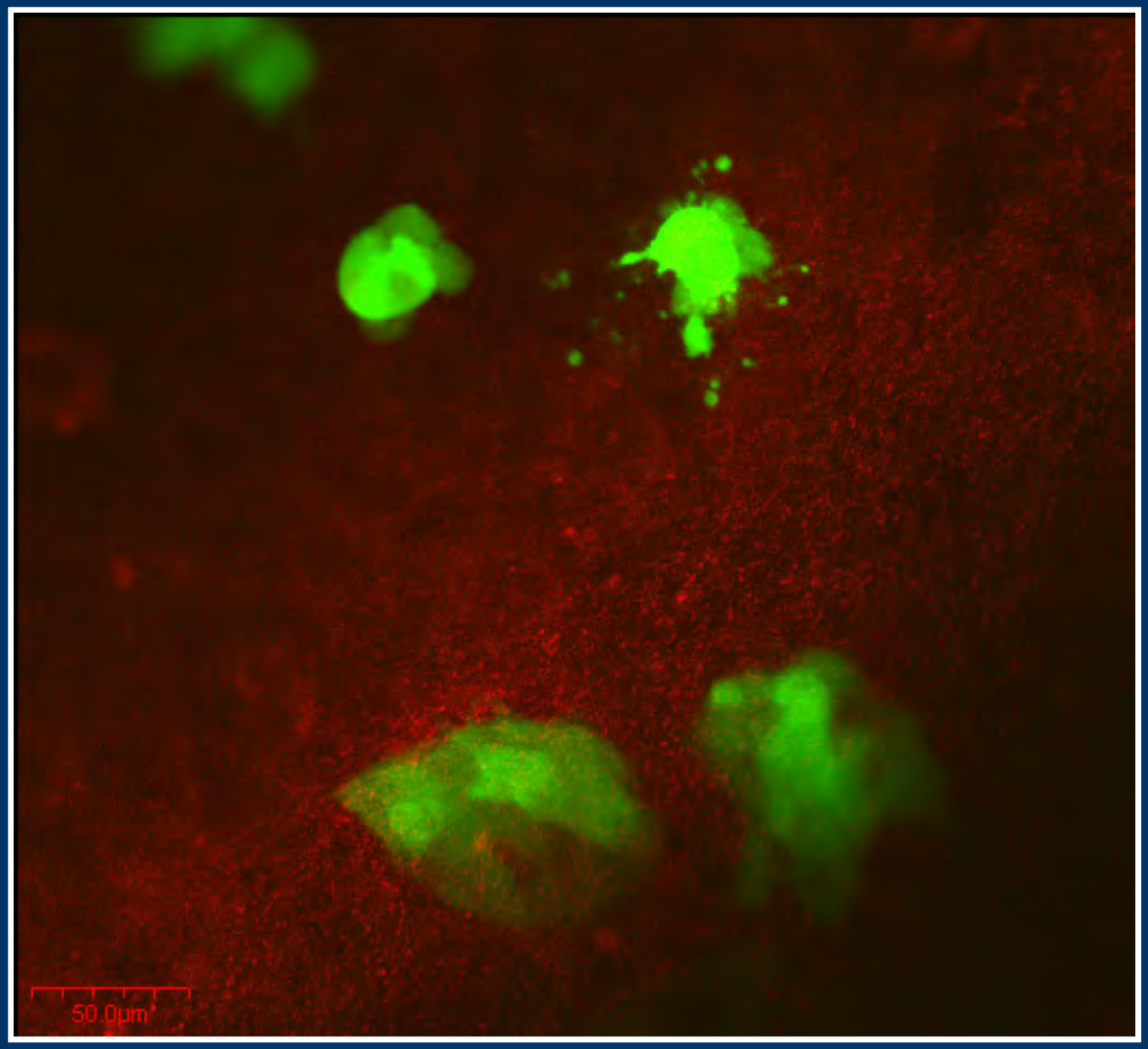

OB + BC +
0.05 µM ZOL

Ruptured breast-cancer cells existed in ZOL treated co-cultures.

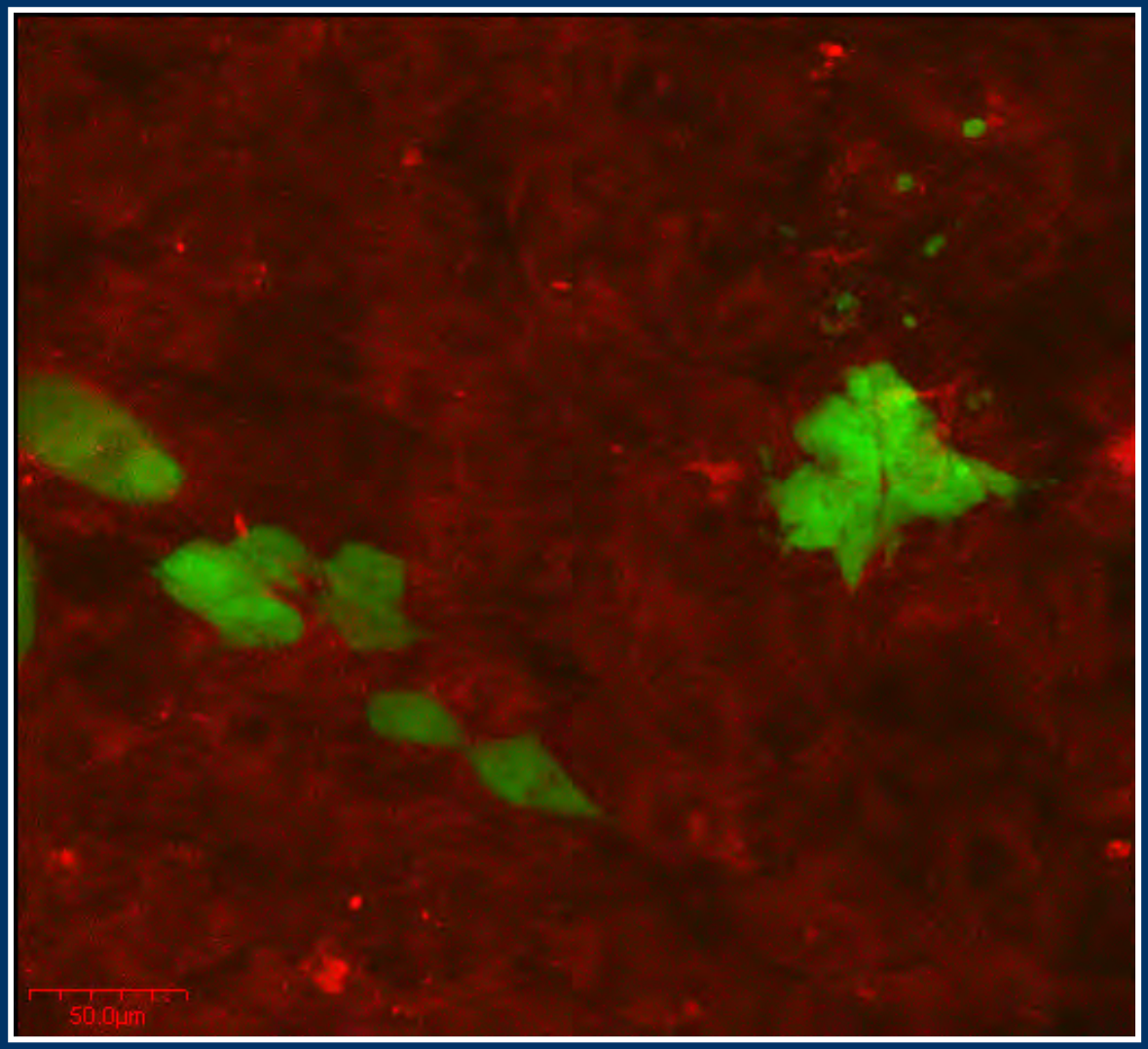

OB + BC +
0.5 µM ZOL

Ruptured breast-cancer cells existed in ZOL treated co-cultures.

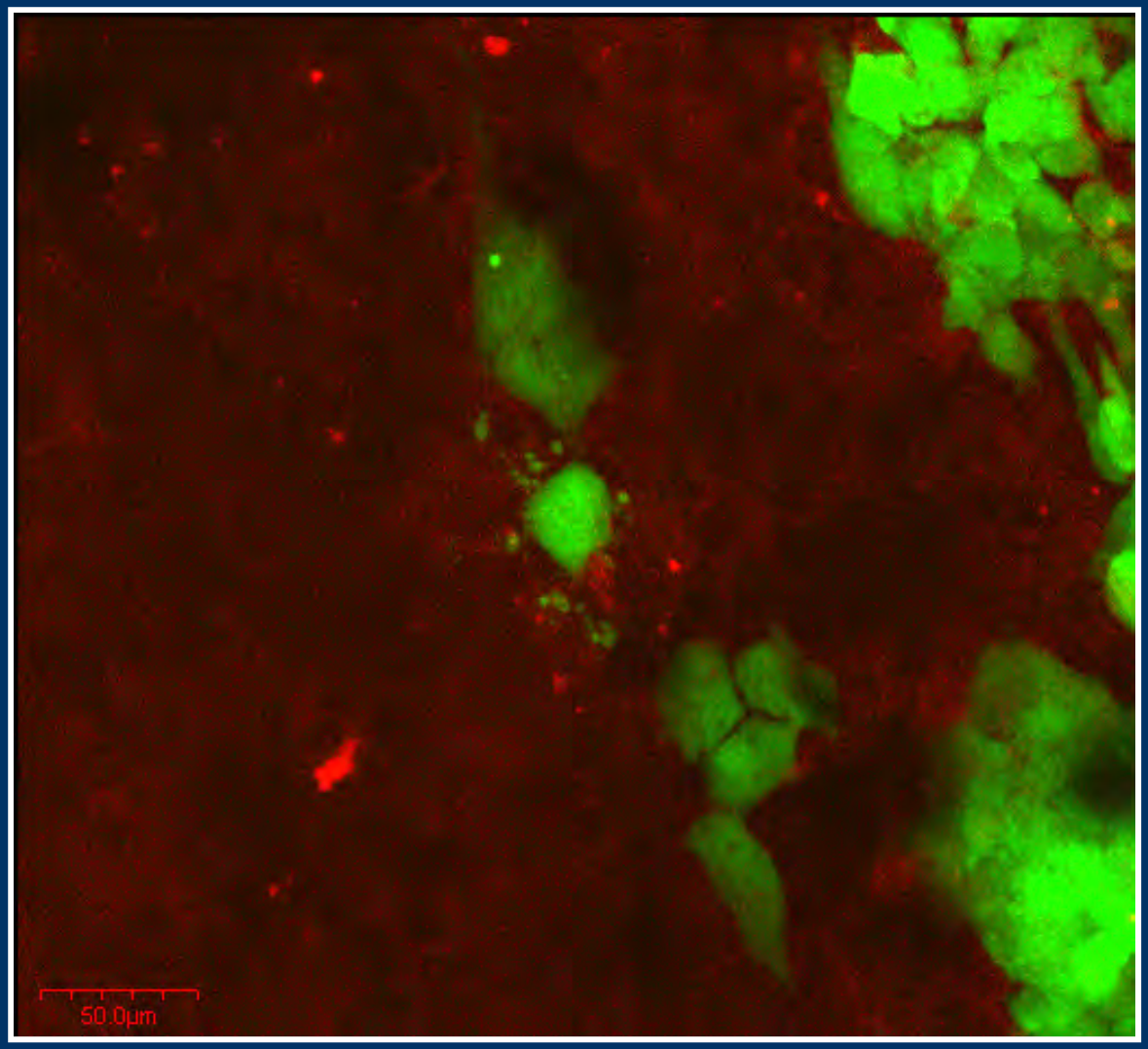

OB + BC +
0.5 µM ZOL

Osteoblasts developed a more spindle-shaped morphology in the untreated co-culture.

Experimental Parameter	Culture/Treatment			
	OB	OB + BC	OB + BC + 0.05µM ZOL	OB + BC + 0.5µM ZOL
BC Colony Formation	n/a	+++	+	++
BC Processes	n/a	+++	+	+
Rounded BC Morphology	n/a	+	+++	++
BC Alignment	n/a	+++	+	++
Ruptured BC Cells	n/a	-	++	++
Spindle-shaped OB Morphology	---	+++	+	+
Tissue Penetration	n/a	+++	+	++

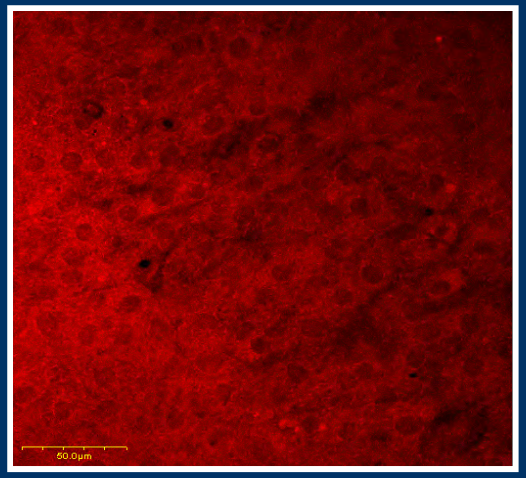

OB

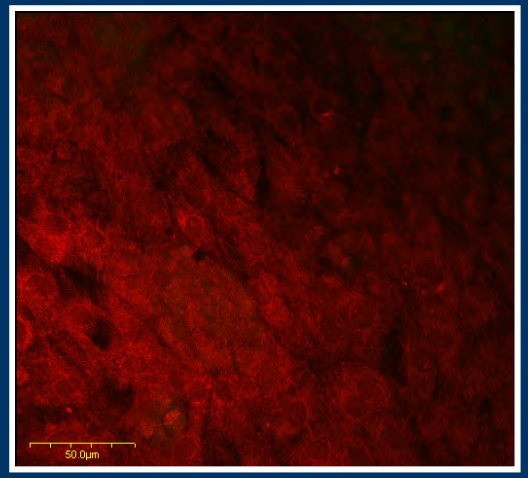

OB + BC
Bottom layer

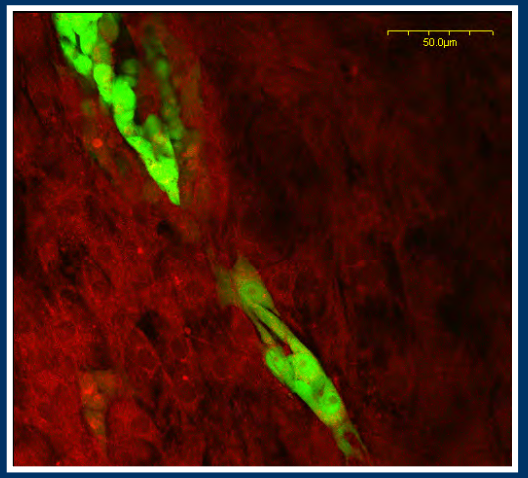

OB + BC +
0.05 µM ZOL

*Phalloidin stained images

Osteoblasts developed a more spindle-shaped morphology in the untreated co-culture.

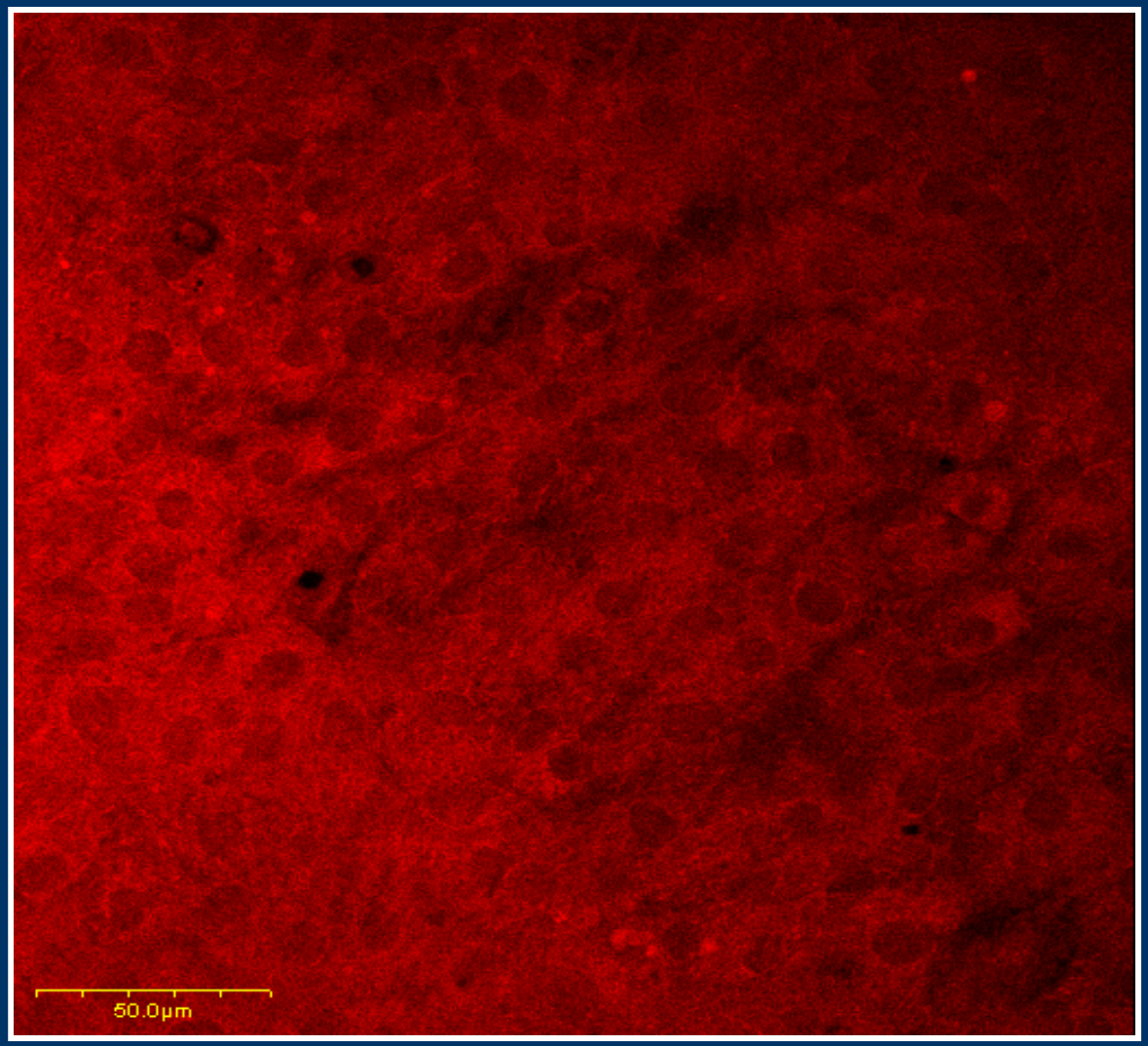

OB

Osteoblasts developed a more spindle-shaped morphology in the untreated co-culture.

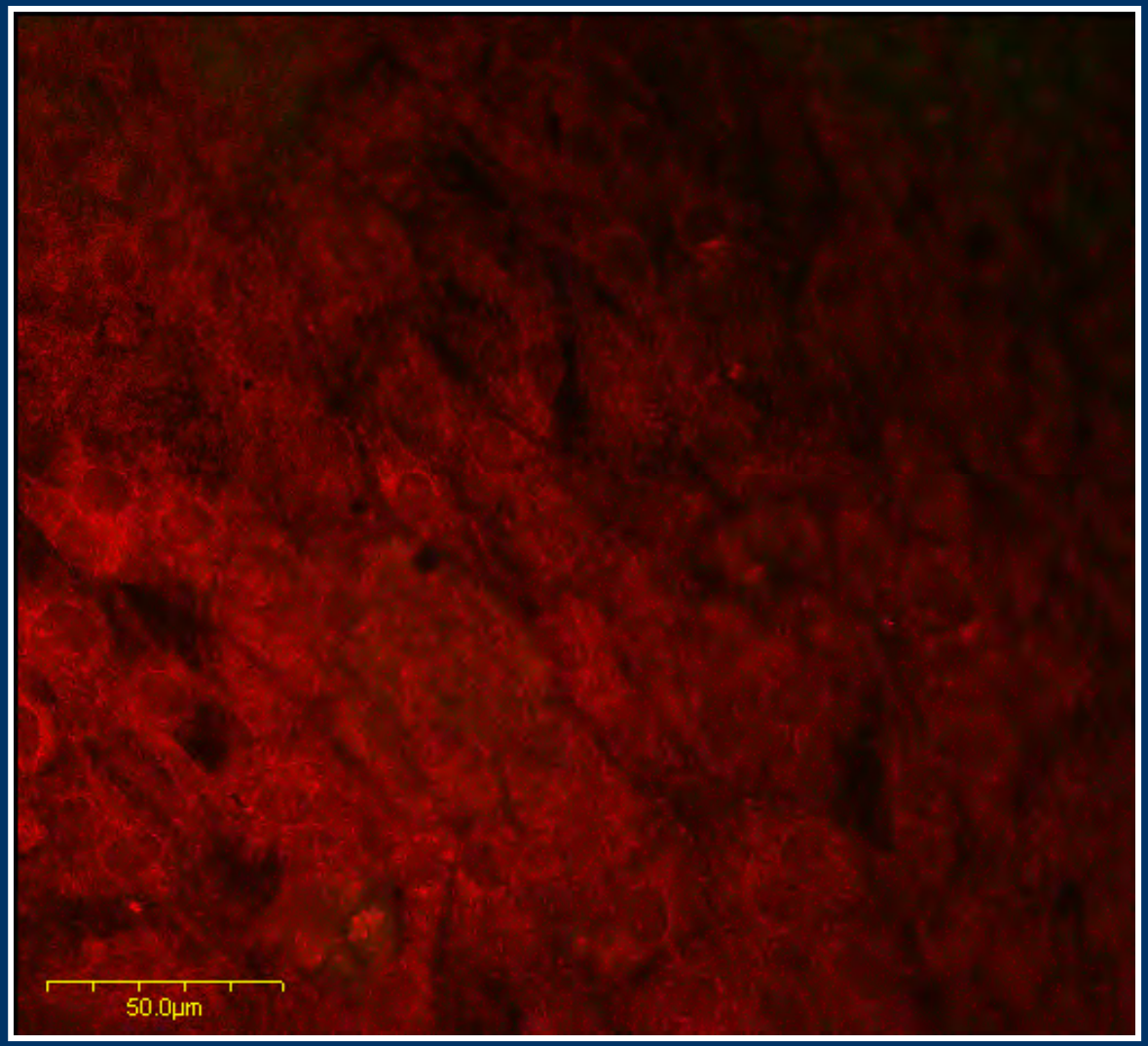

OB + BC
Bottom layer

Osteoblasts developed a more spindle-shaped morphology in the untreated co-culture.

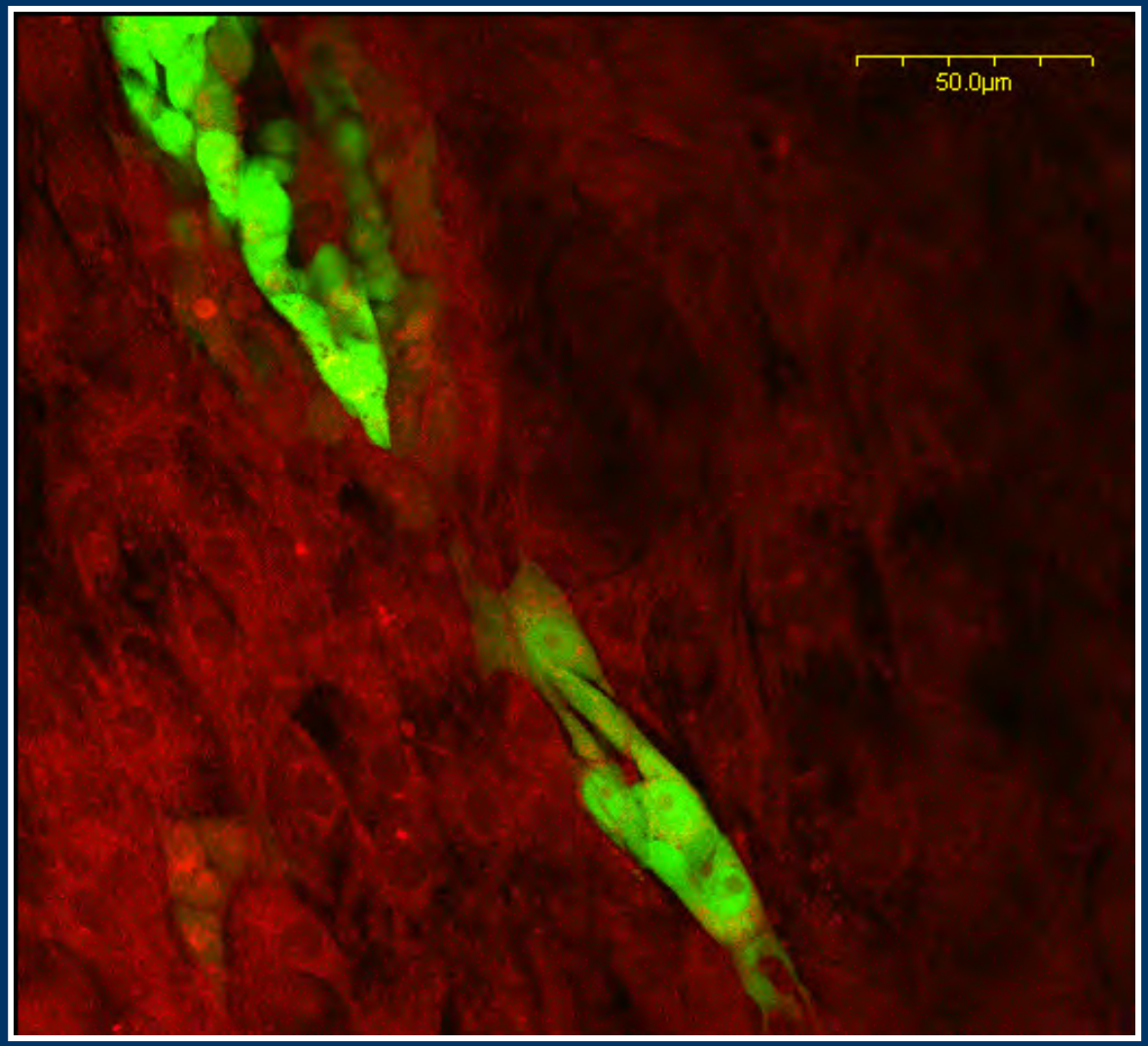

OB + BC +
0.05 µM ZOL

Breast-cancer cells penetrated further into the untreated co-culture than into ZOL treated cultures.

Experimental Parameter	Culture/Treatment			
	OB	OB + BC	OB + BC + 0.05µM ZOL	OB + BC + 0.5µM ZOL
BC Colony Formation	n/a	+++	+	++
BC Processes	n/a	+++	+	+
Rounded BC Morphology	n/a	+	+++	++
BC Alignment	n/a	+++	+	++
Ruptured BC Cells	n/a	-	++	++
Spindle-shaped OB Morphology	---	+++	+	+
Tissue Penetration	n/a	+++	+	++

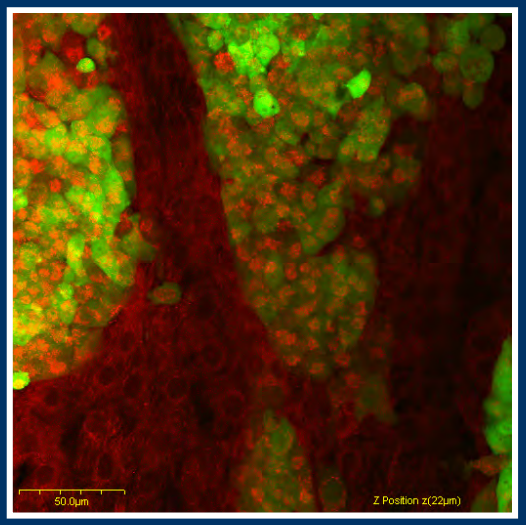

OB + BC

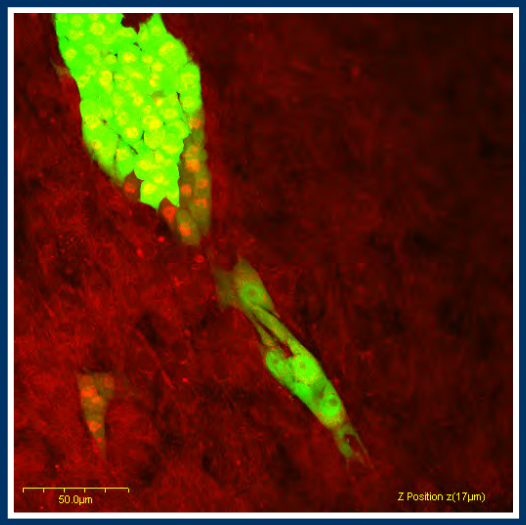

OB + BC + 0.05 µM ZOL

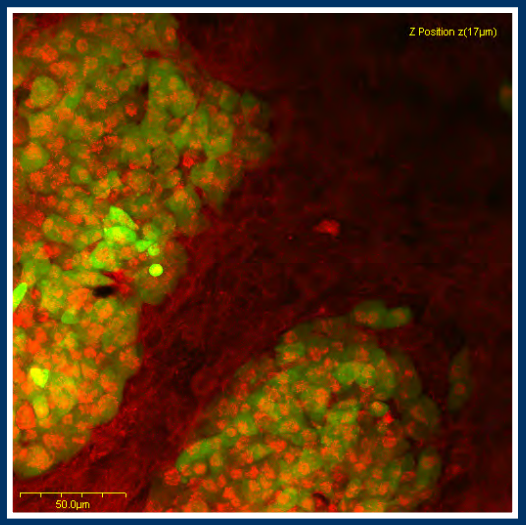

OB + BC + 0.5 µM ZOL

*Phalloidin stained Z-stacks

Breast-cancer cells penetrated further into the untreated co-culture than into ZOL treated cultures.

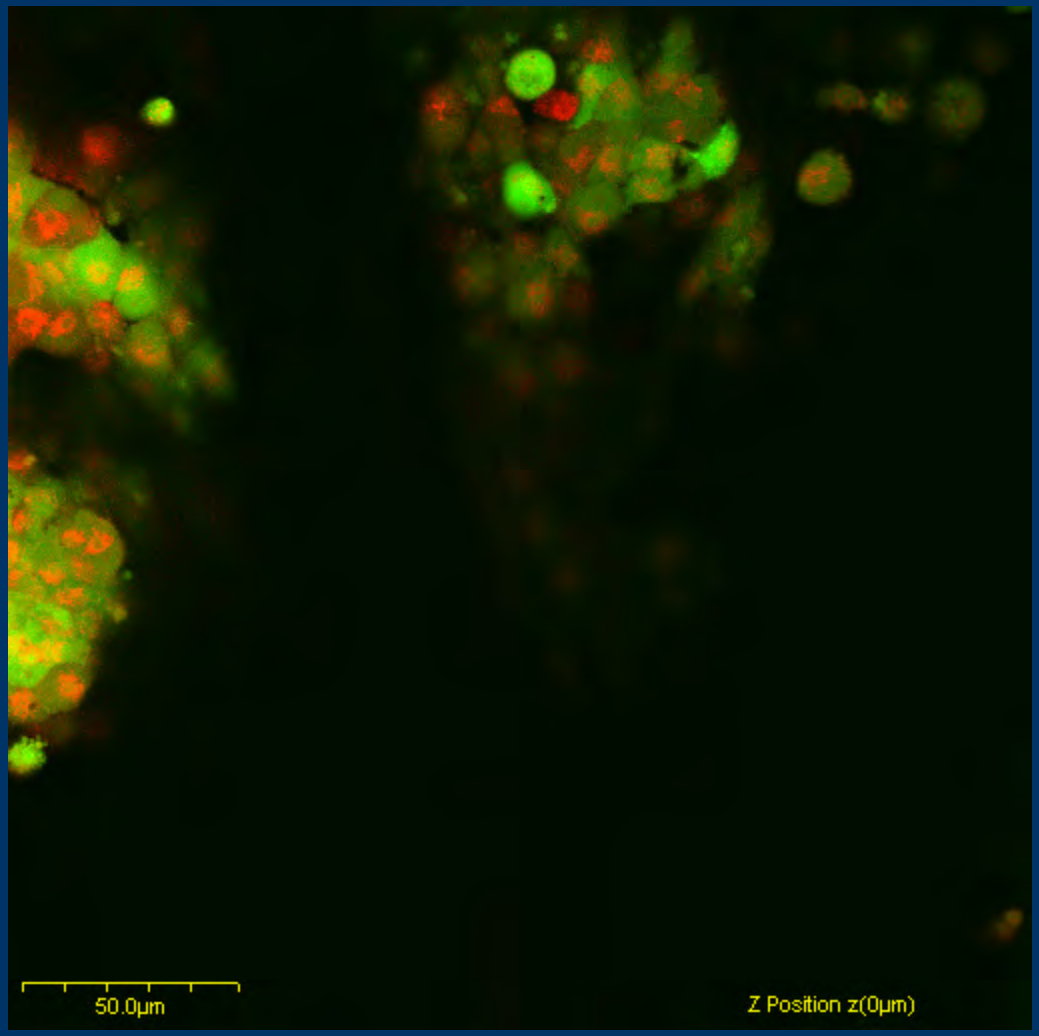

OB + BC

Breast-cancer cells penetrated further into the untreated co-culture than into ZOL treated cultures.

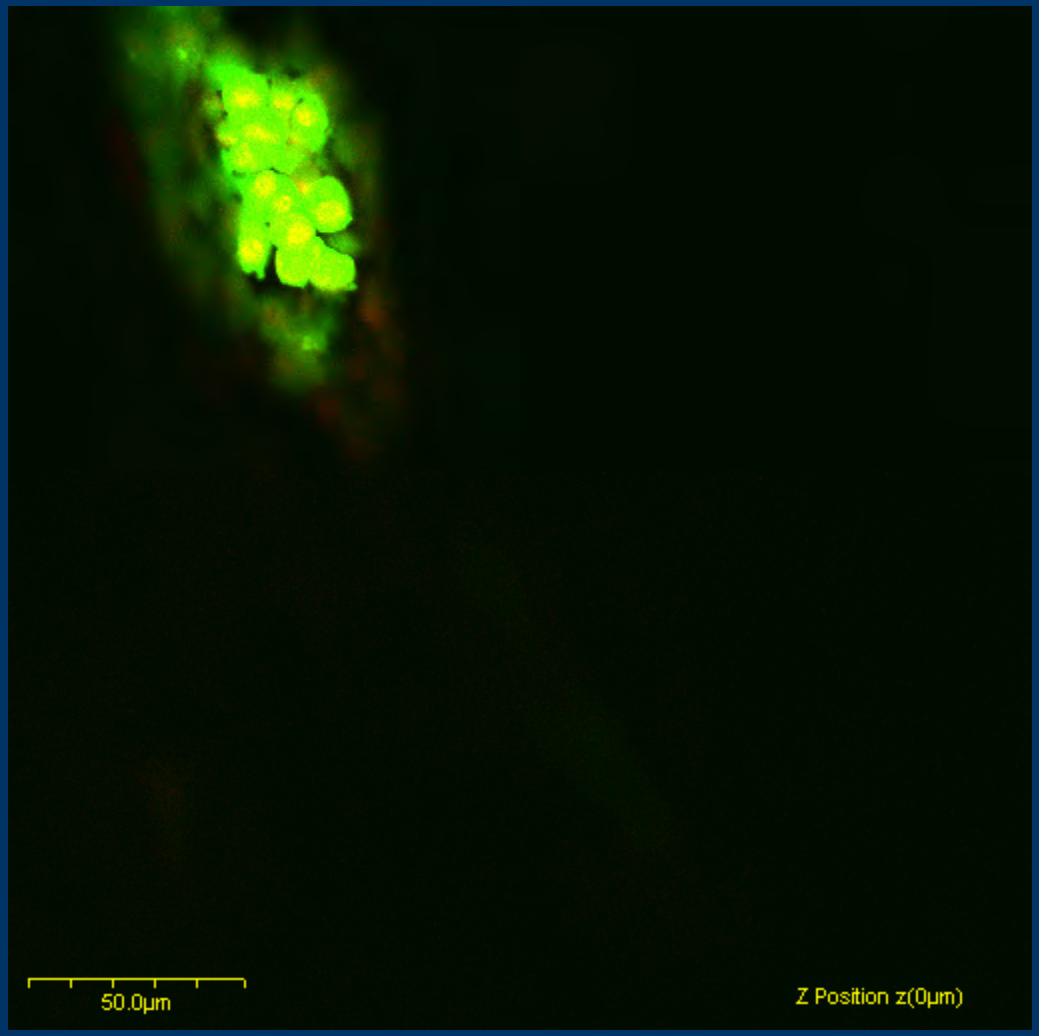

OB + BC +
0.05 µM ZOL

Breast-cancer cells penetrated further into the untreated co-culture than into ZOL treated cultures.

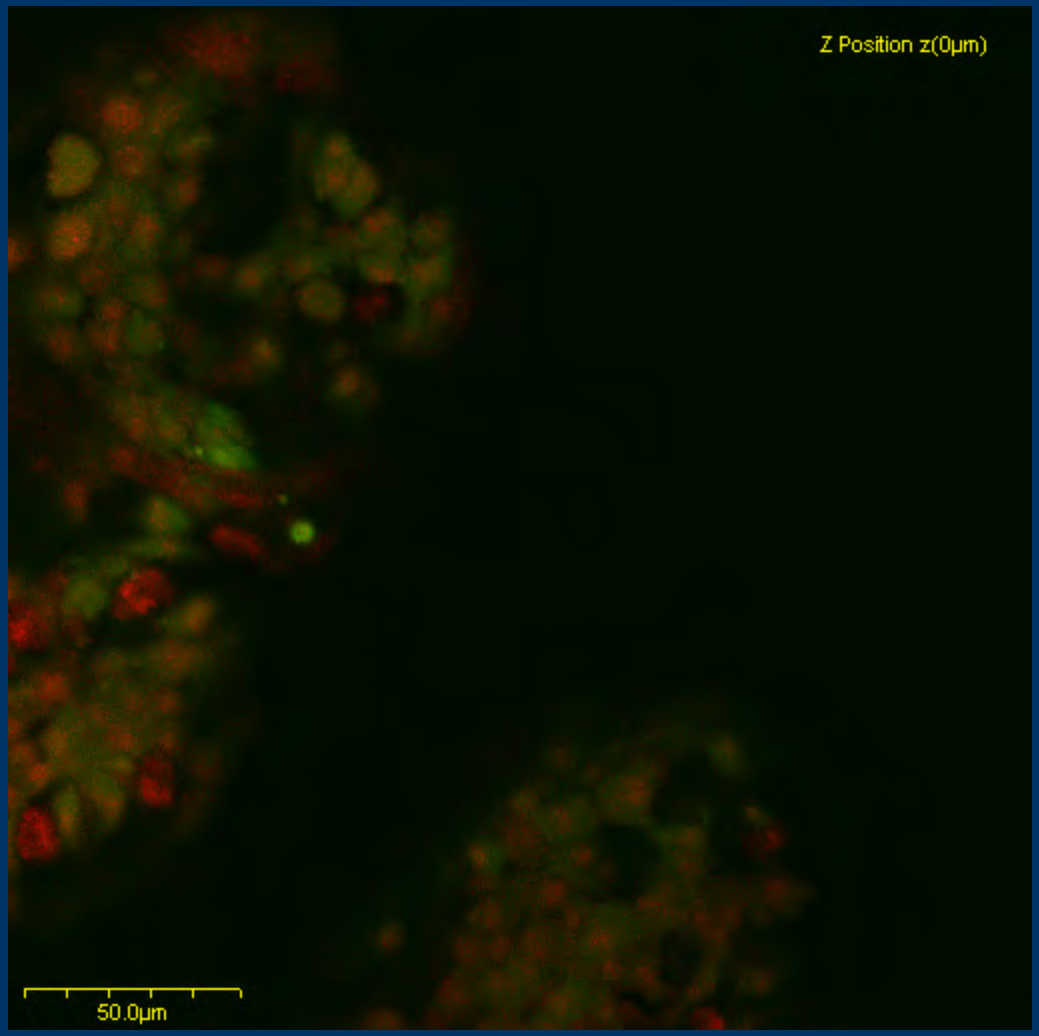

OB + BC +
0.5 µM ZOL

Conclusions

Low dose (0.05 µM) Zoledronic acid has the most profound effect on breast-cancer cells co-cultured with osteoblast tissue.

ZOL initially disrupts BC colony formation and inhibits normal BC progression.

Experimental Parameter	Culture/Treatment			
	OB	OB + BC	OB + BC + 0.05µM ZOL	OB + BC + 0.5µM ZOL
BC Colony Formation	n/a	+++	+	++
BC Processes	n/a	+++	+	+
Rounded BC Morphology	n/a	+	+++	++
BC Alignment	n/a	+++	+	++
Ruptured BC Cells	n/a	-	++	++
Spindle-shaped OB Morphology	---	+++	+	+
Tissue Penetration	n/a	+++	+	++

Future Work

- Gene expression (Osteocalcin, Type I Collagen, etc.)
- ELISAs (MCP-1 and IL-6)
- Specific Aims 2 and 3

Hypothesis: Combination therapy of a bisphosphonate (zoledronic acid) and a taxane (docetaxel) will inhibit breast cancer colonization of osteoblast tissue to a greater degree than a bisphosphonate alone.

Specific Aim 1: To characterize the effect of zoledronic acid on breast cancer colonization of osteoblast tissue.

→ ***Specific Aim 2: To characterize the effect of docetaxel on breast cancer colonization of osteoblast tissue.***

→ ***Specific Aim 3: To characterize the effect of a combination treatment of zoledronic acid and docetaxel on breast cancer colonization of osteoblast tissue.***

Selenium modifies the osteoblast inflammatory stress response to bone metastatic breast cancer

Yu-Chi Chen[1], Donna Sosnoski[1], Leah Novinger[1], Ujjawal H. Gandhi,[2] K. Sandeep Prabhu,[2*] and Andrea M. Mastro[1*]

[1]The Department of Biochemistry and Molecular Biology, [2]The Department of Veterinary and Biomedical Sciences, The Pennsylvania State University, University Park, PA 16802

*Corresponding Authors

K. Sandeep Prabhu
Penn State University
Department of Veterinary and Biomedical Sciences
115 Henning Building
University Park, PA 16802
Phone: 814-863-6140
E-mail: ksp4@psu.edu

Andrea M. Mastro
Penn State University
Department of Biochemistry and Molecular Biology
431 S. Frear Building
University Park, PA 16802
Phone 814-863-0152
Fax 814-863-7024
A36@psu.edu

Abstract

Breast cancer frequently metastasizes to the skeleton where it results in bone degradation due to osteoclast activation. The metastases also downregulate differentiation and the bone rebuilding function of osteoblasts. Moreover, breast cancer cells trigger an inflammatory stress response in osteoblasts. Pro-inflammatory mediators such as IL-6, MCP-1, COX-2, and iNOS, expressed by osteoblasts (MC3T3-E1) stimulated with human breast cancer cell (MDA-MB-231) conditioned medium, are pivotal to osteoclast activation and metastasis progression. Given that all these genes are regulated by NF-κB, a redox- sensitive transcription factor, we hypothesized that selenium could abrogate the inflammatory stress response of osteoblasts to metastatic breast cancer cells by modulating NF-κB. Caffeic acid phenethylether and parthenolide inhibited NF-κB activation, as seen by gel-shift assays and immunoblotting for p65 in nuclear fractions, as well as production of IL-6 and MCP-1. Supplementation of MC3T3-E1 osteoblasts with methylseleninic acid (500 nM to 4 μM) reduced the activation of NF-κB further leading to a decrease in the expression of IL-6, MCP-1, COX-2 and iNOS, in response to the MDA-MB-231 conditioned medium. In summary, our data indicate that the osteoblast response to metastatic breast cancer cells is regulated by NF-κB activation, which can be effectively suppressed by selenium. Thus, selenium supplementation may prevent the osteoblast inflammatory stress-response pathway or dampen the viscous cycle established when breast cancer cells, osteoblasts, and osteoclasts interact.

Introduction

The skeleton is a preferred site for breast cancer metastasis. In spite of many rounds of chemotherapy and an often long latency period, metastases in this sanctuary grow and in the process, bring about osteolytic lesions. Bone loss is not a direct function of the cancer cells, but is largely due to activated osteoclasts. According to the "vicious cycle" paradigm, cancer cells activate osteoblasts, which in turn attract, differentiate and activate osteoclasts to resorb bone. Upon degradation, the matrix releases many stored growth factors including TGFβ which can feed back upon the cancer cells[1].

There is no cure for bone metastasis, but bisphosphonates such as Aledronate™ are used to inhibit osteoclasts. While this therapy slows lesion progression, the bone does not heal[2]. One possible reason is that in the presence of the cancer cells, the function of osteoblasts, the bone forming cells is impaired[3,4]. We tested this possibility using an *in vitro* where human metastatic breast cancer cells or their medium were co-cultured with osteoblast lines. We found that breast cancer cells or their conditioned media (BCCM) increase the prevalence of osteoblast apoptosis[5], prevent differentiation and mineralization, and cause a change in osteoblast morphology[6]. Furthermore, in an *in vivo* study, we confirmed that osteoblasts no longer differentiated and were lost over time following arrival of the cancer cells into the femur[7]

Both direct and indirect contact (i.e., conditioned medium) of breast cancer cells with osteoblasts, result in the down-regulation of the expression of osteoblast differentiation proteins such as osteocalcin, osteonectin, alkaline phosphatase, and bone sialoprotein[8].

However, we also found that osteoblasts in the presence of BCCM greatly increased expression of several pro-inflammatory molecules, interleukin-6 (IL-6), interleukin-8 (IL-8) and monocyte chemoattractant protein-1 (MCP-1). These cytokines, normally produced in low levels by osteoblasts, play a role in the activation of osteoclasts[9], and have been implicated in metastasis[10]. Together, these molecules provide a potent stimulus for bone osteolysis. Their production by osteoblasts also suggests that it is not necessary to invoke cancer cells or immune cells such as macrophages or lymphocytes as the sources of inflammatory molecules, although they undoubtedly play a role *in vivo.* Interestingly, IL-6, IL-8, and MCP-1 also are expressed as part of the immediate early inflammatory stress response in osteoblasts in the presence of prosthesis debris in bone implants in humans [11]. This chronic inflammatory process also leads to bone resorption.

It has long been suspected from both experimental and epidemiological studies that inflammation is strongly linked to cancer[10,12]. A key regulatory molecule in the inflammatory process is the redox-sensitive transcription factor NF-κB, which, upon activation, initiates the expression of a cascade of cytokines, including IL-6, IL-8, and MCP-1. The NF-κB recognition motifs are found in the 5' regulatory regions of these cytokines. NF-κB represents a ubiquitously expressed family of transcription factors that participate in the regulation of diverse biological processes, including immune, inflammatory, and apoptotic responses[13]. For the purposes of this study, we concentrated on NF-κB regulation of the inflammatory cytokines IL-6, and MCP-1[13]. Control of NF-κB activation could potentially interfere with the production of pro-

inflammatory mediators as well as the osteoblast stress response and the activation of osteoclasts.

Recently, we have shown that cellular Se status, via the incorporation of Se into proteins (selenoproteins), can modulate the activation of the NF-κB pathway in macrophages [14]. Of the thirty- some selenoproteins, two major selenoenzymes that play a pivotal role in the maintenance of cellular redox balance are glutathione peroxidase (GPx) and thioredoxin reductases (TrxrR)[14,15]. GPx 1-4 exhibits high peroxidase activity towards certain reactive oxygen species, including H_2O_2 and fatty acid hydroperoxides [16,17]**.** Thus, Se is an essential micronutrient required for normal physiological function. Early epidemiological studies have suggested that there is a unique relationship between Se levels and cancer[18]. More recent studies have provided evidence that Se is protective; and that administration of supra-nutritional levels has demonstrated chemopreventive activity. Literature indicates that Se acts both at the steps of tumor initiation and progression. A reduction in the levels of the selenoprotein, GPx, is inversely related to cancer progression and disease stage[19]. Moreover, reduced GPx activity and Se levels have been found in the blood of cancer patients with metastases[20]. Nonetheless, the mechanisms are not clear. It is known that Se is required for the syntheses of anti-oxidant selenoenzymes important for maintaining oxidative balance. Because oxidative stress can lead to mutations and cancer, these anti-oxidative enzymes may be critical in blocking tumor formation. Roebuck et al.[21] related oxidative stress to increased NF- κB activity in the osteoblast inflammatory response to titanium particles. However, the regulation of the osteoblast inflammatory response during metastasis via Se-dependent control of NF-κB has not been investigated.

The objective of this study was to determine if modification of the Se status of osteoblasts affected their inflammatory response to BCCM. We examined the relationships among NF-κB activation, selenium status, and proinflammatory protein production by osteoblasts exposed to conditioned medium from a human metastatic breast cancer cell line, MDA-MB-231. We found that IL-6, MCP-1 and additionally cyclooxygenase (COX)-2 and inducible nitric oxide synthase (iNOS) production were diminished in the presence of methylseleninic acid (MSA). MSA supplementation also effectively inhibited NF-κB activation.

Materials and Methods

Cells

MC3T3-E1, an osteoblast line derived from murine calvaria that differentiates in culture[22], was a gift from Dr. Norman Karin, Pacific Northwest National Laboratory. The cells were maintained in growth medium, α-MEM plus 10% fetal bovine serum (FBS, Cansera, Roxdale, Ontario), penicillin 100 U/ml/streptomycin 100 μg/ml. They were passaged every 3 to 4 days with 0.002% pronase and not used beyond passage 20. For experiments, the cells were transferred to differentiation medium, i.e. growth medium plus 50μg/ml ascorbic acid and 10 mM β-glycerophosphate. The cells were usually used after about 2 weeks in differentiation medium as indicated for individual experiments.

MDA-MB-231, a human metastatic breast cancer line originally derived from a pleural effusion[23], forms bone metastasis in immunodeficient mice following injection into the

left ventricle of the heart. These cells were a gift from Dr. Danny Welch, University of Alabama at Birmingham. They were maintained in DMEM containing 5% FBS.

MDA-MB-231 BCCM preparation

MDA-MB-231 cells were cultured until they reached about 90% confluency. The culture medium was replaced with serum-free αMEM for 24 hours to allow accumulation of secretory molecules. The medium was collected and centrifuged at 300 x g for 10 min to remove cell debris. The supernatant (BCCM) was aliquoted and stored at -20°C. For comparison, we tested the same medium, vehicle control medium (VM) that was not exposed to breast cancer cells.

Selenium levels

Osteoblast Se levels were manipulated by the Se content of the serum and by addition of Se. The Se concentration of the lot of FBS (Cansera) used for most experiments was determined to be 363 nM by atomic absorption spectrometry. To obtain selenium-deficient cells, MC3T3-E1 and MDA-MB-231, were plated in 5% FBS for a Se concentration of 18.2 nM. Under these conditions, normal cell growth and osteoblast differentiation (production of alkaline phosphatase and positive staining for von Kossa , data not shown) were seen. Cells were cultured for at least four passages in the selenium-deficient medium and their Se status was measured by GPx1 expression and activity assays. In some experiments, osteoblast cultures were supplemented with 500 nM to 4 μM of methylseleninic acid (MSA, Sigma, St. Louis, MO) for 7 days before the

experiment. MSA was preferred over sodium selenite given the possible toxicity associated with the latter compound [24,25].

Reagents and cell treatments

NF-κB inhibitors, caffeic acid phenethyl ester (CAPE) [26] and parthenolide[27] purchased from CalBiochem (San Diego, CA) and were dissolved in DMSO. For all inhibitor treatments, osteoblasts were incubated with inhibitors for 1or 2 hrs before the addition of BCCM. DMSO (0.2 % v/v) was added to control cultures at the same time as the other compounds. Osteoblasts were washed with PBS and treated with 50% BCCM or VM for the indicated time.

iNOS expression by RT-PCR

After incubation with BCCM or VM for 4 hrs, cells were washed one time with PBS; RNA was extracted using the RNeasy kit (QIAGEN, Valencia, CA) and quantified on the basis of A_{260}. The RNA samples were treated with RNase-free DNase to eliminate genomic DNA contamination. Equal amounts of RNA (1 μg) from each sample were used in RT-PCR with iNOS-specific sense (5'-AATGGCAACATCAGGTCGGCCATCACT-3') and antisense (5'-GCTGTGTGTCACAGAAGTCTC-3') primers. B–Actin was used as the control as described previously[28] .

Total cell lysate preparation and western blot analysis

After treatment, cells were lysed with a buffer containing 0.5M Tris-HCl, pH 6.8, 19% (v/v) glycerol and 10% (w/v) SDS. Protease and phosphatase inhibitors, 2 ng/ml aprotinin, 1 μg/ml pepstatin, 7.5mM NaF, 1mM $NaVO_3$, and 1mM DMSF, were also added to the lysis buffer. Total proteins (40 μg) from each sample were used to carry out the western blot. Samples of cells treated for 4 hrs were used for COX-2 expression. COX-2 antibody was purchased from Cayman Chemical (Ann Arbor, Michigan) and actin antibody was from Cell Signaling (Dover, MA). SDS-PAGE followed by western blot analysis was performed as described earlier [29]. B-actin or GAPDH were used as loading controls.

Nuclear extract preparation and electrophoretic mobility shift assay (EMSA)

After 1 hr of treatment, cells were washed and collected for nuclear extraction following a modification of the procedure of NE-PER® Nuclear and Cytoplasmic Extraction (Pierce Biotechnology, Rockford, IL) as described from our laboratory[29]. Nuclear extracts (50 μg) were used in the western blot assay. Antibody to p65 was purchased from Santa Cruz (CA). Actin was also used as a loading control.

For EMSA, the sense strand of the NFκB oligonucleotide, 5'-GATCCAGTTGAGGGGACTTTCCCAGGC-3' (Qiagen), was annealed with its complementary strand and 10 μl (4pmol/μl) of the resultant double-stranded oligonucleotide was labeled with [γ-^{32}P]-ATP (3000Ci/mol at 10mCi/ml) using T4-polynucleotide kinase (New England Biolabs, Ipswich, MA), with an incubation at 37 °C for 30 min followed by gel filtration chromatography in Biogel P6 spin columns (Bio-

Rad, Hercules, CA) to remove the unincorporated 32P. For the binding reaction, 10μg of nuclear extracts were incubated for 10 min at room temperature with 5x gel-shift binding buffer (5mM MgCl2, 2.5mM DTT, 2.5mM EDTA, 250mM NaCl, 50mM Tris-HCl pH 7.5), 50μg/ml poly (dI-dC) and sufficient ddH2O to bring samples to 15μl. ^{32}P-labeled NFκB oligonucleotide (40000 CPM) was added to the reaction, and incubated for 15 min at room temperature. The samples were loaded on pre-cast 4% acrylamide gels (Biorad,) for electrophoresis at 120V for 45-50 min in TBE buffer. The gel was dried, exposed to X-ray film overnight at -80°C and subsequently developed. The NFκB bands were confirmed by competition using a >100-fold excess of unlabeled oligonucleotide.

Cytokine detection

After 4 hr incubations with the cells, the culture media were collected to measure the expression of murine IL-6 and MCP-1 by ELISA. All antibodies and standards were purchased from R & D Systems (Minneapolis, MN); 96-well plates with MaxiSorp™ surfaces (Greiner Bio One, Montroe, NC) were coated with antibody to IL-6 at 2 μg/ml or antibody to MCP-1 at 0.4 μg/ml and incubated at 4℃ overnight. After being washed with PBS, the plates were blocked with 1% BSA for 2 hrs. Samples and standards were added and incubated at 4℃ overnight. After another wash, detection antibody was added at 25 ng/ml for IL-6 antibody or 100 ng/ml for MCP-1 antibody and incubated at room temperature for 2hrs. Samples were washed, and NeutrAvidin™ horseradish peroxidase conjugate (Pierce) was added and the incubation continued at room temperature for 30min. Samples were washed again and incubated with ABTS (Sigma) peroxidase

substrate at room temperature. The absorbance was detected at 405nm. All ELISAs were performed twice, each time with duplicate samples.

GPx activity assays

Osteoblasts were cultured in various Se-containing medium for at least 2 passages. The cells were harvested, lysed with M-PER (Pierce) containing protease inhibitor cocktail and 1mM PMSF and centrifuged (14000 x g) for 10 min. Total protein was measured in the resulting supernatant using the BCA reagent (Pierce). The samples were assayed immediately for GPx activity, according to a published method using H_2O_2 as a substrate[30]. The GPx activity was expressed as nmoles of NADPH oxidized per minute per milligram of protein.

Results

NF-κB was activated during stimulation with BCCM and was critical for cytokine induction

To confirm that NF-κB was activated, we tested for p65 translocation into the nucleus following osteoblast stimulation by BCCM. Nuclei were isolated from cells 1 hr after treatment with BCCM. Pilot experiments indicated this time was optimal for NF-κB activation (data not shown). The presence of activated NF-κB in the nucleus was evaluated both by western blotting for p65 and by NF-κB EMSA (Figure 1, A-C). We observed an increase in p65 translocation to the nucleus at 1 hr post BCCM treatment. We also found an increase in DNA-bound NF-κB. Taken together, these data suggested that NF-κB was activated by BCCM. It was also reasonable to expect a rapid activation

of NF-κB considering its function as an upstream transcription factor. NF-κB is one of many transcription factors associated with the regulation of cytokines. Some common transcription factors, such as AP-1 and CRE, have also been reported to be involved[31,32]. In order to demonstrate the importance of NF-κB in the osteoblast response, we treated MC 3T3-E1 cells with NF-κB inhibitors, CAPE and parthenolide in separate experiments, to determine if blocking NF-κB would result in the reduction of the cytokine response (Figure 1, D and E). Both IL-6 and MCP-1 production by BCCM were reduced by the NF-κB inhibitors in a dose-dependent manner. Control samples with the addition of 0.2% DMSO showed no response. Both inhibitors blocked NF-κB translocation into the nucleus (Figure 1C). Thus both NF-κB translocation and DNA binding activity were clearly abrogated by both CAPE and parthenolide. To verify that the reduction of cytokines was not due to cell death, viability was tested by trypan-blue staining. After 5 hrs of incubation with parthenolide or 6 hrs with CAPE and 0.2% DMSO, cell viability remained nearly 100% even in the highest concentration of inhibitor (data not shown). Together, the data indicated that NF-κB was a common regulator for IL-6 and MCP-1, and was critical for their induction in osteoblasts by BCCM.

Breast cancer CM stimulates NF-κB-regulated COX-2 and iNOS expression

Cytokine expression is only one part of the inflammatory response. In addition to testing for IL-6 and MCP-1, we evaluated COX-2 and iNOS expression in MC3T3-E1 after treatment with BCCM, because these two proteins are usually induced during inflammation, and are downstream targets of NF-κB[14,15]. After 4 hr treatment of MC3T3-E1 with BCCM, COX-2 protein and iNOS mRNA were both increased by

BCCM treatment compared to those treated with VM (Figure 2. A and B). These data as well as the induction of IL-6, MC-P-1, and IL-8 that we reported earlier[33], suggests that NF-κB controls a wide-range of proinflammatory reactions in osteoblasts in response to breast cancer stimulation.

Osteoblast response to methylseleninic acid

There are many reports that Se can decrease NF-κB activation under different situations. However, the responses towards Se are cell-type and Se compound-specific[34,35]. For examples, Li et al. demonstrated that inorganic Se, selenite, and organic Se, MSA, activated different apoptotic pathways in the same cell type [36]. Therefore, we tested a less toxic form, MSA, in our studies. Osteoblasts were cultured in Se-deficient differentiation medium for 7 days before addition of MSA for another 7 days. At this time, osteoblasts were treated with BCCM for 4 hours, and IL-6 and MCP-1 concentrations were measured in the culture media (Figure 3, A and B). With MSA supplementation, both IL-6 and MCP-1 declined in a dose-dependent manner. These results suggested that MSA was able to downregulate the proinflammatory response. To ensure that the reduction in cytokines was not due to a loss of cell viability, the cells were staine with trypan blue after 7 days of MSA supplementation. Nearly 100% of the cells were viable (data not shown). These data indicated that MSA was a biologically effective Se compound capable of reducing the cytokine response of osteoblasts towards BCCM.

To determine if MSA could affect expression of iNOS and COX-2, we tested for the expression of these molecules after 4 hrs treatment with BCCM (Figure 3 C and D).

MSA supplementation inhibited both iNOS expression and COX-2 induction by BCCM. Taken together, these data suggested that a wide-range inflammatory response could be regulated by MSA. Interestingly, a comparison of the dose responses of iNOS, COX-2 and IL-6 indicated that more than 1 μ M MSA was required in each case.

GPx activity may be a marker of adequate Se status but might not reflect the inflammatory status.

Selenium is required for the maintenance of intracellular redox status. It is critical to both biosynthesis and function of reactive oxygen species (ROS)-scavenging enzymes, e.g. glutathione peroxidase (GPx). The Se-dependent GPx would not be functional in the absence of Se, leading to intracellular ROS accumulation and eventually cause oxidative stress. Our data so far indicated that MSA-supplemented osteoblasts gave a reduced inflammatory response to BCCM. Thus we tested if the effect was related to the level of GPx activity which affects intracellular oxidative stress.

Osteoblasts were cultured in MSA-containing medium for two passages in order to reach a steady state level of Se. Total cell lysates were then used to measure GPx activity (Figure 4). In the absence of added Se, osteoblasts showed no detectable GPx activity, as expected following depletion of Se. With the gradual increase of MSA supplementation, the activity of GPx was restored. We detected an obvious increase of GPx activity with as low as 50 nM MSA supplementation, which implied that osteoblasts could absorb and use MSA efficiently. However, when we further evaluated the correlation between the GPx activity and the reduction of inflammatory responses (Figure 3), we did not see the

same dose response. GPx activity appeared to be almost saturated when osteoblasts were supplemented with 1μM MSA; higher concentrations of MSA, caused no additional increase in GPx activity (data not shown). On the other hand, we found that MSA supplementation of 1μM had little or no effect on IL-6 and MCP-1 production. Taken together, we suggest that while the level and activity of GPx was sensitive to Se supplementation and could be used as an indicator, GPx may not be the main selenoprotein or Se-containing intermediate involved in the regulation of IL-6 and MCP-1 production.

MSA supplementation blocked the activation of NF-κB by BCCM in osteoblasts

To determine whether MSA regulated IL-6 and MCP-1 expression through the NF-κB pathway, we examined the activation of NF-κB after MSA treatment. Osteoblasts were supplemented with MSA (100 nM to 4 μM) and treated with VM or BCCM for 1 hr. The translocation of p65 into the nuclear fraction was detected by western blot (Figure 5A). Without added Se, p65 accumulation in the nuclear fraction was apparent. With MSA supplementation as low as 1 μM, there was less p65 present in the nucleus. With 4 μM MSA supplementation, no nuclear p65 was detectable. The EMSA findings also supported this result (Fig, 5B). There was more DNA-bound NF-κB when osteoblasts were supplemented with no or low MSA and treated with BCCM. However, when osteoblasts were supplemented with 4 μM MSA, BCCM treatment did not efficiently trigger the activation of NF-κB. Therefore, less NF-κB translocated to the nucleus and bound to the DNA. These data suggested that MSA supplementation inhibited the activation of NF-κB and consequently, reduced the expression of its target genes.

Discussion

In the present study, we investigated the role of NF-κB on the regulation of the inflammatory response of osteoblasts to conditioned medium from MDA-MB-231, metastatic breast cancer cells. We found not only the increased production of IL-6, and MCP-1, but other inflammatory molecules, COX-2 and iNOS, were significantly enhanced with BCCM. These findings indicated that a wide range of inflammatory responses was triggered in the osteoblasts upon interaction with the BCCM. The data also supported the hypothesis that NF-κB was activated by BCCM and was critical to IL-6 and MCP-1 expression.

NF-κB is a member of ubiquitously expressed family of transcription factors which regulates more than 200 genes including COX-2[14] and iNOS[15]. The data strongly indicated that NF-κB played an important role in the inflammatory responses of osteoblasts to BCCM. Therefore, the regulation of activation of NF-κB activation is a possible approach to reduce cytokines and other inflammatory molecules. For example, by supplemention of osteoblasts with MSA, which increased cellular selenoproteins, abrogated BCCM-induced cytokine production by the osteoblasts.

Selenium, an essential element in the mammalian diet, provides protection from oxidative damage [37]. Severe Se deficiency observed primarily in certain areas in China is associated with an endemic disease called Kashin-Beck disease. It is an osteoarticular disease with symptoms of the necrosis of articular and growth plate chondrocytes, resulting in degenerative and necrotic lesions[37]. Several reports indicate that bone

tissues in man are affected by Se deficiency[38,39]. For example, in healthy infants, there is a correlation between the Se level in the urine and bone resorption[39]. This literature suggests a link between Se and bone turnover. However, the importance and detailed mechanism of Se in this case remain unclear.

Selenium is also known to prevent several degenerative diseases, such as atherosclerosis, arthritis, central nervous system pathologies, altered immunological function, and cancers[18]. Many epidemiological studies describe an inverse correlation between Se levels and cancers, such as stomach, pancreas, lung and breast[18]. In the Nutritional Prevention of Cancer Trial (NPC Trial)[40], researchers tested the effect of Se supplementation on a large population and measured the cancer incidence. The results of the trial indicated an impressive preventative effect of Se supplementation, especially in lung, colorectal and prostate cancers[41]. However, a concern to be addressed from the NPC trail is that only very few of the subject's (6/1,312) plasma level were below 80 ng/ml Se[42], which is the minimum requirement of plasma Se to produce maximum selenoproteins. This finding may indicate that the preventive effect of Se does not work through selenoproteins, at least those such as GPx, but through other selenoproteins or active metabolites. In a more recent study, the SELECT trial, Se-Met or vitamin E supplementation did not prevent the occurrence of new cases of prostate cancer in a relatively healthy population [43]. While there may always be design questions with this trial [44], for our purposes, this study did not deal with metastasis, specifically mestastasis to bone, a common site for prostate cancer.

Selenium compounds can generally be separated into two groups: organic and inorganic. Organic Se is present in foods in the form of Se-Met, Se-Cys, and methylselenocysteine, while inorganic Se is usually in the forms of selenate or selenite in the soil[45]. After ingestion, these Se compounds follow different metabolic pathways in the body but enventually form a common intermediate, selenide (Se^{2-}) which is then incorporated into proteins[46]. Inorganic Se compounds convert into selenide with the help of GSH, while organic Se compounds more likely form the methylselenol (CH_3SeH) first. It is known that when cells generate too much selenide, it reacts with oxygen to produce superoxide radicals (O_2^-), which are toxic to cells[46]. On the other hand, it is a well-accepted concept that methylselenol is involved in the anti-cancer effects of Se [46]. Taken together, different forms of Se compounds may enter the metabolic pathway at different points and may have different effects on different types of cells[34,35]. In this regard, MSA has been demonstrated not to cause oxidative stress, unlike selenite, and is, therefore, less toxic [24]. Therefore, we restricted our investigation to MSA.

The bone remodeling process shares some similarities with inflammation[47]. Many inflammatory molecules that are secreted by immune cells are produced by osteoblasts. Some, such as IL-1, IL-6, IL-8, MCP-1, PGE_2 and COX-2, are also osteoclastogenic [48]. They attract and activate osteoclasts, which results in bone matrix degradation followed by the release of many growth factors from the matrix including TGF-β[1]. The abundance of growth factors makes the bone microenvironment more affable to breast cancer cells.

Interleukin-6 receptors are expressed by osteoclasts and when stimulated, initiate osteoclast differentiation and thus, the bone resorption process[9]. Some reports indicate that increased plasma IL-6 is a negative indicator of metastasis [49]. IL-6 is also associated with increased breast cancer cell migration[48]. MCP-1(a CC chemokine) regulates bone resorption by stimulating the migration of monocyte-osteoclast progenitor cells to the bone[9,33]. MCP-1 is also associated with angiogenesis and cancer cell survival[48]. COX-2 contributes to the activation of osteoclasts and the creation of a favorable niche for cancer cells[48]. COX-2 expression is associated with growth, invasion, apoptosis and angiogenesis in breast cancer [48]. Taken together, their increased expression by osteoblasts may affect the equilibrium in the bone microenvironment and promote breast cancer osteolytic bone metastasis. By controlling their common regulator, NF-κB, it may be possible to reduce the damage caused by breast cancer bone metastasis. Currently there is no way to restore existing osteolytic lesions; however, limiting the effect of bone metastasis may significantly improve the quality of life of individuals with breast cancer bone metastasis.

In the clinic, it is not unusual to observe metastasis after surgery or chemotherapy. Metastatic lesions originate from a group of tumor cells which disseminate from the primary tumor mass and may undergo a period of dormancy in the target tissue [50]. Some reports showed that in breast cancer, tumor cell dissemination may occur in the early stages from non-invasive tumors[51]. Dormant cells can rest in the secondary metastatic site or in the lymph node for years before they grow to a detectable tumor [52]. All together, it may be very difficult to totally prevent metastasis since it is difficult to

define the time or the critical stage of this event. However, reducing the damage from the metastasis is still a useful approach. By supplementing Se in the diet, we can increase intracellular Se levels sufficient to produce useful intermediates. By the time dormant micro-metastases of breast cancer in bone begin to proliferate, the higher Se levels in osteoblasts may prevent or reduce their responses to breast cancer cells, which in turn may slow the metastatic growth and break the vicious cycle. There are many reports that Se functions in both cancer initiation and progression. Our results offer the possibility that Se can also affect the metastasis process.

Animal models are commonly conducted to establish the link between dietary Se and cancers. However, the majority of those animal studies focus on the chemoprevention effect of Se[18]; only few reports demonstrate the relationship between Se and metastasis. In a recent study, mice fed a Se-supplemented diet showed not only fewer mammary tumors, but tumor cells with Se supplementation also showed an inhibition of migration *in vitro*[53]. We plan to test a mouse breast cancer model to evaluate the effect of Se on metastasis *in vivo*.

In summary, we found that Se supplementation reduced the inflammatory response of osteoblasts to metastatic breast cancer cells by regulating the activation of NF-κB. The expression of NF-κB –dependent genes, which a play an important role in metastasis, were down-regulated implying that Se supplementation may negatively impact the metastasis process.

Acknowledgments

This work was supported by the American Institute for Cancer Research (#06027) with some additional support from the National Foundation for Cancer Research, Center for Metastatic Research, University of Alabama at Birmingham (AMM), and NIH R01 DK 077152 (KSP). The President's Fund for Undergraduate Research provided summer funding for L.N. We thank Drs. Karam El-Bayoumy and Arun Das for measuring the selenium content of the serum.

References

1. Guise, T.A. and Mundy, G.R. (1998) Cancer and bone. *Endocr Rev*, **19**, 18-54.
2. Lipton, A. (2000) Bisphosphonates and breast carcinoma: present and future. *Cancer*, **88**, 3033-7.
3. Delmas, P.D., Demiaux, B., Malaval, L., Chapuy, M.C., Edouard, C. and Meunier, P.J. (1986) Serum bone gamma carboxyglutamic acid-containing protein in primary hyperparathyroidism and in malignant hypercalcemia. Comparison with bone histomorphometry. *J Clin Invest*, **77**, 985-91.
4. Stewart, A.F., Vignery, A., Silverglate, A., Ravin, N.D., LiVolsi, V., Broadus, A.E. and Baron, R. (1982) Quantitative bone histomorphometry in humoral hypercalcemia of malignancy: uncoupling of bone cell activity. *J Clin Endocrinol Metab*, **55**, 219-27.
5. Mastro, A.M., Gay, C.V., Welch, D.R., Donahue, H.J., Jewell, J., Mercer, R., DiGirolamo, D., Chislock, E.M. and Guttridge, K. (2004) Breast cancer cells induce osteoblast apoptosis: a possible contributor to bone degradation. *J Cell Biochem*, **91**, 265-76.
6. Mercer, R., Miyasaka, C. and Mastro, A.M. (2004) Metastatic breast cancer cells suppress osteoblast adhesion and differentiation. *Clin Exp Metastasis*, **21**, 427-435.
7. Phadke, P.A., Mercer, R.R., Harms, J.F., Jia, Y., Frost, A.R., Jewell, J.L., Bussard, K.M., Nelson, S., Moore, C., Kappes, J.C., Gay, C.V., Mastro, A.M. and Welch, D.R. (2006) Kinetics of metastatic breast cancer cell trafficking in bone. *Clin Cancer Res*, **12**, 1431-40.
8. Mercer, R.R., Miyasaka, C. and Mastro, A.M. (2004) Metastatic breast cancer cells suppress osteoblast adhesion and differentiation. *Clin Exp Metastasis*, **21**, 427-35.
9. Manolagas, S.C. (1995) Role of cytokines in bone resorption. *Bone*, **17**, 63S-67S.
10. Balkwill, F. and Coussens, L.M. (2004) Cancer: an inflammatory link. *Nature*, **431**, 405-6.

11. Fritz, E.A., Glant, T.T., Vermes, C., Jacobs, J.J. and Roebuck, K.A. (2002) Titanium particles induce the immediate early stress responsive chemokines IL-8 and MCP-1 in osteoblasts. *J Orthop Res*, **20**, 490-8.
12. Taranova, A.G., Maldonado, D., 3rd, Vachon, C.M., Jacobsen, E.A., Abdala-Valencia, H., McGarry, M.P., Ochkur, S.I., Protheroe, C.A., Doyle, A., Grant, C.S., Cook-Mills, J., Birnbaumer, L., Lee, N.A. and Lee, J.J. (2008) Allergic pulmonary inflammation promotes the recruitment of circulating tumor cells to the lung. *Cancer Res*, **68**, 8582-9.
13. Baud, V. and Karin, M. (2009) Is NF-kappaB a good target for cancer therapy? Hopes and pitfalls. *Nat Rev Drug Discov*, **8**, 33-40.
14. Zamamiri-Davis, F., Lu, Y., Thompson, J.T., Prabhu, K.S., Reddy, P.V., Sordillo, L.M. and Reddy, C.C. (2002) Nuclear factor-kappaB mediates over-expression of cyclooxygenase-2 during activation of RAW 264.7 macrophages in selenium deficiency. *Free Radic Biol Med*, **32**, 890-7.
15. Prabhu, K.S., Zamamiri-Davis, F., Stewart, J.B., Thompson, J.T., Sordillo, L.M. and Reddy, C.C. (2002) Selenium deficiency increases the expression of inducible nitric oxide synthase in RAW 264.7 macrophages: role of nuclear factor-kappaB in up-regulation. *Biochem J*, **366**, 203-9.
16. Bjornstedt, M., Hamberg, M., Kumar, S., Xue, J. and Holmgren, A. (1995) Human thioredoxin reductase directly reduces lipid hydroperoxides by NADPH and selenocystine strongly stimulates the reaction via catalytically generated selenols. *J Biol Chem*, **270**, 11761-4.
17. Saito, Y., Hayashi, T., Tanaka, A., Watanabe, Y., Suzuki, M., Saito, E. and Takahashi, K. (1999) Selenoprotein P in human plasma as an extracellular phospholipid hydroperoxide glutathione peroxidase. Isolation and enzymatic characterization of human selenoprotein p. *J Biol Chem*, **274**, 2866-71.
18. Patrick, L. (2004) Selenium biochemistry and cancer: a review of the literature. *Altern Med Rev*, **9**, 239-58.
19. Mantovani, G., Maccio, A., Madeddu, C., Mura, L., Massa, E., Gramignano, G., Lusso, M.R., Murgia, V., Camboni, P. and Ferreli, L. (2002) Reactive oxygen species, antioxidant mechanisms and serum cytokine levels in cancer patients: impact of an antioxidant treatment. *J Cell Mol Med*, **6**, 570-82.
20. Guven, M., Ozturk, B., Sayal, A., Ozeturk, A. and Ulutin, T. (1999) Lipid peroxidation and antioxidant system in the blood of cancerous patients with metastasis. *Cancer Biochem Biophys*, **17**, 155-62.
21. Roebuck, K.A., Vermes, C., Carpenter, L.R., Fritz, E.A., Narayanan, R. and Glant, T.T. (2001) Down-regulation of procollagen alpha1[I]] messenger RNA by titanium particles correlates with nuclear factor kappaB (NF-kappaB) activation and increased rel A and NF-kappaB1 binding to the collagen promoter. *J Bone Miner Res*, **16**, 501-10.
22. Sudo, H., Kodama, H.A., Amagai, Y., Yamamoto, S. and Kasai, S. (1983) In vitro differentiation and calcification in a new clonal osteogenic cell line derived from newborn mouse calvaria. *J Cell Biol*, **96**, 191-8.
23. Cailleau, R., Young, R., Olive, M. and Reeves, W.J., Jr. (1974) Breast tumor cell lines from pleural effusions. *J Natl Cancer Inst*, **53**, 661-74.

24. Ip, C., Thompson, H.J., Zhu, Z. and Ganther, H.E. (2000) In vitro and in vivo studies of methylseleninic acid: evidence that a monomethylated selenium metabolite is critical for cancer chemoprevention. *Cancer Res*, **60**, 2882-6.
25. Li, G.X., Lee, H.J., Wang, Z., Hu, H., Liao, J.D., Watts, J.C., Combs, G.F., Jr. and Lu, J. (2008) Superior in vivo inhibitory efficacy of methylseleninic acid against human prostate cancer over selenomethionine or selenite. *Carcinogenesis*, **29**, 1005-12.
26. Haddad, J.J. (2002) Nuclear factor (NF)-kappa B blockade attenuates but does not abrogate LPS-mediated interleukin (IL)-1 beta biosynthesis in alveolar epithelial cells. *Biochem Biophys Res Commun*, **293**, 252-7.
27. Hehner, S.P., Hofmann, T.G., Droge, W. and Schmitz, M.L. (1999) The antiinflammatory sesquiterpene lactone parthenolide inhibits NF-kappa B by targeting the I kappa B kinase complex. *J Immunol*, **163**, 5617-23.
28. Prabhu, K., Zamamiri-Davis, F., Stewart, J., Thompson, J., Sordillo, L. and Reddy, C. (2002) Selenium deficiency increases the expression of inducible nitric oxide synthase in RAW 264.7 macrophages: role of nuclear factor-kappaB in up-regulation. *Biochem. J.*, **366**, 203-209.
29. Palempalli, U.D., Gandhi, U., Kalantari, P., Vunta, H., Arner, R.J., Narayan, V., Ravindran, A. and Prabhu, K.S. (2009) Gambogic acid covalently modifies IkappaB-kinase-beta subunit to mediate suppression of lipopolysaccharide-induced activation of NF-kappaB in macrophages. *Biochem J*.
30. Paglia, D.E. and Valentine, W.N. (1967) Studies on the quantitative and qualitative characterization of erythrocyte glutathione peroxidase. *J Lab Clin Med*, **70**, 158-69.
31. Nettles, K.W., Gil, G., Nowak, J., Metivier, R., Sharma, V.B. and Greene, G.L. (2008) CBP Is a dosage-dependent regulator of nuclear factor-kappaB suppression by the estrogen receptor. *Mol Endocrinol*, **22**, 263-72.
32. Zenz, R., Eferl, R., Scheinecker, C., Redlich, K., Smolen, J., Schonthaler, H.B., Kenner, L., Tschachler, E. and Wagner, E.F. (2008) Activator protein 1 (Fos/Jun) functions in inflammatory bone and skin disease. *Arthritis Res Ther*, **10**, 201.
33. Kinder, M., Chislock, E., Bussard, K.M., Shuman, L. and Mastro, A.M. (2008) Metastatic breast cancer induces an osteoblast inflammatory response. *Exp Cell Res*, **314**, 173-83.
34. Park, J.M., Kim, A., Oh, J.H. and Chung, A.S. (2007) Methylseleninic acid inhibits PMA-stimulated pro-MMP-2 activation mediated by MT1-MMP expression and further tumor invasion through suppression of NF-kappaB activation. *Carcinogenesis*, **28**, 837-47.
35. Jiang, C., Ganther, H. and Lu, J. (2000) Monomethyl selenium--specific inhibition of MMP-2 and VEGF expression: implications for angiogenic switch regulation. *Mol Carcinog*, **29**, 236-50.
36. Li, G.X., Hu, H., Jiang, C., Schuster, T. and Lu, J. (2007) Differential involvement of reactive oxygen species in apoptosis induced by two classes of selenium compounds in human prostate cancer cells. *Int J Cancer*, **120**, 2034-43.
37. Turan, B., Can, B. and Delilbasi, E. (2003) Selenium combined with vitamin E and vitamin C restores structural alterations of bones in heparin-induced osteoporosis. *Clin Rheumatol*, **22**, 432-6.

38. Moreno-Reyes, R., Egrise, D., Neve, J., Pasteels, J.L. and Schoutens, A. (2001) Selenium deficiency-induced growth retardation is associated with an impaired bone metabolism and osteopenia. *J Bone Miner Res*, **16**, 1556-63.
39. Tsukahara, H., Deguchi, Y., Miura, M., Hata, K., Hori, C., Hiraoka, M., Kusaka, Y. and Sudo, M. (1996) Selenium status and skeletal tissue metabolism in young infants. *Eur J Pediatr*, **155**, 148-9.
40. Clark, L.C., Combs, G.F., Jr., Turnbull, B.W., Slate, E.H., Chalker, D.K., Chow, J., Davis, L.S., Glover, R.A., Graham, G.F., Gross, E.G., Krongrad, A., Lesher, J.L., Jr., Park, H.K., Sanders, B.B., Jr., Smith, C.L. and Taylor, J.R. (1996) Effects of selenium supplementation for cancer prevention in patients with carcinoma of the skin. A randomized controlled trial. Nutritional Prevention of Cancer Study Group. *Jama*, **276**, 1957-63.
41. Combs, G.F., Jr., Clark, L.C. and Turnbull, B.W. (2001) An analysis of cancer prevention by selenium. *Biofactors*, **14**, 153-9.
42. Duffield-Lillico, A.J., Reid, M.E., Turnbull, B.W., Combs, G.F., Jr., Slate, E.H., Fischbach, L.A., Marshall, J.R. and Clark, L.C. (2002) Baseline characteristics and the effect of selenium supplementation on cancer incidence in a randomized clinical trial: a summary report of the Nutritional Prevention of Cancer Trial. *Cancer Epidemiol Biomarkers Prev*, **11**, 630-9.
43. Lippman, S.M., Klein, E.A., Goodman, P.J., Lucia, M.S., Thompson, I.M., Ford, L.G., Parnes, H.L., Minasian, L.M., Gaziano, J.M., Hartline, J.A., Parsons, J.K., Bearden, J.D., 3rd, Crawford, E.D., Goodman, G.E., Claudio, J., Winquist, E., Cook, E.D., Karp, D.D., Walther, P., Lieber, M.M., Kristal, A.R., Darke, A.K., Arnold, K.B., Ganz, P.A., Santella, R.M., Albanes, D., Taylor, P.R., Probstfield, J.L., Jagpal, T.J., Crowley, J.J., Meyskens, F.L., Jr., Baker, L.H. and Coltman, C.A., Jr. (2009) Effect of selenium and vitamin E on risk of prostate cancer and other cancers: the Selenium and Vitamin E Cancer Prevention Trial (SELECT). *Jama*, **301**, 39-51.
44. Kristal, A.R. (2008) Are clinical trials the "gold standard" for cancer prevention research? *Cancer Epidemiol Biomarkers Prev*, **17**, 3289-91.
45. Rikiishi, H. (2007) Apoptotic cellular events for selenium compounds involved in cancer prevention. *J Bioenerg Biomembr*, **39**, 91-8.
46. Suzuki, K.T., Kurasaki, K., Ogawa, S. and Suzuki, N. (2006) Metabolic transformation of methylseleninic acid through key selenium intermediate selenide. *Toxicol Appl Pharmacol*, **215**, 189-97.
47. Rodan, G.A. (2003) The development and function of the skeleton and bone metastases. *Cancer*, **97**, 726-32.
48. Bussard, K.M., Gay, C.V. and Mastro, A.M. (2008) The bone microenvironment in metastasis; what is special about bone? *Cancer Metastasis Rev*, **27**, 41-55.
49. Yoneda, T., Nakai, M., Moriyama, K., Scott, L., Ida, N., Kunitomo, T. and Mundy, G.R. (1993) Neutralizing antibodies to human interleukin 6 reverse hypercalcemia associated with a human squamous carcinoma. *Cancer Res*, **53**, 737-40.
50. Aguirre-Ghiso, J.A. (2007) Models, mechanisms and clinical evidence for cancer dormancy. *Nat Rev Cancer*, **7**, 834-46.

51. Schardt, J.A., Meyer, M., Hartmann, C.H., Schubert, F., Schmidt-Kittler, O., Fuhrmann, C., Polzer, B., Petronio, M., Eils, R. and Klein, C.A. (2005) Genomic analysis of single cytokeratin-positive cells from bone marrow reveals early mutational events in breast cancer. *Cancer Cell*, **8**, 227-39.
52. Karrison, T.G., Ferguson, D.J. and Meier, P. (1999) Dormancy of mammary carcinoma after mastectomy. *J Natl Cancer Inst*, **91**, 80-5.
53. Unni, E., Kittrell, F.S., Singh, U. and Sinha, R. (2004) Osteopontin is a potential target gene in mouse mammary cancer chemoprevention by Se-methylselenocysteine. *Breast Cancer Res*, **6**, R586-92.

Figure Legends

Figure 1. NF-kB activation in osteoblasts exposed to BCCM. MC3T3-E1 were cultured and differentiated for 2 weeks before stimulation with 50% BCCM for different times. (A) p65 translocation was detected by western blot using nuclear extracts prepared from MC3T3-E1 one hr after treatment with BCCM. (B) NF-kB gel mobility shift analysis (EMSA) of samples prepared as in A. CC: cold oligonucleotide competitor. NS: non-specific binding. (C) Inhibition of NF-kB binding. Osteoblasts were pre-treated with inhibitors CAPE for 2 hrs or with parthenolide for 1hr before addition of BCCM for 1 hr. NF-kB DNA binding activity was detected by EMSA. (D) IL-6, and (E) MCP-1 production by osteoblasts treated with NF-kB inhibitors CAPE for 2 hrs or with parthenolide for 1hr before incubation with BCCM for 4 hrs. DMSO (0.2%) treatment was used as control. Cytokines in the culture media were detected by ELISA. All experiments were performed twice and each sample was assayed in duplicate. Cell viability remained nearly 100% after inhibitor treatment as confirmed by trypan-blue staining (data not shown).

Figure 2. COX-2 (A) and iNOS (B) induction by MC3T3-E1 osteoblasts in response to human MDA-MB-231 breast cancer cells. MC3T3-E1 were cultured and differentiated for 2 weeks before they treated with 50% MDA-MB-231 BCCM for 4 hours. (A) COX-2 expression was detected by western blot using total cell lysate. (B) iNOS expression was detected by RT-PCR. Actin expression was used as a loading control in both assays. All experiments were performed at least in duplicate and each experiment was performed at least twice. Pilot experiments were carried out to determine the optimal treatment period.

Figure 3. Response of osteoblasts to MSA supplementation. Osteoblasts were cultured and differentiated in a selenium-deficient culture medium (18.2 nM Se) for 7 days before supplementation with methylseleninic acid (MSA) for another 7 days for selenium to reach a steady state within the cells. After 2 weeks of culture, osteoblasts were treated with 50% BCCM for 4 hrs. (A) IL-6, (B) MCP-1, and (C) COX-2 and (D) iNOS expression were used as indicators of the effects of selenium compounds. Cytokines were measured by ELISA; COX-2 expression was detected by western blot; iNOS expression was evaluated by RT-PCR. Actin was used as a loading control in COX-2 and iNOS detection. Cell viability was not affected by 7days of MSA supplementation as seen by trypan blue staining (data not shown). Indicated are the concentrations of MSA added to the cultures.

Figure 4. Intracellular GPx activity in MSA supplemented osteoblasts. Osteoblasts were cultured in the presence of MSA for 2 passages at the concentration indicated. Cells

lysates were used to measure GPx activity with hydrogen peroxide as substrates as described in the methods section. The activity is presented as nmoles of NADPH oxidized per minute per milligram of protein.

Figure. 5 NF-kB inhibition by MSA supplementation.

Osteoblasts were cultured in Se-deficient medium (18.2 nM) for 7 days before adding MSA to the culture system for another 7 days. On day 14, osteoblasts were treated with BCCM for 1 hr and nuclear extracts were prepared. NF-kB activation was measured by (A) p65 translocation and (B) NF-kB EMSA. Actin was used as a loading control. CC: cold oligonucleotide competitor. NS: non-specific binding.

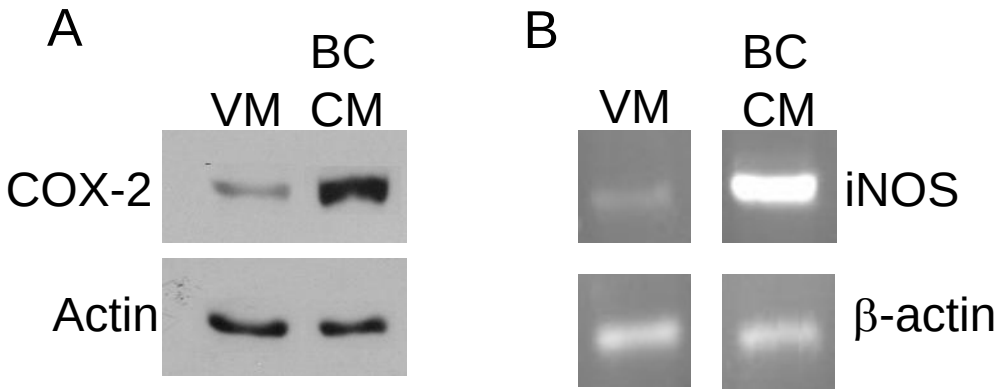

Figure 1. **COX-2 (A) and iNOS (B) induction by MC3T3-E1 osteoblasts in response to human MDA-MB-231 breast cancer cells.** MC3T3-E1 were cultured and differentiated for 2 weeks before they treated with 50% MDA-MB-231 BCCM for 4 hours. (A) COX-2 expression was detected by western blot using total cell lysate. (B) iNOS expression was detected by RT-PCR. Actin expression was used as a loading control in both assays. All experiments were performed at least in duplicate and each experiment was performed at least twice. Preliminary experiments were performed to determine the optimal treatment period.

A

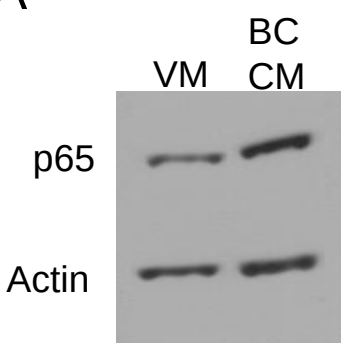
VM
BC CM
p65
Actin

B

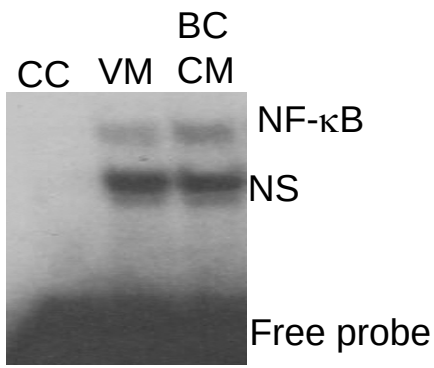
CC
VM
BC CM
NF-κB
NS
Free probe

D

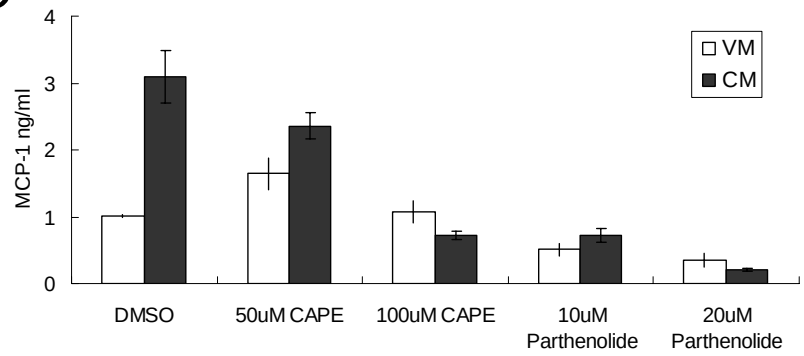
MCP-1 ng/ml
4
3
2
1
0
VM
CM
DMSO
50uM CAPE
100uM CAPE
10uM Parthenolide
20uM Parthenolide

C

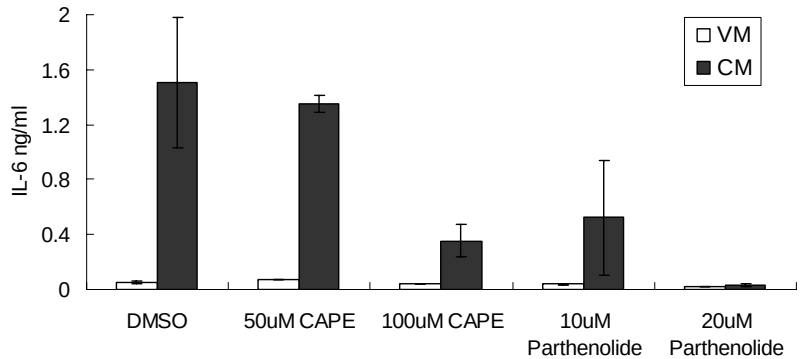
IL-6 ng/ml
2
1.6
1.2
0.8
0.4
0
VM
CM
DMSO
50uM CAPE
100uM CAPE
10uM Parthenolide
20uM Parthenolide

E

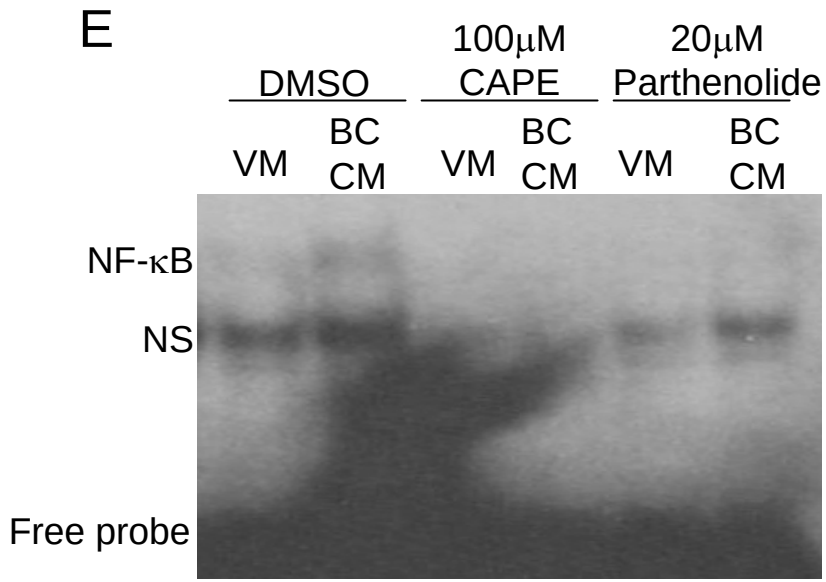
DMSO
100μM CAPE
20μM Parthenolide
VM
BC CM
VM
BC CM
VM
BC CM
NF-κB
NS
Free probe

Figure 2. **NF-κB activation in osteoblasts exposed to BCCM.** MC3T3-E1 were cultured and differentiated for 2 weeks before stimulating with 50% BCCM for different times. (A) p65 translocation. Osteoblasts were treated with BCCM for 1h. p65 translocation was detected by western blot using nuclear extracts. Actin was used as a control. (B) NF-κB gel mobility shift analysis (EMSA). Samples were prepared as in A. CC: cold oligonucleotide competitor. NS: non-specific binding. (C) IL-6, (D) MCP-1 reduction by NF-κB inhibitors. Osteoblasts were treated with CAPE for 2 hrs or with parthenolide for 1hr before incubating with 50% BCCM for 4 hrs. DMSO 0.2% treatment was used as control. Cytokines production was detected by ELISA using culture medium after treatment. All experiments were performed in duplicate and each sample was assayed in duplicate. Cell viability remained nearly 100% after inhibitors treatment confirmed by trypan-blue staining (data not shown). (E) Inhibition of NF-κB binding. Samples were pre-treated with inhibitors as in (C), (D) and treated with 50% BCCM for 1 hr. NF-κB DNA binding activity was detected by EMSA using nuclear extracts.

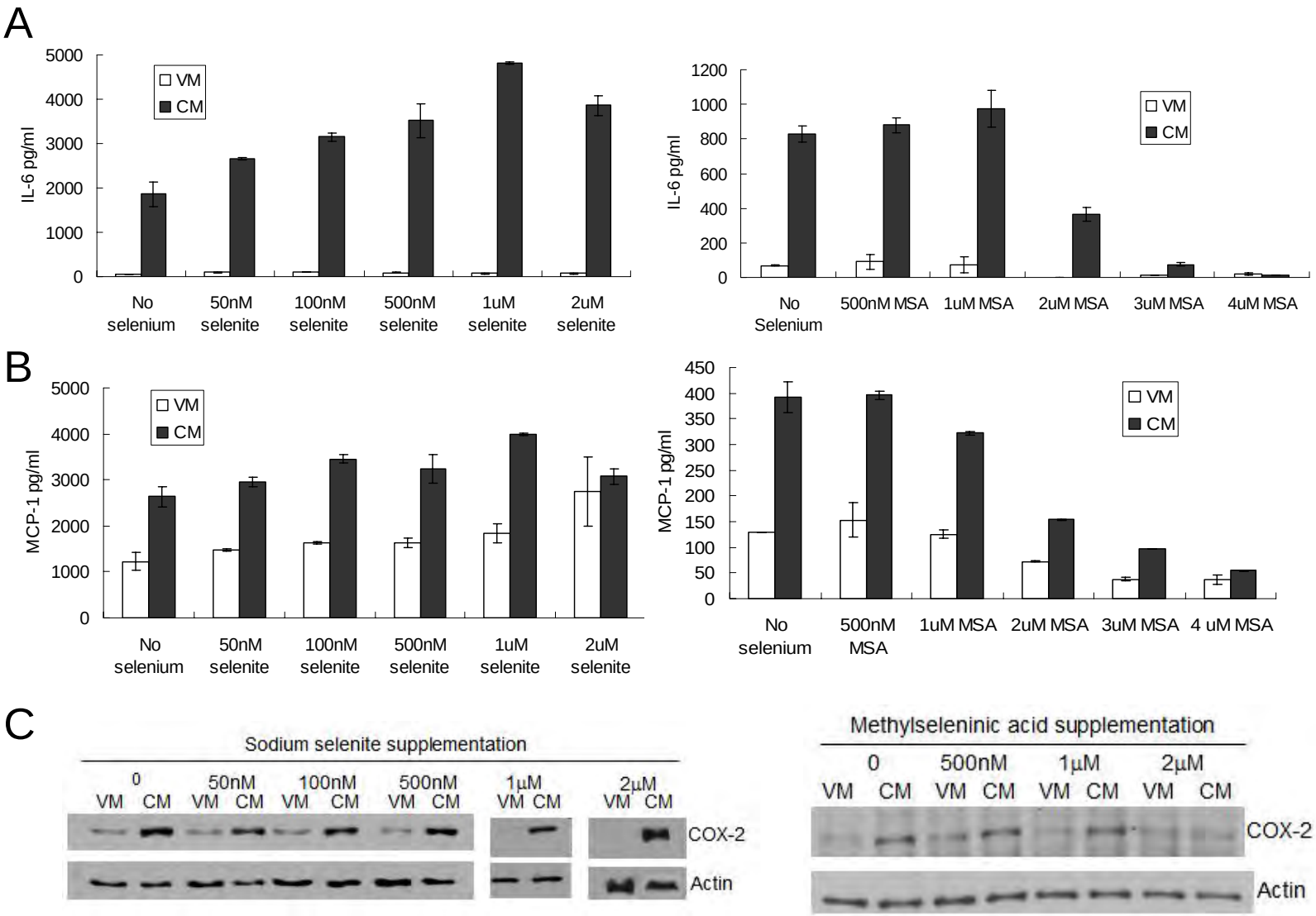
A
IL-6 pg/ml
VM
CM
No selenium
50nM selenite
100nM selenite
500nM selenite
1uM selenite
2uM selenite
No Selenium
500nM MSA
1uM MSA
2uM MSA
3uM MSA
4uM MSA
B
MCP-1 pg/ml
No selenium
50nM selenite
100nM selenite
500nM selenite
1uM selenite
2uM selenite
500nM MSA
1uM MSA
2uM MSA
3uM MSA
4 uM MSA
C
Sodium selenite supplementation
0
50nM
100nM
500nM
1μM
2μM
COX-2
Actin
Methylseleninic acid supplementation
0
500nM
1μM
2μM
COX-2
Actin

Figure 3. **Responses of osteoblasts to different selenium compounds.** Osteoblasts were cultured and differentiated in a selenium-deficient culture system (18.2 nM) for 7 days before supplemented with two selenium compounds (sodium selenite, methylseleninic acid [MSA]) for another 7 days to reach a selenium balance within cells. After 2 weeks of culture, osteoblasts were treated with 50%BCCM for 4 hrs. (A) IL-6, (B) MCP-1, and (C) COX-2 expression was used as indicators to evaluate the effects of selenium compounds. Cytokine production was measured by ELISA; COX-2 expression was detected by western blot. Cell viability remained nearly 100% after 7days of MSA supplementation confirmed by trypan blue staining (data not shown).

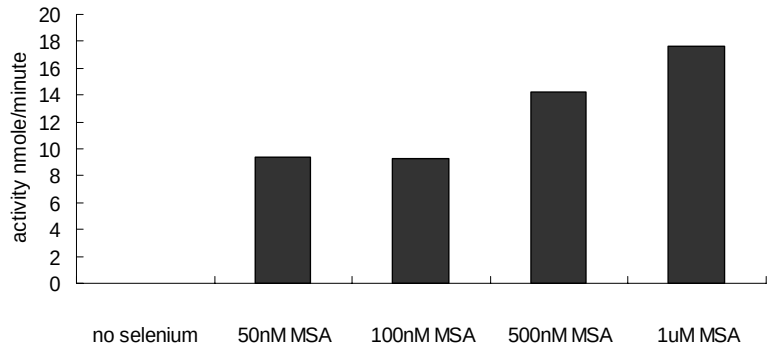

Figure 4. **Intracellular GPX activity in MeSA-supplemented osteoblasts.** Osteoblasts were cultured in the presence of MSA for 2 passages at the concentration indicated to reach a selenium balance. Cells lysates were used to measure GPX activity with hydrogen peroxide as substrates. The activity was described as nmoles of NADPH oxidized per minute per milligram of protein.

A

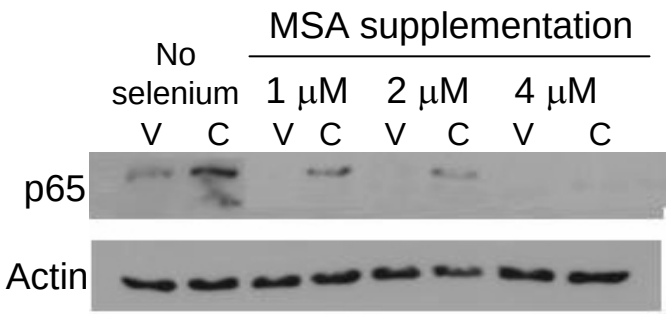
MSA supplementation
No selenium
1 μM
2 μM
4 μM
V C V C V C V C
p65
Actin

B

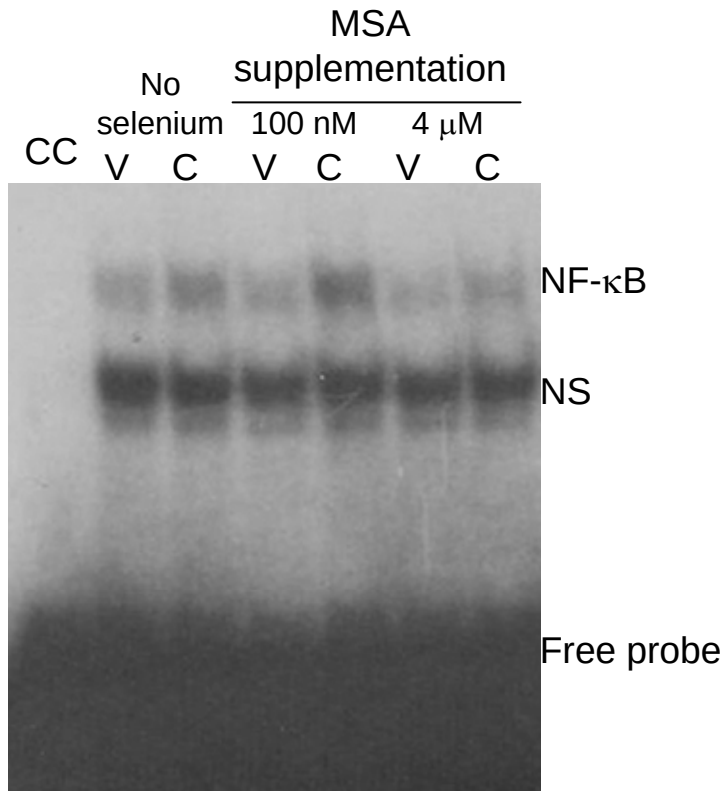
MSA supplementation
No selenium
100 nM
4 μM
CC
V C V C V C
NF-κB
NS
Free probe

Figure. 5 **NF-kB inhibition by MSA supplementation.**
Osteoblasts were cultured in Se-deficient medium (18.2 nM) for 7 days before adding MSA to the culture system for another 7 days. On day 14, osteoblasts were treated with BCCM for 1 hr and nuclear extracts were prepared. NF-κB activation was measured by (A) p65 translocation and (B) NF-κB EMSA. Actin was used as a loading control. CC: cold oligonucleotide competitor. NS: non-specific binding.